

CRWR Online Report 98-8

Use of Digital Soil Maps in a Rainfall-Runoff Model

by

Seann M. Reed, B.S., M.S.

Graduate Research Assistant

and

David Maidment, Ph.D.

Principal Investigator

December 1998

CENTER FOR RESEARCH IN WATER RESOURCES

Bureau of Engineering Research • The University of Texas at Austin
J.J. Pickle Research Campus • Austin, TX 78712-4497

This document is available online via World Wide Web at
<http://www.ce.utexas.edu/centers/crwr/reports/online.html>

Acknowledgements

For helping me through all my years as a student, I would first like to thank my parents, John and Kathie, and my sister, Monise.

During my graduate studies at The University of Texas, I have had the good fortune to interact with many wonderful people. Most importantly, I met my wife, Cindy, who has brought great joy to my life.

I wish to thank my faculty advisor, David Maidment, not only for his scholarly advice, but also for his never-ending optimism and kindness. I would also like to thank my other dissertation committee members, especially Jay Famiglietti, who has made me feel welcome to participate in activities with the Geological Sciences department.

A special thank you also goes to Francisco Olivera who has been both friend and mentor.

I greatly appreciate the financial support provided by the Hydrologic Engineering Center (HEC) and the technical guidance provided by John Peters and Arlen Feldman of HEC.

Other colleagues who I would like to thank for providing help with technical issues throughout my graduate studies include Zichuan Ye, Tom Evans, Dean Djokic, Pawel Mizgalewicz, John Burgin, Laurie Wood, Tim Plover, and Ty Lehman.

I will always remember the warmth of the students, faculty, and staff in EWRE. Thank you to the ultimate frisbee players for all the fun times.

I would like to acknowledge the support of the following organizations for providing data used in this research free of charge:

- Agricultural Research Service, Grazinglands Research Laboratory, El Reno, OK.
- Atmospheric Radiation Measurement (ARM) Program sponsored by the U.S. Department of Energy, Office of Energy Research, Office of Health and Environmental Research, Environmental Sciences Division.
- U.S. Geological Survey EROS Data Center, Sioux Falls, SD.
- U.S. Geological Survey, Oklahoma District, Oklahoma City, OK.
- U.S. Department of Agriculture Natural Resources Conservation Service.
- U.S. Environmental Protection Agency.
- National Weather Service Arkansas-Red Basin River Forecast Center, Tulsa, OK.
- EOS Distributed Active Archive Center (DAAC), NASA Goddard Space Flight Center, Greenbelt, MD.

Use of Digital Soil Maps in a Rainfall-Runoff Model

Publication No. _____

Seann Mischa Reed, Ph.D.
The University of Texas at Austin, 1998

Supervisor: David R. Maidment

Computer programs, collectively named the Soil-water Balance Modeling System (SWBMS), are developed to evaluate alternative methods for using digital soil maps in rainfall-runoff modeling. The two soils databases of interest are the State Soil Geographic Database (STATSGO — 1:250,000 scale) and the Soil Survey Geographic Database (SSURGO — 1:24,000 scale), both maintained by the U.S. Department of Agriculture. In SWBMS, simple conceptual models are used to describe infiltration, percolation, and evaporation processes. Use of simplified process models is justified because there are large uncertainties involved with the specification of soil hydraulic properties and in quantifying rainfall. Representative soil hydraulic properties are assigned based on USDA texture class. Distributed soil properties are used in conjunction with distributed NEXRAD Stage III rainfall data to make to make rainfall excess calculations.

SWBMS is applied using hydrologic data from the Little Washita watershed in southwestern Oklahoma. The performance of SWBMS in predicting runoff is evaluated using different levels of spatial complexity to describe soil properties. Spatial complexity is varied in three different ways. (1) Differences between a one and a two-layer conceptual soil model are considered. (2) Simulations in which a single surface soil texture is assigned to the entire watershed, a single surface soil

texture is assigned to each NEXRAD rainfall cell, and multiple surface soil textures are considered within each NEXRAD rainfall cell are compared. (3) Soil texture properties are assigned using soil maps created from sources at two different scales (1:250,000 and 1:24,000).

Calibration and validation of the SWBMS model has yielded interesting insights. In the two-layer conceptual soil model, the top layer controls direct runoff, but the bottom layer serves as an important control on how much water evaporates and how much water percolates to the groundwater reservoir. When the spatial variability of surface texture is reduced through resampling of soil properties, model performance decreases. Although the 1:250,000 scale soil map contains considerably less spatial detail than the 1:24,000 scale map, use of each data set as input in model validation runs produced similar results. Further simulations should be made to verify these conclusions.

TABLE OF CONTENTS

LIST OF TABLES	x
LIST OF FIGURES	xii
NOMENCLATURE.....	xvi
CHAPTER 1. INTRODUCTION	1
1.1. Motivation.....	1
1.2. Objectives and scope.....	3
1.3. Study area.....	7
1.4. Organizational statement.....	9
CHAPTER 2. LITERATURE REVIEW	10
2.1. Surface and subsurface runoff: definition of terms.....	10
2.2. Lumped versus distributed modeling.....	11
2.2.1. NEXRAD Data.....	11
2.2.2. Partial area effects	13
2.3. Soil-water balance modeling.....	16
2.4. Infiltration	17
2.5. Evaporation	18
2.6. Percolation	22
2.7. Existing streamflow simulation modeling programs	22
2.8. GIS and Hydrologic Modeling.....	23
2.8.1. Terrain analysis	23
2.8.2. GIS preprocessors for hydrology models	24
2.8.3. Use of soils data.....	25
2.9. Summary	26
CHAPTER 3. METHODOLOGY	27
3.1. Overview.....	27

3.2. Data description	29
3.2.1. Topographic data	32
3.2.2. Soils Data.....	35
3.2.2.1. STATSGO vs. SSURGO	35
3.2.2.2. Estimation of soil hydraulic properties	42
3.2.2.2.1. Soil attribute tables.....	42
3.2.2.2.2. The lookup table approach	45
3.2.2.2.3. Selecting representative parameter values for texture classes	51
3.2.2.3. One-layer model versus a two-layer model	61
3.2.3. Land use data	68
3.2.4. NEXRAD data and spatial variability	70
3.2.5. Data used to estimate evaporation	74
3.2.6. Data used for calibration and validation.....	74
3.3. Process Representation	77
3.3.1. Direct runoff computation	77
3.3.1.1. Green-Ampt model	79
3.3.1.2. Estimating wetting front suction head	85
3.3.1.3. Computational scheme for Green-Ampt infiltration under variable rainfall	87
3.3.2. Evaporation.....	90
3.3.2.1. Surface Resistance	90
3.3.2.2. Data analysis: evaporation	92
3.3.2.3. Plotting surface resistance against soil piezometric head	104
3.3.2.4. Evaporation method used in this study: practical considerations	111
3.3.3. Percolation.....	112
3.3.4. Soil layer mass balance.....	113
3.3.4.1. Non-event mass balance for an individual time step	113
3.3.4.2. Event mass balance	114
3.3.5. Runoff transform method : “modClark”	118
3.3.6. Baseflow	122
3.3.6.1. Single linear reservoir model	122
3.3.6.2. Baseflow separation	123
3.3.7. Special considerations for the Little Washita	126
3.4. Summary	127

CHAPTER 4. COMPUTER IMPLEMENTATION	130
4.1. Collecting and reformatting input data	130
4.2. The ArcView Pre-Processor (AV-SWBMS)	131
4.2.1. Pre-processing for a one-layer model.....	133
4.2.2. Pre-processing for a two-layer model.....	138
4.3. The Visual Basic Hydrology Program (VB-SWBMS).....	141
4.4. Summary	144
 CHAPTER 5. ANALYSIS AND RESULTS.....	 145
5.1. Overview	145
5.2. Calibration and validation procedures	145
5.2.1. Calibration	147
5.2.2. Validation	147
5.3. Comparison of NEXRAD and Micronet rainfall	152
5.4. One-layer vs. two-layer model.....	163
5.4.1. Direct runoff	163
5.4.2. Baseflow	166
5.5. Horizontal soil variations	169
5.6. Sensitivity analysis.....	173
 CHAPTER 6. CONCLUSIONS AND RECOMMENDATIONS FOR FUTURE WORK	 177
6.1. Conclusions.....	177
6.2. Recommendations for future work	182
 APPENDICES	 184
A. Description of the AV-SWBMS and VB-SWBMS programs	185
B. Time series data processing programs.....	205

C. Description of files on the CD-ROM that was produced to archive the research presented in this dissertation.....	217
D. Table used to reclassify 719 STATSGO texture names into 12 basic USDA classes and the "other" category.....	222
REFERENCES.....	238
VITA	247

LIST OF TABLES

Table 3.1 List of data sources.	30
Table 3.2 Projection parameters.....	32
Table 3.3 Mean values and coefficients of variation for hydraulic parameters in the 12 basic USDA texture classes. A comparison of values reported by Rawls, Brakensiek, and Saxton (1982) and Carsel and Parrish (1988).	52
Table 3.4 Estimates for Green-Ampt wetting front suction head (h_f) for an initially dry soil.....	61
Table 3.5 Description of soil drainage classes specified in the STATSGO comp table.....	66
Table 3.6 Impervious percentages associated with selected land use classes.....	66
Table 3.7 Natural saturation values corresponding to the 12 USDA texture classes.	82
Table 4.1 Spatial data required to run AV-SWBMS	132
Table 4.2 Description ArcView pre-processing programs under the menu “SWBMS.”.....	135
Table 4.3 Description of menu items used to create input files for a two-layer model.	138
Table 4.4 Input files for VB-SWBMS	142
Table 4.5 Output files for VB-SWBMS.....	143
Table 5.1 Model parameters not specified from soils databases.....	151
Table 5.2 Comparison of storm rainfall totals between Micronet and NEXRAD data.	153
Table 5.3 Calibrated parameter values for NEXRAD and adjusted NEXRAD simulations.	157
Table 5.4 Statistics describing NEXRAD and adjusted NEXRAD calibration and validation runs.....	158
Table 5.5 Calibrated parameter values for the one-layer and two-layer models. .	163
Table 5.6 Statistics describing one-layer and two-layer calibration and validation runs.....	164

Table 5.7 Calibrated parameter values and validation statistics for the one-layer model with different levels of model resampling and different soil map inputs.	172
Table 5.8 Statistics for level 2, STATSGO and level 0, 30 m grid simulations on 5/7/97 - 5/24/97.....	173
Table A1 Suggested AV-SWBMS menu sequences for different modeling options..	190
Table A2. VB-SWBMS File Names.	191
Table B1: Procedure for processing NEXRAD StageIII data.....	215

LIST OF FIGURES

Figure 1.1 Conceptual illustration of three resampling options.....	5
Figure 1.2 Location reference for the Little Washita River watershed.....	9
Figure 2.1 Typical soil moisture extraction function (adapted from Shuttleworth, 1993)	20
Figure 3.1 Conceptual storage zone model schematic	28
Figure 3.2 Watersheds delineated from 100-m and 30-m digital elevation models respectively.	34
Figure 3.3 Flow length to the watershed outlet for the 30 m digital elevation model.	35
Figure 3.4 STATSGO and 30 m soils grid.....	39
Figure 3.5 Mapunit OK103 polygons.	40
Figure 3.6 Comparison of surface texture composition for the STATSGO soils map and the 30-m soils grid with (a) soils grouped into the 12 USDA texture classes and (b) loamy sand and sandy loam grouped together along with loam and silt loam.....	41
Figure 3.7 Relationships among the mapunit, comp, and layer table.	43
Figure 3.8. Example wetting and drying water retention curves for a loam soil with $h_b = 27.8$ and $\lambda = 0.56$	45
Figure 3.9 Mean porosity values for USDA texture classes with 1 standard deviation error bars.	55
Figure 3.10 Mean residual saturation values for USDA texture classes with 1 standard deviation error bars.....	56
Figure 3.11 Mean λ values for USDA texture classes with 1 standard deviation error bars.	57
Figure 3.12 Mean h_b values for USDA texture classes with 1 standard deviation error bars.	58
Figure 3.13 Rawls, Brakensiek, and Saxton h_b values on the USDA textural triangle.	59
Figure 3.14 Carsel and Parrish h_b values on the USDA textural triangle.	60

Figure 3.15 Percentage of soil components with 1, 2, 3, 4, 5, or 6 layers (a) with multiple distinguishing characteristics and (b) with the 12 basic USDA soil classes as the only distinguishing characteristic.	63
Figure 3.16 Total depth of the soil zone defined for the two-layer model.	67
Figure 3.17 Land use in the Little Washita watershed.....	68
Figure 3.18 Intersecting NEXRAD cells with watershed boundary.....	71
Figure 3.19 Locations for gravimetric soil moisture sampling during SGP97.	76
Figure 3.20 Locations of Micronet stations.	77
Figure 3.21 Average percent imperviousness in each NEXRAD cell.	79
Figure 3.22 Curved wetting front formed during infiltration into a homogeneous, uniformly wetted soil.	80
Figure 3.23 Idealized infiltration into a homogeneous, uniformly wetted soil with a sharp wetting front.	80
Figure 3.24 Relative permeability curve for wetting. ($\lambda = 0.56$, $h_b = 27.8$)	86
Figure 3.25 Pseudo-code for computation of Green-Ampt infiltration under variable rainfall.	89
Figure 3.26 Locations of 22 ARM Measurement Sites	95
Figure 3.27 Surface radiation budget components at ARM SGP Site EF7 on July 29, 1997.....	97
Figure 3.28 30 minute Bowen ratio values at the ARM SGP Site EF7 on July 29, 1997.....	98
Figure 3.29 Wind speed (m/s) at site EF7 on July 29, 1997.....	99
Figure 3.30 Temperature ($^{\circ}\text{C}$) and relative humidity (RH) at site EF7 on July 29, 1997.....	100
Figure 3.31 Vapor pressure deficit and vapor pressure at site EF7 on July 29, 1997.	100
Figure 3.32 Surface resistance (r_s) vs. $\ln(h+z)$ for EF7 at a depth of 5 cm (a) with regression line for all data points (b) with regression lines for individual months.....	103
Figure 3.33. Surface resistance (r_s) vs. $\ln(h+z)$ for EF7 at a depth of 15 cm (a) with regression line for all data points (b) with regression lines for individual months.....	106
Figure 3.34 Surface resistance (r_s) vs. $\ln(h+z)$ for EF7 at a depth of (a) 25 cm, (b) 35 cm, (c) 60 cm, (d) 85 cm, (e) 125 cm, and (f) 175 cm.....	108

Figure 3.35 A comparison of surface resistance (r_s) vs. $\ln(\psi+z)$ at two sites: EF7 and EF4.	110
Figure 3.36 Post-infiltration mass balance flow chart for the two-layer model. ...	117
Figure 3.37 Post-infiltration mass balance flow chart for the one-layer model....	118
Figure 3.38 Average flow length from each model polygon to the watershed outlet.	120
Figure 3.39 Baseflow separation method. (a) estimating baseflow at $t = 2$, (b) estimating baseflow at $t = 3$, and (c) estimating baseflow at $t = 4$	125
Figure 3.40 Baseflow separation using $n = 15, 30$, and 60 hours.	126
Figure 4.1 Screen capture of menus that are part of AV-SWBMS.....	133
Figure 4.2 Example input files for the one-layer model.	137
Figure 4.3 Example input files for the two-layer model.	140
Figure 4.4 Pseudo-code describing the overall computational sequence for VB-SWBMS.	142
Figure 5.1 A comparison of Micronet and NEXRAD Stage III rainfall estimates for 8 hours of the 7/10/97 storm.	156
Figure 5.2 Calibrated flows using (a) NEXRAD and (b) adjusted NEXRAD rainfall.	159
Figure 5.3 Validation runs using parameters from Table 5.3. (a) NEXRAD and (b) adjusted NEXRAD rainfall.	160
Figure 5.4 Comparison of modeled and observed average daily soil moisture for (a) a loamy sand in cell (557, 309) and observed data averaged from sites 3, 4, and 5; (b) a sandy loam in cell (559, 305) and observed data from site 17; (c) a loam in cell (560, 309) and observed data averaged from sites 11, 12, and 13; and (d) a silt loam in cell (555, 307) and observed data averaged from sites 8 and 9.	162
Figure 5.5 Flow during the validation period for the one-layer and two-layer models.	164
Figure 5.6 Attempts to simulate baseflow using the one-layer soil model. (a) recession constant $\chi = 240$ hours (b) recession constant $\chi = 17520$ hours...	168
Figure 5.7 Hydrographs from two-layer simulation with $\chi = 240$ hours and $p_2 = 0.0015$ cm/hour.	169

Figure 5.8 Comparison of direct runoff from watershed level resampling, STATSGO simulation with direct runoff from a no resampling, 30-m grid simulation for 5/7/97 - 5/24/97.	172
Figure 5.9 Tornado diagram showing deviations from the base case based on high and low parameter values.	175
Figure A1 Menus for AV-SWBMS.	185
Figure A2 SWBMS user interface for a one-layer model with no baseflow simulation.	194
Figure B1 Graphical User Interface for several data processing programs.	206

NOMENCLATURE

(Symbols are listed in alphabetical order with lower case letters first, followed by upper case letters, lower case Greek letters, and upper case Greek letters.)

Symbol	Description	Units
c_p	specific heat of moist air	$\text{J kg}^{-1} \text{ } ^\circ\text{C}^{-1}$
d	layer depth	cm
d_r	rooting depth	cm
e	vapor pressure	kPa
e_s	saturation vapor pressure	kPa
$f(\theta)$	soil moisture extraction function	
h	suction head	cm
h_b	air entry head (a.k.a. bubbling pressure head)	cm
h_c	estimated crop height	m
h_{we}	air exit head or water entry head	cm
h_f	wetting front suction head	cm
h_i	initial suction head	cm
h_p	ponding depth	cm
i	infiltration rate	cm hour^{-1}
k_f	hydraulic conductivity calibration factor	
k_{rw}	relative hydraulic conductivity	
l	latent heat of vaporization	J kg^{-1}
n	baseflow separation parameter	
p	percolation rate	cm hour^{-1}
q	Darcy flux	cm hour^{-1}
r	rainfall rate	cm hour^{-1}
r_a	aerodynamic resistance	s m^{-1}
r_s	surface resistance	s m^{-1}
r_{smin}	minimum surface resistance	s m^{-1}
t_p	time to ponding	hours
u_z	wind speed at height z	m s^{-1}
Z	elevation	cm
Z_e	height at which humidity measurements are made	m
Z_{om}	roughness height for momentum transfer	m
Z_{ov}	roughness height for turbulent transfer of water vapor	m
Z_u	height at which wind measurements	m

	are made	
CV	coefficient of variation	
D	vapor pressure deficit	kPa
E	actual evaporation	mm day ⁻¹
E _m	mass flux of water vapor	kg m ⁻² s ⁻¹
E _r	reference crop evaporation	mm day ⁻¹
FL _{avg}	average flowlength from a rainfall cell to the watershed outlet	m
FL _{max}	maximum flowlength from a rainfall cell to the watershed outlet	m
G	ground heat flux	W m ⁻²
GSM	gravimetric soil moisture	
H	sensible heat flux	W m ⁻²
I	cumulative infiltration	cm
I _p	cumulative infiltration at ponding time	cm
K _{ns}	saturated hydraulic conductivity at natural saturation	cm hour ⁻¹
K _s	saturated hydraulic conductivity	cm hour ⁻¹
LAI	leaf area index	
L _f	wetting front depth	cm
N	van Genuchten water retention parameter	
P	total percolation from a soil layer during a given time step	cm
P _a	atmospheric pressure	kPa
Q	flow	m ³ s ⁻¹
Q _o	observed flow	m ³ s ⁻¹
Q _s	simulated flow	m ³ s ⁻¹
Q ^d	direct runoff	m ³ s ⁻¹
Q ^{din}	direct runoff into the linear storage reservoir	m ³ s ⁻¹
Q ^{dout}	direct runoff out of the linear storage reservoir	m ³ s ⁻¹
R	modClark storage coefficient	hours
R _n	net radiation	W m ⁻²
RH	relative humidity	
S	groundwater storage	m ³
T	air temperature	°C
T _c	modClark time of concentration	hours
T _m	travel time from a rainfall cell to the watershed outlet	hours

α	van Genuchten water retention parameter	cm^{-1}
β	Bowen ratio	
χ	groundwater storage constant	hours
ε	layer root fraction	
ϕ	porosity	
γ	psychrometric constant	$\text{kPa } ^\circ\text{C}^{-1}$
κ_c	crop coefficient	
κ_{co}	potential crop coefficient	
λ	Brooks and Corey water retention parameter	
μ	mean	
θ	volumetric water content	
θ_{fc}	water content at field capacity	
θ_i	initial water content	
θ_{ns}	water content at natural saturation	
θ_r	residual water content	
θ_{wp}	water content at plant wilting point	
ρ_a	density of moist air	kg m^{-3}
ρ_b	bulk density	g cm^{-3}
ρ_w	density of water	g cm^{-3}
Δ	gradient of the saturation vapor pressure curve	$\text{kPa } ^\circ\text{C}^{-1}$
Θ	effective saturation	
Θ_d	drying phase effective saturation	
Θ_i	initial effective saturation	
Θ_{ns}	natural saturation	
Θ_w	wetting phase effective saturation	

CHAPTER 1. INTRODUCTION

1.1. Motivation

Traditionally, runoff simulation models have used lumped (watershed average) rainfall and infiltration parameter values. This approach has been practical because rain-gage networks are typically sparse and use of data from these gages does not justify a more detailed spatial model. Development of next generation radar (NEXRAD) products by the National Weather Service has made spatially distributed hydrologic modeling a more practical alternative. With gridded rainfall products, distributed or quasi-distributed methods for watershed modeling merit further investigation.

Researchers at the Hydrologic Engineering Center (HEC) of the U.S. Army Corps of Engineers are interested in enhancing the capabilities of their Hydrologic Modeling System (HMS) software to include capabilities for considering distributed soil properties. Geographic Information System (GIS) pre-processing software programs have recently been developed to implement a quasi-distributed runoff transform method called modClark in HMS (Peters and Easton, 1996; Reed and Maidment, 1995; HEC, 1995; HEC, 1996). This software is designed to work with NEXRAD data. Although this software makes it practical to transform rainfall excess from gridded rainfall cells to the watershed outlet, it has only limited capabilities for computing distributed loss rates. GIS programs are available to estimate the average Soil Conservation Service (SCS) curve number for each NEXRAD grid cell. Although knowing the spatial distribution of Curve Numbers is an improvement over using watershed average loss rate parameters, this is a rather unsatisfactory approach for dealing with losses when considering the many weaknesses of the SCS Curve Number method, particularly when it is used in an attempt to reproduce historical events — not the purpose for which it was originally developed (Goldman, 1989; Pilgrim and Cordery, 1993). In addition to problems

with the SCS Curve Number method noted by Goldman (1989) and Pilgrim and Cordery (1993), this method is ill suited for incorporation into a continuous soil-moisture accounting model which can be used to predict antecedent moisture conditions. Methods to continuously model soil-water content through time are important because rainfall excess is sensitive to antecedent moisture conditions (Pilgrim and Cordery, 1993; Coles *et al.*, 1997).

The focus of this manuscript is on the computation of rainfall excess using distributed soil parameters and distributed rainfall estimates. Use of distributed rainfall and soils data may help to alleviate some limitations of lumped continuous simulation modeling methods currently being tested at HEC. In simulations made using the Continuous Soil Moisture Accounting Model being developed for HEC-HMS, engineers have noticed that a model calibrated to large storms may predict no response for small storms (Peters, pers. com., 1998). Missing the small storms could perhaps be due to the inability of a lumped model to capture partial area effects or due to inaccurate estimation of antecedent soil moisture conditions. These issues are investigated in this research.

The ability of the soil to transmit and retain water influences the rate of runoff during a storm and the rate at which the soil dries out between storms. To model the water fluxes into and out of the soil on a continuous basis, physically based process representations are attractive — as opposed to strictly empirical methods like the SCS method. For an appropriately formulated soil-water balance model, parameters with a physical basis can be estimated using digital soils databases maintained by the U.S. Department of Agriculture (USDA). To date, the information in USDA soils databases like STATSGO (State Soil Geographic Database) and SSURGO (Soil Survey Geographic Database) has not been fully exploited by practicing hydrologists. This is due in part to the fact that practical schemes for using these data in soil-water balance and rainfall-runoff modeling are lacking. It would be

useful to be able to estimate parameter values that control infiltration, percolation, and evaporation using information from these databases.

Distributed rainfall data, digital soils data, and the computer software to easily manage these data sets are now available. The challenging task is to develop new methods to use these data and to determine the effectiveness of these new methods. To evaluate new methods, a common approach is to compare predicted and observed streamflows. Although the total runoff generated in a watershed can be compared with observed streamflow, it is often difficult to understand what is going on within the watershed. Just knowing the fraction of rainfall that does not become streamflow does not provide information about how much of this water is stored in the soil and groundwater and how much evaporates. New data sets from intensive hydrology field campaigns that are geared towards improving land surface and cloud parameterizations in General Circulation Models offer unprecedented soil moisture and meteorological measurements that may help to validate and parameterize soil-water balance models. Some of these data are used in this study.

The current investigation focuses on the soil-water balance component of streamflow simulation models because this is an area where currently available soils data and experimental observations have not been fully utilized.

1.2. Objectives and scope

The objectives of this study are:

- Develop a practical and automated method for using U.S. Department of Agriculture digital soils data in a rainfall-runoff model.
- Compare the performance of modeling alternatives that use different levels of spatial complexity.
- Quantify the uncertainties involved with the specification of soil hydraulic properties.

- Make recommendations to HEC regarding the use of spatial soils data in HEC-HMS.

To more specifically define the research scope, a summary of the modeling issues to be addressed is provided here.

Spatial complexity:

Because the rainfall intensity is assumed to be uniform within a NEXRAD cell, NEXRAD rainfall cell boundaries define the major units in which vertical flux calculations are made. A key issue addressed in this research is how to describe spatial soil variability. In the analysis of spatial data, resampling procedures are often used to simplify complex data sets. Some alternatives for resampling spatially complex soils data are considered here.

- No resampling: Estimate the percentage of each soil type or the percentage of each distinct soil component within each NEXRAD cell, and make vertical flux calculations separately for each of these units.
- NEXRAD cell level resampling: Assign a representative soil type to each NEXRAD cell.
- Watershed level resampling: Assign a representative soil type to the entire watershed (a lumped approach).

These three resampling options are illustrated in Figure 1.1. For each of these three resampling levels, modeling results may vary depending on the map scale of the soils data. The differences in simulation results obtained using 1:250,000 scale soil maps (STATSGO) and 1:24,000 scale soil maps (SSURGO) are considered. The map scale issue is of particular interest because 1:250,000 scale data are readily available for all of the United States, but 1:24,000 scale data are more difficult to obtain.

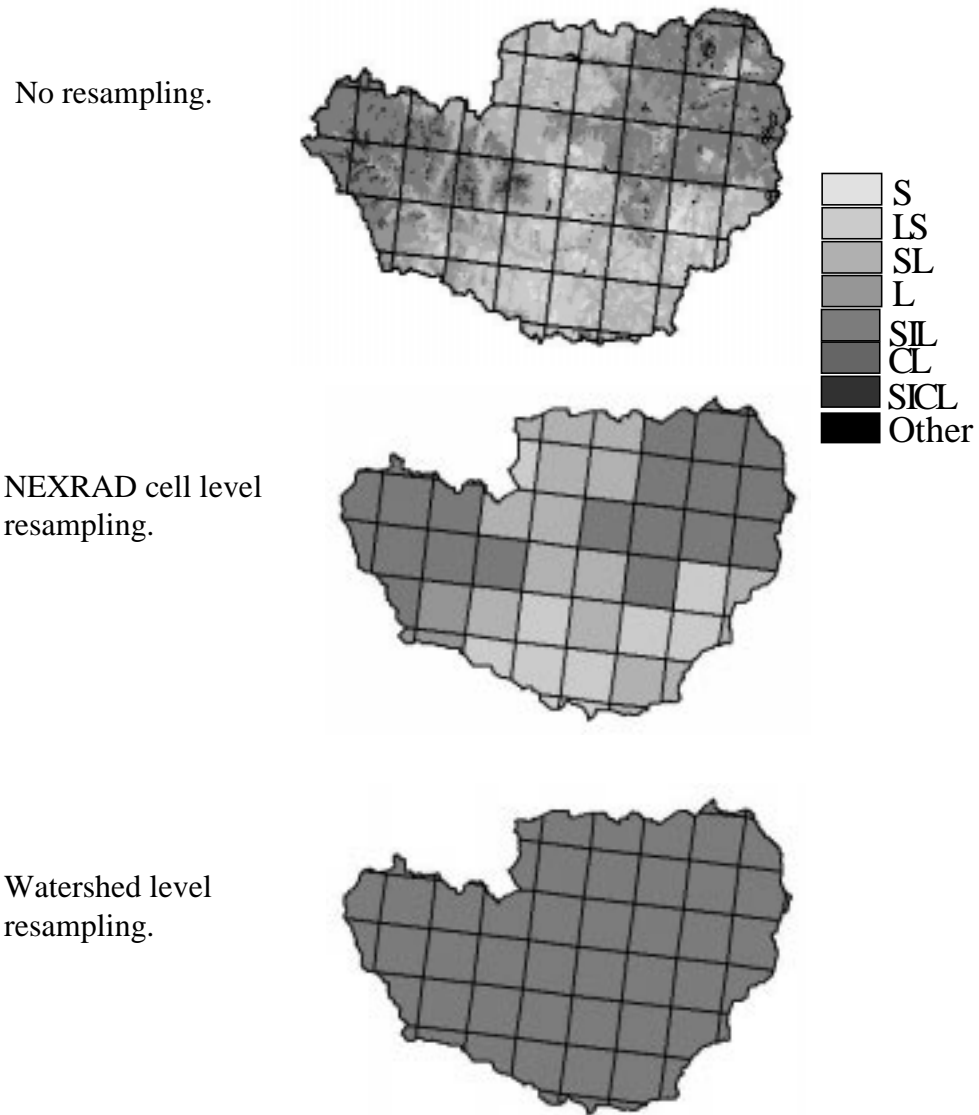


Figure 1.1 Conceptual illustration of three resampling options.

In addition to considering horizontal variations in soil properties, tradeoffs between parameterizing only near surface soils (one-layer model) and parameterizing both surface soils and a second soil layer (two-layer model) that restricts percolation to groundwater are investigated. Given the results of this investigation, a goal of this research is to assess whether further vertical partitioning is desirable and could be supported by the available data.

Parameterization:

A simple scheme for estimating soil hydraulic properties based on the texture attribute listed in standard soils data tables is proposed and implemented. In the two-layer model, other attributes in the soils data tables are considered to define the lower boundary for the soil zone.

Process representation:

The soil-water balance is computed by estimating infiltration, percolation, evaporation, and change in soil-water storage. A concerted effort is made to maintain an approximate physical basis for process representation whenever possible. Simple, straightforward equations (i.e. the Green-Ampt infiltration equation) for computing infiltration and percolation as a function of measurable soil properties and the current soil-water content are described in the literature. Relating evaporation rates to soil properties and soil-water content is more complex because evaporation is dependent on many factors in addition to soil characteristics. Methods used to estimate evaporation from soils range from very simple empirical methods (bucket models) to very complex soil-vapor-atmosphere transfer schemes (SVATS). An effort is made in this research to take advantage of newly available soil moisture and surface energy budget data in an effort to gain a greater understanding of soil drying rates due to evaporation. Using this data, the possibility of deriving empirical relationships that define effective daily values of evaporative surface resistance as a function of soil-water potential is investigated.

Computer implementation:

Using ArcView GIS and standard spatial data (i.e. STATSGO and 3" digital elevation models) model pre-processing routines are automated, making it easy to set up the model at any location in the United States. The ramifications of model

complexity on computer implementation are discussed, particularly with regard to the transfer of information from the GIS system to a hydrologic model like HEC-HMS.

Evaluation:

The accuracy of alternatives for describing spatial complexity is evaluated by comparing simulated runoff with observed runoff and simulated soil moisture with observed soil moisture.

1.3. Study area

The Little Washita River Watershed in southwestern Oklahoma was selected as the study area for this project for the following reasons:

- With a 600 km² drainage area, the Little Washita River basin is at the lower end of the size range for modeling units typical used by the U.S. Army Corps of Engineers and the National Weather Service for river basin forecasting.
- Archived Stage III NEXRAD Data, the most advanced National Weather Service weather radar product, is publicly available for this area from the Arkansas-Red Basin River Forecast Center.
- The state of Oklahoma is rich in meteorological and hydrological observations. Three research observation networks overlap in Oklahoma, including the Department of Energy's Atmospheric Radiation Measurement Program's Southern Great Plains Cloud and Radiation Testbed (DOE ARM SGP CART) (www.arm.gov), the Oklahoma Mesonet operated jointly by the University of Oklahoma and Oklahoma State University (okmesonet.ocs.ou.edu), and the U.S. Department of Agriculture Agricultural Research Service (USDA ARS) Micronet operated in the Little

Washita Watershed (grl.ars.usda.gov/sgp97-1.html). In addition to the high density of automated meteorological observations, a unique feature of these three observation programs is the large number of automated soil moisture observations that are being taken. More than 90 locations within a 10,000 km² area are now instrumented to produce profiles of soil-water and temperature (Schneider and Fisher, 1997). This network of 90 soil moisture measurement stations has been given the name MOISTNET (Schneider and Fisher, 1997). Not all of the MOISTNET data are available free of charge and some of the new equipment being used is still being calibrated. Therefore, only a small sampling of the data from the MOISTNET sites is analyzed in this study. Rain gage data from the Little Washita Micronet are compared with NEXRAD Stage III radar rainfall estimates in this study. Gravimetric soil moisture measurements taken in the Little Washita watershed during the Southern Great Plains 1997 Hydrology Experiment (daac.gsfc.nasa.gov/CAMPAIGN_DOCS/SGP97/sgp97.html) are also used for model calibration.

- County level (1:24,000 scale) soils are not generally available, but are available for the Little Washita watershed.

The location of the Little Washita River, a tributary of the Chickasha River is shown in Figure 1.2.

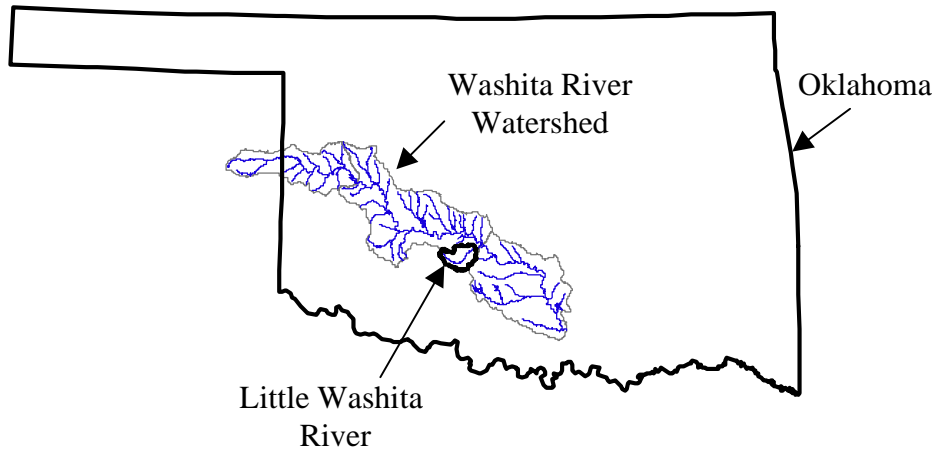


Figure 1.2 Location reference for the Little Washita River watershed

1.4. Organizational statement

The remainder of this dissertation includes:

- Chapter 2: A literature review.
- Chapter 3: A methodology chapter that includes a description of all input data, methods used to estimate model parameters using GIS software, and mathematical equations used to describe hydrologic processes.
- Chapter 4: A description of how the proposed model is implemented on a computer.
- Chapter 5: An analysis and results chapter that describes calibration and validation simulation runs and insights gained from these simulations related to the study objectives.
- Chapter 6: Conclusions and recommendations for future work.

The methodology chapter is the longest because a large amount of the research effort in this project has gone towards model development.

CHAPTER 2. LITERATURE REVIEW

This section includes a review of literature relevant to the stated objectives. Topics covered include a summary of runoff terminology, NEXRAD data, partial area effects, soil-water balance modeling, infiltration, evaporation, percolation, existing streamflow simulation programs, and GIS applications for hydrologic modeling. Additional references related to the infiltration, evaporation, and percolation models that have been selected for use in this study are provided in the Chapter 3. Chapter 3 also includes more information about the input data used in this research.

2.1. Surface and subsurface runoff: definition of terms

Streamflow prediction is a fundamental problem in hydrology that has been studied for many years. Streamflow produced from flow over the land surface is typically computed in a different manner than the flow that passes through the subsurface because different mechanisms control the volume and timing of surface and subsurface flows. Subsurface flow is produced when soil-water or groundwater discharges directly to a stream. Subsurface flow with a short-term response is often referred to as subsurface stormflow while flow that persists for long times after a rainfall event is often referred to as baseflow. The term direct runoff is used to refer to streamflow generated from water that does not infiltrate and flows over that land surface. Direct runoff may be generated if the rainfall rate exceeds the infiltration capacity of the soil (infiltration excess) or if the soil surface becomes saturated from below (saturation excess). The saturation excess mechanism for direct runoff generation tends to be more important in watersheds with humid climates, concave footslopes, and wide valley bottoms (Dunne, 1978). In arid and sub-humid climates and watersheds disturbed by human influence (i.e. agricultural watersheds), the infiltration excess runoff mechanism tends to dominate.

2.2. Lumped versus distributed modeling

2.2.1. NEXRAD Data

A hydrologic model commonly used by the National Weather Service, the Sacramento Soil Moisture Accounting Model (Burnash, Ferral, and McGuire, 1973), and a hydrologic model commonly used by the U.S. Army Corps of Engineers, HEC-1, are both lumped models in which rainfall is assumed to be uniform over an entire subwatershed. Lumped models are currently used by the 13 National Weather Service River Forecast Centers (RFCs) to provide daily discharge and stage forecasts at over 4,000 locations nationwide (Smith *et al.*, 1996b). The installation of a national network of radars (Weather Surveillance Radar 1988-Doppler (WSR88-D)) by the National Weather Service as part of the Next Generation Weather Radar (NEXRAD) program makes the move from lumped models to distributed models a real possibility. NEXRAD products provide precipitation estimates at higher spatial and temporal resolutions than have traditionally been available for hydrologic modeling. Better precipitation estimates offer the potential to improve streamflow forecasts, increase the number of river forecast points, and improve reservoir operations (Shedd and Fulton, 1993). Other applications for NEXRAD data include flash flood forecasting, long term water supply forecasting, climatology, and engineering hydrometeorology (Smith *et al.*, 1996b).

Several levels of NEXRAD processing have been developed for different uses. The lowest level NEXRAD product, Stage I, uses radar information alone to generate 1-hour rainfall estimates. In Stage II processing, rain gage data, satellite information, and surface temperature information are used to improve the radar estimates from Stage I. In Stage III, rainfall estimates from several radars are mosaicked into a common grid system at National Weather Service River Forecast Centers (RFCs) so that basin-wide stream flow forecasts can be made. Stage III also incorporates interactive quality control by the forecaster. Stage IV is a national

mosaic of hourly rainfall that uses both Stage II and Stage III data as input (Shedd and Fulton, 1993).

The accuracy of NEXRAD data products is still a matter of study. Smith *et al.* (1996a) provide a good discussion of errors associated with measurement of rainfall using WSR-88D radars based on a study of radar data from the Southern Great Plains of the United States. The conclusions of Smith *et al.* (1996a) include the following: (1) radar rainfall estimates are range-dependent with a tendency to produce low biased estimates at close (0-40 km) and far (beyond 150 km) ranges and higher estimates at intermediate ranges, (2) systematic differences in comparing signals from overlapping radars indicate that calibrations may be inconsistent among different radar sites, resulting in a 30% difference in average predicted rainfall in the example provided, (3) improvements in NEXRAD algorithms have eliminated a number of problems with anomalous propagation (high rainfall estimates due to high radar reflectivity from areas not receiving rainfall) but anomalous propagation is still problematic if embedded in actual precipitation, (4) a comparison between radar and gage estimates indicates that radar systematically underestimates rainfall, particularly at close and far ranges, and (5) despite the noted problems, WSR-88D radars are far superior to rain gage networks in monitoring heavy rainfall because it was found that a number of storm systems producing heavy rain were completely missed by gage networks. The NEXRAD Stage III estimates used in this study incorporate information from several overlapping radars and have been adjusted to reflect rain gage information; therefore, it is impossible to predict whether an underestimate or overestimate of rainfall would be expected based on the observations of Smith *et al.* (1996a). In a study of nine watersheds near the Oklahoma-Arkansas-Missouri state boundaries, Finnerty and Johnson (1997) found that 7-month mean areal rainfall accumulations computed from NEXRAD Stage III data were 10-25% lower than 7-month mean areal rainfall accumulations computed from rain gage data alone.

Both the National Weather Service Hydrologic Research Lab (HRL) and the U.S. Army Corps of Engineers Hydrologic Engineering Center (HEC) are currently researching methods to use NEXRAD data in hydrologic forecasting. As an intermediate step between existing lumped basin models and grid-cell level modeling, a “semi-distributed” modeling approach has been adopted by the Hydrologic Research Lab in which the basins in existing models are sub-divided into smaller sub-basins and mean areal precipitation estimates are computed for these basins using NEXRAD data (Smith *et al.*, 1996b). It is apparent from the research of Smith *et al.* (1996b) that the Sacramento Soil Moisture Accounting Model parameters that have been used in the past will require re-calibration if the semi-distributed modeling approach using NEXRAD data is used. As one might expect, Smith *et al.* (1996b) show that spatially averaging rainfall data over different size sub-basins produces notable differences (as high as a 600% difference in surface runoff in the example given) if model parameters remain unchanged. HEC has implemented a “quasi-distributed” cell-based model for using NEXRAD data in the HEC-Hydrologic Modeling System (HEC-HMS) software. Rainfall excess is computed for each NEXRAD cell and routed to the watershed outlet using an adaptation of the Clark unit hydrograph method called modClark (HEC, 1995; Peters and Easton, 1996). ModClark is “quasi-distributed” rather than distributed because there is no cell-to-cell flow routing.

2.2.2. Partial area effects

It is a well documented phenomenon that not all portions of a watershed contribute equally to direct runoff during a storm. This is due to both rainfall variability and land surface heterogeneity. Betson (1964) used the term *partial areas* to refer to this phenomenon. Betson (1964) did not observe large changes in the partial areas contributing to direct runoff among different storms on the same watershed, except during extreme conditions. A similar term, *variable source areas*

(Hewlett and Hibbert, 1965), refers more specifically to the expansion and contraction of saturated soil zones under different rainfall conditions, causing variations in saturation excess runoff generation.

A number of hydrologic models have been formulated so that the soil heterogeneities and/or spatially variable infiltration properties of a watershed are described using statistical distributions. In the Stanford watershed model and subsequent variations thereof, the infiltration capacity in a watershed at a given time is characterized by a simple probability distribution function (Hydrocomp, 1970). It is assumed that the infiltration capacity in a watershed can be described using a uniform distribution ranging from a minimum to a maximum infiltration capacity. This assumption has no physical basis but has proven to be effective in matching observed runoff (Hydrocomp, 1970; Dawdy, Lichty, and Bergman, 1972). This same scheme is used in the U.S. Geological Survey Precipitation Runoff Modeling System (PRMS) (Leavesley *et al.*, 1983). In a parameterization for a General Circulation Model, Entekhabi and Eagleson (1989) described the spatial variability of surface soil moisture using a probability distribution function that fits "well" with field observations of other researchers. Sivapalan and Wood (1986) and Wood *et al.* (1988) used a lognormal distribution to describe the spatial variability of saturated hydraulic conductivity for numerical experiments. Assumed distributions for soil properties or soil moisture are used to calculate the amount of runoff generated by infiltration excess and the amount of evaporation.

Researchers have also developed simplified ways to explicitly model direct runoff generated by the saturation excess mechanism. This is done by using topographic maps in conjunction with soil maps. Localized areas of soil saturation are predicted by effectively reducing the 3-dimensional watershed to two dimensions using a topographic wetness index. A topographic wetness index is derived by assuming that surface saturation will occur where the accumulated drainage flux exceeds the local transmissivity of the soil. A common assumption is

that a perched water table forms at some depth due to the presence of a low permeability layer and that surface saturation will occur when this water table rises to the surface. Beven and Kirkby (1979) and O'Loughlin (1981) were the first to describe the use of topographic wetness indices. A number of modelers have used variations on Beven and Kirkby's TOPMODEL (Beven, 1986; Sivapalan *et al.*, 1987; Famiglietti and Wood, 1994) and O'Loughlin's wetness index (O'Loughlin, 1986; Moore *et al.*, 1986; Moore *et al.*, 1988). The models of Beven (1986), Sivapalan *et al.* (1987), and Famiglietti and Wood (1994) explicitly account for both the infiltration excess and saturation excess mechanisms of runoff generation.

To a certain extent, field observations have validated the use of topographic index methods as an indicator of lateral soil moisture distributions (Anderson and Burt, 1977; Dunne, Moore, and Taylor, 1975; Zaslavsky and Sinai, 1981; and Burt and Butcher, 1985). Zaslavsky and Sinai (1981) observed higher soil-water contents in hollows when compared with spurs even in situations where no perched water table or impermeable layer existed. Zaslavsky and Sinai (1981) mathematically relate observed soil moisture to plan curvature. Burt and Butcher (1985) compare several different topographic indices with observed soil moisture (a/s , $\ln(a/s)$, plan curvature, etc.) and find that perhaps the best correlation with observed soil moisture results from the product plan curvature multiplied by (a/s) . In these expressions, a is the upslope drainage area and s is the local slope in percent. The analysis of Burt and Butcher (1985) was done on a 1.4 hectare hillslope. Based on their analysis alone, it is uncertain how well these topographic indexes would perform if computed using digital elevation models with relatively large cell sizes. In a 100-m digital elevation model, for example, each cell covers 0.01 km^2 so there would only be 1.4 cells in a 1.4 hectare area.

2.3. Soil-water balance modeling

A soil-water balance model is used to keep track of water content changes in the soil zone. Soil-water content is an important state variable that influences fluxes into and out of the soil zone (infiltration, evaporation, and percolation) and the energy balance at the land surface. Soil-water balance models treat the soil zone as a control volume. The control volume approach provides a consistent means for applying physical laws to hydrologic systems (Chow, Maidment, and Mays, 1988). Using this approach, direct runoff, evaporation, and percolation are treated as losses from the hydrologic system.

Thorough validation of soil-water balance models is typically only possible on small, well-instrumented plots of land where the fluxes across the soil zone boundaries are measured. On small plots, evaporation is often estimated by measuring rainfall or irrigation, changes in soil-water content, and sometimes percolation. Weighing lysimeters or neutron probes are typically used to measure changes in soil-water content (ASCE, 1990). Percolation may be measured with some types of lysimeters or assumed negligible if measurements are taken several days after irrigation (ASCE, 1990). Evaporation may also be measured using an energy balance approach like the Bowen ratio method or a mass transfer approach like eddy correlation. Descriptions of these methods are given by Brutsaert (1982) and Kanemasu *et al.* (1992). The Bowen ratio and eddy flux measurement techniques require extensive instrumentation so data of this type has typically been available only for short research studies (ASCE, 1990). Data from the Department of Energy's Atmospheric Radiation Measurement Program (ARM) (ARM, 1998; Peppler, Sisterson, and Lamb, 1997) provide unique data sets that might be helpful in validating water balance models. At some ARM measurement sites, Bowen ratio measurement systems are co-located with soil-water measurement systems. Schneider and Fisher (1997) note that the devices that are used to measure soil moisture at these sites are still (as of the publication date) undergoing calibration but

some interesting insights related to evaporation can be still be drawn from the available data sets as discussed in Section 3.3.2.

In the soil-water balance model described in this dissertation, changes in soil-water content are estimated by making an initial guess at soil-water content and then estimating infiltration, evaporation, and percolation fluxes using physically-based mathematical equations and climatic forcing data. To the extent possible, gravimetric measurements of soil-water content from the 1997 Southern Great Plains Hydrology Experiment are used to help calibrate the model (SGP, 1997).

2.4. Infiltration

Infiltration is the downward flow of water into the soil. Infiltration rates are controlled by soil properties and by the supply of moisture at the surface. Infiltration is one mechanism for “losses,” defined as the quantity of rainfall that does not contribute to direct runoff. Other loss mechanisms include interception, depression storage, and streambed losses.

It is often adequate to use simple, non-physical models such as an initial abstraction and constant loss rate model when calibrating an event simulation model with gaged data (Goldman, 1989); however, it is desirable to relate loss rates to physical characteristics of the watershed in continuous simulation so that loss rates may be computed as a function of soil moisture conditions at the beginning of a storm. In addition, a model with a physical basis may be suitable for application in ungaged areas. Approximate theory-based solutions to Richard’s equation like the Green-Ampt and Philip models and empirical loss models like Holtan’s method and the SCS Curve Number method have parameters that relate to measurable watershed characteristics. Reviews of these methods are provided by Rawls *et al.* (1993) and Goldman (1989). The Green-Ampt and Philip methods are more practical to apply than the Holtan method because simple relationships are available for deriving Green-Ampt and Philip parameters from water retention and relative hydraulic

conductivity parameters of a given soil (Neuman, 1976; Clapp and Hornberger, 1978). The SCS method is not considered as an option for the research described herein because it is not well-suited for incorporation into a continuous soil moisture simulation scheme and because it has a poor theoretical basis for time-varying calculations. In this research, the Green-Ampt model is selected over the Philip model because the Green-Ampt model has received more attention in the engineering literature, and the physical interpretation of Green-Ampt parameters is more straightforward.

The Green-Ampt model has performed well in laboratory studies (Mein and Larson, 1973; Rawls and Brakensiek, 1985), but uncertainty remains as to its performance under field conditions with variable rainfall rates and heterogeneous soil conditions. A scheme for using the Green-Ampt model with variable rainfall rates and heterogeneous soil conditions is proposed here. Use of a simplified model like the Green-Ampt model is justified when field data describing soil hydraulic properties show large spatial variability, which is often the case (Govindaraju *et al.*, 1992).

2.5. Evaporation

Following the convention used by Shuttleworth (1993) the term evaporation in this document refers to the “rate of liquid water transformation to vapor from open water, bare soil, or vegetation with soil beneath.” Major factors that govern the rate of evaporation from open water include the energy available at the surface and the vapor pressure deficit. Evaporation from bare soil is more complex because it also depends on soil-water content and soil type. Evaporation from plants is even more complex because plant stomata open and close to control the release of water vapor. Thus, the evaporation rate from plants is a function of the stomatal density and the degree to which stomata are opened. Guard cells on plant leaves may vary the size of stomatal openings as a function of the amount of sunlight, the CO₂ concentration,

the leaf-air vapor pressure gradient, the leaf temperature, and the leaf water content (soil-water content can be used as a surrogate for leaf water content) (Dingman, 1994). Modeling evaporation is further complicated because many of the factors that influence evaporation vary significantly throughout the day and it is often the case that only daily observations of meteorological variables are available.

Evaporation research has been conducted by investigators in many different scientific and engineering disciplines with different purposes. Agricultural and civil engineers are interested in estimating irrigation requirements and evaporation rates from surface water impoundments while climatologists and atmospheric scientists are interested in the relationships between evaporation and regional and/or global climate. Perhaps the most rigorous evaporation models have been developed for use with General Circulation Models (GCM) — biophysically “realistic” models developed by Dickinson (1984) and Sellers *et al.* (1986) consider diurnal variations in heat and vapor fluxes and complex feedbacks between plant growth, momentum transfer, and the surface energy balance. In these models, truly interdependent parameters such as albedo, roughness length, and soil moisture are not prescribed independently as is often the case (Sellers, 1992). In engineering practice, such biophysically realistic models are generally considered too complex to be practical — parameters can often be determined only through numerical experiments and the detailed meteorological inputs required are not generally available (outside of a GCM).

Shuttleworth (1993) and ASCE (1990) provide thorough reviews of common methods for estimating evaporation in engineering applications. A widely accepted approach for estimating evaporation from irrigated field crops is to first estimate the so-called reference crop evaporation (E_r) [mm day^{-1}] and then multiply this by an empirical crop coefficient (κ_c) which depends on the crop type, stage of development, and to some degree on the average climate where the empirical calibration was carried out. The crop coefficient also depends on the dryness of the

soil when the calibration was carried out. A slightly different crop coefficient is defined for conditions when the water supply is adequate so that plant growth is not limited (κ_{co}). Under conditions when soil moisture becomes a significant limiting factor on evaporation, empirical studies have been made to determine the relationship between the ratio of actual evaporation (E) to reference crop evaporation (E_r) and soil-water content. Dyck (1983), Shuttleworth (1993), and Brutsaert (1982) summarize the work of several researchers who have plotted empirical relationships between soil-water content (θ) and the evaporation ratio (E/E_r). Although the precise relationship between θ and E/E_r varies under different conditions, Shuttleworth (1993) notes that the results of many investigators follow the general trend shown in Figure 2.1.

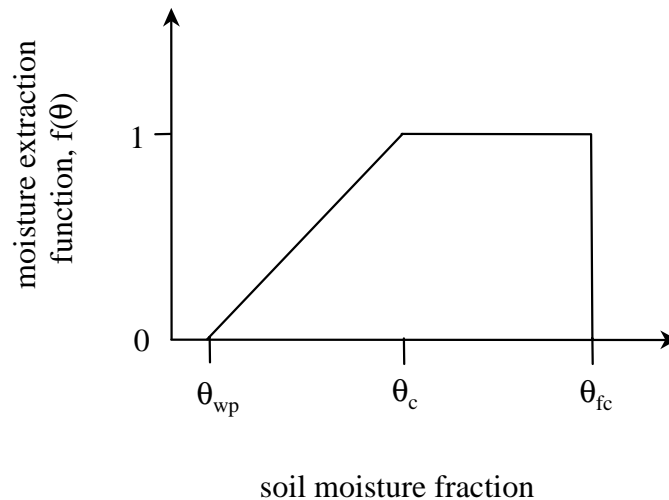


Figure 2.1 Typical soil moisture extraction function (adapted from Shuttleworth, 1993)

In Figure 2.1, θ_{wp} is the wilting point and θ_{fc} is the field capacity. According to the relationship in Figure 2.1, drying proceeds unrestricted by soil-water content until a critical level (θ_c) is reached. At this point, the evaporation rate decreases until the wilting point is reached and the evaporation becomes zero. θ_c is typically 50 to 80

% of θ_{fc} . Using this type of relationship, the evaporation from a vegetated surface is estimated as:

$$\text{Equation 2.1 } E = f(\theta)\kappa_{co}E_r \quad [\text{mm day}^{-1}]$$

The amount of water accessible to plants for evaporation depends on the rooting depth, which varies with location and season. When a soil root zone is divided into multiple layers, one approach to estimating evaporation from each layer is to take layer evaporation as the product of E_r , the fraction of roots in that layer, and $f(\theta)$ (Shuttleworth, 1993). This approach is discussed further in Section 3.3.2.

Part of the reason for the variability found in the literature for plots like that shown in Figure 2.1 may be that the true relationship is dependent on soil type, which makes sense because, as noted by Shuttleworth (1993), plants are more sensitive to suction head (h) than soil-water content (θ) and the relationship between θ and h varies for different soils. Zahner (1967) used different $f(\theta)$ relationships for sand, loam, and clay while making soil-water balance calculations. The relationships proposed by Zahner (1967) are also used in the USGS PRMS model (Leavesley *et al.*, 1983).

The method of Equation 2.1 is attractive because of its simplicity. For practical application with agricultural crops, empirical κ_{co} factors for different stages in the plant growth cycle are tabulated for different crop types and different climates (Doorenbos and Pruitt, 1977; Shuttleworth, 1993). However, Shuttleworth (1993) points out that the crop coefficient κ_c is poorly defined and has implicit meteorological dependence (the same point would apply to κ_{co}). Shuttleworth (1993) also recommends that future research projects into plant control on evaporation should attempt to estimate and document a purer measure of stomatal control, surface resistance (r_s), rather than the crop coefficient (κ_c). An empirical study that attempts to relate a daily average surface resistance (r_s) to soil-water

matric potential is presented in Section 3.3.2. This approach is investigated as a possible alternative to using Equation 2.1.

2.6. Percolation

Kinematic models for the redistribution and percolation of infiltrated water are discussed by Jury, Gardner, and Gardner (1991) and Charbeneau (1989). A simple kinematic model for percolation is used in this study, as described in Section 3.3.3.

2.7. Existing streamflow simulation modeling programs

This section is not intended to be an exhaustive review of existing streamflow simulation programs. Reviews of well-known hydrologic simulation programs are provided by DeVries and Hromadka (1993), Francini and Pacciani (1991) and McFadden (1994). None of the programs described in these reviews includes the capability to use digital soil maps to automatically estimate soil hydraulic properties or the capability to use distributed radar rainfall estimates. Francini and Pacciani (1991) compare the predictive capabilities of seven conceptual storage models (Stanford, Sacramento, TANK, APIC, SSARR, Xinanjiang, and Arno). Francini and Pacciani conclude that all of these models (with the exception of APIC) produce “similar and equally valid results.” Therefore, the most attractive models are those that are easy to calibrate, require few parameters, and consider the physics of the problem (Francini and Pacciani, 1991). The model described in this dissertation meets all of these criteria.

Streamflow simulation models are often calibrated and validated using observed streamflow data. Models with a large number of parameters are often difficult to calibrate. In models with many parameters, more than one parameter can have a similar effect on the predicted hydrograph. In these cases, one approach to calibration is to isolate times in the hydrologic record when a certain parameter

has the most effect (USACE, 1994). It takes a minimum of 5 to 8 years of hydrologic data to properly calibrate the Sacramento model used by the National Weather Service (Smith *et al.*, 1996b). Estimating some model parameters directly from physical watershed characteristics simplifies calibration procedures.

2.8. GIS and Hydrologic Modeling

Geographic Information System (GIS) software programs provide tools for storing, analyzing, and visualizing geographical and related tabular data. Different data structures are used in a GIS to store different types of data. Three of the most common data structures are (1) the vector data structure, which uses points, lines, and polygons to represent features in two dimensions, (2) the raster data structure which uses a regular grid of cells to represent continuous surfaces and categorical data, and (3) triangulated irregular networks (TINs) which are used to model 3-dimensional surfaces. The GIS programs described in this dissertation use the ArcView 3.0a GIS with its Spatial Analyst 1.1 extension to manipulate vector and raster data describing topography, soils, land use, and rainfall cells. The Avenue script language is used to manipulate objects in ArcView and automatically prepare an input file for hydrologic calculations. Previous work on preparing input data for streamflow models is discussed briefly in this section. Many other hydrology related GIS applications are not discussed. A review of some other hydrology related applications is provided on the GISHydro98 CD-ROM (CRWR-ESRI, 1998).

2.8.1. Terrain analysis

Digital terrain models are widely used in hydrology. A digital terrain model is an ordered array of elevation values, commonly stored in one of three data structures: contours, grids, or triangulated irregular networks (TINs). Moore, Grayson, and Ladson (1991) review the advantages and disadvantages of each of

these three data structures. Grid terrain models are attractive because they are widely available, terrain analysis methods with the grid model are simple, and the grid structure is compatible with remote sensing techniques. A grid terrain model consists of regularly spaced elevation values in two dimensions. The term adopted by the USGS to describe digital terrain data in a grid format is digital elevation model (DEM).

A basic task that can be accomplished easily with GIS software is the delineation of drainage paths and watershed boundaries from a digital elevation model. Other hydrologic parameters that can be estimated from a digital elevation model include drainage area, slope, aspect, and flow path length. A more exhaustive list of topographically derived attributes is provided by Moore, Grayson, and Ladson (1991). A simple and widely used method for approximating cell-to-cell flow paths and delineating drainage areas from a digital elevation model is described by O'Callaghan and Mark (1984) and Jensen and Domingue (1988). Both the Arc/Info and the ArcView 3.0 with the Spatial Analyst software packages contain built in functions for terrain analysis and watershed delineation based on the algorithms described by Jensen and Domingue (1988). Maidment and Mizgalewicz (1993) and Reed and Maidment (1995) describe Arc/Info procedures for watershed delineation. The ArcView GUI offers a more convenient user interface to do the same types of analysis. Customized ArcView programs for watershed and stream network delineation are briefly summarized in the introduction section of Olivera, Reed, and Maidment (1998).

2.8.2. GIS preprocessors for hydrology models

Customized tools for hydrologic modeling have been developed to pass information from GIS databases to widely used engineering hydrology models. Programs described by Hellweger (1997) with modifications described by Olivera, Reed, and Maidment (1998) are capable of preparing a basin file for the Hydrologic

Modeling System (HMS). This basin file contains enough information for HMS to automatically create a schematic network for lumped hydrologic modeling. Reaches and watersheds in this model are automatically attributed with parameters derived from the topography, soil, and land use data layers. Arc/Info GIS software programs that can be used to prepare a cell parameter file for HEC's quasi-distributed modClark routing program (a component of HMS) are described by Reed and Maidment (1995) and HEC (1996). The Watershed Modeling System developed at the Brigham Young University Engineering Computer Graphics Laboratory has the capability to use GIS data in preparing an input file for the HEC-1 hydrology model and other models used for hydrologic and hydraulic design (WMS, 1998).

2.8.3. Use of soils data

In this dissertation, a systematic approach is proposed to estimate hydrologic soil properties from standard soils data distributed and maintained by the U.S. Department of Agriculture. In previous work, Miller and White (1998) have developed a 1 km grid with multi-layer hydrologic soil characteristics for the conterminous United States by interpreting and processing information in the USDA STATSGO database. In attempting to develop a generic gridded database intended for applications such as soil-vegetation atmosphere transfer schemes (SVAT), climatology, and other environmental models, Miller and White (1998) were forced to make numerous assumptions in the interpretation of STATSGO data. Although different assumptions are preferred for the current work, the work of Miller and White (1998) is similar to the present study in the sense that both are geared towards making soil information more accessible to hydrologic modelers.

Additional references describing spatial data sources (topography, soils, and land use) and procedures for processing and interpreting these data are provided in Chapter 3.

2.9. Summary

Distributed rainfall estimates from NEXRAD products offer the potential to improve streamflow prediction models. Traditional, lumped approaches to hydrologic modeling need to be adapted in order to fully utilize the spatial information provided by NEXRAD products. Efforts to use distributed rainfall estimates in operational models have been initiated by the U.S. Army Corps of Engineers Hydrologic Engineering Center (HEC) and the National Weather Service Hydrologic Research Lab (HRL). Geographic Information Systems provide useful tools for implementing distributed modeling schemes.

Existing distributed modeling schemes lack the ability to describe spatially variable loss rates. Digital soil maps (STATSGO and SSURGO) maintained by the U.S. Department of Agriculture contain spatial information that may be used along with distributed rainfall to estimate distributed loss rates. Research is needed to develop and evaluate practical methods for using these soil maps in operational hydrology models. The remaining chapters of this dissertation address this issue.

Loss rates depend on the wetness of the soil at the beginning of a storm. A continuous soil-water balance model can be used to model the changes in soil-water content due to infiltration, evaporation and percolation. Because field data describing soil properties show large spatial variability, it is believed that the use of simple process models, like the Green-Ampt infiltration equation, is justified. The parameters for simple flow models can be estimated using information in the STATSGO and SSURGO databases. A method to parameterize simple infiltration, evaporation, and percolation equations is proposed in Chapter 3.

CHAPTER 3. METHODOLOGY

3.1. Overview

This section describes a conceptual model, input data, data interpretation methods, and model equations. The conceptual model and model equations are specifically chosen to maintain a physical basis when practical, use methods that are well supported by previous studies, require a small number of calibration parameters, and be practical to apply using spatial rainfall and soils data. In terms of input data and data processing, the most emphasis is placed on the estimation of soil hydraulic properties; however, all of the input data sets are described in some detail in Section 3.2.

A diagram illustrating the proposed conceptual storage zone model is shown in Figure 3.1. Well-known streamflow simulation models like the USGS Precipitation Runoff Modeling System (Dawdy, Lichty, and Bergmann, 1972; Leavesley *et al.*, 1983), the Sacramento model (Burnash, Ferral, and McGuire, 1973), and the Streamflow Synthesis and Reservoir Regulation Model (USACE, 1994) all contain components similar to those shown in Figure 3.1. All of these models are more complex, dealing with additional factors such as snowmelt, interception and depression storage, and explicitly estimating interflow, but the fundamental approach is the same. The surface and subsurface are divided into zones in which the storage and movement of water are controlled by different factors. Equations are formulated to describe the movement of water into and out of these zones and mass balance equations are used to keep track of the water stored in each zone. Forcing data, including rainfall and other meteorological variables used to estimate evaporation, are used to drive the model.

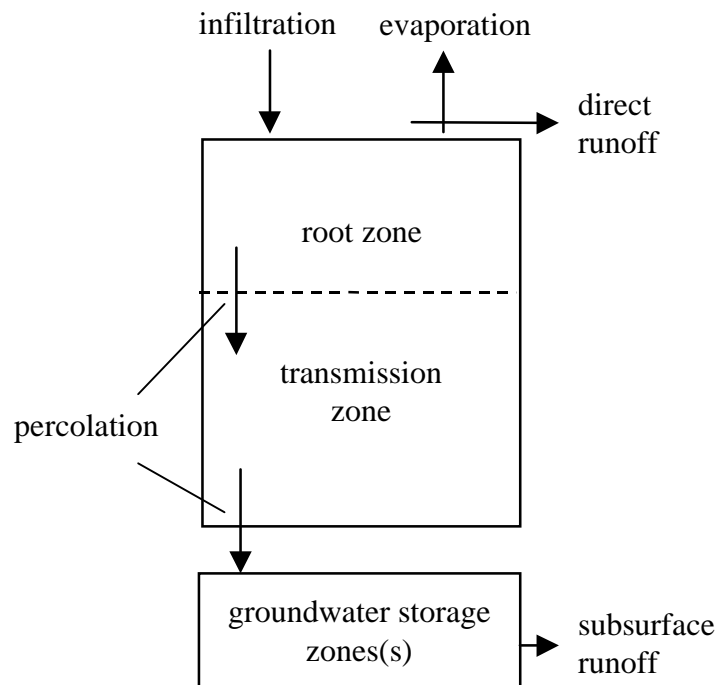


Figure 3.1 Conceptual storage zone model schematic

The simplified conceptual model in Figure 3.1 is used in this research because the emphasis here is on developing and testing parameterizations for the soil zone. Infiltration, evaporation, and percolation estimates are point calculations. Different soil properties in different parts of a watershed will result in different amounts of excess runoff when subjected to the same amount of rainfall. The routing of excess runoff from different points in the watershed to the watershed outlet depends on overland flow velocity and storage effects. These effects are approximated using the modClark method (see Section 3.3.5). Although the spatial variability of soil properties within a watershed are considered in this model, the subsurface response is modeled as a function of a single lumped parameter. Two alternatives for determining baseflow are used in this research, simulating baseflow with a simple linear reservoir model and applying a baseflow separation technique to observed flow data. Reasons for using these two baseflow approaches are discussed in Section 3.3.6.

In this research, all spatial analysis tasks are automated using ArcView GIS and all hydrologic calculations are done using Visual Basic. Computer implementation and data management are discussed further in Chapter 4.

3.2. Data description

A summary of data used in this research is provided in Table 3.1. Not all of the data sources listed in Table 3.1 are required to run a simulation. Required inputs include a digital elevation model, a soil map (STATSGO or SSURGO), a land use map that uses the Anderson Level II classification scheme, rainfall data and an associated map of rainfall cells, and enough meteorological data to make an estimate of reference crop evaporation. The meteorological variables required to estimate reference crop evaporation depend on the estimation method used. In this research, the Penman-Monteith reference crop equation is used, requiring estimates of available heating, temperature, relative humidity, atmospheric pressure, and wind speed; however, a program user may compute reference crop evaporation using any method and store these values in a model input file. The model operates using a nominal time step of one hour because this is the time interval for which NEXRAD rainfall data are available. All of the required inputs for this model are relatively easy to obtain. Other data sets listed in Table 3.1 that are used for calibration and validation are unique to the Southern Great Plains region and/or the Little Washita River watershed.

Table 3.1 List of data sources.

Category	Description	Map Scale	Source of Information	Method of Acquisition	Dates for Which Data was Obtained
Topography	30 m digital elevation model	~ 1:24,000	ARS-GRL, El Reno, OK grl.ars.usda.gov	Personal request	
	3" (~100 m) digital elevation model	1:250,000	USGS EROS Data Center. edcwww.cr.usgs.gov/webgis	Internet download	
Soils	STATSGO for Oklahoma	1:250,000	USDA NRCS, www.ftw.nrcs.usda.gov/soi	Internet download	
	30 m soils grid – SSURGO level of spatial detail; attribute tables are structured similarly to STATSGO.	~ 1:24,000	ARS-GRL, El Reno, OK grl.ars.usda.gov	Personal request	
Land Use/Land Cover	GIRAS Landuse/Landcover files w/ Anderson Level II land use classification scheme.	1:250,000	EPA. www.epa.gov/ngispgm3/ns	Internet download	
	NWS NEXRAD Stage III data: hourly estimates of precipitation on grid cells approximately 4 km on a side.		NWS Arkansas-Red Basin River Forecast Center. info.abrfc.noaa.gov	Internet download	The archived product is available June 24, 1994 – present. Data was obtained for October 1995 – September 1997
Meteorological Data	Micronet: 5-minute cumulative rainfall estimates from 42 gages in and around the Little Washita watershed. Used to check the NEXRAD data.		ARS-GRL, El Reno, OK. grl.ars.usda.gov/sgp97-1.html	Internet download	June, July, and August, 1997 * many of the data for early and mid-June are missing

Table 3.1 (cont.)

Category	Description	Map Scale	Source of Information	Method of Acquisition	Dates for Which Data was Obtained
Meteorological Data (cont.)	DOE ARM SGP-CART: 30 minute Energy Budget Bowen Ratio (EBBR) data stream; data from site EF26 used to estimate potential evaporation for simulations in the Little Washita, data from sites EF4 and EF7 used for evaporation study (see Section 3.3.2).		DOE-ARM. www.archive.arm.gov/data/ordering.html	Internet download	EF26: October 1995 – September 1997; EF4: May, June, July, 1997; EF7: June, July, August, September, 1997.
	DOE ARM SGP-CART: 30 minute Surface Meteorological Observation System (SMOS) data stream; data from sites EF4 and EF7 used for evaporation study (see Section 3.3.2).		DOE-ARM. www.archive.arm.gov/data/ordering.html	Internet download	EF4: May, June, July, 1997; EF7: June, July, August, September, 1997.
Streamflow	15 minute flow data for USGS gaging station on Little Washita R. East of East Ninnekah, OK, 07327550.		Oklahoma USGS	Personal request	October 1995 – October 1997.
Observed Soil Moisture	DOE ARM SGP-CART: 30 minute Soil Water and Temperature Systems (SWATS) data stream; matric potential data from sites EF4 and EF7 used for evaporation study (see Section 3.3.2).		DOE-ARM. www.archive.arm.gov/data/ordering.html	Internet download	EF4: May, June, July, 1997; EF7: June, July, August, September, 1997.
	Southern Great Plains Hydrology Experiment 1997, SGP '97. Twice daily gravimetric soil moisture measurements.		USDA/NASA, daac.gsfc.nasa.gov/CAMP AIGN_DOCS/SGP97/grav i_moist.html	Internet download	June 18 – July 16, 1997.

In order to use spatial data from different sources in conjunction with one another, each data layer must be transformed into a common map projection. The map projection used in this study is the same map projection used in USGS Open-File Report 95-727 for watershed and elevation maps of Oklahoma. The parameters for this projection are given in Table 3.2.

Table 3.2 Projection parameters

Projection	Albers Equal Area Conic
Datum	NAD83
Units	Meters
Spheroid	GRS1980
Xshift	0
Yshift	0
1st standard parallel	34.0
2nd standard parallel	36.5
Central meridian	-98.0
Latitude of projection's origin	33.0
False easting (meters)	0
False northing (meters)	0

3.2.1. Topographic data

Digital elevation models derived from map sources at two different scales are used in this study. A 3-arc-second digital elevation model was obtained from the U.S. Geological Survey. The horizontal and vertical spacing between elevation values in this data set is 3-arc-seconds, hence the name. 3 arc-second spacing is equivalent to 92 meters at the Equator. The earth distance between elevation values along parallels of latitude decreases with increasing latitude, but the earth distance between elevation values along meridians of longitude changes very little. The 3-arc-second data are projected and resampled to a 100-m grid for use in this study.

The map scale associated with these 3-arc-second data is 1:250,000 because the data were derived from topographic information on maps of this scale.

A 30-meter digital elevation model was obtained from the Agricultural Research Service Grazinglands Research Laboratory in El Reno, Oklahoma. The map scale associated with the 30-m digital elevation model is 1:24,000.

The area draining to the streamflow gage of interest, USGS 07327550 East of Ninnekah, Oklahoma was delineated using each of the two digital elevation models. Procedures for watershed delineation using Arc/Info and ArcView are reviewed in the Watershed Characterization Module of GISHydro '98 (CRWR-ESRI, 1998). The watershed delineation method used in these programs requires that an integer flow direction value be assigned to each grid cell, indicating to which of its eight neighboring cells water will flow. Flow from a given cell must go to one and only one of its neighboring cells. This flow direction model is sometimes referred to as the D8 or eight-direction pour-point model. All cells draining to a selected outlet cell can be determined using the flow direction grid, thus defining the watershed for that outlet. Also using the grid of flow directions, the path from each cell to the watershed outlet cell can be traced, allowing the approximate flow length to the watershed outlet to be determined for each grid cell. Diagrams illustrating grid-based flow direction and flow length calculations are provided in the online documentation for Arc/Info and ArcView software.

Watersheds delineated from the 100-m and 30-m elevation grids are illustrated in Figure 3.2. The areas delineated using the two different terrain models are 597.0 km² (59,700 cells) for the 100-m grid and 600.1 km² (666,778 cells) for the 30-m grid. The flow path traced from a selected cell (A) in the watershed to the outlet (B) is also shown in Figure 3.2. The average flow length from this point to the watershed outlet is 31,155 m using the 100-m grid and 31,444 m using the 30-m grid. A map showing the flow length from each cell in the 30-m grid to the

watershed outlet is shown in Figure 3.3. The way in which flow length values are used in runoff transform calculations is discussed in Section 3.3.5.

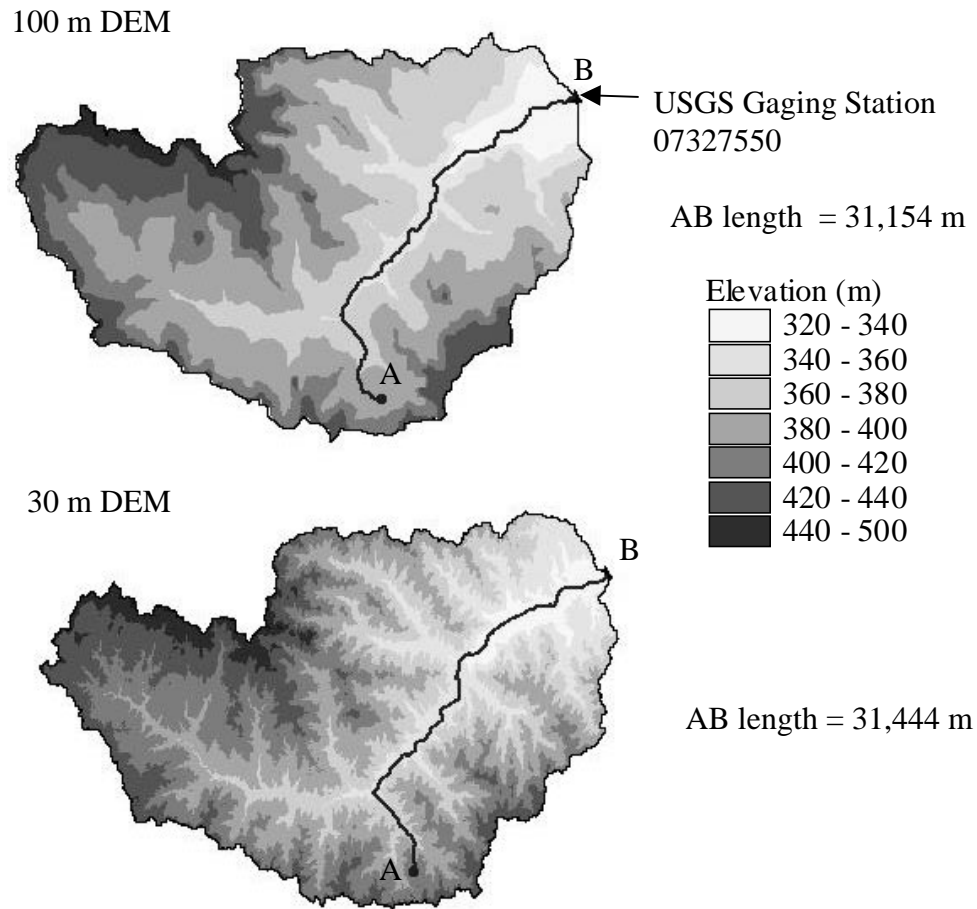


Figure 3.2 Watersheds delineated from 100-m and 30-m digital elevation models respectively.

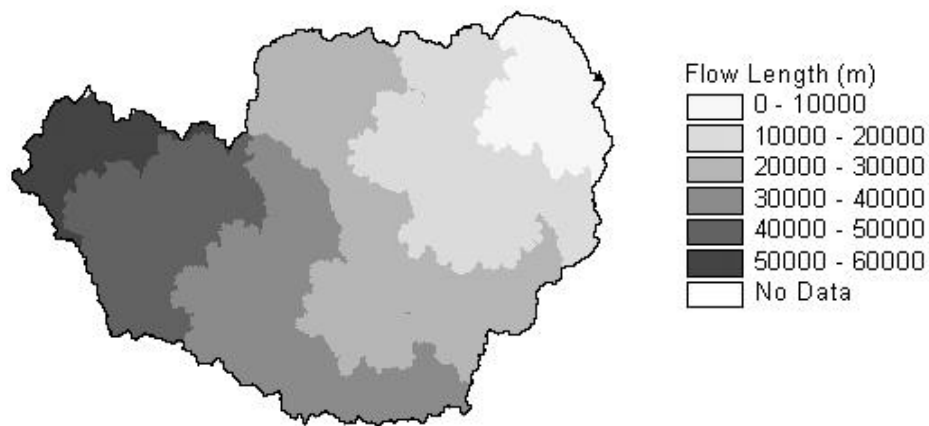


Figure 3.3 Flow length to the watershed outlet for the 30 m digital elevation model.

3.2.2. Soils Data

3.2.2.1. STATSGO vs. SSURGO

Two soils databases maintained by the United States Department of Agriculture are of interest in this study, the Soil Survey Geographic (SSURGO) database and the State Soil Geographic (STATSGO) database. The SSURGO database contains a greater level of spatial detail than STATSGO. SSURGO maps are created using field methods at scales ranging from 1:12,000 to 1:63,360, and are designed primarily for landowner, township, and county level natural resources planning and management (USDA, 1995). STATSGO maps are created either by generalizing more detailed soil maps such as SSURGO or by assimilating data on geology, topography, vegetation, and climate and deducing the probable classification and extent of various soil types. With the exception of Alaska, the STATSGO data are mapped at 1:250,000 scale. STATSGO data are designed primarily for regional, river basin, state, and multi-state level planning (USDA, 1994).

Both STATSGO and SSURGO maps are divided into map units. “A map unit is a collection of areas defined and named the same in terms of their soil components or miscellaneous areas or both.” (USDA, 1993) A soil component is typically associated with a single soil series phase (USDA, 1994). A soil series

consists of soils with similar properties. Miscellaneous areas are areas that have little or no soil such as a rock outcrop. Rock outcrop areas are listed as separate components in the STATSGO attribute tables.

The attribute database associated with STATSGO and SSURGO includes a description of the physical and chemical properties of 18,000 soil series in the United States. Soil series are differentiated primarily by the kind and character of soil properties and the arrangement of horizons within the profile. Soil series are the most homogeneous classification category used for soils in the United States (USDA, 1993). Since map components are commonly associated with a single soil series phase, map components are also relatively homogeneous. However, even map units that only contain a single component are likely to contain some inclusions. Map units are typically designed so that inclusions for which use and management might differ constitute less than 15% of the map unit area.

There is a distinct difference between the amount of spatial detail provided in the STATSGO and SSURGO databases. STATSGO map units may consist of anywhere from 1 to 21 components for which the spatial delineations are not shown, while SSURGO map units most commonly contain only 1 component but may contain up to 3 components (for which the spatial delineations are not shown). STATSGO map units may consist of one or more non-contiguous polygons while map units in SSURGO consist of a single polygon. The location of individual components within map unit polygons is not shown on the map.

Currently, STATSGO data files for any of the 50 United States are readily available from the USDA Natural Resource Conservation Service (NRCS). The availability of SSURGO data is much more limited. Information about the current status of SSURGO data is provided on the NRCS World Wide Web page for soils (www.ftw.nrcs.usda.gov/soils_data.html). As of July 1, 1998, certified SSURGO data files were only available for 2 counties in Oklahoma and 17 counties in Texas. In some areas, the availability of SSURGO data is increasing. In the past year, the

number of counties for which data is available in Texas increased from 5 to 17. The USDA Natural Resources Conservation Service (NRCS) is proposing to digitize 150 county soil surveys in Texas and share costs through the Strategic Mapping Initiative (www.tnris.state.tx.us/stratmap.html). One goal of this research is to assess the value of using the more detailed SSURGO data for hydrologic modeling. If the SSURGO level of detail is shown to be much more valuable then availability becomes an issue. Although certified SSURGO maps are not available for the three counties intersecting the Little Washita watershed (Caddo, Grady, and Comanche), a 30-m soils grid for the watershed has been obtained from the Agricultural Research Service Grazinglands Research Laboratory. The spatial detail in this grid is equivalent to that in SSURGO maps, and the data tables associated with this grid are very similar to those used for STATSGO/SSURGO, although the differences are significant enough to require separate GIS pre-processing routines.

Figure 3.4 illustrates the differences in spatial detail provided by the STATSGO and the 30-m soils grid. The soil types listed in the legend correspond to the predominant soil surface texture. The shading scheme in Figure 3.4 is selected so that darker shades represent soils with a tendency to produce more runoff. The location of different soil components within a STATSGO mapunit is not known. For example, there are 14 components associated with Mapunit OK103. The percentage of each component in OK103 is known and the component surface texture is also known. Surface texture names reported in the database tables are reclassified into the 12 basic USDA soil texture classes as explained in Section 3.2.2.2. Using this information, it was determined that the surface texture at any point in OK103 has a 56% likelihood of being a Loam, a 30% likelihood of being a Silt Loam, and a 14% likelihood of being a Sandy Loam. The portion of STATSGO Mapunit OK103 shown in Figure 3.4 is shaded as if it were a Loam because this is the predominant soil type. These percentages do not guarantee, however, that any soil with a Silt Loam (for example) surface texture lies within the

Little Washita portion of Mapunit OK103 or that the surface texture in the Little Washita portion of Mapunit OK103 is not entirely Silt Loam. The Little Washita portion of Mapunit OK103, in fact, constitutes only 10% of the total area for Mapunit OK103. Figure 3.5 shows the location of all polygons in Mapunit OK103 polygons relative to the Little Washita watershed.

The percentage of the Little Washita watershed with surface textures specified as each of the 12 basic USDA soil textures was computed using both STATSGO and the 30-m soils grid. The results of this calculation are shown in Figure 3.6a. For calculations with the 30-m soils grid, some grid cells may have two possible surface textures. The predominant texture was used in calculations for Figure 3.6a. Nearly all of the surface soils in the Little Washita fall into one of four categories — loamy sand, sandy loam, loam, or silt loam. At first glance, there appear to be significant differences in the surface texture compositions estimated from the two different map scales. However, the hydraulic properties of loamy sand and sandy loam are similar and the hydraulic properties of loam and silt loam are similar as discussed in Section 3.2.2.2.3. If these two sets of soil types are grouped together, then the surface texture compositions predicted by the two soil maps are very similar (Figure 3.6b). This observation may explain the small differences in simulation results obtained when the two different data sets are used (See Chapter 5).

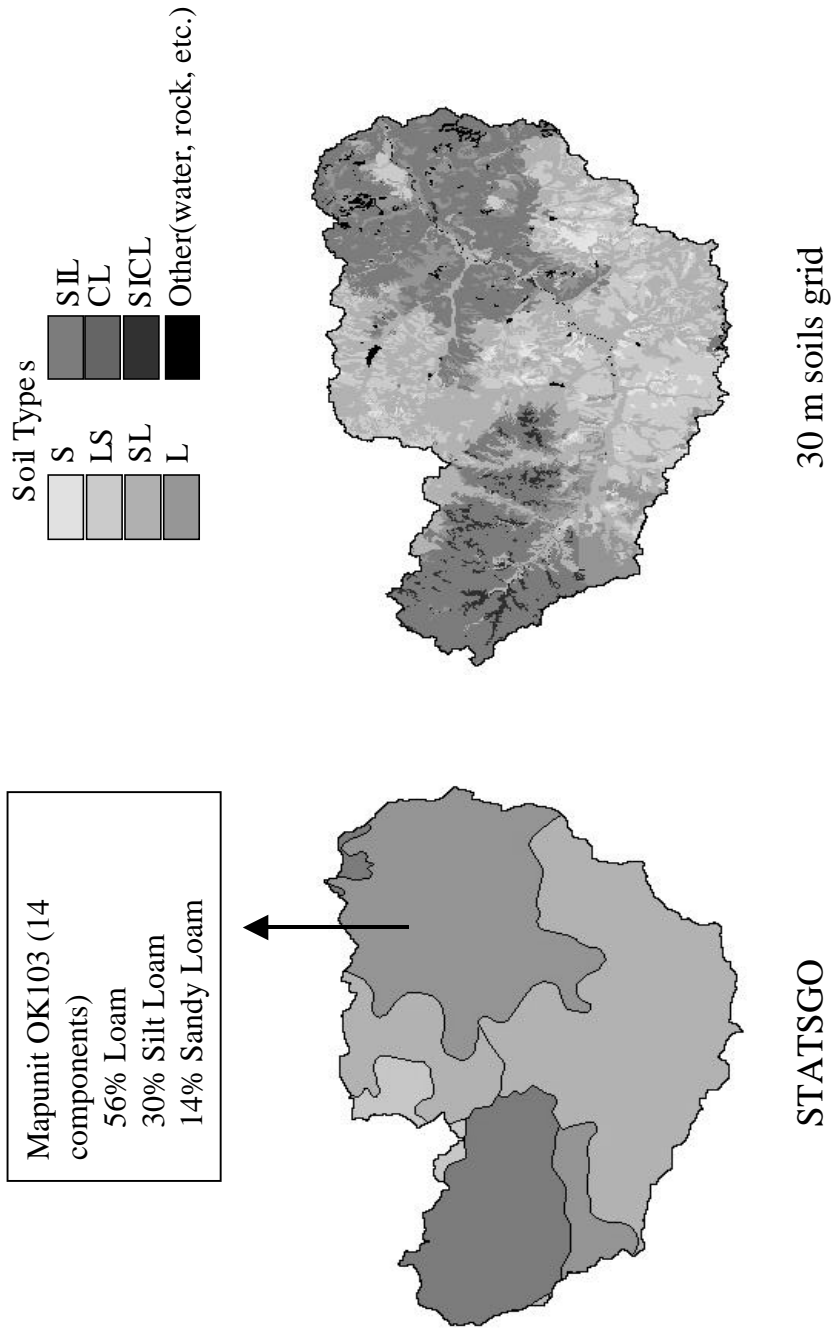


Figure 3.4 STATSGO and 30-m soils grid.

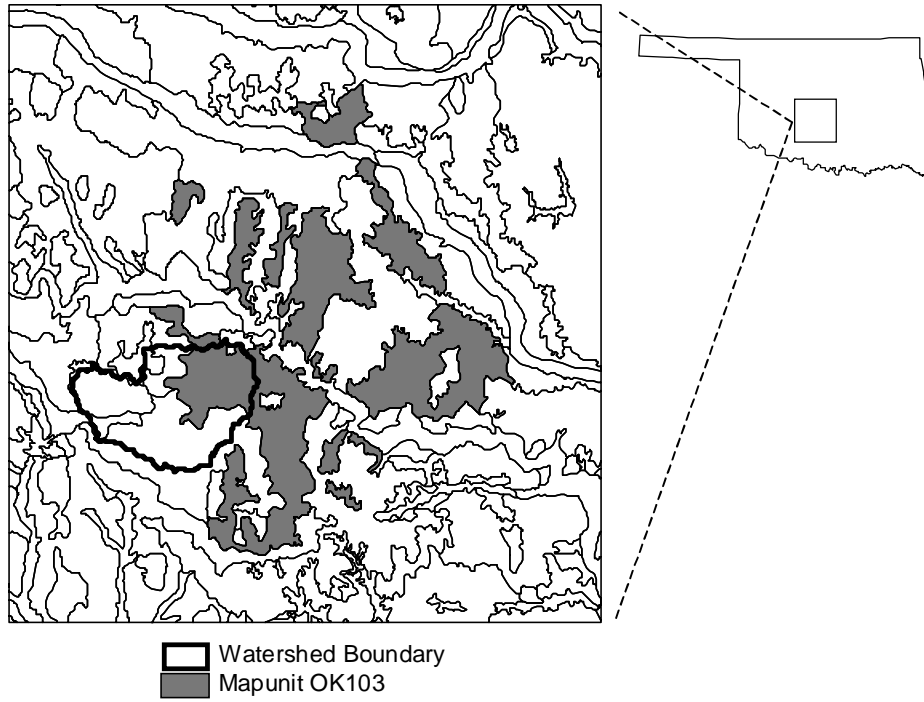


Figure 3.5 Mapunit OK103 polygons.

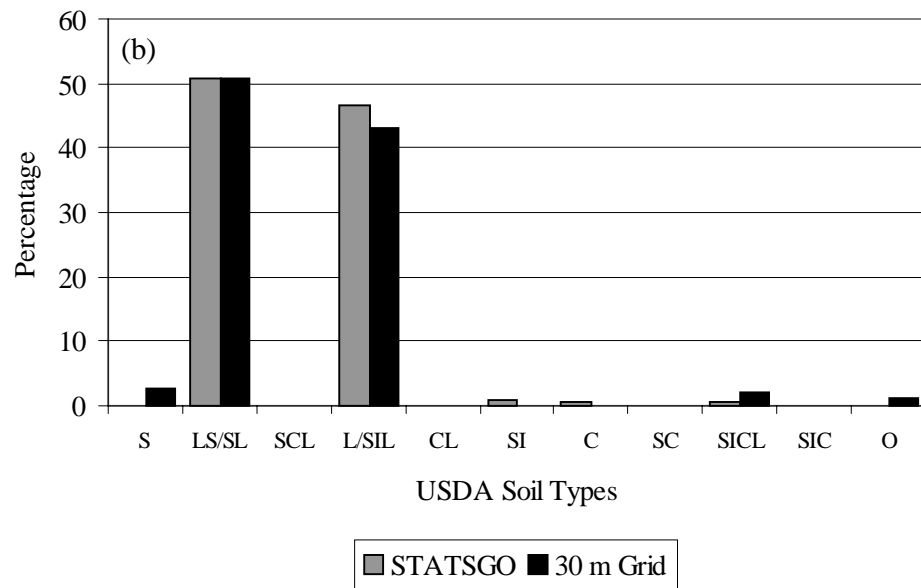
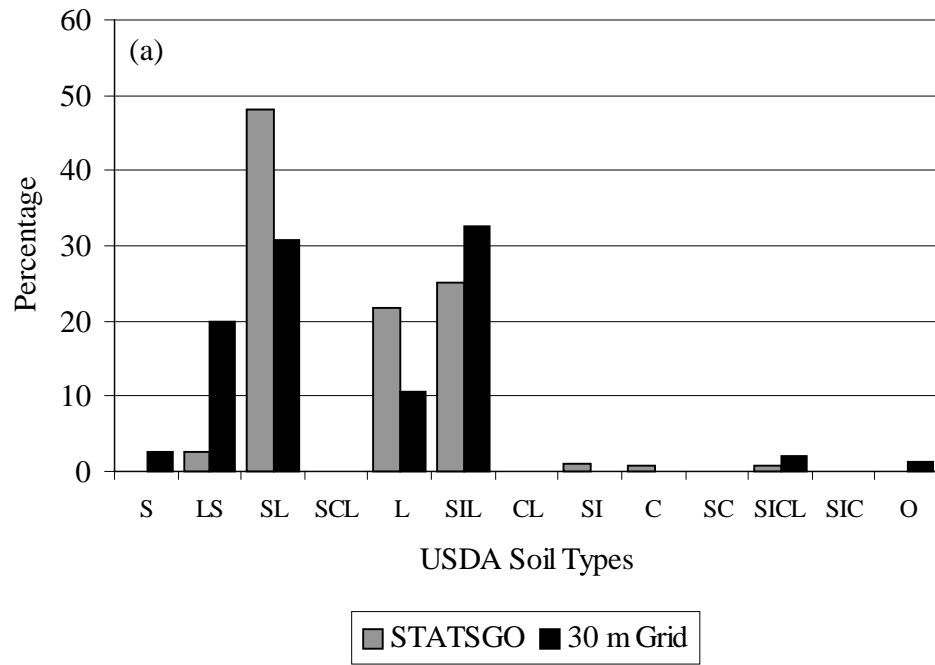


Figure 3.6 Comparison of surface texture composition for the STATSGO soil map and the 30-m soil grid with (a) soils grouped into the 12 USDA texture classes and (b) loamy sand and sandy loam grouped together along with loam and silt loam.

3.2.2.2. Estimation of soil hydraulic properties

3.2.2.2.1. Soil attribute tables

Many soil attributes are stored in tables associated with the STATSGO and SSURGO soil maps. STATSGO tables are described here. The tables associated with the 30-m soils grid contain most of the same information. The attribute tables of interest here are the *mapunit* table, the *comp* (component) table, and the *layer* table. The *mapunit* table holds the key to relating soil attributes to polygons on the map. One record exists in the *mapunit* table for each mapunit. A single record in the *mapunit* table relates to one or more components in the *comp* table. In STATSGO there can be up to 21 components in a mapunit while SSURGO mapunits typically contain only 1 component but may contain up to 3. A single record in the *comp* table relates to 1 to 6 records in the *layer* table. The relationships among these three tables is illustrated in Figure 3.7 for mapunit OK103. The total number of attributes available in the *comp* table is 53 and the total number of attributes available in the *layer* table is 55. Several attributes in the *comp* and *layer* tables are relevant to hydrology but interpretation and use of these values for modeling is not straightforward.

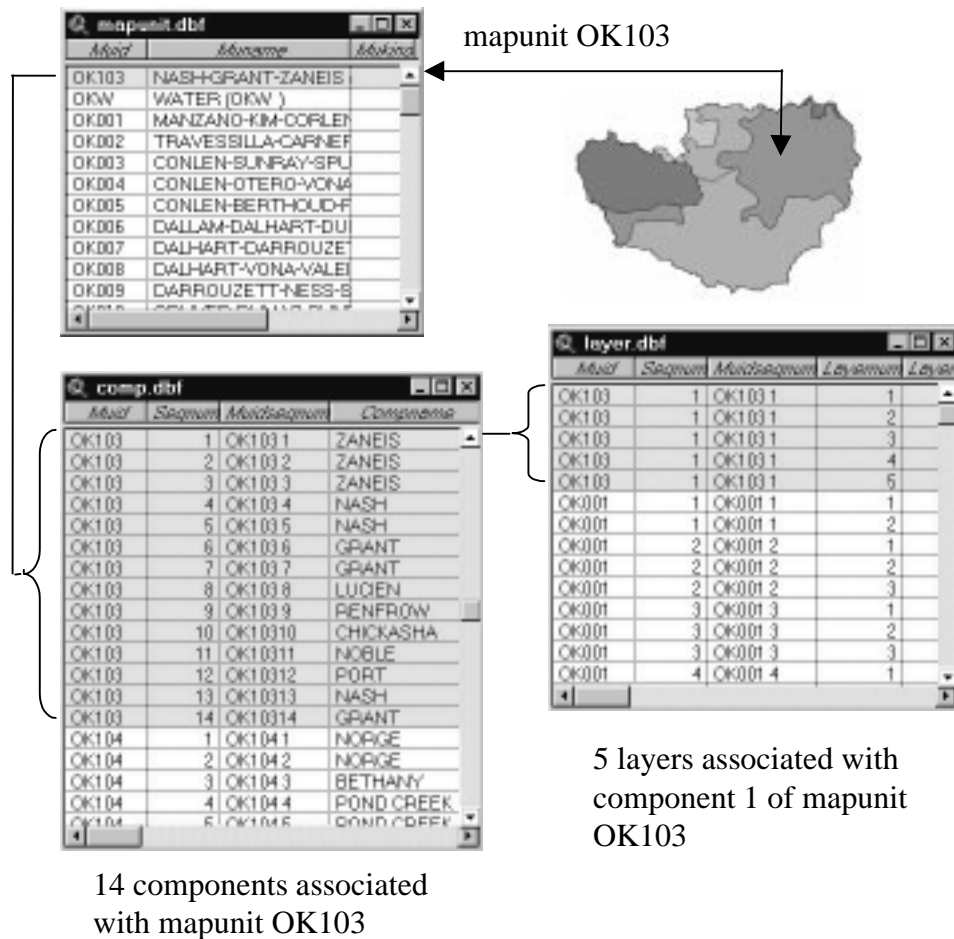


Figure 3.7 Relationships among the mapunit, comp, and layer table.

The following soil properties must be estimated in order to use the infiltration, evaporation, and percolation equations that are described in Section 3.3: saturated hydraulic conductivity (K_s), porosity (ϕ), residual water content (θ_r), the Brooks and Corey water retention parameters (λ and h_b) defined by Equation 3.1, field capacity (θ_{fc}), and wilting point (θ_{wp}). θ_{fc} and θ_{wp} do not need to be prescribed independently because they can be computed from λ and h_b . In Equation 3.1, Θ_d is the effective saturation associated with soil drying and h is the absolute value of suction head [cm]. Equation 3.2 shows a similar equation that is used to describe the water

retention function in the wetting phase. Differences in soil behavior during the wetting and drying phases is referred to as hysteresis (Jury, Gardner, and Gardner, 1991). The distinction between wetting and drying phases becomes important in the derivation of the equations to estimate wetting front suction head given in Section 3.3.1.2. In Equation 3.2, h_{we} [cm] is the water entry head. Although h_b in Equation 3.1 is sometimes referred to as the air entry head, use of the symbol h_b (the subscript b stands for bubbling pressure head) is commonly seen in the literature and will be used here. Based on the experimental work of Bouwer (1966), h_{we} is commonly taken as half of h_b . An illustration of the wetting and drying water retention curves for a loam soil is given in Figure 3.8.

$$\text{Equation 3.1} \quad \Theta_d = \frac{\theta - \theta_r}{\phi - \theta_r} = \left(\frac{h_b}{h} \right)^\lambda$$

$$\text{Equation 3.2} \quad \Theta_w = \frac{\theta - \theta_r}{\phi - \theta_r} = \left(\frac{h_{we}}{h} \right)^\lambda$$

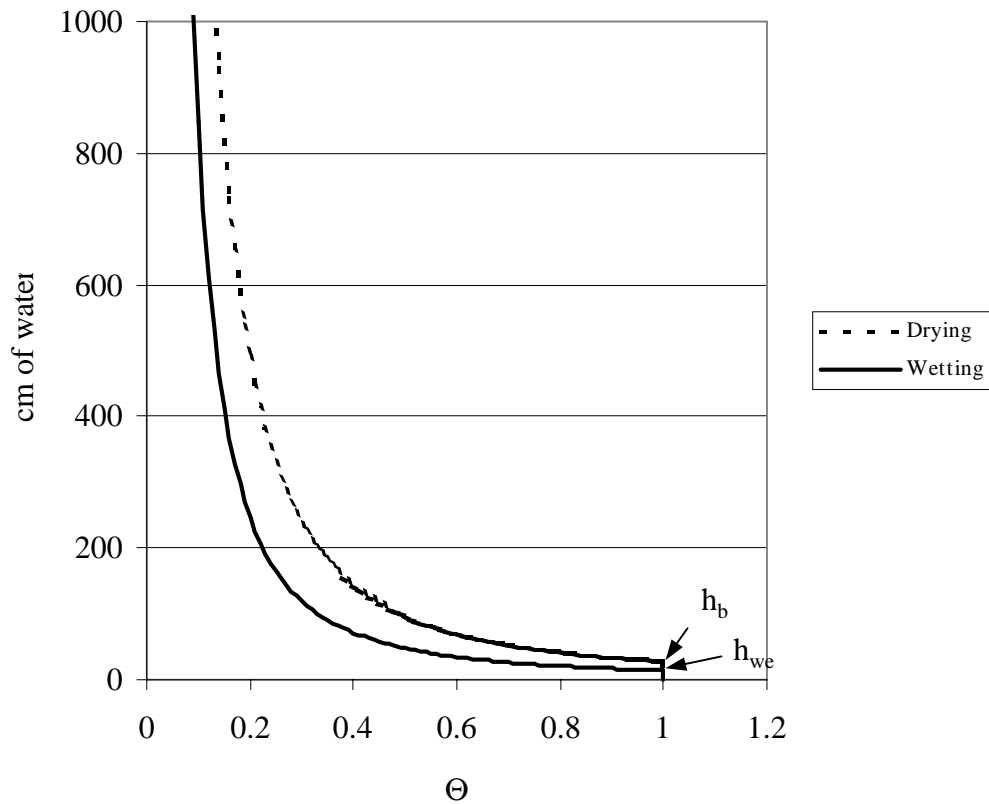


Figure 3.8. Example wetting and drying water retention curves for a loam soil with $h_b = 27.8$ and $\lambda = 0.56$.

The model equations described in Section 3.3 have been selected in part because a rational method for estimating the required parameters is available.

3.2.2.2.2. The lookup table approach

A good deal of attention has been paid in the literature to the estimation of hydraulic properties from the information in soils databases. McCuen, Rawls, and Brakensiek (1981) concluded that Brooks and Corey water retention parameters and the Green-Ampt infiltration parameters vary systematically across the USDA soil texture classes, thus suggesting that representative hydraulic properties for each of the 12 USDA soil texture classes might be used in hydrologic models when only the

soil texture is known. To arrive at this conclusion, McCuen, Rawls, and Brakensiek (1981) analyzed 1085 water retention data sets and used statistical analysis to show that the Brooks and Corey and Green-Ampt infiltration parameters are statistically different among soil classes. Rawls, Brakensiek, and Saxton (1982) performed a similar analysis on a larger data set and presented a table with means and standard deviations for ϕ , θ_r , λ , h_b , θ_{fc} , and θ_{wp} within 11 of the 12 basic USDA textural classes. Clapp and Hornberger (1978) had also performed a similar analysis on a subset of the data used by Rawls, Brakensiek, and Saxton (1982). Rawls, Brakensiek, and Saxton (1982) also “visually” estimated representative values of saturated hydraulic conductivity (K_s) for each of the 11 texture classes from plots of experimental data but emphasize that other characteristics besides texture will influence K_s .

Rawls and Brakensiek (1985) developed regression equations that can be used to estimate θ_r , h_b , λ , and K_s as a function of percent clay, percent sand, and porosity. Using a large soils database with information on bulk density, sand, and clay contents for thousands of soils, Carsel and Parrish (1988) used the regression equations of Rawls and Brakensiek (1985) to produce empirical distributions for K_s , θ_r , and the van Genuchten water retention parameters (α and N) defined by Equation 3.3.

$$\text{Equation 3.3} \quad \theta = \theta_r + \frac{(\phi - \theta_r)}{[1 + (\alpha h)^N]^{(1-1/N)}}$$

Subsequently, Carsel and Parrish (1988) used statistical techniques to determine the means, variances, and covariances for each of these parameters (K_s , θ_r , α , N) within each of the 12 USDA texture classes. Carsel and Parrish (1988) used the relationships presented in Equation 3.4 and Equation 3.5 in order to use the Rawls and Brakensiek (1985) regression equations for λ and h_b to predict α and N . Thus,

the representative values presented by Carsel and Parrish for α and N can precisely be converted back to λ and h_b using these same equations.

$$\text{Equation 3.4} \quad \lambda = N - 1$$

$$\text{Equation 3.5} \quad h_b = \frac{1}{\alpha}$$

The Brooks and Corey (λ and h_b) and van Genuchten (α and N) relationships become identical at large capillary heads when Equation 3.4 and Equation 3.5 hold true.

Considering this previous work, two general approaches may be considered for estimating the parameters K_s , ϕ , θ_r , λ , h_b , θ_{fc} , and θ_{wp} from the information in STATSGO or SSURGO data tables, a regression approach or a lookup table approach. A third alternative might be considered for estimating K_s and ϕ alone. The first, more complex, approach would be to try to use *layer* table attributes describing the percent of soil passing through American Society for Testing Materials sieves (Attribute names are No10l, No10h, No200l, and No200h, where No10l is the low estimate for the fraction of soil passing the number 10 sieve and No10h is the high estimate and so forth.) in conjunction with information about percent clay (clayl and clayh) to estimate the percent sand and percent clay. Using this information along with bulk density (bdh and bdl) to estimate porosity (ϕ), the regression equations of Rawls and Brakensiek (1985) could be applied to estimate K_s , θ_r , λ , and h_b . There are at least two practical difficulties in using this approach. In Oklahoma, some inconsistencies are found between the sieve values and the percent clay estimates if high and low attribute values are averaged. For example, in some layers the average percent material passing sieve No. 200 is greater than the average percent clay, a condition that should not be possible. Miller and White (1998) note similar difficulties in estimating percent, sand, silt, and clay in Pennsylvania. A second difficulty with using the regression approach is that some

non-water, non-bedrock layers in the Oklahoma layer table have zero values for bulk density, preventing direct estimates of porosity for these layers. Miller and White (1998) also note this problem in Pennsylvania.

A simpler parameter estimation approach adopted here is to estimate K_s , θ_r , λ , and h_b as a function of USDA texture class by using a lookup table. Field capacity (θ_{fc}) and wilting point (θ_{wp}) values are estimated using the lookup table values for λ and h_b and Equation 3.1. The matric potential corresponding to field capacity is taken as -10 kPa for coarse textured soils (S, LS, SL) and -20 kPa for medium to fine textured soils (SCL, L, SIL, CL, SI, C, SC, SICL, SIC) as recommended in ASCE (1990).

Although all of the required soil parameters can be derived using the texture lookup table approach advocated here, one might argue that layer attributes other than texture should be considered to estimate K_s and ϕ more directly. The reasons for not doing this are discussed briefly here.

The bulk density (bdh, bdl) attribute might be used to estimate porosity more directly; however, as stated previously, non-water, non-bedrock layers with zero values for bulk density cause problems with this approach.

The “permeability” attribute (with units of inches/hour) might be used to estimate K_s , but a study of the physical meaning and derivation of permeability attribute in STATSGO and SSURGO has led the author to conclude that this approach would be no better than the lookup table approach and more complex to implement. The USDA *Soil Survey Manual* (1951) describes two methods for determining soil permeability. One method is a laboratory test to determine the drainage through a saturated soil core sample subject to a constant ponded head and the other is to assign a permeability class to a soil based on structure, texture, porosity, cracking and other horizon characteristics. The USDA *Soil Survey Manual* (1993) describes a similar system for assigning a saturated hydraulic conductivity class to soils based on texture and bulk density. The term saturated

hydraulic conductivity in the 1993 manual is used in lieu of permeability that was used in the 1951 manual. Measured values of saturated hydraulic conductivity can easily vary by an order of magnitude within a soil series or even between soil samples taken within centimeters of one another (USDA, 1993). Different measurement techniques may produce drastically different results; however, field measurement techniques are generally preferred over laboratory techniques (USDA, 1993). Of the model parameters (ϕ , θ_r , K_s , λ , h_b) used in this study, K_s has by far the largest coefficient of variation based on the analysis of Carsel and Parrish (1988). This is a major reason why a hydraulic conductivity factor is chosen for model calibration (see Chapter 5).

Upon examination of the STATSGO layer data for Oklahoma, it seems likely that reported saturated hydraulic conductivity values are based on a general classification system like that described in the USDA *Soil Survey Manual* (1951). Typically only ranges of values like 0-0.06 inches/hour, 0.2-0.6 inches/hour, 0.6–2.0 inches/hour, 2-6 inches/hour, 6-20 inches/hour etc., are given in STATSGO. The ranges prescribed by the 1951 manual are 0-0.05 inches/hour, 0.05-0.2 inches/hour, 0.2-0.8 inches/hour, 0.8-2.5 inches/hour, 2.5-5 inches/hour, 5-10 inches/hour, and > 10 inches/hour. 2927 out of 7597 (39%) of the soil layers in Oklahoma have the permeability range 0.6-2.0 inches/hour. At least 6 different USDA texture classes have permeability specified in this range. Thus, other factors besides texture are influencing the permeability class, perhaps bulk density or layering. Using both bulk density and texture to estimate saturated hydraulic conductivity would be better than using texture alone; however, the additional complications introduced by using this approach seem to outweigh the benefits at this time, particularly since hydraulic conductivity will be used in model calibration and there are missing data values in STATSGO for bulk density. Carsel and Parrish (1988) showed that there is a significant statistical correlation between samples of K_s and the water retention

parameters within each texture class. Therefore, an additional advantage of using a lookup table alone is that all parameter values are mutually consistent.

One last argument in favor of using texture as the only distinguishing factor among components is that this significantly simplifies model data management, at least for the one-layer model discussed in the next section. When only a single distinguishing factor is used, components with a common texture can be lumped together and the spatial soils information passed from the GIS to the hydrology model is set at 13 different specifications (12 USDA texture classifications and an “other” category). If multiple distinguishing factors are used, then components with a common surface texture may differ in other characteristics so that there is a need to pass more information about individual components to the hydrology model.

In application, the texture names specified in the STATSGO database cannot be passed directly to a texture-parameter lookup table because the letter codes used to specify soil texture may include qualifiers or letters used in lieu of texture. BY-SL (bouldery sandy loam) and CB-SL (cobble sandy loam) are examples of texture codes with qualifiers. PEAT and UWB (unweathered bedrock) are examples of codes used in lieu of texture. Miller and White (1998) compiled a lookup table that reclassifies all 719 possible texture name combinations listed in STATSGO into one of the 12 basic USDA classes or the other category. A slightly modified version of the Miller and White reclassification table is used here. With two exceptions, the reclassifications specified in the Miller and White table make sense. In the original table, LFS (loamy fine sand) and LCOS (loamy coarse sand) were reclassified as S (sand). These reclassifications were changed to LS (loamy sand) for the current application because this seemed more intuitive. Due to its length, presentation of this lookup table is left to the Appendix D.

3.2.2.2.3. Selecting representative parameter values for texture classes

Both Rawls, Brakensiek, and Saxton (1982) and Carsel and Parrish (1988) present tables with representative values for K_s , ϕ , θ_r , λ , and h_b in the basic USDA texture classes. Rawls, Brakensiek, and Saxton and Carsel and Parrish used information from thousands of soil samples to derive their respective tabulated parameter values; however, their approaches used to derive parameter values differed and so do their tabulated results.

Rawls, Brakensiek, and Saxton visually estimated values of K_s for each texture class by plotting unsaturated hydraulic conductivity data from the literature, but noted that other factors besides texture will influence K_s . Both Rawls, Brakensiek, and Saxton and Carsel and Parrish report means and standard deviations for porosity (ϕ) based on sample values obtained directly from soil survey reports. To estimate values of θ_r , λ , and h_b , Rawls, Brakensiek, and Saxton plotted water retention-matric potential data from the literature and used optimization to determine the parameter values (θ_r , λ , h_b) that best fit each data set. Rawls, Brakensiek, and Saxton report the mean values for these fitted parameters and values corresponding to plus and minus one standard deviation. In contrast, Carsel and Parrish generated a sampling of values for K_s , θ_r , α , and N in each texture class by using regression equations developed by Rawls and Brakensiek (1985). Carsel and Parrish used Equations 3.3 and 3.4 to compute α and N from regression equations for λ and h_b . The inputs to these regression equations are percent clay, percent sand, and porosity (ϕ) (values obtained from Soil Conservation Service Soil Survey Information Reports). Carsel and Parrish statistically analyzed the K_s , θ_r , α , and N samples in each texture class and reported means and standard deviations as well as the correlations among the parameters in each texture class.

A tabulation of the parameter means (μ) and coefficients of variation (CV) from Rawls, Brakensiek, and Saxton and Carsel and Parrish is presented in Table 3.3. Rawls, Brakensiek, and Saxton do not report the coefficients of variation but

do report values corresponding to one standard deviation above and below the mean (x^+ , x^-). Approximate coefficients of variation (CV*) from Rawls, Brakensiek, and Saxton are computed using the following equation.

$$\text{Equation 3.6} \quad CV^* = \frac{(x^+ - x^-)/2}{\mu} * 100$$

Table 3.3 Mean values and coefficients of variation for hydraulic parameters in the 12 basic USDA texture classes. A comparison of values reported by Rawls, Brakensiek, and Saxton (1982) and Carsel and Parrish (1988).

	Saturated Hydraulic Conductivity			Porosity			
	R,B, & S K_s μ	C & P K_s μ	CV(%)	R, B, & S ϕ μ	CV*(%)	C & P ϕ μ	CV(%)
S	23.6	29.7	52	0.44	14	0.43	15
LS	5.98	14.6	78	0.44	16	0.41	22
SL	2.18	4.42	127	0.45	23	0.41	21
SCL	0.3	1.31	209	0.40	17	0.39	18
L	1.32	1.04	175	0.46	19	0.43	22
SIL	0.68	0.45	275	0.50	16	0.45	19
CL	0.2	0.26	267	0.46	12	0.41	22
SI		0.25	130			0.46	17
C	0.06	0.2	210	0.48	10	0.38	24
SC	0.12	0.12	234	0.43	14	0.38	14
SICL	0.2	0.07	289	0.47	11	0.43	17
SIC	0.1	0.02	453	0.48	11	0.36	20

Residual Water Content

Lambda

	R, B, & S		C & P		R, B, & S		C & P	
	θ_r	CV*(%)	θ_r	CV(%)	λ	CV*(%)	λ	CV(%)
	μ		μ		μ		μ	
S	0.02	95	0.045	22	0.69	57	1.68	20
LS	0.035	91	0.057	26	0.55	58	1.28	12
SL	0.041	129	0.065	27	0.38	63	0.89	9
SCL	0.068	101	0.1	6	0.32	75	0.48	9
L	0.027	137	0.078	17	0.25	66	0.56	7
SIL	0.015	193	0.067	22	0.23	55	0.41	9
CL	0.075	116	0.095	10	0.24	71	0.31	7
SI	0.015		0.034	30			0.37	3
C	0.09	108	0.068	50	0.17	78	0.09	8
SC	0.109	88	0.1	13	0.22	78	0.23	8
SICL	0.04	148	0.089	11	0.18	78	0.23	5
SIC	0.056	121	0.07	34	0.15	73	0.09	5

h_b

	R, B, & S		C&P	
	h_b	CV*(%)	h_b	CV(%)
	μ		μ	
S	7.3	257	6.9	20
LS	8.7	230	8.1	35
SL	14.7	200	13.3	49
SCL	28.1	242	17.0	65
L	11.2	335	27.8	57
SIL	20.8	281	50.0	65
CL	25.9	212	52.6	78
SI			62.5	45
C	37.3	241	125.0	160
SC	29.2	286	37.0	62
SICL	32.6	233	100.0	62
SIC	34.2	233	200.0	114

* Computed using Equation 3.6.

With the exception of porosity (ϕ), the Rawls, Brakensiek, and Saxton parameter estimates tend to have much higher coefficients of variation than those of Carsel and Parrish. K_s has by far the highest variability among the parameter values reported by Carsel and Parrish. Rawls, Brakensiek, and Saxton do not report

uncertainty for K_s . The h_b values have the highest coefficients of variation among the parameter estimates tabulated by Rawls, Brakensiek, and Saxton. The most striking differences in the mean values from the two data sets occurs in the λ values for coarse textured soils and the h_b values for fine soils.

Plots of the mean values of ϕ , θ_r , λ , and h_b with one standard deviation error bars have been prepared to provide a visual basis for comparing the two sets of values. These plots are shown in Figures 3.9 - 3.12. In these figures, textures are listed in order of decreasing saturated hydraulic conductivity from top to bottom. Preparation of the Rawls, Brakensiek, and Saxton data series on these plots is straightforward because their paper reports parameter values corresponding to one standard deviation above and below the mean. From the Carsel and Parrish paper, the parameter values corresponding to these points are not explicitly reported and must be computed for the skewed distributions. Statistical parameter values reported in Table 6 of Carsel and Parrish for the transformed θ_r , α , and N values were untransformed to create the error bars in these figures.

The Carsel and Parrish estimates for ϕ tend to be lower than those of Rawls, Brakensiek, and Saxton but the differences between mean ϕ values tend to be no more than one standard deviation, with the exception of silty clay (SIC). Mean θ_r values from Carsel and Parrish tend to be higher than mean values from Rawls, Brakensiek, and Saxton. For λ , there seems to be an increasing discrepancy in the mean parameter values from the two data sets when moving from fine to coarse textured soils. The error bars do not even overlap in Figure 3.11 for loam, sandy loam, loamy sand, and sand soils. For h_b , discrepancies in the mean values increase when moving from fine textured soils to coarse textured soils. The error bars for h_b still overlap for coarse textured soils because of the large uncertainty in the h_b values reported by Rawls, Brakensiek, and Saxton.

Another way of visualizing the variations in parameter values across the different texture classes is to use the USDA textural triangle. Figures 3.13 and 3.14

show h_b values printed on the USDA textural triangle. Looking at the textural triangle, one would intuitively expect bubbling pressure head to increase with decreasing sand content (along the line from point 1 to point 2) and increase with increasing clay content (along the line from point 1 to point 3). This trend is seen in both Figures 3.13 and 3.14 with one notable exception, the Rawls, Brakensiek, and Saxton h_b value for the loam soil appears to be too low. If figures similar to 3.13 and 3.14 are created for the λ values, all parameter values are consistent with the expected trends for both data sets.

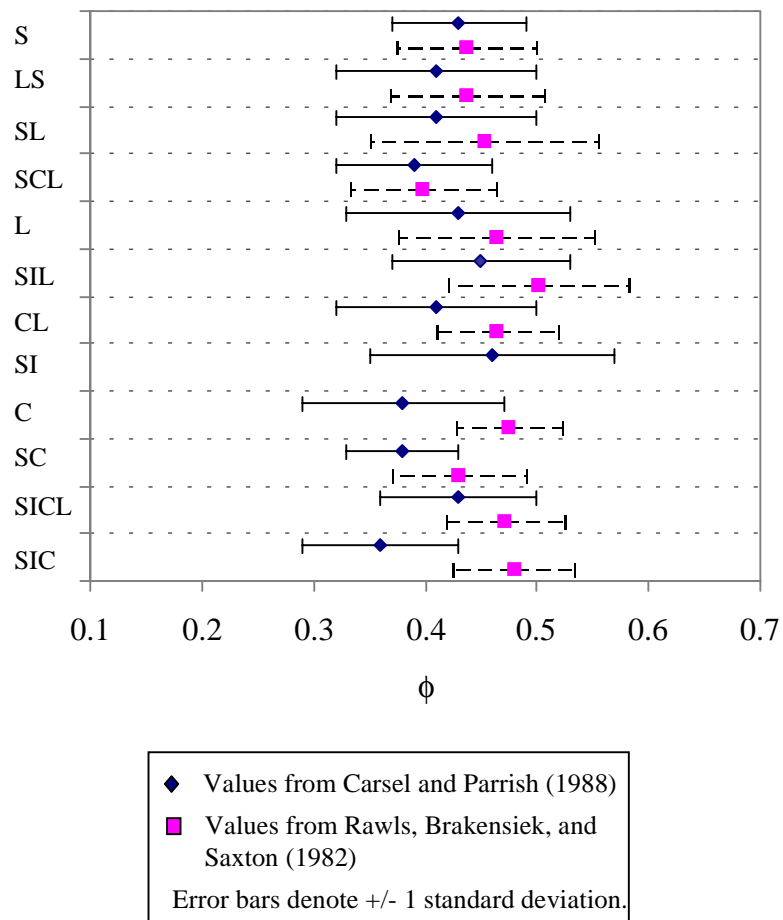
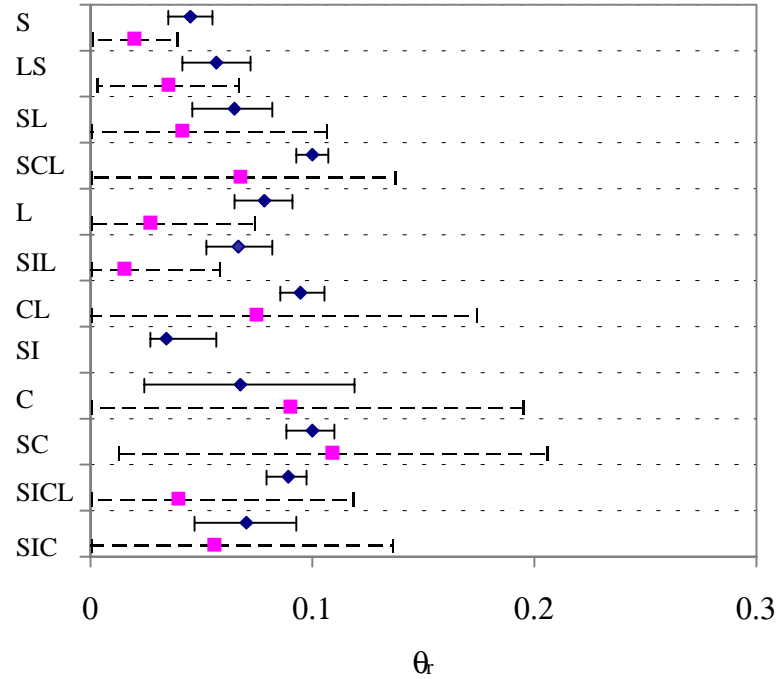


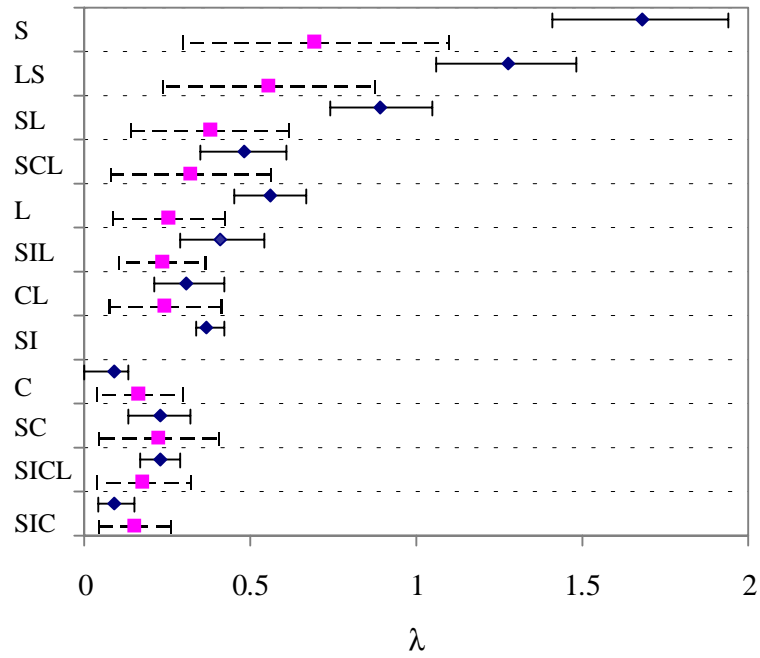
Figure 3.9 Mean porosity values for USDA texture classes with 1 standard deviation error bars.



◆ Carseel and Parrish (1988)
 Error bar end points are determined by back-transforming values corresponding to +/- 1 standard deviation above and below the mean in a transformed space.

■ Rawls, Brakensiek, and Saxton (1982)
 Error bars correspond to +/- 1 standard deviation values reported by Rawls, Brakensiek, and Saxton (1982).

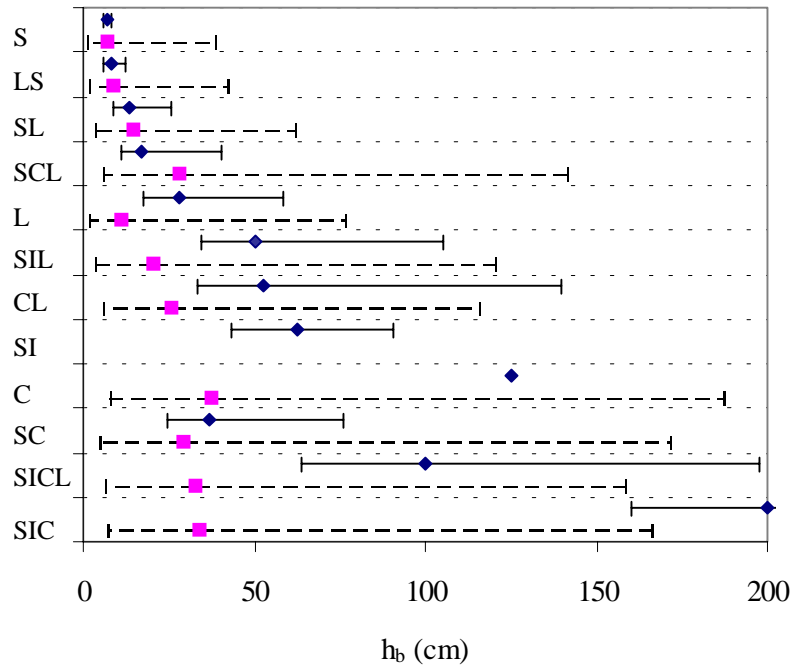
Figure 3.10 Mean residual saturation values for USDA texture classes with 1 standard deviation error bars.



◆ Carsel and Parrish (1988)
 Error bar end points are determined by back-transforming values corresponding to ± 1 standard deviation above and below the mean in a transformed space.

■ Rawls, Brakensiek, and Saxton (1982)
 Error bars correspond to ± 1 standard deviation values reported by Rawls, Brakensiek, and Saxton (1982).

Figure 3.11 Mean λ values for USDA texture classes with 1 standard deviation error bars.



◆ Carseel and Parrish (1988)
 Error bar end points are determined by back-transforming values corresponding to +/- 1 standard deviation above and below the mean in a transformed space.

■ Rawls, Brakensiek, and Saxton (1982)
 Error bars correspond to +/- 1 standard deviation values reported by Rawls, Brakensiek, and Saxton (1982).

Figure 3.12 Mean h_b values for USDA texture classes with 1 standard deviation error bars.

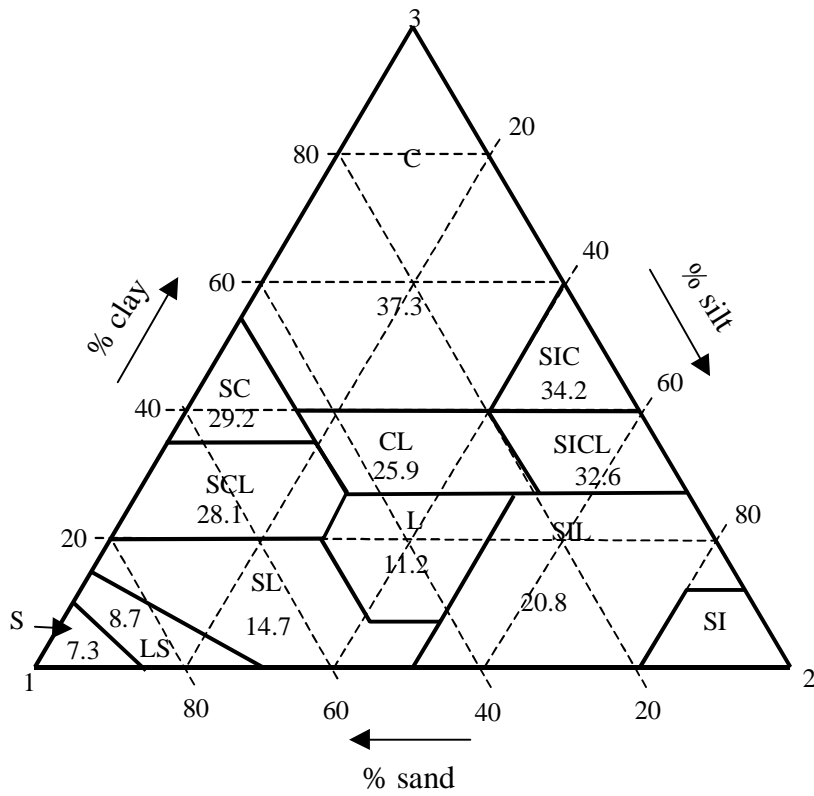


Figure 3.13 Rawls, Brakensiek, and Saxton h_b values on the USDA textural triangle.

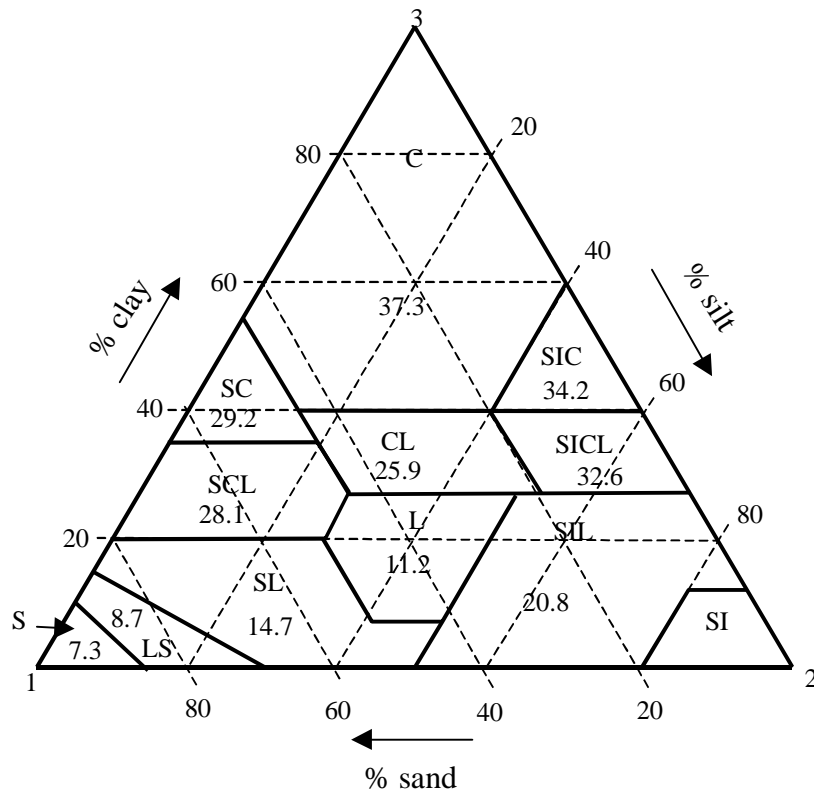


Figure 3.14 Carsel and Parrish h_b values on the USDA textural triangle.

A method for computing Green-Ampt wetting front suction head (h_f) values from the Brooks and Corey water retention parameters (λ , h_b) is discussed in detail in Section 3.3.1.2. For discussion here, the Green-Ampt wetting front suction head parameter values computed from the Rawls, Brakensiek, and Saxton mean λ and h_b values and the Carsel and Parrish mean λ and h_b values for an initially dry soil are given in Table 3.4. The wetting front suction head values derived from the Carsel and Parrish λ and h_b parameter values are much more consistent with values of wetting front suction head shown graphically in Figure 5.5.4 of Rawls *et al.* (1993). For this reason, and the fact that there is an internal inconsistency in the h_b value for loam soil shown in Figure 3.13, the Carsel and Parrish mean parameter values are used for simulations described in Chapter 5. To get a sense of the impact of

parameter uncertainty on simulation results, a simple sensitivity analysis is included in Section 5.6.

Table 3.4 Estimates for Green-Ampt wetting front suction head (h_f) for an initially dry soil.

Texture	h_f from Rawls, Brakensiek, and Saxton (cm)	h_f from Carsel and Parrish (cm)
S	4.8	4.0
LS	6.0	4.9
SL	11	8.5
SCL	22	12
L	8.7	19
SIL	16	36
CL	20	40
SI		46
C	31	112
SC	23	29
SICL	27	78
SIC	29	179

3.2.2.3. One-layer model versus a two-layer model

One of the questions to be addressed in this research is whether increased vertical detail in representing soil water processes is beneficial, in addition to the increased horizontal detail associated with moving from lumped to distributed models. Therefore, the tradeoffs between using a one-layer and a two-layer soil model are considered. It is hypothesized that partitioning beyond two layers would introduce unnecessary complication into the model. Computer codes have been written in this research to use a one-layer or a two-layer approach.

The interpretation of soil component data for use in a one-layer model is straightforward. The texture for the one layer is simply taken from the surface texture attribute (*surftex*) of the *comp* table and translated into soil hydraulic parameters using the lookup tables described in the Section 3.2.2.2. The top layer is assumed to be homogeneous in terms of its hydraulic properties. The top layer is

loosely defined as the depth of soil that reacts quickly to atmospheric forcing. The depth of the top layer is important conceptually because infiltrated water is averaged over the depth of the top layer at the end of a rainstorm. If the depth of the top layer is too large, then a realistic degree of soil moisture variability is not simulated. In the model, each soil component is assigned the same top layer depth, and top layer depth essentially becomes a model parameter.

Each component in either the STATSGO or SSURGO database corresponds to anywhere from 1 to 6 layers in the *layer* table. The percentage of soil components with 1, 2, 3, 4, 5, or 6 layers in STATSGO for Oklahoma is illustrated in Figure 3.15a. 92% of the components have 4 or fewer layers and 71% of the components have 3 or fewer layers. When information about multiple layers exist, it is often the case that adjacent layers correspond to the same basic USDA texture class, effectively reducing the amount of vertical heterogeneity given the proposed modeling scheme. Differences in soil characteristics other than texture distinguish these adjacent layers. Considering adjacent layers of the same basic USDA texture as one layer, the percentage of components with 1, 2, 3, 4, or 5 distinct layers is illustrated in Figure 3.15b. In this case, 93% of the Oklahoma STATSGO components contain 3 or fewer layers and 64% of the components contain 2 or fewer layers. In light of this information, it does not seem that any vertical discretization (based on texture) beyond 3 layers could be supported by the available data and only a two-layer model could be supported in the majority of components.

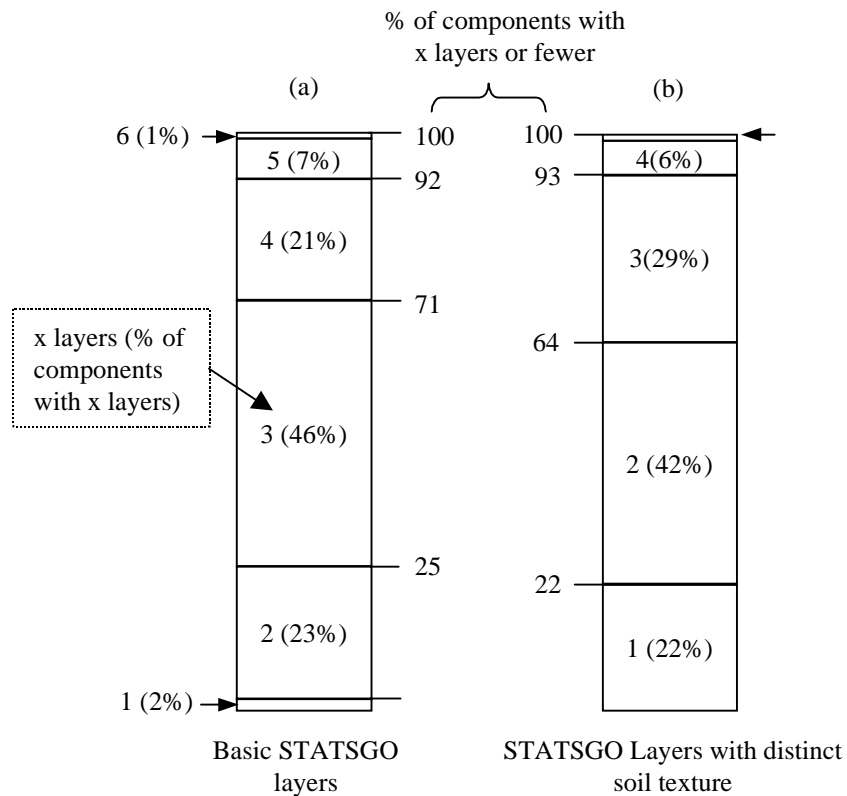


Figure 3.15 Percentage of soil components with 1, 2, 3, 4, 5, or 6 layers (a) with multiple distinguishing characteristics and (b) with the 12 basic USDA soil classes as the only distinguishing characteristic.

The idea in this study is to use both a one-layer and a two-layer model and evaluate whether adding the complexity of a second layer is valuable. The coding, data management and calibration for a two-layer model is significantly more complex than for a one-layer model, as discussed in Chapters 4 and 5; therefore, adding a third layer was not considered, a decision which appears to be justified based on modeling results.

The two-layer model developed in this study is only an approximation of the layering that exists in the soils databases. For implementation, the soil hydraulic properties of the second model layer are taken as the properties associated with the layer below the top layer with the lowest saturated hydraulic conductivity (K_s). This

approach is used because it is common that the most restrictive layer controls percolation out of the soil zone (USDA, 1951). As in the one-layer model, the depth of the top layer in the two-layer model is treated as a model parameter. The total soil zone depth is specified based on additional information in the soil layer table as described in the next paragraph, and the depth of the second layer is taken as the difference between the total soil zone depth and the depth of the top layer. The second layer serves as a reservoir from which water may evaporate or percolate to the groundwater reservoir. This approach is sensible in terms of restricting the percolation out of the soil zone based on the most impermeable layer, but does not reflect the true thickness of the soil whose properties are assigned to the second layer and may not be the most appropriate assumption in terms of estimating evaporation from the second layer. The emphasis here is on simplicity.

The total depth for the soil zone determines the depth of the second layer in each soil component. The depth of the second layer influences the water content of the second layer which in turn influences the rate of percolation out the bottom of the second layer and thus the recharge rate to groundwater. Information in the soils layer tables is used to estimate the total depth of the soil zone. In the proposed model, there are three pieces of information that may define the bottom of the soil zone. The total soil zone depth is taken as the minimum of (1) the deepest layer depth reported, (2) the depth to a non-soil, low permeability layer if one exists, and (3) the depth to an assumed water table if it exists. The definitions of non-soil, low permeability layers and the rationale for assuming a water table depth are discussed in the next paragraph. One motivating factor for estimating the total soil zone depth is to determine whether shallow soil layers exist that may become saturated during heavy rainfall.

The layer texture codes are used to identify any non-soil, low permeability layers at depth. In this study, the top depth (laydepl) for a layer with any of the following codes is taken as the bottom of the soil zone: cemented (CEM), indurated

(IND), unweathered bedrock (UWB), and weathered bedrock (WB). If limited by such a layer, the water storage capacity and the evaporation parameters for the second layer are determined by the properties of the soil above such a layer, but this low permeability layer now limits the percolation. These layers are not assumed to be entirely impermeable because, if they are, simulations show that there will not be enough recharge to the groundwater. The model user specifies a constant percolation rate for these layers.

Information about the depth to water table in STATSGO is implicit in the “drainage” attribute of the *comp* table. Drainage classes for soils defined by the USDA are listed in Table 3.5. In excessively (E), somewhat excessively (SE), and well (W) drained soils the depth to the water table is greater than 6 feet and the presence of a water table is not considered in the soil-water balance model. For other drainage classes, water table depths are assumed based on information in Table 3.5. Clearly the water table depths will vary with season, and the values in Table 3.5 are only a first approximation. In the Little Washita soils data obtained for this study, the STATSGO *comp* table contains the drainage class attribute but the *comp* table associated with the 30-m soils grid does not. Based on the STATSGO database, the most limiting drainage class that actually exists in the Little Washita is SP (somewhat poorly) with an assumed water table depth of 2 ft. In the model runs described in Chapter 5, the SP drainage class does not influence direct runoff because soils with this drainage class never become fully saturated.

Table 3.5 Description of soil drainage classes specified in the STATSGO comp table.

Drainage Class	Symbol	Description*	Assumed water table depth.
Very poorly	VP	“Soils are wet to the surface most of the time. Depth to water table is less than 1 foot, or is ponded.”	15.2 cm (0.5 ft)
Poorly	P	“Soils may have a saturated zone, a layer of low hydraulic conductivity or seepage. Depth to water table is less than 1 foot.”	15.2 cm (0.5 ft)
Somewhat poorly	SP	“Soils commonly have a layer with low hydraulic conductivity, wet state high in profile, etc. Depth to water table is 1 to 3 feet.”	61 cm (2 ft)
Moderately well	MW	“Soils have a layer of low hydraulic conductivity, wet state high in the profile. Depth to water table is 3 to 6 feet.”	137 cm (4.5 ft)
Well	W	“Soils have intermediate water holding capacity. Depth to water table is more than 6 feet.”	--
Somewhat excessively	SE	“Soils have high hydraulic conductivity and low water holding capacity. Depth to water table is more than 6 feet.”	--
Excessively	E	“Soils have very high and high hydraulic conductivity and low water holding capacity. Depth to water table is more than 6 feet.”	--

* Descriptions are from USDA (1994).

A map showing the total depth of the soil zone (used for the two-layer model only) derived from the 30-m soils grid is shown in Figure 3.16. The total soil zone depth in 47% of the watershed is defined by a non-soil, low permeability layer.

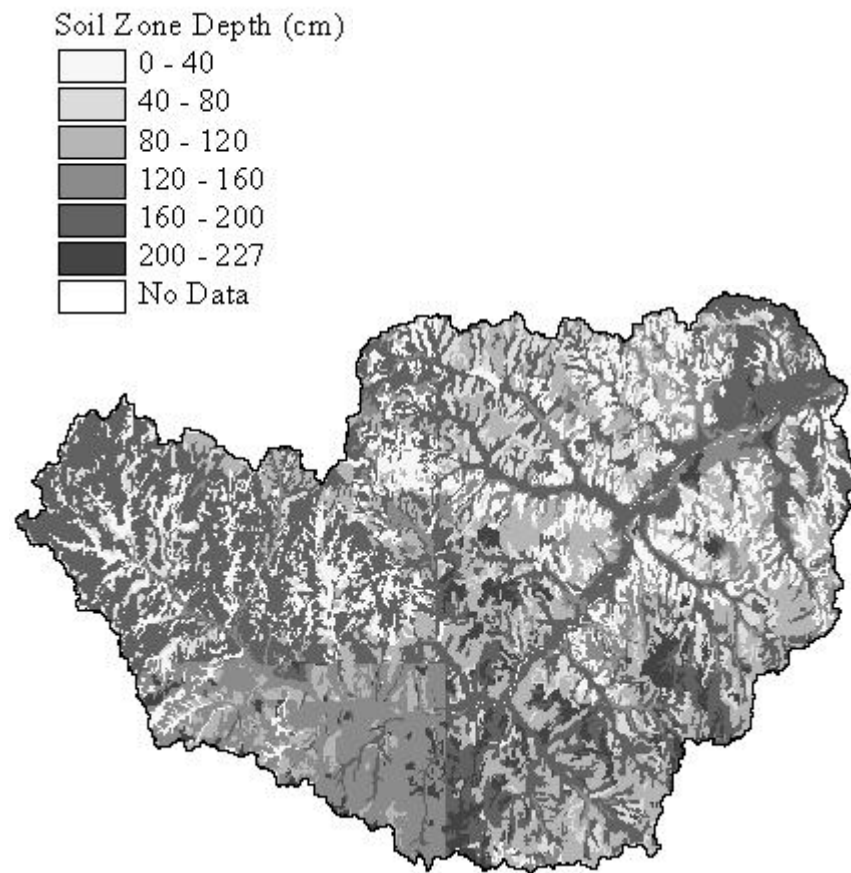


Figure 3.16 Total depth of the soil zone defined for the two-layer model.

Assessing the value of using the more complex two-layer approach is one goal of this research. There are two reasons why the added complexity of a two-layer model is of interest. By defining a lower limit on the soil zone, a limit is now placed on the cumulative infiltration that may occur. There is no limit on the cumulative infiltration in the one-layer model. If the infiltration depth predicted using the Green-Ampt model exceeds the capacity of the top layer in the one-layer model, then any excess infiltration is passed to the groundwater reservoir or treated as a sink. In contrast, if the predicted infiltration volume exceeds the capacity of the soil zone in the two-layer model, any infiltration that is not accommodated adds to

the direct runoff. The second reason that adding a second layer is of interest is that it provides an additional storage zone for water before it is passed to the groundwater reservoir.

3.2.3. Land use data

In this research, land use data are used to estimate impervious areas in a watershed. 1:250,000 scale GIRAS Land Use/Land Cover (LULC) files covering the Little Washita watershed were obtained from the EPA Internet site listed in Table 3.1. Data in these files were originally collected by the U.S. Geological Survey and converted to Arc/Info format by the U.S. Environmental Protection Agency. Land use characteristics in these files were specified in the mid 1970's and early 1980's. In some parts of the United States, significant land use changes have occurred since this time; however, this is not as big issue in the Little Washita watershed. A map showing broad land use classes in the Little Washita is provided in Figure 3.17. It is interesting to note overall similarities between land use and soils (Figure 3.4). Areas with sandy soils correspond to rangeland while silty and loamy soils correspond to agricultural land.

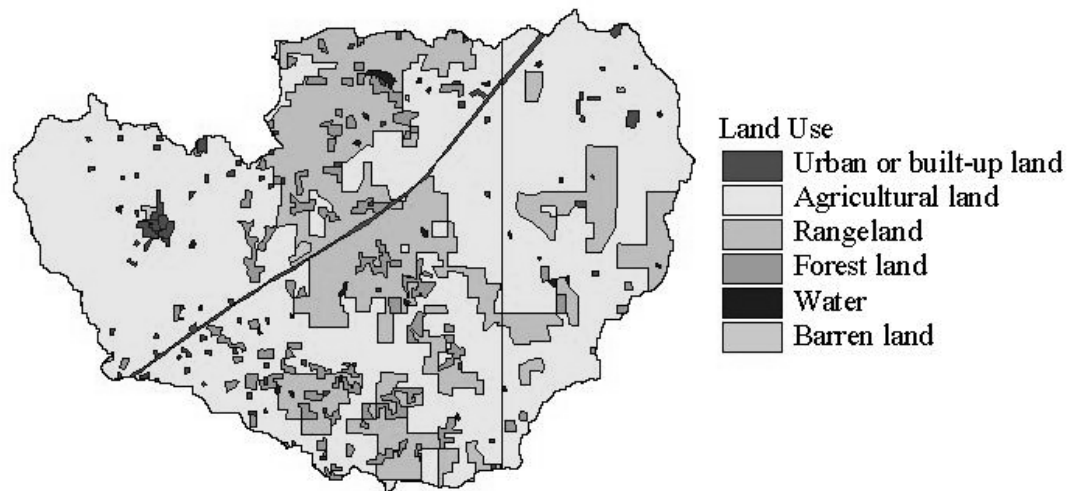


Figure 3.17 Land use in the Little Washita watershed

Each polygon in an LULC map is assigned a code indicating land use type based on the Anderson Level II land use classification scheme (Anderson *et al.*, 1976). Anderson Level II codes consist of two integers, the first integer specifies a general category (i.e. 1 = urban or built-up land) and the second integer is more specific (i.e. 11 = residential). In this study, Table 3.6 has been developed to associate an impervious cover percent with several of the Anderson level II land use codes. Impervious percent estimates for codes 11, 12, and 13 are made based on information in Chow, Maidment, and Mays (1988) Table 5.5.2. Other estimates are considered reasonable guesses. Zero impervious percent is assumed for land use categories not listed (i.e. agriculture, rangeland, and forest land). Subcategories of the Tundra (8) and Perennial Snow or Ice (9) Level 1 categories are not considered here.

Table 3.6 Impervious percentages associated with selected land use classes.

Land use code	Description	Assigned % Imperv.
11	Residential	36
12	Commercial and services	85
13	Industrial	72
14	Transportation, communication, utilities.	100
16	Mixed urban or built-up land	50
17	Other urban or built-up land	50
51	Streams and canals	100
52	Lakes	100
53	Reservoirs	100
54	Bays and estuaries	100
61	Forested wetland	100
62	Non-forested wetland	100
74	Bare exposed rock	100

3.2.4. NEXRAD data and spatial variability

The primary rainfall data used for this study are hourly NEXRAD Stage III data from the National Weather Service Arkansas-Red Basin River Forecast Center (ABRFC). NEXRAD Stage III data are mapped using the Hydrologic Rainfall Analysis Project (HRAP) grid (Greene and Hudlow, 1982) with cells that are approximately 4 km on a side in Oklahoma. A detailed discussion of mapping issues associated with using HRAP grid cells in GIS-based hydrologic modeling is provided by Reed and Maidment (1998). The NEXRAD rainfall cells define the modeling units for this study. Programs developed by Reed and Maidment (1995) were used to create a polygon coverage of rainfall cells covering the Little Washita watershed. These cells are intersected with the watershed boundary as shown in Figure 3.18. Portions of 55 different NEXRAD cells intersect the watershed boundary. Many of the NEXRAD cells that intersect near the watershed boundary form small polygons that are only a fraction of the NEXRAD cell size. The number of whole NEXRAD cells within the Little Washita watershed can be estimated by dividing the watershed area (600 km^2) by the approximate area of NEXRAD cells (16 km^2) giving 38 cells. Thus, it would take about 40 gages uniformly spread around the watershed to get the same spatial resolution.

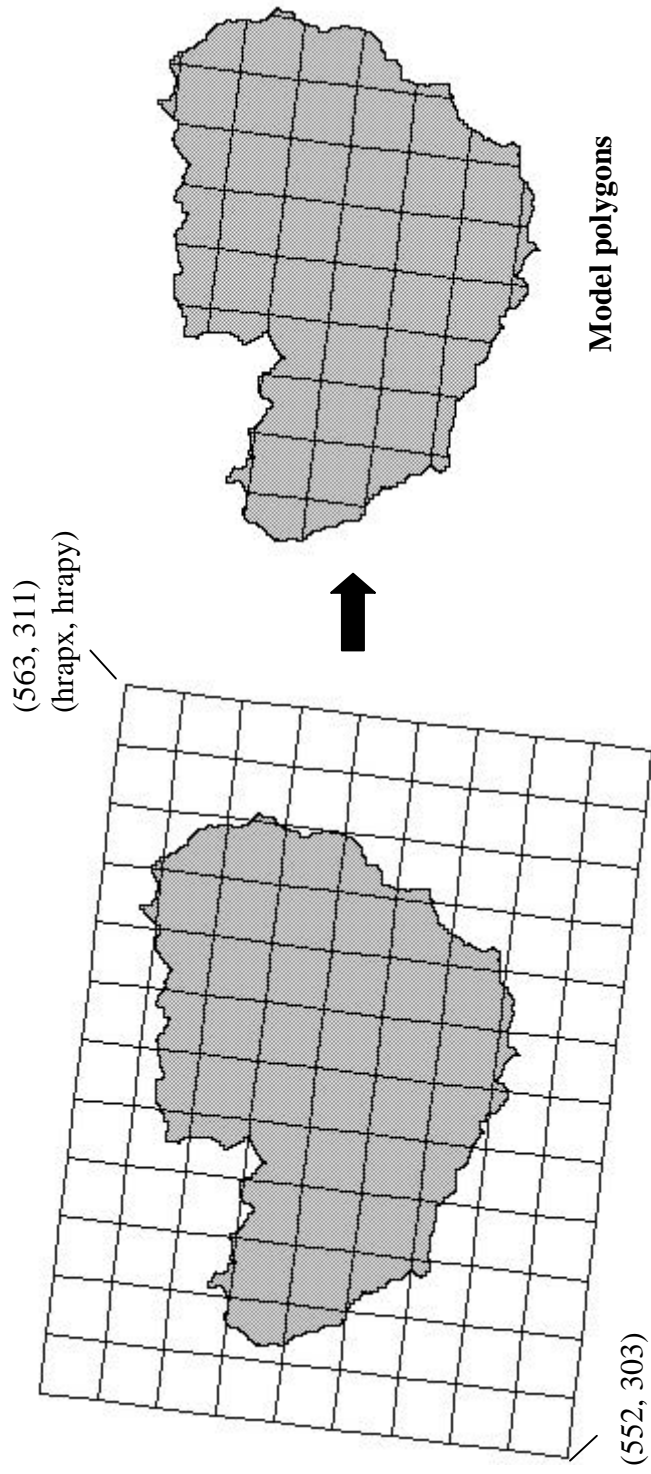


Figure 3.18 Intersecting NEXRAD cells with watershed boundary.

Three levels of resampling are considered for simplifying the description of soil properties in the model.

- No resampling: Estimate the percentage of each soil type or the percentage of each distinguishable soil component profile within each cell, and make vertical flux calculations separately for each of these units.
- NEXRAD cell level resampling. Assign a representative soil type to each NEXRAD cell.
- Watershed level resampling: Assign a representative soil type to the entire watershed.

The same rainfall data are used at all three levels; therefore, watershed level resampling is lumped in terms of soil properties but not lumped in terms of rainfall. For NEXRAD cell and watershed level resampling, the representative property is assigned based on the predominant soil type in the watershed or NEXRAD cell respectively. This approach is used rather than a weighted average because complex issues arise when trying to average soil properties such as water retention parameters that exhibit and control non-linear behavior. For each of the three resampling levels, soil properties may be estimated using either the STATSGO data or the 30-m soils grid.

Both the one-layer and two-layer models are considered for the case of no resampling. For the one-layer model this means that the percentage of each surface texture class (and the “other” class) falling within each NEXRAD cell must be computed. For the two-layer model, a list of components and the percentage area covered by each component are computed. In addition, a list of soil properties associated with each component is also computed for the two-layer model. A description of how this information is transferred from Arcview GIS to the hydrologic model written in Visual Basic is provided in Chapter 4. For all resampling levels, several non-soil parameters are computed for each NEXRAD cell

including area, average flow length to the watershed outlet, and percent imperviousness.

Although NEXRAD cells are used exclusively in this study, the spatial analysis programs used are general enough so that any polygons could be used to define uniform rainfall units (i.e. Thiessen polygons).

The acquisition of rainfall time series data is a somewhat tedious process. Archived, hourly Stage III data files are available from the Arkansas-Red Basin River Forecast Center (ABRFC) from July 24, 1994, to present. The Arkansas-Red Basin River Forecast Center is responsible for flood forecasting over a 538,487 km² area that covers seven states. Hourly Stage III files produced at ABRFC contain 53,265 data values. The archived files are in a special binary format called netCDF (Network Common Data Format) developed at the Unidata Program Center in Boulder, Colorado. Semi-automated procedures were developed to download and process netCDF rainfall files into a more tractable format, consisting of a comma delimited text file containing one column of time series data for each of the 55 NEXRAD cells intersecting the Little Washita watershed.

NetCDF files are obtained from the ABRFC through their Internet server (address given in Table 3.1). After downloading the data, a UNIX shell script is executed which runs a series of processing routines including a freeware program that converts netCDF files into ASCII files, and C and FORTRAN routines that are used to reformat the files and extract only the data for cells in the area of interest. The specific cells of interest in the Little Washita watershed are hardwired into the code. These programs are described further in Appendix B. Two months of netCDF data files (1440 files) can be processed in about 30 minutes running this procedure on a Sun Ultrasparc1. Comma delimited rainfall files containing data for the area of interest were prepared for October, 1995 – September, 1997, although not all of these data are used for analysis.

3.2.5. Data used to estimate evaporation

A conventional approach to estimating evaporation was discussed in Chapter 2. The development of an alternative method is considered in Section 3.3.2. Data from Department of Energy Atmospheric Radiation Measurement program Southern Great Plains Cloud and Radiation Testbed (DOE ARM SGP CART) sites are used in the development of the proposed method and a description of these data is left to Section 3.3.2. Although the data used for analysis in Section 3.3.2 are for locations outside of the Little Washita watershed, data from a different SGP CART site that lies within the Little Washita is used for simulation runs. The use of these data is also discussed in Section 3.3.2.

3.2.6. Data used for calibration and validation

15 minute runoff data for USGS gaging station 07327550 near Ninnekah, Oklahoma, for October, 1995, - October, 1997, were obtained from the Oklahoma USGS office. A Visual Basic program was written to compute hourly totals, flag missing data, and put the data into a more usable format. Further description of this data processing program is provided in Appendix B.

Gravimetric soil moisture measurements from Southern Great Plains 1997 Hydrology (SGP97) experiment are used in this study. SGP97 was an intensive hydrology field experiment organized jointly by the USDA and NASA that took place from June 18 - July 17, 1997. There were several objectives in SGP97 related to the use of in-situ and remote sensing observations to understand soil moisture and energy balance dynamics at different spatial scales. Numerous field and remote sensing measurements were taken during SGP97. A subset of the gravimetric soil moisture observations taken in SGP97 are used for model calibration in this study.

Gravimetric soil samples were taken at 23 different sites in the Little Washita watershed from June 18 – July 16, 1997. The locations of these sampling sites is shown in Figure 3.19. 9 to 14 samples were taken from the top 5 cm of soil twice

daily at each of the sites. Daily averages and standard deviations for gravimetric soil moisture ($GSM = \text{mass water(g)}/\text{mass of soil(g)}$) and bulk density ($\rho_b = \text{mass of soil(g)}/\text{total volume(cm}^3\text{)}$) were obtained from the SGP Internet site listed in Table 3.1. Using this information, daily average water content ($\bar{\theta}$) values for the top 5 cm of soil are computed using Equation 3.7.

$$\text{Equation 3.7} \quad \bar{\theta} = GSM * \frac{\rho_b}{\rho_w}$$

In Equation 3.7, ρ_w is the density of water taken as 0.997 g/cm^3 .

The soil textures at each of the 23 sampling sites are provided in the SGP documentation. Among the 23 sites, four different soil textures are represented: sandy loam (SL), loamy sand (LS), loam (L), and silt loam (SIL). Sites 3, 4, and 5 are all loamy sand sites and fall within the same NEXRAD cell (557, 309). The daily values from these three sites are averaged so that a comparison can be made with simulated results for loamy sand in cell (557, 309). Other sites chosen for analysis include sites 8 and 9 with silt loam soils that fall within cell (555, 307), sites 11, 12, and 13 with loam soils that fall within cell (560, 309), and site 17 with sandy loam soil that falls within cell (559, 305). Use of observed soil moisture for model calibration is discussed in Chapter 5.

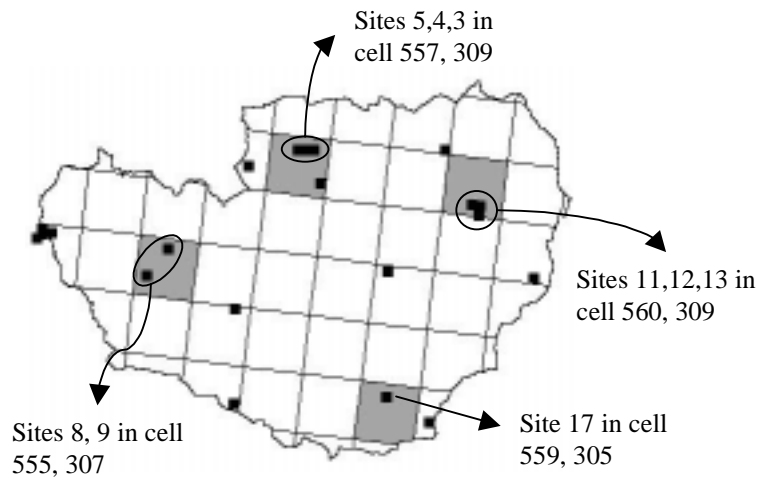


Figure 3.19 Locations for gravimetric soil moisture sampling during SGP97.

A dense meteorological observation network operated by the Agricultural Research Service Grazinglands Research Laboratory includes 42 stations covering areas in and around the Little Washita. This network is called the Micronet. The Micronet, which contains about 1 rain gage per NEXRAD cell, has an unusually high network density that cannot be found at many locations in the world. The locations of the Micronet rain gages are shown in Figure 3.20. Rainfall data from this network are available for the months of June, July, and August, 1997, from the SGP Internet site listed in Table 3.1, although many stations were not reporting until mid-June. Hourly average values for the Little Washita as a whole were computed from 5 minute cumulative totals available for each gage. As discussed in Chapter 5, these hourly averages are compared with spatially averaged NEXRAD Stage III radar estimates to try to assess the quality of the NEXRAD data being used for simulations.

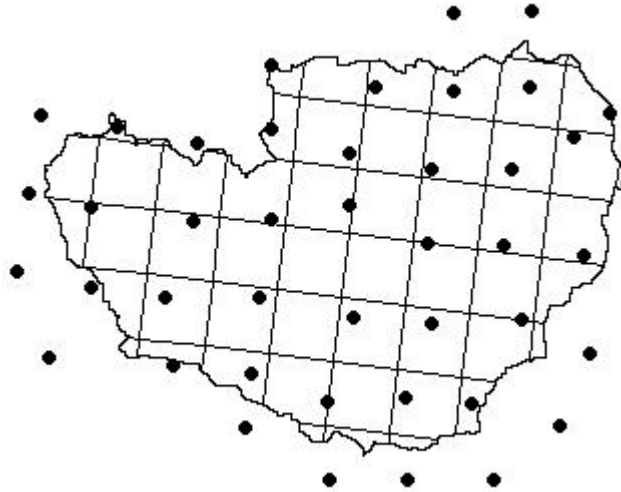


Figure 3.20 Locations of Micronet stations.

3.3. Process Representation

3.3.1. Direct runoff computation

Direct runoff forms the rapidly varying portions of watershed hydrographs. In event simulation, direct runoff can be defined as the fraction of rainfall that is not lost to interception, depression storage, or infiltration. In this study, infiltration is the only loss mechanism that is explicitly modeled, in part, because infiltration parameters can be estimated from available data, but no satisfactory scheme has been developed to parameterize other mechanisms such as interception, depression storage, and channel storage. Direct runoff could evaporate while flowing to the watershed outlet, but this additional loss mechanism is not considered in this study due to the relatively short time of concentration (12 hours).

Interception is an important factor in forested areas, accounting for as much as 40% of the gross precipitation in some forests (Dingman, 1994) but is not as important in the agricultural and rangeland areas, which predominate in the Little Washita watershed. Previous researchers have used the leaf area index (LAI),

defined as the leaf area per unit of ground area to estimate interception. It is difficult to support seasonally varying estimates of leaf area index with the data used in this research. Although beyond the scope of this research, the use of remote sensing data to estimate leaf area index values is discussed briefly in Section 3.3.2 on evaporation. The model described in this manuscript has proven useful and insightful without an explicit parameterization for interception.

Since the Little Washita watershed is an agricultural watershed in a sub-humid climate with moderately rolling topography (Allen and Naney, 1991), the dominant control on direct runoff generation is assumed to be soil texture. Although topography influences soil moisture locally, it appears from the remote sensing images of Jackson *et al.* (1996) that soil texture plays a bigger role than vegetation or topography in controlling large scale soil moisture distributions in the Little Washita watershed.

Impervious areas will significantly influence direct runoff production in a watershed. The percent impervious area in each model polygon is computed using the land use coverage (Figure 3.15) and Table 3.6. Impervious areas generate direct runoff even during small storms when the infiltration capacity of even the least permeable soils is never exceeded. The percent imperviousness for each model polygon in the Little Washita is shown in Figure 3.21.

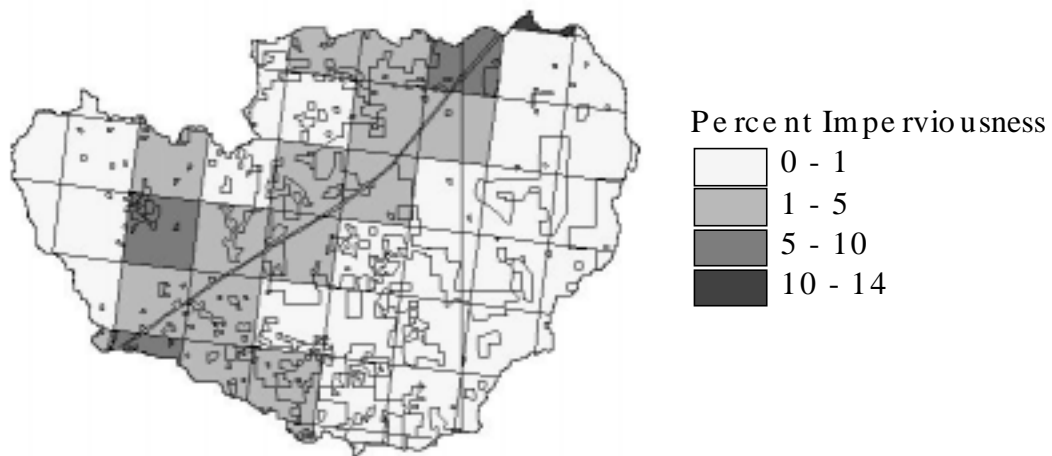


Figure 3.21 Average percent imperviousness in each NEXRAD cell.

3.3.1.1. Green-Ampt model

For reasons discussed in Section 2.4, the Green-Ampt infiltration model is used in this study. The Green-Ampt model approximates vertical infiltration into a semi-infinite homogeneous soil under ponded surface conditions. Experimental evidence indicates that a short period of time after surface ponding, a plot of soil moisture versus depth reveals a curved wetting front, which maintains a constant shape as it advances into the soil (Jury, Gardner, and Gardner, 1991). An analogy is often made between this wetting front and the movement of a piston, which advances but does not change shape (Figure 3.22). To derive a simple expression for the infiltration rate as a function of cumulative infiltration, an abrupt wetting front is assumed in the Green-Ampt model as shown in Figure 3.23. Two parameters that control the rate of infiltration are the hydraulic conductivity behind the wetting front and the average wetting front suction head.

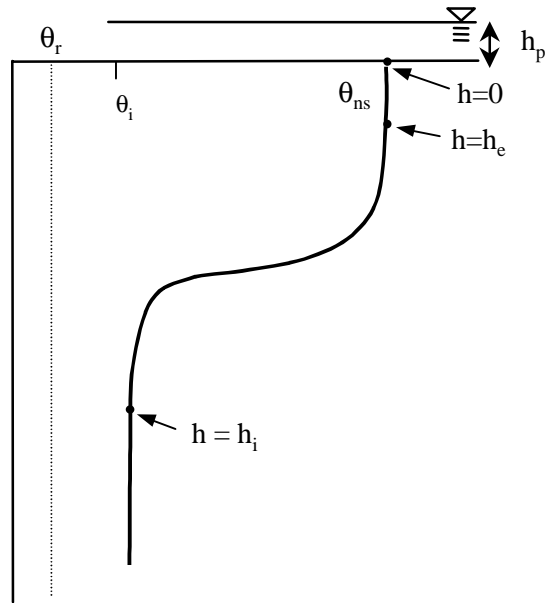


Figure 3.22 Curved wetting front formed during infiltration into a homogeneous, uniformly wetted soil.

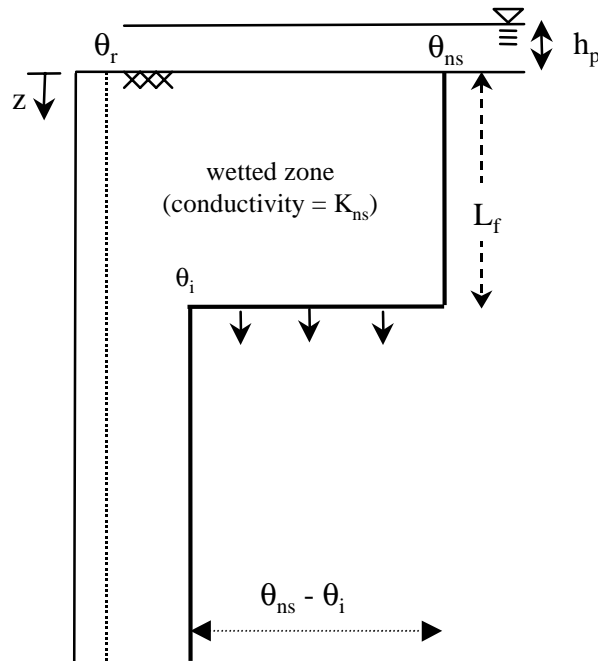


Figure 3.23 Idealized infiltration into a homogeneous, uniformly wetted soil with a sharp wetting front.

The rate of infiltration and the wetting front suction head (h_f) itself are both functions of the initial water content of the soil (θ_i). The physical meaning of the wetting front suction head (h_f) has been the subject of debate in the literature. Mein and Larson (1973) suggest that h_f can be estimated using Equation 3.8.

$$\text{Equation 3.8} \quad h_f = \int_0^{h_i} k_{rw}(h)dh$$

In Equation 3.8, k_{rw} is the relative permeability ($K(h)/K_s$), h is suction head, h_i is the suction head at the initial saturation of the soil. Evaluation of the integral in Equation 3.8 is discussed in the next section. Neuman (1976) shows how the expression in Equation 3.8 can be derived theoretically by presenting a formal derivation of the Green-Ampt infiltration equation. The derivation of Neuman is reproduced here.

Darcy's law quantifies the vertical flux at any point in the soil column. With the z -coordinate positive downward as in Figure 3.23, Darcy's can be written as:

$$\text{Equation 3.9} \quad q = K(h) \left(\frac{d(h+z)}{dz} \right) = K(h) \left(\frac{dh}{dz} + 1 \right)$$

Considering Figure 3.22, the total flux into the soil column can be estimated by rearranging Equation 3.9 and integrating from the ponded surface to the bottom edge of the wetting front.

$$\text{Equation 3.10} \quad \int_0^{L_f} qdz = \int_{h_p}^{h_i} K(h)dh + \int_0^{L_f} K(h)dz$$

or

$$\text{Equation 3.11} \quad \int_0^{L_f} qdz = \int_{h_p}^0 K(h)dh + \int_0^{h_i} K(h)dh + \int_0^{L_f} K(h)dz$$

It is assumed that the hydraulic conductivity is constant between ponding depth (h_p) and elevation zero. Because an abrupt wetting front is assumed, then q is constant and the hydraulic conductivity is constant from the ground surface to the abrupt front. Neuman (1976) takes the constant hydraulic conductivity behind the wetting

front as K_s , the saturated hydraulic conductivity associated with air entry that is normally reported in the literature. Based on these assumptions, the integral on the left-hand-side of Equation 3.11 and the first and third integrals on the right-hand-side can be evaluated as follows:

$$\text{Equation 3.12} \quad qL_f = K_s h_p + \int_0^{h_i} K(h)dh + K_s L_f$$

Factoring K_s out of the remaining integral and dividing through by L_f yields an equation for infiltration rate (i).

$$\text{Equation 3.13} \quad i = q = \frac{K_s (L_f + \int_0^{h_i} k_{rw} dh + h_p)}{L_f}$$

The remaining integral is the same as Equation 3.8 and defines the wetting front suction head term (h_f). A method for evaluating this integral (h_f) is presented in the next section.

Bouwer (1969) notes that the actual hydraulic conductivity of the wetted zone in the Green-Ampt model is less than the saturated hydraulic conductivity (K_s) due to entrapped air. Bouwer (1969) suggests estimating the hydraulic conductivity of the wetted zone as half of the saturated hydraulic conductivity (K_s) based on his review of hydraulic conductivity-suction head relationships presented in the literature. This assumption is cited by Rawls, Brakensiek, and Miller (1983) and Charbeneau and Asgian (1991). Following Charbeneau and Asgian (1991), the term natural saturation (K_{ns}) will be used here to refer to the hydraulic conductivity behind the wetting front that is taken as half of K_s .

$$\text{Equation 3.14} \quad K_{ns} = \frac{K_s}{2}$$

Replacing K_s by K_{ns} in Equation 3.13 and assuming surface ponding (h_p) is negligible yields:

$$\text{Equation 3.15} \quad i = \frac{K_{ns} (L_f + \int_o^{h_i} k_{rw} dh)}{L_f}$$

Strictly speaking, the term K_{ns} should be substituted for K_s in Equation 3.12 rather than in Equation 3.13. Doing this would produce a factor of 1/2 in front of the integral expression for h_f , giving the value of h_f as half of the value computed using Equation 3.8. In evaluating the integral expression for h_f (described in the next section), this factor of 1/2 is not included so that the results are consistent with the expression for h_f derived by Brakensiek (1977) that appears to have gained acceptance in the literature.

Given the assumption that there is trapped air in the wetted soil, the wetted zone does not have a saturation equal to 1. During an event, the water content jumps from its initial value (θ_i) to the water content (θ_{ns}) that corresponds natural saturation (Θ_{ns}) (Charbeneau and Asgian, 1991). θ_{ns} can be computed by substituting $K_{ns} = 1/2 K_s$ into the Brooks and Corey relative permeability relationship (Equation 3.16) and then solving for θ_{ns} (Equation 3.17).

$$\text{Equation 3.16} \quad \frac{K_{ns}(\theta)}{K_s} = (\Theta_{ns})^{3+2/\lambda} = \left(\frac{\theta_{ns} - \theta_r}{\phi - \theta_r} \right)^{3+2/\lambda} = \frac{1}{2}$$

$$\text{Equation 3.17} \quad \theta_{ns} = (\phi - \theta_r) \left(\frac{1}{2} \right)^{\left(\frac{1}{3+2/\lambda} \right)} + \theta_r$$

Using the Carsel and Parrish values for the Brooks and Corey parameters given in Table 3.3, natural saturation values for each of the 12 USDA soil texture classes are computed and given in Table 3.7. In the proposed model, the top layer water content is not allowed to exceed θ_{ns} to ensure that the water deficit ($\theta_{ns} - \theta_i$) is always positive. In natural soils, θ_{ns} may be exceeded if water is not drained and trapped air has time to escape from the soil.

Table 3.7 Natural saturation values corresponding to the 12 USDA texture classes.

Class Name	Symbol	Θ_{ns}
sand	S	0.85
loamy_sand	LS	0.86
sandy_loam	SL	0.88
sandy_clay_loam	SCL	0.91
loam	L	0.90
silt loam	SIL	0.92
clay_loam	CL	0.93
silt	SI	0.92
clay	C	0.97
sandy_clay	SC	0.94
silty_clay_loam	SICL	0.94
silty_clay	SIC	0.97

The jump in water content from θ_i to θ_{ns} defines the relationship between cumulative infiltration (I) and the depth of the wetting front (L_f)

$$\text{Equation 3.18} \quad I = (\theta_{ns} - \theta_i)L_f$$

Solving Equation 3.18 for L_f and substituting into Equation 3.13 yields an equation where the infiltration rate (i) is a function of cumulative infiltration (I).

$$\text{Equation 3.19} \quad i = \frac{dI}{dt} = \frac{K_{ns}(I + h_f(\theta_{ns} - \theta_i))}{I}$$

An expression for the cumulative infiltration as a function of time can be derived by separating and integrating Equation 3.19 from 0 to t.

$$\text{Equation 3.20} \quad I - h_f(\theta_{ns} - \theta_i) \ln \left[\frac{I}{h_f(\theta_{ns} - \theta_i)} + 1 \right] = K_{ns}t$$

This equation can be solved for I using iterative substitution or by using the Newton-Raphson root finding method. The Newton-Raphson method is used in the computer codes developed for this study. Equations 3.19 and 3.20 only apply if the rainfall has ponded to a small depth at the soil surface, meaning that the rainfall rate

has exceeded the potential infiltration rate. Therefore, time to ponding must be determined in order to make direct runoff computations.

Mein and Larson (1973) describe a method for determining ponding time under a constant rainfall rate (r). The assumption is that all rainfall infiltrates before ponding occurs and ponding begins when the potential infiltration rate (computed with Equation 3.19) drops below the rainfall rate. Therefore, time to ponding (t_p) occurs when the potential infiltration rate (i) equals the rainfall rate (r). Since all rainfall that occurs before ponding infiltrates, the cumulative infiltration at ponding time (I_p) equals rt_p when the rainfall rate is constant. Substituting this expression for I_p into Equation 3.19 and setting $i = r$ yields an expression for the cumulative infiltration at ponding under a constant rainfall rate.

$$\text{Equation 3.21} \quad I_p = rt_p = \frac{K_{ns} h_f (\theta_{ns} - \theta_i)}{(r - K_{ns})}$$

Computing infiltration under variable rainfall conditions is discussed in Section 3.3.1.3.

3.3.1.2. Estimating wetting front suction head

The derivation method presented here follows that of Brakensiek (1977). To estimate the wetting front suction head at the onset of each storm, the Brooks and Corey relative permeability relationship is substituted into the integral defining the wetting front suction head in Equation 3.8. Graphically, h_f is the area under the relative permeability curve for wetting shown in Figure 3.24 (for a loam soil) and described by Equation 3.22.

$$\text{Equation 3.22} \quad k_{rw} = (\Theta_w)^{3+2/\lambda} = \left(\frac{h_{we}}{h} \right)^{3\lambda+2}$$

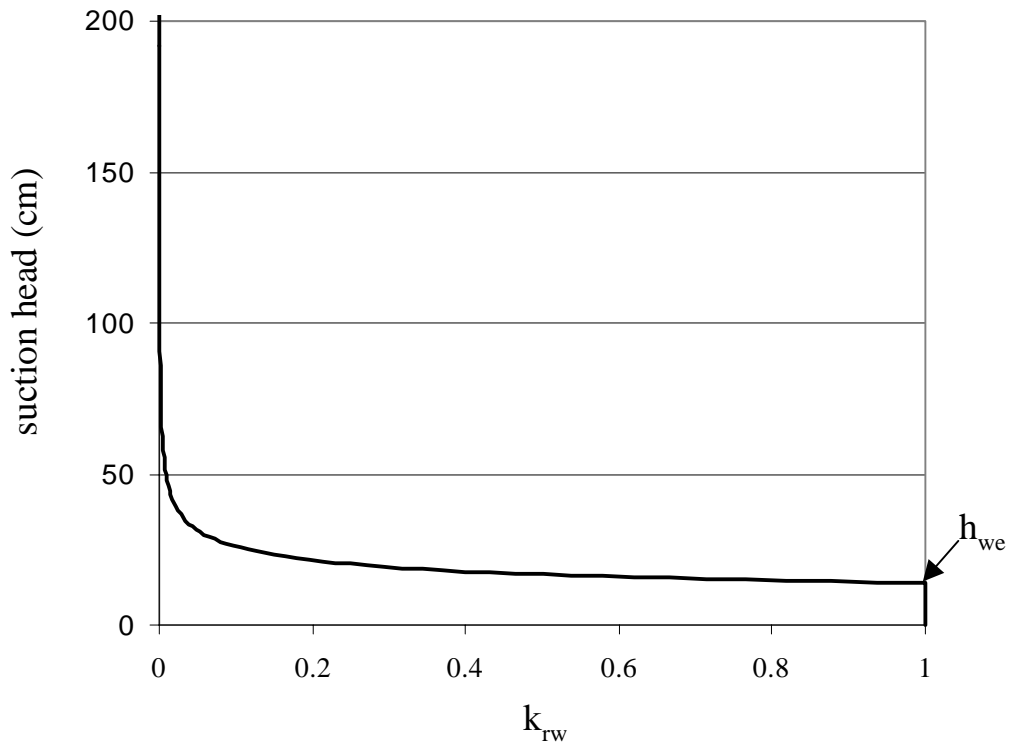


Figure 3.24 Example relative permeability curve for wetting ($\lambda = 0.56$, $h_b = 27.8$).

Following Brakensiek (1977), the wetting front suction head can be calculated by breaking Equation 3.8 into two parts as shown in Equation 3.23.

$$\text{Equation 3.23} \quad h_f = \int_0^{h_i} k_{rw}(h)dh = \int_0^{h_{we}} dh + \int_{h_{we}}^{h_i} k_{rw}(h)dh$$

During sorption, $k_{rw}(h)$ is 1 between $h = 0$ and $h = h_{we}$. Above h_{we} , $k_{rw}(h)$ begins to decrease. Given the relationship shown in Equation 3.22, the second integral on the right hand side of Equation 3.23 can be written in terms of effective saturation and solved. To do this, a variable substitution is made by solving Equation 3.22 for suction (h) as a function of effective saturation (Θ) and taking the derivative of h with respect to Θ .

$$\text{Equation 3.24} \quad \frac{dh}{d\Theta_w} = -\frac{h_{we}}{\lambda} \Theta_w^{(-1/\lambda-1)}$$

Equation 3.23 then becomes

$$\text{Equation 3.25} \quad h_f = h_{we} - \int_1^{\Theta_i} \Theta_w^{(3+2/\lambda)} \frac{h_{we}}{\lambda} \Theta_w^{(-1/\lambda-1)} d\Theta$$

which evaluates to

$$\text{Equation 3.26} \quad h_f = -\frac{h_{we} \Theta_w^{(3+1/\lambda)}}{3\lambda+1} + \frac{h_{we}}{3\lambda+1} + h_{we}$$

This result is consistent with the result presented by Brakensiek (1977) for wetting front suction head into a completely dry soil if the effective saturation is set equal to zero and the substitution $h_{we} = h_b/2$ is made. That result is:

$$\text{Equation 3.27} \quad h_f = \frac{h_b}{2} \left(\frac{2+3\lambda}{3\lambda+1} \right)$$

3.3.1.3. Computational scheme for Green-Ampt infiltration under variable rainfall

To make infiltration calculations under variable rainfall using the Green-Ampt model, the computational scheme described in Figure 5.4.1 of Chow, Maidment, and Mays (1988) is used. This solution scheme uses the integral form of the infiltration equation rather than a time stepping method so there is no error associated with the numerical algorithm. A key idea in implementing this method is that the cumulative infiltration at the end of a time interval Δt can be written as a function of the cumulative infiltration at the beginning of that interval as follows.

$$\text{Equation 3.28} \quad I_{t+\Delta t} - I_t - h_f(\theta_{ns} - \theta_i) \ln \left[\frac{I_{t+\Delta t} + h_f(\theta_{ns} - \theta_i)}{I_t + h_f(\theta_{ns} - \theta_i)} \right] = K_{ns} \Delta t$$

Equation 3.28 is derived by writing Equation 3.20 for both time t and time $t+\Delta t$ and then subtracting the two equations.

The pseudo-code in Figure 3.25 summarizes the scheme for computing infiltration.

In both the one-layer and two-layer soil models, the top layer properties are assumed to control infiltration.

```

'-----
' variables:
' I      final cumulative infiltration
' i      potential infiltration rate
' r      rainfall rate
' subscripts t and t+dt refer to current and next time step respectively
' subscript p refers to the ponding time
' first_time: boolean variable that is true if t = 1
'-----

Initialize I, It, and It+dt, to 0

MAIN LOOP: For all time steps t with positive precipitation
If this is the first time step
    Set It = 0
    Set first_time = True
Endif
If this is not the first time step then
    Compute infiltration rate at time t (it) with Equation ___
Endif
If (ponding has not occurred (it > rt)) or (if this is the first time step)
    Calculate tentative values I't+dt and i't+dt assuming that all rainfall infiltrates
    If (i't+dt > rt) then ponding does not occur in the interval
        It+dt = I't+dt
    Else ponding occurs at some point in the interval
        Calculate the cumulative infiltration at ponding Ip based on Equation ___
        with r = rt
        Determine the ponding time t+Δt' where Δt' = (Ip - It) / rt
        Solve Equation 3.28 iteratively for It+dt with It = Ip and Δt = Δt - Δt' using
        the Newton-Raphson method
    End If
    first_time = False
Else ponding occurs throughout interval
    Solve Equation 3.28 for It+dt using the Newton-Raphson method
End If
' reinitialize cumulative infiltration before the next time step
It = It+dt

END MAIN LOOP through time steps

```

Figure 3.25 Pseudo-code for computation of Green-Ampt infiltration under variable rainfall.

3.3.2. Evaporation

In Section 2.5, a conventional method for estimating evaporation was described that uses an empirical crop coefficient. Shuttleworth (1993) notes that the crop coefficient has a poor theoretical basis and implicitly has meteorological dependence. He recommends that future research be directed towards estimating surface resistance values rather than crop coefficients. An analysis of data from SGP CART sites presented here lends insight into the relationship between surface resistance and soil moisture, and an alternative to the conventional method of estimating evaporation under moisture limiting conditions (Figure 2.1) is investigated.

3.3.2.1. Surface Resistance

The Penman-Monteith method is a widely accepted approach for estimating reference crop evaporation. The Penman-Monteith method is attractive because it has a sound physical basis and because its accuracy is proven when compared with lysimeter measurements. In fact, this method was rated first in accuracy among twenty methods for estimating reference crop evaporation in ASCE (1990). The Penman-Monteith equation can be written as follows:

$$\text{Equation 3.29} \quad lE_m = \frac{\Delta(R_n + G) + \rho_a c_p D / r_a}{\Delta + \gamma(1 + r_s / r_a)}$$

In Equation 3.29, lE_m is the energy flux used for evaporation [W m^{-2}] (l is the latent heat of vaporization in [J kg^{-1}] and E_m is the mass flux of water vapor [$\text{kg m}^{-2} \text{s}^{-1}$]), R_n is the net radiation absorbed at the land surface [W m^{-2}], G is the ground heat flux [W m^{-2}], Δ is the gradient of the saturation vapor pressure curve [$\text{kPa } ^\circ\text{C}^{-1}$], ρ_a is the density of moist air [kg m^{-3}], c_p is the specific heat of moist air [$\text{J kg}^{-1} \text{ } ^\circ\text{C}^{-1}$],

D is the vapor pressure deficit [kPa], γ is the so-called psychrometric constant [kPa °C⁻¹], r_a is the aerodynamic resistance to diffusive mass transfer of water vapor [s m⁻¹], and r_s is the surface resistance to mass transfer due to the vegetation canopy [s m⁻¹]. The variables and parameters R_n , G , Δ , ρ_a , c_p , and γ in Equation 3.29 can either be measured directly or estimated in a fairly straightforward manner from temperature and pressure. Critical variables that cannot be measured directly and are more difficult to estimate are the aerodynamic (r_a) and surface (r_s) resistances. The units for r_a and r_s are [s m⁻¹] because these resistances are equal to a concentration difference [kg m⁻³] divided by a mass flux [kg m⁻² s⁻¹].

The aerodynamic resistance (r_a) is a function of both the crop height and the wind profile. r_a is often estimated by assuming a logarithmic wind profile and making an estimate of the surface roughnesses for heat and vapor transfer as a function of the crop height.

The surface resistance (r_s) refers to the total resistance of all leaves in a canopy. When estimates of reference crop evaporation are made, a specific crop type (grass or alfalfa) and height are assumed. With this information, the minimum surface resistance (r_{smin}) may be estimated using an approximation for surface resistance as a function of leaf area index (LAI) (Shuttleworth, 1993). The variable r_{smin} here is equivalent to the parameter " r_s " used by Shuttleworth (1993). Surface resistance is inversely proportional to leaf area index. The minimum surface resistance (r_{smin}) is the value of surface resistance when there is no water stress (when potential evaporation is occurring).

Use of the Penman-Monteith equation to estimate reference crop evaporation is feasible and is done commonly in practice. It is a much more difficult problem to predict actual evaporation when soil-water is limiting by using Equation 3.29. Monteith (1980) notes that "it is impossible to predict with confidence how r_c [equivalent to r_s used here] will change during a growing season as soil water is depleted by root extraction and replenished by rain or irrigation." The two key

factors cited by Monteith (1980) that control surface resistance are changes in soil-water content which affects the leaf water content and therefore the stomatal resistance of individual leaves, and changes in the leaf area index which affect the net resistance for the entire canopy.

Using an analogy to electrical resistance for parallel resistors, the net surface resistance (r_s) for a canopy is approximated as the individual leaf resistance (r_{leaf}) divided by the leaf area index. Monteith (1980) suggests that empirical evidence may be used to determine a value for r_s as a function of soil-water potential. Monteith also suggests that “progress [in calculating the actual evaporation rate as a function of soil-water content] in the immediate future calls for the shrewd interpretation of evidence from carefully designed field experiments rather than the development of more comprehensive simulation models.” The work presented in the following sections represents an attempt to pursue this line of thinking, although the field experiments were not carefully designed by the author — rather, selected data sets from sites being extensively monitored for other purposes are used to illustrate an idea. The idea is to see if useful empirical relationships between surface resistance (r_s) and soil-water potential can be derived.

3.3.2.2. Data analysis: evaporation

This section describes the analysis of field data that were collected as part of the Department of Energy’s Atmospheric Radiation Measurement (ARM) program. The ARM data collection program is an ongoing effort to improve scientific understanding of radiative energy fluxes in the Earth's atmosphere. One goal of the program is to improve radiative transfer parameterizations in General Circulation Models. Three field measurement sites called Cloud and Radiation Testbeds (CART) are part of the ARM program. These sites include the Southern Great Plains site in Kansas and Oklahoma, USA, a Tropical Western Pacific Site, and a

North Slope of Alaska site. More information about this program can be found on the Internet at www.arm.gov.

Three data streams from the Southern Great Plains site are used in the analysis presented here. The word “streams” is used by in the ARM program to refer to the stream of measurements that are produced by selected group of instruments. These data streams include Energy Balance and Bowen Ratio (EBBR) data, Surface Meteorological Observation System (SMOS) data, and Soil Water and Temperature Sensors (SWATS) data. EBBR, SMOS, and SWATS data for certain facility locations and time periods are easily accessible from the ARM Archive Internet site (www.archive.arm.gov/data/ordering.html). The EBBR and SMOS data streams are classified as "production" data streams because these data streams have routine and well-developed procedures for instrument operations, data processing, and data review. The SWATS data streams are classified as "developmental" data streams as of June 1, 1998, indicating that data quality control procedures are relatively immature (www.arm.gov/docs/instruments/static/swats.html). Calibrations to convert SWATS matric potential estimates into volumetric water content estimates are still being refined.

The idea proposed here is to examine functional relationships between surface resistance and soil-water potential using EBBR, SMOS, and SWATS data. In theory, this type of relationship could be used in a continuous soil-water balance model to estimate r_s at any given time. Values of r_s are estimated by solving Equation 3.29 for r_s and determining values for all other variables in Equation 3.29 using the EBBR and SMOS data. Before describing these calculations in more detail, further description of the ARM data sets is provided.

There are a number of instrumented sites in the ARM SGP study area covering central Oklahoma and south-central Kansas. To give an idea of the areal extent of the SGP study area, the locations for 22 of the instrumented sites are shown in

Figure 3.26. These points were plotted based on latitude and longitude values for extended facilities provided by Peppler, Sisterson, and Lamb (1997).

Many different instruments are used throughout the ARM SGP study area, but the instrumentation varies from site to site. To facilitate the proposed analysis, the EBBR, SMOS, and SWATS instrument sets must coexist at selected sites and data from these instruments must be available for coincident time periods. According to Peppler, Sisterson, and Lamb (1998), 8 of 26 extended facilities should be equipped with all three required instrument sets by the end of 1997. Unfortunately, one or more of the desired data streams at some of these sites were either not available from the ARM data archive or contained measurements of suspect quality. Data from extended facilities EF-4 (Plevna, KS) and EF-7 (Elk Falls, KS) were used for analysis because the necessary data were available for these sites at the time of this study. Data from these two sites are adequate to illustrate the proposed idea. Large volumes of data that could support further study are continuously being created at the ARM sites.

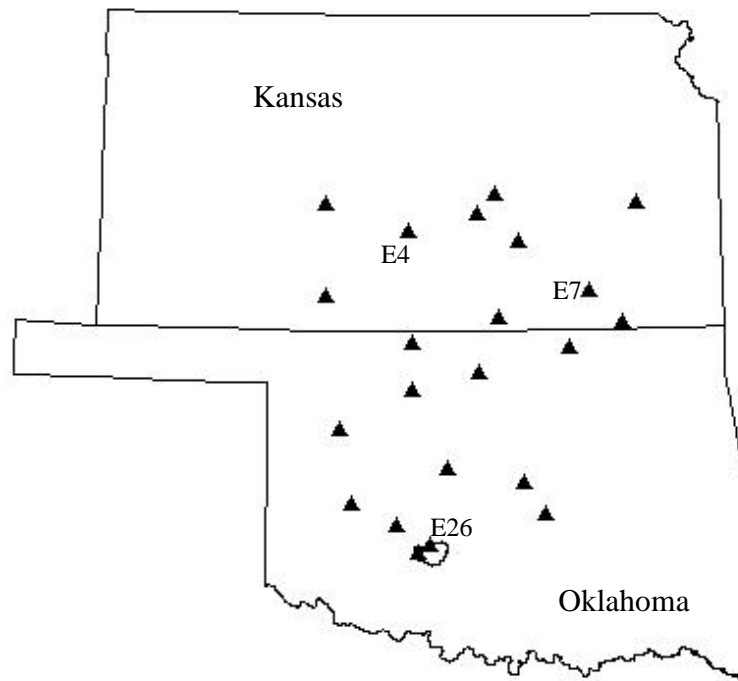


Figure 3.26 Locations of 22 ARM Measurement Sites

Equation 3.29 is rearranged here so that r_s is written as a function of variables that can be determined from instrument measurements.

$$\text{Equation 3.30} \quad \bar{r}_s = \left[\frac{\overline{\Delta(R_n + G)} + \frac{\bar{\rho}_a c_p \bar{D}}{\bar{r}_a}}{\bar{\gamma} \bar{E}} - \frac{\bar{\Delta}}{\bar{\gamma}} - 1 \right] \bar{r}_a$$

Bars over the variables indicate daily average values. Although the Penman-Monteith equation is only theoretically valid at a single instant in time and is more accurate when used with hourly data than with daily data, the Penman-Monteith equation can provide reliable estimates of evaporation when daily mean climatic input values are used (ASCE, 1990). Although the ARM data would support estimating hourly values of r_s , meteorological observations available in most areas will not support hourly computations for evaporation. For these reasons, representative daily surface resistance values are computed here rather than hourly r_s

values. Monteith, Szeicz, and Waggoner (1965) showed that surface resistance can vary considerably throughout the day. A large part of this variation is attributable to the amount of sunlight received by the plants, which influences the degree to which stomata are opened. Making daily calculations averages out diurnal variations in surface resistance. When r_s is computed using Equation 3.30, the result is really the combined resistance due to both bare soil and plants; however, when vegetation is dense or when the soil surface is dry, evaporation from the bare soil is negligible (Monteith, Szeicz, and Waggoner, 1965).

In Equation 3.30, R_n , G , and lE are estimated using EBBR data; Δ , ρ_a , D , γ , and r_a are estimated using SMOS data; and c_p , the specific heat of moist air, is taken as $1013 \text{ J kg}^{-1} \text{ C}^{-1}$.

The Energy Balance Bowen Ratio (EBBR) systems are primarily designed to estimate vertical fluxes of sensible and latent heat at the land surface. Net radiation (R_n) absorbed at the Earth's surface is consumed by either heating the air (sensible heat flux, H), converting liquid water into water vapor (latent heat flux, lE), or heating the soil (ground heat flux, G). The sum of the energy fluxes at the Earth's surface is equal to zero.

$$\text{Equation 3.31} \quad R_n + H + lE + G = 0$$

In Equation 3.31, the units of each term are $[\text{J m}^{-2} \text{ s}^{-1}]$ or $[\text{W m}^{-2}]$. At each EBBR location, R_n and G are measured. The sum of R_n and G is sometimes referred to as the available heating.

The Bowen ratio (β), the ratio of sensible heat flux to latent heat flux (H/lE), is used to partition the available heating between latent and sensible heat fluxes. The Bowen ratio is estimated using measurements of temperature and relative humidity (converted to vapor pressure) at two heights. Derivations of equations that can be used to estimate the Bowen ratio from such measurements are presented by Chow, Maidment, and Mays (1988). Given 30 minute average estimates of R_n , G , and β , 30 minute average estimates of lE and H are estimated using

Equation 3.32
$$lE = \frac{-(R_n + G)}{(1 + \beta)}$$

and

Equation 3.33
$$H = \beta lE$$

For use in Equation 3.30, daily average values of R_n , G , and lE are computed from the 30 minute values. The Bowen ratio method becomes unstable if β is close to -1 , which may occur in the evening or morning hours when the sensible heat flux changes direction. To avoid this type of problem, the lE estimates for time periods in which $-1.5 < \beta < -0.65$ are not considered in the daily averaging.

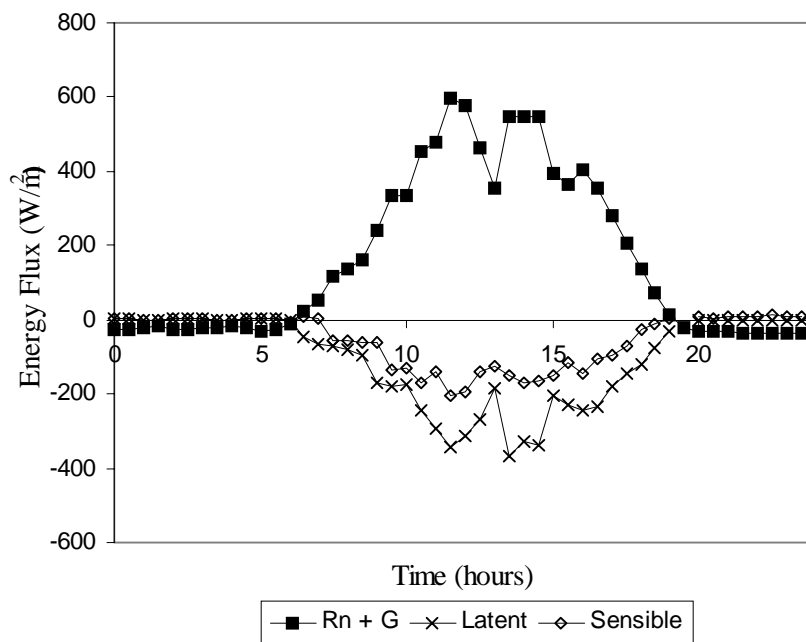


Figure 3.27 Surface radiation budget components at ARM SGP Site EF7 on July 29, 1997.

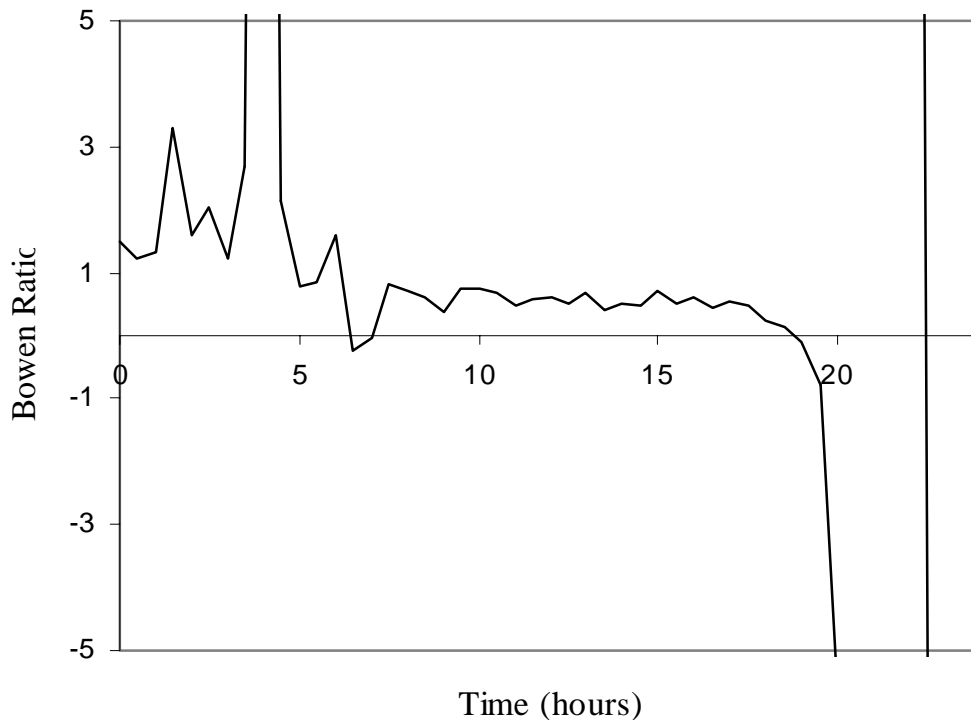


Figure 3.28 30 minute Bowen ratio values at the ARM SGP Site EF7 on July 29, 1997.

Typical surface radiation flux values and Bowen ratio values are shown in Figures 3.27 and 3.28 for ARM SGP site EF7 on July 29, 1997. Negative radiation fluxes are directed away from the earth's surface and positive fluxes are directed towards the earth's surface. Net radiation is positive during the day but becomes slightly negative during the night. A downward spike occurs in the 27th half-hour period for the day, 1:00 - 1:30 p.m. A possible explanation for this spike is that a cloud covered the measurement site during this time. The measured Bowen ratio often remains relatively constant during daytime hours but can become unstable at night.

The gradient of the saturation vapor pressure curve (Δ), the air density ρ_a , the vapor pressure deficit (D), the psychrometric constant (γ), and the aerodynamic resistance (r_a) are estimated using SMOS data. The SMOS measurements that are

used for these calculations include wind speed at 10 m, air temperature and relative humidity (RH) at 2 m, and barometric pressure at 1 m. Although 24 hour averages of these variables are used for calculations, it is interesting to see plots showing how some of these meteorological variables vary throughout the day. Plots of wind speed, temperature and relative humidity, and vapor pressure deficit are shown in Figures 3.28, 3.29, and 3.30 for ARM SGP site EF7 on July 29, 1997.

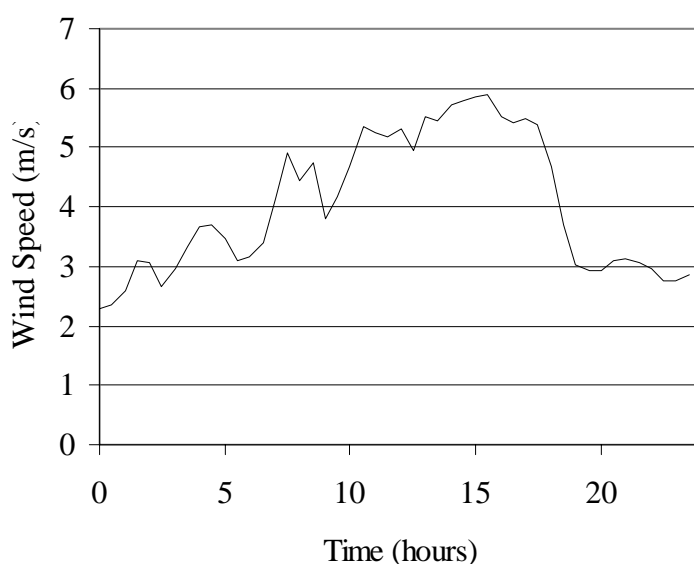


Figure 3.29 Wind speed (m/s) at site EF7 on July 29, 1997.

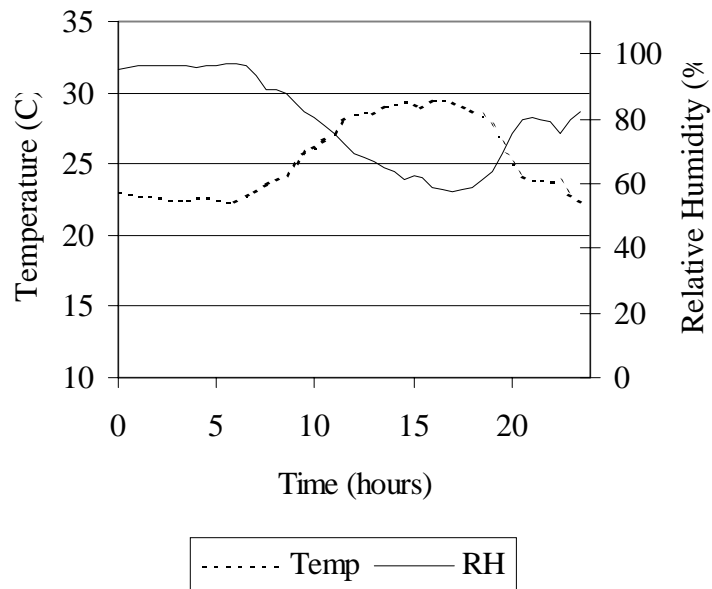


Figure 3.30 Temperature (°C) and relative humidity (RH) at site EF7 on July 29, 1997.

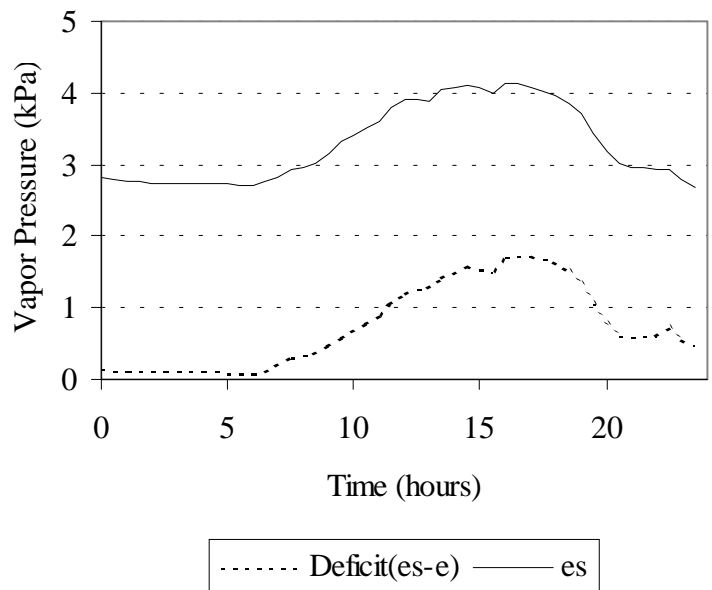


Figure 3.31 Vapor pressure deficit and vapor pressure at site EF7 on July 29, 1997.

Δ is computed using the average daily air temperature (T) at 2 m and the following two equations:

$$\text{Equation 3.34} \quad e_s = 0.6108 \exp\left(\frac{17.27T}{237.3+T}\right)$$

$$\text{Equation 3.35} \quad \Delta = \frac{4098e_s}{(237.3+T)^2}$$

T is air temperature [$^{\circ}\text{C}$] and e_s is the saturation vapor pressure [kPa] corresponding to the temperature T. The density of moist air [kg m^{-3}] is estimated as

$$\text{Equation 3.36} \quad \rho_a = 3.486 \frac{P}{273+T}$$

following Shuttleworth (1993). P is atmospheric pressure [kPa] and T is temperature [$^{\circ}\text{C}$]. Daily average values for P and T were used to make calculations. The vapor pressure deficit (D) [kPa] is the difference between the saturation vapor pressure and the actual vapor pressure.

$$\text{Equation 3.37} \quad D = e_s - e = e_s(1 - RH)$$

$$\text{Equation 3.38} \quad RH = \frac{e}{e_s}$$

This deficit appears in Equation 3.30 because the gradient between saturated air inside the leaf stomata and ambient air is one of the driving forces for evaporation. The average daily deficit is estimated as the average of 24 hourly deficit values. When hourly values are not available, approximate methods for estimating daily average deficits are used — these different methods may yield significantly different results due to the non-linear nature of Equation 3.34. Alternative methods for estimating a representative daily vapor pressure deficit are described by Shuttleworth (1993) and ASCE (1990). Shuttleworth (1993) recommends specific methods depending on the types of meteorological measurements available.

γ [kPa °C⁻¹], the so-called psychrometric "constant" is a function of pressure (P) and the latent heat of vaporization (l) [MJ kg⁻¹](l is a function of temperature). The following two equations are used to estimate γ :

$$\text{Equation 3.39} \quad l = 2.501 - 0.002361T_s$$

$$\text{Equation 3.40} \quad \gamma = 0.0016286 \frac{P}{l}$$

T_s should be temperature at the water surface [°C] but the ambient air temperature is used here as a surrogate for water temperature. Daily average pressure and temperature values are computed from 30 minute observations and substituted into Equations 3.41 and 3.42.

The aerodynamic resistance term, r_a , is computed using Equation 4.2.25 from Shuttleworth (1993).

$$\text{Equation 3.41} \quad r_a = \frac{\ln[(z_u - 0.67h_c) / z_{om}] \ln[z_e - 0.67h_c / z_{ov}]}{(0.41)^2 u_z}$$

$$\text{Equation 3.42} \quad z_{om} = 0.123h_c$$

$$\text{Equation 3.43} \quad z_{ov} = 0.0123h_c$$

In this equation, z_u is the height at which wind measurements are made (10 m), z_e is the height at which relative humidity measurements are made (2 m), u_z is the observed wind speed, h_c is an estimated crop height, z_{om} is the roughness height for momentum transfer, and z_{ov} is the roughness height for turbulent transfer of water vapor. Average crop heights (h_c) were estimated for the EF 4 and EF 7 sites used in this study based on limited information available from the EBBR data files — notes in the EBBR files describe the vegetation found during instrument installation (both instruments were installed during September). An estimated grass height of 1.25 m was used for EF 4 and 0.25 m was used for EF 7. Substituting values for z_u , z_e , and h_c into Equations 3.41-3.43 for EF 4 and EF 7 yields the relationships.

Equation 3.44 $r_a = \frac{105}{u_z}$ for EF4

Equation 3.45 $r_a = \frac{219}{u_z}$ for EF7

Daily average values for wind speed (u_z) are used to calculate r_a in this study.

In the ARM SWATS developmental data streams for sites EF4 and EF7, estimates of soil temperature, matric potential, and volumetric water content are provided at eight different depths. The SWATS systems use heat dissipation sensors to measure matric potential in the soil (Reece, 1996). The theory behind heat dissipation sensors is that the thermal conductivity of a ceramic cylinder in contact with the soil can be computed knowing the rate of heat dissipation from a line heat source at the center of the cylinder. The thermal conductivity of the ceramic cylinder changes with the water content in the cylinder. In the laboratory, temperature changes observed by the sensor are calibrated against matric potential, rather than water content. For ARM SWATS field installations, the soil-water retention curve of the soil surrounding the sensors is determined in order to translate matric potential into volumetric water content (Schneider and Fisher, 1997). Because the accuracy of calibrations that are used to convert matric potential estimates to volumetric water content are still being assessed (www.arm.gov/docs/instruments/static/swats.html), only matric potential measurements are used in this study. This may be a logical approach regardless of the data quality because plants are more sensitive to matric potential than water content and a derived empirical relationship between r_s and matric potential is independent of soil type.

All of the ARM data sets used in this study were downloaded from the ARM Archive accessible from the Internet (www.arm.gov/docs/data.html). Data obtained from the ARM Archive were distributed in network Common Data Format (netCDF). All netCDF files were converted to ASCII files using a freeware utility,

and Visual Basic programs were written to read and manipulate data from these files. A description of the programs used to manipulate ARM data is provided in Appendix B.

3.3.2.3. Plotting surface resistance against soil piezometric head

The intent here is to investigate how daily surface resistance (r_s) to evaporation changes as the soil dries out. r_s values are computed using Equation 3.30 and plotted against soil piezometric head values ($h + z$). Piezometric head values are used rather than matric potential so graphs showing measurements at different depths can be compared without bias. An interesting question that can be explored is how surface resistance relates to piezometric head measured at different depths.

At site EF7, concurrent EBBR, SMOS, and SWATS data were available for June, July, August, and September of 1997. Computed r_s and ($h + z$) values at a 5 cm depth are plotted in Figure 3.32. Not all days in June, July, August, and September are represented by points on Figure 3.32 because (1) during some days there were obvious errors or unusual behavior in the input data (i.e. values were out of a reasonable range or missing), and (2) days during which rain occurred were not considered. The abscissas in Figure 3.32 show the natural logarithms of the absolute values of the piezometric heads rather than their absolute values, because it was found that using a logarithmic scale makes the data easier to interpret. If data for all four months are looked at collectively (Figure 3.32 a), the correlation between increasing $\ln(h + z)$ and increasing r_s is very weak. It is interesting to note, however, that correlations for individual months are better, as shown in Figure 3.32 b, indicating that a seasonal factor such as vegetation is influencing surface resistance. A similar observation can be made for plots of r_s versus ($h + z$) at a 15 cm depth as shown in Figure 3.33a and b.

Similar plots of r_s versus ($h + z$) at greater depths are shown in Figure 3.34 (a-f). In these plots the correlations for data points for individual months begin to

deteriorate as the depth increases. Data points for individual months become aligned vertically, indicating that there is little variation in soil matric potential among the days plotted. Because many data points are aligned vertically, no regression lines have been included in Figure 3.34 (a-f). At the ARM EF7 site, there are actually two instrumented profiles separated by 1 meter, a west profile and an east profile. The data shown in Figures 3.31, 3.32, and 3.33 are for the west profile.

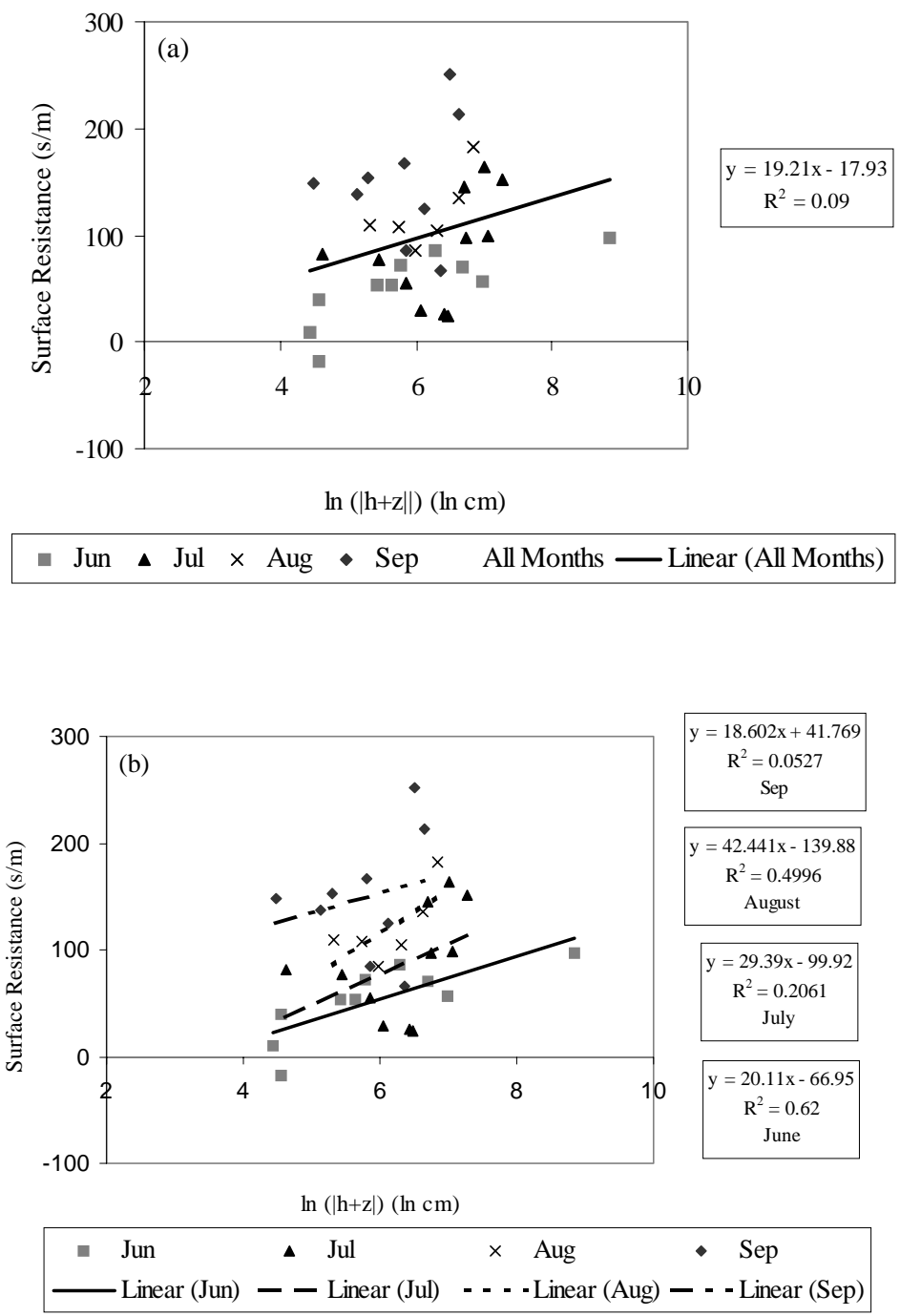


Figure 3.32 Surface resistance (r_s) vs. $\ln(|h+z|)$ for EF7 at a depth of 5 cm (a) with regression line for all data points (b) with regression lines for individual months.

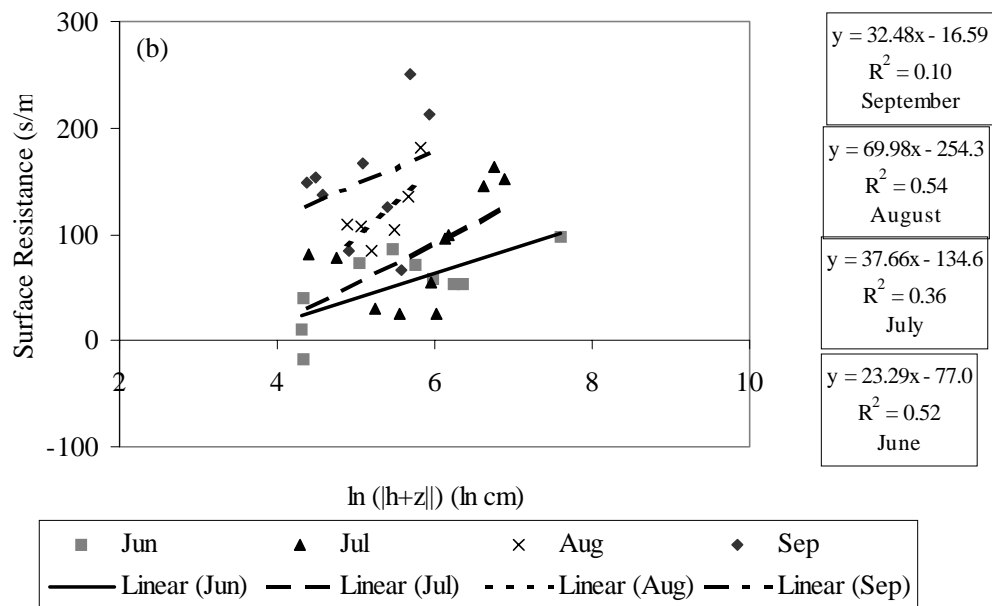
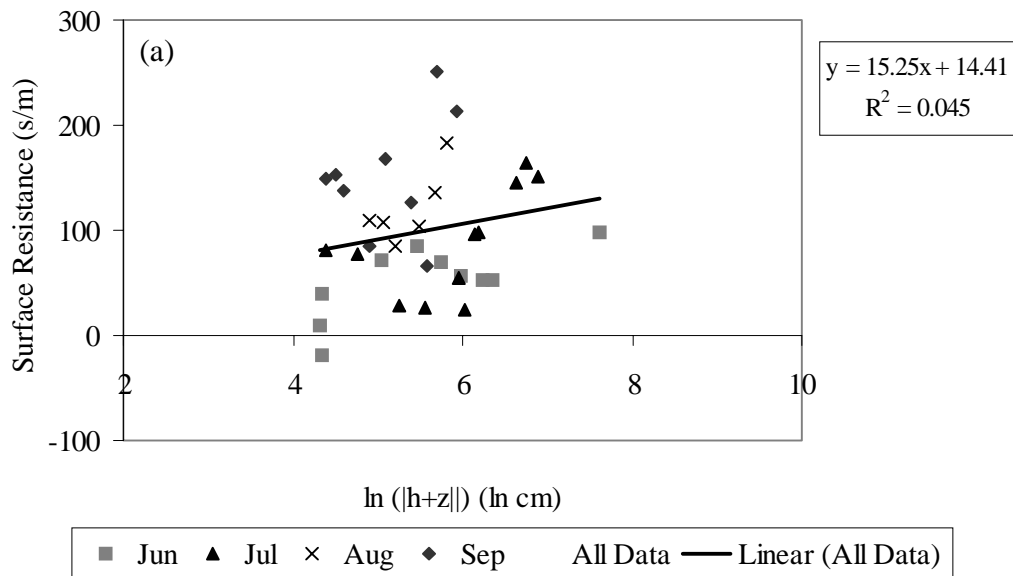


Figure 3.33. Surface resistance (r_s) vs. $\ln(|h+z|)$ for EF7 at a depth of 15 cm (a) with regression line for all data points (b) with regression lines for individual months.

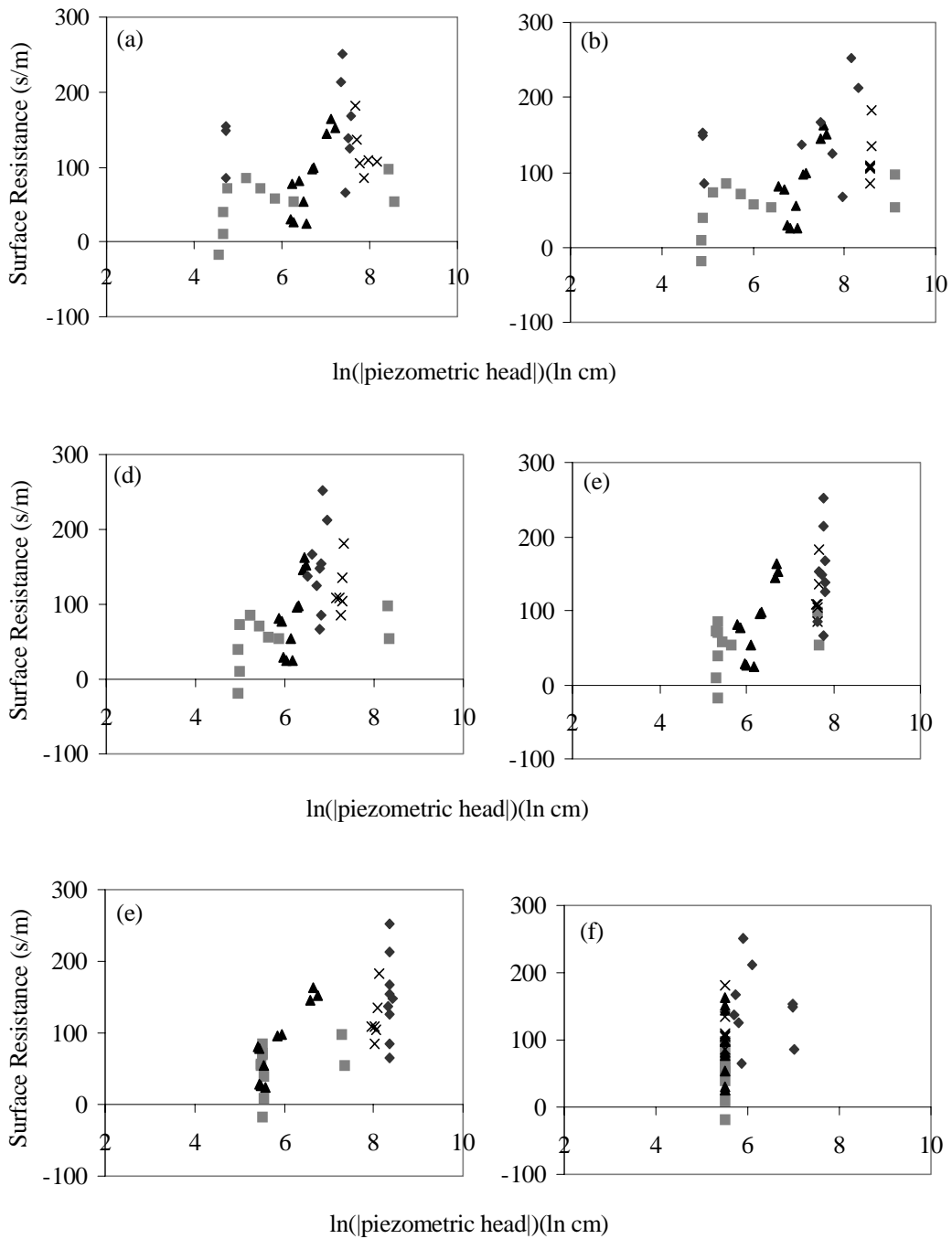


Figure 3.34 Surface resistance (r_s) vs. $\ln(|h+z|)$ for EF7 at a depth of (a) 25 cm, (b) 35 cm, (c) 60 cm, (d) 85 cm, (e) 125 cm, and (f) 175 cm.

It appears from Figures 3.32 and 3.33 that factors other than soil piezometric head influence the surface resistance and perhaps a key factor is the month of the year. Monteith, Szeicz, and Waggoner (1965) showed that values of surface resistance computed in a manner similar to that used here are sensitive to leaf area index. Although additional factors that influence stomatal openings might come into play (i.e. solar radiation, air temperature, humidity deficit, and CO₂ concentration), Fukami *et al.* (1995) indicate that soil moisture and leaf area index (LAI) are the most important factors controlling surface resistance based on modeling "experience."

If leaf area index data were available (LAI data were not available for this study.), then graphs like those shown in Figures 3.32 and 3.33 could be normalized to surface resistance for a single leaf by multiplying the surface resistance by LAI. Perhaps this would bring results for different months closer together. With this being considered, the results in Figures 3.32b and 3.33b are consistent with models for surface resistance used by Dickinson (1984) and Noilhan and Planton (1989) in which surface resistance is inversely proportional to water content and leaf area index. An inverse relationship with water content is similar to a linear relationship with the logarithm of piezometric head shown here if one considers the popular water retention relationship of Brooks and Corey in which water content is exponentially related to the inverse of matric potential. Knowledge of LAI would not only be valuable for estimating surface resistance but can also be related to vegetation height, which would help in computing the aerodynamic resistance (r_a).

Although beyond the scope of this study, the use of remote sensing Advanced Very High Resolution Radiometer Normalized Difference Vegetation Index (AVHRR NDVI) data to infer leaf area index is a promising science. Senay and Elliot (1997) use AVHRR NDVI data to characterize seasonal vegetation changes in the state of Oklahoma.

Surface resistance for selected days was also computed at site EF4. The concurrent availability and quality of required data (EBBR, SMOS, and SWATS) was more limited at this site. Therefore, only values for selected days in June, 1997, are plotted. Figure 3.35 shows a comparison of June 1997 values at the two sites (EF7 and EF4) at a 5 cm depth. Surface resistance values at site EF4 far exceed those at site EF7. Not enough information is available to determine the reason for large discrepancies between sites EF4 and EF7, but clearly factors other than matric potential are influencing the surface resistance. Based on the discussion of leaf area index in the last paragraph, one might infer that the leaf area index at site EF4 is lower than that at EF7. Unfortunately, leaf area index data were not available for this study.

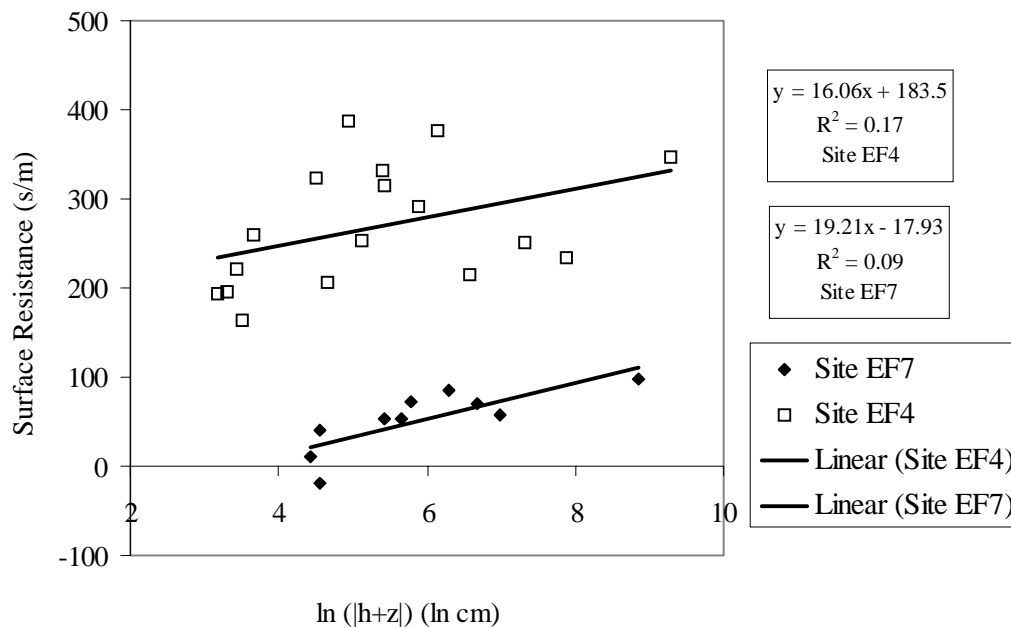


Figure 3.35 A comparison of surface resistance (r_s) vs. $\ln(|\psi+z|)$ at two sites: EF7 and EF4.

3.3.2.4. Evaporation method used in this study: practical considerations

In the preceding sections, an attempt was made to develop empirical equations for estimating surface resistance as a function of piezometric head. The graphs developed indicate that other factors besides soil piezometric head significantly influence surface resistance. There appears to be a seasonal influence on surface resistance. It is suspected that this seasonality is related to vegetation growth and could perhaps be quantified using the leaf area index; however, leaf area index data were not available for this study. Further investigation into the use of the leaf area index subject is suggested as future work.

Based on a review of the literature and the empirical analysis presented here, the conventional approach to estimating evaporation under conditions of limiting soil moisture specified by Equation 2.1 in Section 2.5 is the most practical approach, and this approach is used for simulations described in Chapter 5.

A difficult question to answer when applying Equation 2.1 (or any function that might be used to estimate evaporation) is to what soil depth is water being extracted by plants. Maximum rooting depth estimates may be obtained in the literature for agricultural crops (Doorenbos and Pruitt, 1977) or for general vegetation types (Canadell *et al.*, 1996), but actual rooting depth is a more difficult parameter to specify. In this research, rooting depth (d_r) is used as a model calibration parameter. Physically-based specification of rooting depth (i.e. as a function of vegetation type and season) is left as a subject for future research.

The amount of water accessible to plants for evaporation depends on the rooting depth, which varies with location and season. When a soil root zone is divided into multiple layers, one approach to estimating evaporation from each layer is to take layer evaporation as the product of E_r , the fraction of roots in that layer (ϵ), and $f(\theta)$ (Shuttleworth, 1993). Thus, in application to individual soil layers, Equation 2.1 is modified to include the layer root fraction (ϵ):

$$\text{Equation 3.46} \quad E = \epsilon f(\theta) \kappa_{co} E_r \quad [\text{mm day}^{-1}]$$

Root fraction is assumed to be proportional to soil layer depth in the proposed model. If the model user specifies a total rooting depth (d_r), then the root fractions for the top layer (layer 1) and bottom layer (layer 2) are given by Equation 3.47 and 3.48 respectively.

$$\text{Equation 3.47} \quad \varepsilon_1 = \frac{d_1}{d_r}$$

$$\text{Equation 3.48} \quad \varepsilon_2 = \frac{d_r - d_1}{d_r} \quad d_r < (d_1 + d_2)$$

In the one-layer model, only the evaporation from layer 1 is computed. For the two-layer model, rooting depth must be less than the total soil zone depth. The rooting depth parameter (d_r) is used to help calibrate the proposed model against observed soil water content as discussed in Chapter 5. Rooting depth significantly effects the drying rate from layer 1 and consequently influences direct runoff.

For the simulation runs described in Chapter 5, the input data used to estimate reference crop evaporation (E_r) are taken from the EBBR data stream at site EF26 shown in Figure 3.19. Equation 3.29 is used to estimate reference crop evaporation. Using the definition prescribed by Shuttleworth (1993) for a reference crop, the surface resistance (r_s) is taken as 69 s m^{-1} and the crop height is taken as 0.12 m. The wind speed at site EF26 is measured at 3.4 m and the humidity measurement used is taken at 1.84 m. Substituting these values into Equations 3.41 - 3.43 yields the following relationship for estimating the aerodynamic resistance:

$$\text{Equation 3.49} \quad r_a = \frac{228}{u_{3.4}} \text{ for EF26}$$

3.3.3. Percolation

In both the one-layer and two-layer models, the water content of layer 1 controls the rate of infiltration into layer 1 and the rate of percolation out of layer 1. The percolation out of layer 1 is a function of the water content in layer 1 only, and

the percolation out of layer 2 (if it exists) is a function of the water content in layer 2 only. In the one-layer model, percolation out of layer 1 is passed directly to the groundwater reservoir. In the two-layer model, percolation from layer 1 is passed to layer 2 and percolation from layer 2 is passed to the groundwater reservoir. Percolation rates are specified using a kinematic model, which assumes that matric potential gradients are negligible relative to gravity. Based on this assumption, the percolation rates for each layer are simply specified as the hydraulic conductivity corresponding to the average effective saturation in the respective soil layers. The Brooks and Corey relationship between hydraulic conductivity and effective saturation is used to define percolation (p)

$$\text{Equation 3.50} \quad p_j = K_{js} (\bar{\Theta}_j)^{(3+2/\lambda_j)} \quad j = 1, 2$$

The subscript j indicates that a separate computation is made for layer 1 and layer 2. The bar over the effective saturation ($\bar{\Theta}$) indicates layer average effective saturation. When percolation is controlled by a non-soil, low permeability layer such as weathered bedrock (see Section 3.2.2.3), p_2 is assigned a constant value specified by the user.

3.3.4. Soil layer mass balance

Using the equations describing infiltration, evaporation, and percolation, the mass balance on each soil layer is computed. Computations during an event are different than computations between events and will be discussed separately in the next two sections.

3.3.4.1. Non-event mass balance for an individual time step

When there is no infiltration occurring, the mass balance equation on layer 1 can be written as follows

$$\text{Equation 3.51} \quad d_1(\phi - \theta_r)_1 \frac{d\bar{\Theta}_1}{dt} - e_1 - p_1 = 0$$

where the first term represents the change in storage, e_1 represents evaporation, and p_1 represents percolation. d_1 is the depth of layer 1. In Equation 3.51 both e_1 and p_1 are non-linear functions of Θ_1 which means that Equation 3.51 is a non-linear, non-separable, ordinary differential equation for which it is difficult if not impossible to determine an analytical solution. For this reason, a time stepping method is used to solve this equation in which estimates of e_1 and p_1 are functions of the effective saturation (Θ) at the beginning of the time step. In the two-layer model, a time stepping method is also used to compute the mass balance on layer 2.

The discrete mass balance equations for the case of no infiltration are:

$$\text{Equation 3.52} \quad \Theta_{1t+dt} = -\frac{(e_1 + p_1)}{d_1(\phi - \theta_r)_1} \Delta t + \Theta_{1t} \quad \text{layer 1}$$

$$\text{Equation 3.53} \quad \Theta_{2t+dt} = \frac{(p_1 - p_2 - e_2)}{d_2(\phi - \theta_r)_2} \Delta t + \Theta_{2t} \quad \text{layer 2}$$

Because of the highly non-linear nature of the percolation function, a limit (0.1) is placed on the amount of change in saturation that can occur during a single time step. If this is not done, then a saturated layer with a coarse textured soil might completely dry out during a one hour period if the percolation rate for the entire hour is assumed to be governed by the effective saturation at the beginning of the hour. If the 0.1 limit is exceeded, the computation time step is cut in half until either this limit is satisfied or a maximum number of time step subdivisions (128) is reached. Additional precautions are taken to make sure that effective saturation in each layer never drops below 0 or exceeds 1.

3.3.4.2. Event mass balance

During a rainfall event, infiltration is modeled as piston flow, and the rate of advancement of this piston is a function of initial water content of soil layer 1 and

the cumulative infiltration for that event. To keep things simple, infiltrated water is not redistributed throughout the soil layer(s) until the rainfall event has ended. Evaporation is assumed to be negligible during a rainfall event, but percolation is not neglected during an event. Initial estimates of event percolation from both layers are made based on the initial saturation levels. By neglecting evaporation and not accounting for infiltrated water until the end of the storm, an analytical solution for the percolation from layer 1 during an arbitrary rainfall period can be determined. The mass balance equation for layer 1 is:

$$\text{Equation 3.54} \quad (\phi_1 - \theta_{1r})d_1 \frac{d\Theta_1}{dt} + K_{s1}(\Theta_1)^{(3+2/\lambda_1)} = 0$$

Equation 3.54 can be separated and integrated from the known initial effective saturation (Θ_{1i}) to the unknown final effective saturation (Θ_{1f}) over the time period t_i to t_f .

$$\text{Equation 3.55} \quad \int_{\Theta_{1i}}^{\Theta_{1f}} \Theta_1^{-(3+2/\lambda_1)} d\Theta_1 = \int_{t_i}^{t_f} -\frac{K_{1s}}{d_1(\phi_1 - \theta_{1r})} dt$$

Solving for Θ_{1f} yields:

$$\text{Equation 3.56} \quad \Theta_{1f} = \left[\frac{2K_{1s}}{d_1(\phi_1 - \theta_{1r})} (t_f - t_i) \left(1 + \frac{1}{\lambda_1}\right) + \Theta_{1i}^{\left(-2 - \frac{2}{\lambda_1}\right)} \right]^{-\frac{1}{2} \left(\frac{\lambda_1}{\lambda_1 + 1} \right)}$$

To simplify the mathematics for layer 2, the initial estimate for layer 2 percolation is calculated independently of the added percolation from layer 1 during the event (making the math identical to that for layer 1). The exception occurs when the percolation rate out the bottom of layer 2 is assumed to be a constant because of a non-soil, low permeability layer. In this case, the equation for the final saturation in layer 2 is as follows:

$$\text{Equation 3.57} \quad \Theta_{2f} = -\frac{P_2}{d_2(\phi_2 - \theta_{2r})} \Delta t + \Theta_{2i}$$

The initial estimates of total percolation (P_j) (note that lower-case p stands for percolation rate) for each layer during a storm are given by Equation 3.58. The units for total percolation are [cm] and the subscript j indicates layer number.

$$\text{Equation 3.58} \quad P_j = (\Theta_{ji} - \Theta_{jf}) (\phi - \theta_r)_j d_j \quad j = 1, 2$$

Although the assumptions that allow these analytical solutions are imperfect from a physical point of view, percolation computations are simplified greatly. As described in the next paragraph, if necessary, adjustments are made to P_1 and P_2 to ensure that the physical limits on effective saturation are not violated.

At the end of a rainfall event, the water contents in each layer are adjusted to account for the event percolation (P_j) defined by Equation 3.58 and event infiltration (I). As much of the infiltrated water as possible remains in the top layer, without allowing the effective saturation to exceed natural saturation. Any remaining infiltrated water is passed to the second layer. The second layer may also become full and if it does, the excess infiltration is added to the storm direct runoff and distributed evenly over the storm time periods. In the one-layer model, the total depth of the soil zone is unspecified so any infiltration that exceeds that capacity of layer 1 is treated as percolation. In both models, layer 1 is allowed to fill only to Θ_{ns} because any higher saturation might cause an error in the infiltration calculations (which only depend on the saturation in the top layer). Layer 2 is allowed to fill to $\Theta = 1$.

Because percolation and infiltration are occurring simultaneously, but the magnitudes for these flux computations are estimated independently from one another, a series of checks are made to ensure that the physical limits on effective saturation are not violated at the end of a storm. A flow chart that illustrates the sequence of calculations ensuring post-infiltration mass balance in the two layer model is shown in Figure 3.37.

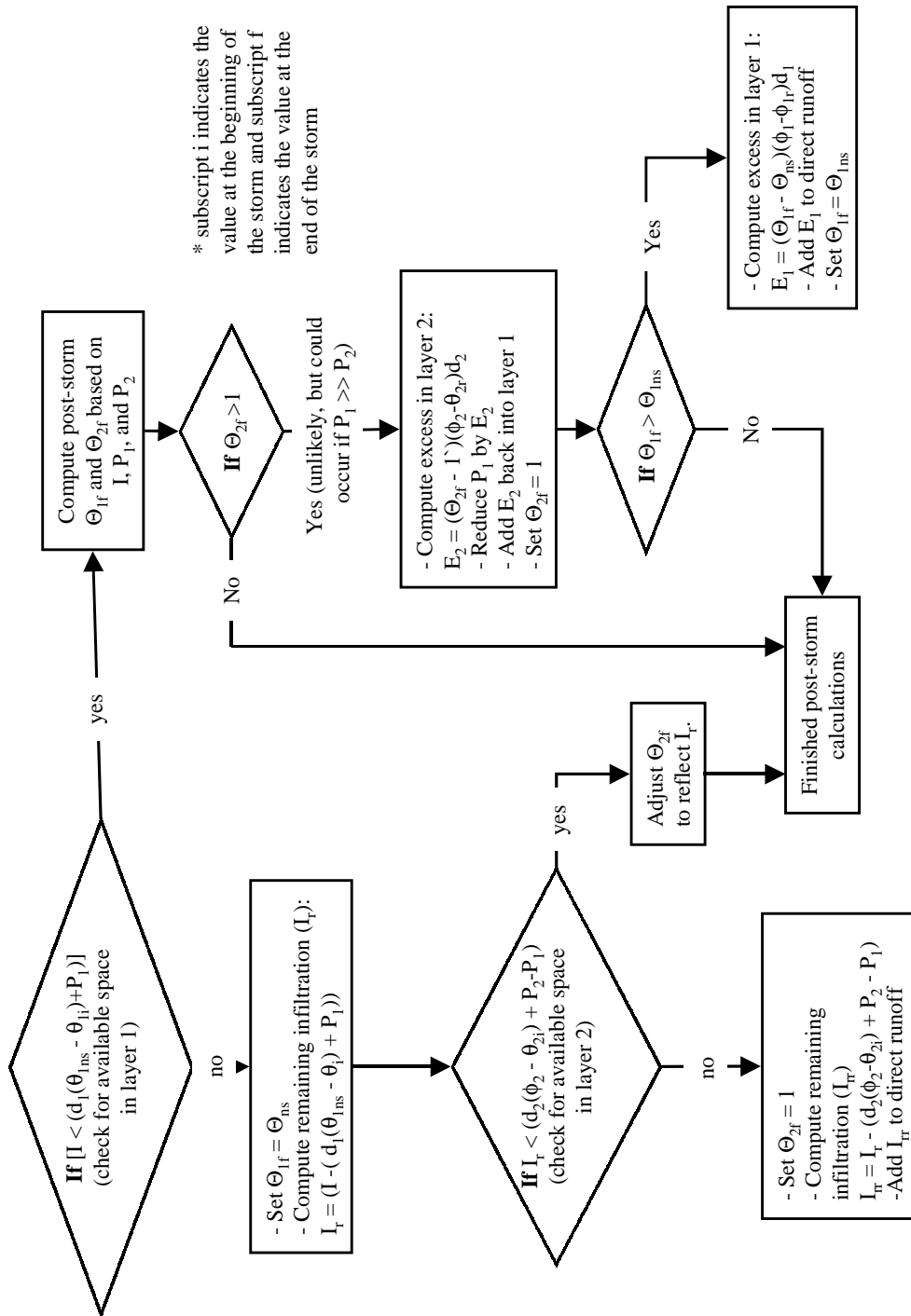


Figure 3.36 Post-infiltration mass balance flow chart for the two-layer model.

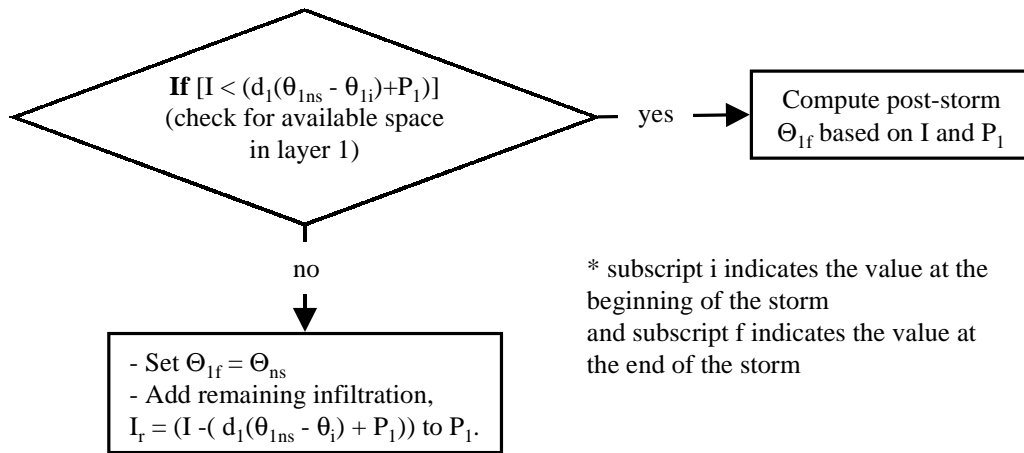


Figure 3.37 Post-infiltration mass balance flow chart for the one-layer model.

3.3.5. Runoff transform method : “modClark”

Although watershed runoff routing is not the focus of this research, a runoff transform method is included so that predicted rainfall excess can be compared with observed runoff. Direct runoff from each model cell is transformed into a streamflow response at the watershed outlet using the modClark transform method. The modClark method was developed at the U.S. Army Corps of Engineers Hydrologic Engineering Center (HEC) for use in quasi-distributed modeling with NEXRAD rainfall data (HEC, 1995; Peters and Easton, 1996). The modClark method is also applied using NEXRAD data here; however, the same methodology can be applied to any arbitrarily defined precipitation polygons. ModClark is an adaptation of the Clark unit hydrograph method. In modClark, direct runoff pulses from each cell are first translated to the outlet based on a travel time that is linearly proportional to travel length. At the outlet, arrays of lagged direct runoff pulses are summed and then passed through a linear reservoir to generate the direct runoff hydrograph. As in the original Clark method, the linear reservoir is intended to represent stream channel storage effects.

In addition to the time series of rainfall excess determined from the soil-water balance, implementation of the modClark method requires estimates of (1) the average flow length from each model cell to the watershed outlet, (2) cell areas, (3) the time of concentration (T_c) for the watershed as a whole, and (4) a linear reservoir storage coefficient (R). Area is an attribute of the model polygons shown in Figure 3.18. The average flow length for each NEXRAD polygon is determined by averaging the flow lengths of all digital elevation model cells (Figure 3.3) within that polygon. There are approximately 1,600 of the 100-m DEM cells and 17,778 of the 30-m DEM cells in a NEXRAD cell. A map showing the average flow length for each model polygon is shown in Figure 3.38. T_c and R may be estimated from previous studies, regionalization, or calibration (Peters and Easton, 1996). The travel time (T_m) from a model cell to the watershed outlet is estimated using the following equation:

$$\text{Equation 3.59} \quad T_m = T_c \frac{FL_{avg}}{FL_{max}}$$

In Equation 3.59, FL_{avg} stands for the average flow length from a given NEXRAD cell and FL_{max} stands for the maximum of the cell average flow lengths.

Equation 3.60 is used to route water through a linear reservoir at the outlet (HEC, 1995).

$$\text{Equation 3.60} \quad Q_t^{dout} = \left[\frac{\Delta t}{R + 0.5\Delta t} \right] \bar{Q}^{din} + \left[1 - \frac{\Delta t}{R + 0.5\Delta t} \right] Q_{t-\Delta t}^{dout}$$

\bar{Q}^{din} is the average flow rate into the linear reservoir during the current time step.

$Q_{t-\Delta t}^{dout}$ is the flow rate out of the linear reservoir at time $t-\Delta t$, and Q_t^{dout} (the unknown quantity) is the flow rate out of the linear reservoir at time t . The “d” in the superscript is intended to distinguish direct runoff from baseflow. To be consistent with the original references, this mathematical equation describing a linear reservoir differs slightly from that developed in the next section for the baseflow component,

however, the numbers resulting from calculation with the two different forms are very similar.

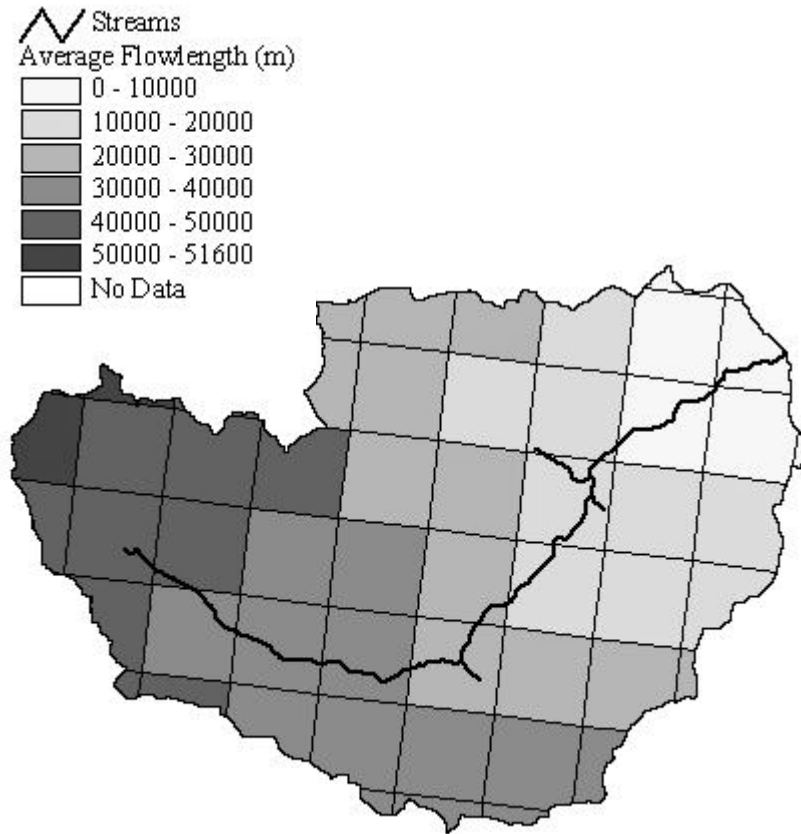


Figure 3.38 Average flow length from each model polygon to the watershed outlet.

3.3.6. Baseflow

Two methods are used to generate baseflow in this study, baseflow simulation with a single linear reservoir model and baseflow separation using observed flow data. Both methods require a single parameter that cannot be estimated from the physical characteristics of the watershed. The baseflow separation approach is simpler to apply and is adequate to address the objectives of this research dealing with the effects of soil heterogeneity on direct runoff generation. When the

baseflow separation method is used, any percolation out the bottom of the soil zone is treated as a sink in the model. With the single linear reservoir baseflow model, percolation out the bottom of the soil zone is passed to the linear reservoir. Although not absolutely necessary to meet the objectives of this research, a baseflow simulation scheme is necessary to apply the proposed model in areas where no observed flow data is available.

It will be shown in Chapter 5 that use of the two-layer soil model in conjunction with the single linear reservoir baseflow model may provide reasonable baseflow results, but when the one-layer soil model is used, the single linear reservoir model is not adequate to simulate baseflow response. This is because too much water gets passed to the linear reservoir in the one layer model. Existing models like PRMS (Leavesley *et al.*, 1983) and the HEC Continuous Soil Moisture Accounting Model (unpublished by Bennett, 1997) allow for multiple groundwater storage reservoirs. One of these reservoirs might serve the same role as the second soil layer in the model used here. Multiple groundwater zones may also be used to distinguish between shorter and longer term recession responses for a basin (sometimes referred to as “subsurface” and “groundwater” flow respectively). The drawback to introducing multiple groundwater zones is the addition of more parameters that cannot be estimated from watershed characteristics. In the HEC Continuous Soil Moisture Accounting model, the user must supply at least two parameters for each groundwater zone — the maximum storage in that zone and a linear reservoir storage coefficient for modeling the release of water. A third parameter, maximum percolation rate, is required for a given zone if another zone exists below it.

More detailed descriptions of the simulation and separation baseflow approaches are provided in the next two sections.

3.3.6.1. Single linear reservoir model

Using a linear reservoir to model baseflow is a popular approach because the linear reservoir model generates exponentially decaying baseflow that is consistent with observed hydrographs and theoretically consistent with the equation for 1-dimensional flow from a phreatic aquifer (USACE, 1994). Although the mathematics of linear reservoirs are widely documented, an explanation is included here for the sake of completeness. By definition, the storage (S [L^3]) in a linear reservoir is proportional to the outflow (Q^b [$L^3 T^{-1}$]) with χ [T] being the constant of proportionality (reservoir constant) as shown in Equation 3.61.

$$\text{Equation 3.61} \quad S = \chi Q_b$$

Combining Equation 3.61 with the continuity equation (Equation 3.62) and then integrating from time t to time $t+\Delta t$ yields Equation 3.63, which can be used to calculate the discharge from the reservoir during any time interval.

$$\text{Equation 3.62} \quad \frac{dS}{dt} = \text{Inflow} - Q^b$$

$$\text{Equation 3.63} \quad Q_{t+\Delta t}^b = Q_t^b e^{-\Delta t/\chi} + \text{Inflow}_t \left(1 - e^{-\Delta t/\chi} \right)$$

Inflow_t is the sum of the percolation out of the bottom soil layer for all soil components in all cells. Q_t^b is the baseflow at time t and $Q_{t+\Delta t}^b$ is the baseflow at time $t+\Delta t$.

Using only one groundwater reservoir, there is only one groundwater parameter, the reservoir storage coefficient (χ). This is a lumped parameter for the entire watershed and is determined by calibration against observed flow data.

3.3.6.2. Baseflow separation

In this study, the purpose of the baseflow separation is to extract a direct runoff hydrograph from the observed flow record for comparison with the direct runoff hydrograph predicted by the soil-water balance model. Historically, a number of different methods have been used for baseflow separation. Chow, Maidment, and Mays (1988) describe three possible baseflow separation techniques. A baseflow separation technique described by Olivera, Maidment, and Charbeneau (1996) is used here. The baseflow separation program described by Olivera, Maidment, and Charbeneau (1996) was written in FORTRAN but has been rewritten in Visual Basic with slight modifications for this research. The main algorithm used by the baseflow separation program is unchanged. This baseflow separation algorithm is illustrated in Figure 3.39. In the example of Figure 3.39, baseflow at the first time step ($t(1)$) is set equal to the total flow $Q^b(1) = Q(1)$ at time 1. The baseflow at the next time step $Q^b(t+1)$ depends on the separation parameter n , which specifies the number of future hours that are considered in estimating $Q^b(t+1)$. The parameter n is taken as 3 hours in Figure 3.39. n lines are drawn from the known point $Q^b(1)$, one to each of the n subsequent observed flow values ($Q(t)$), and the slopes of these lines are calculated. The baseflow hydrograph is assumed to follow the minimum slope defined by this set of lines. Thus $Q^b(t+1)$ is computed using the following equation:

$$\text{Equation 3.64} \quad Q_{t+1}^b = Q_t^b + \min\left(\frac{Q_{t+1} - Q_t^b}{1}, \frac{Q_{t+2} - Q_t^b}{2}, \dots, \frac{Q_{t+n} - Q_t^b}{n}\right)$$

Choice of the parameter n can significantly influence the baseflow estimates derived using this method. An example application using streamflows from July 7 – July 17 at the USGS flow station East of Ninnekah on the Little Washita River is shown in Figure 3.40 to illustrate this point. For the observed direct runoff hydrographs shown in Chapter 5, an n value of 60 hours was used. If a different n value was chosen, then some of the calibrated parameter values presented in

Chapter 5 would change. The absolute accuracy of direct runoff predicted in the validation runs might also change, but the relative performance of the different modeling scenarios would likely remain the same.

Although there is no physical basis for selecting an n value, there is no physical basis for the specification of the storage constant (χ) used in the baseflow simulation scheme either. The baseflow separation method described here is attractive because it is easily automated and can be applied consistently to different storms in a long flow record.

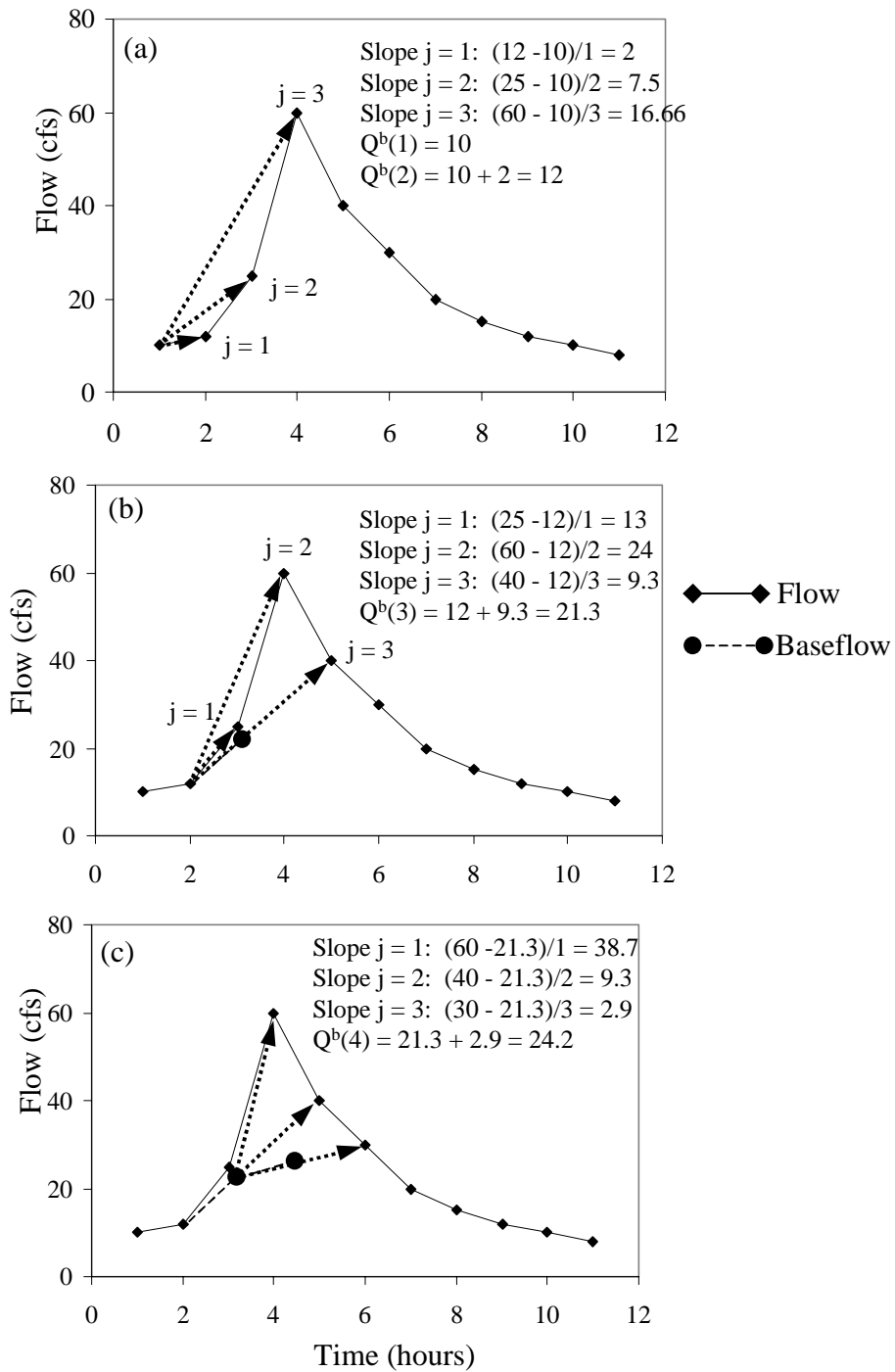


Figure 3.39 Baseflow separation method. (a) estimating baseflow at $t = 2$, (b) estimating baseflow at $t = 3$, and (c) estimating baseflow at $t = 4$.

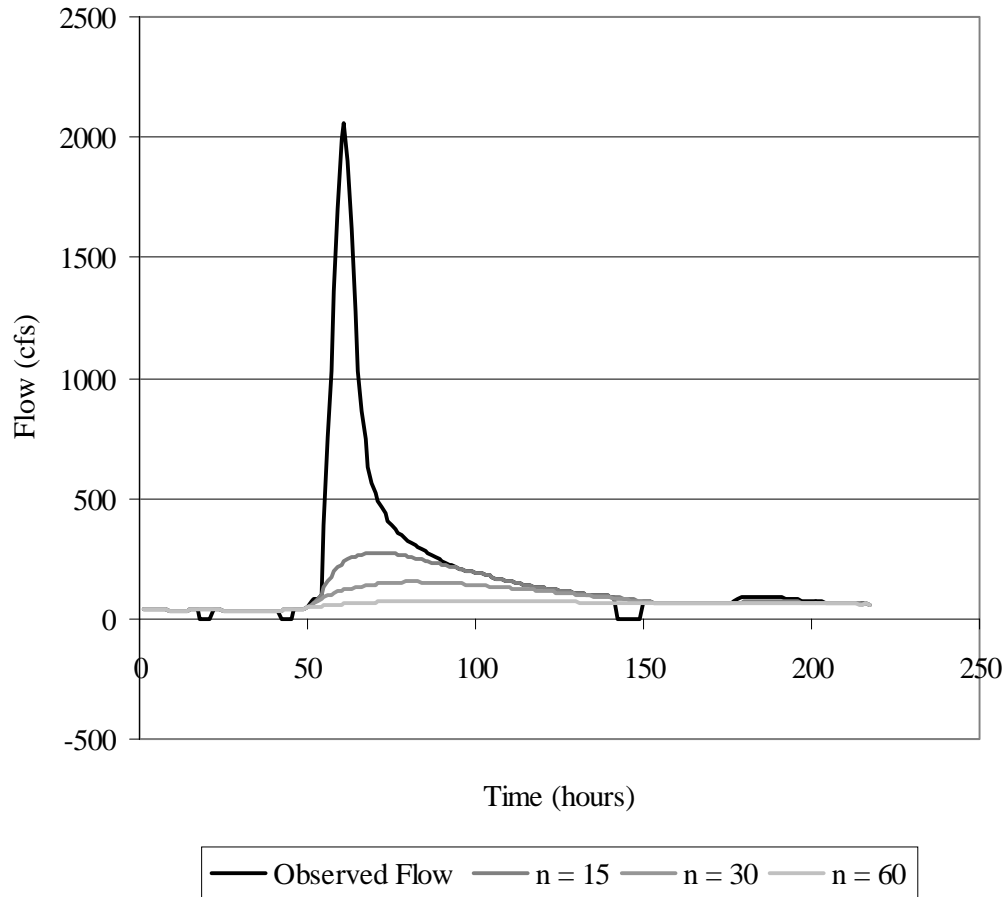


Figure 3.40 Baseflow separation using n = 15, 30, and 60 hours.

3.3.7. Special considerations for the Little Washita

Although the Little Washita River Watershed is an attractive study area due to the large amount and variety of hydrologic data available, one drawback in studying this watershed is that it contains 45 floodwater detention structures (as of 1985) installed by the Soil Conservation Service (Allen and Naney, 1991) which alter the natural hydrology of the watershed. These detention structures influence 46% of the watershed area, and appear to have a significant influence on the hydrographs. It is

hypothesized that the recession limbs of storm hydrographs do not exhibit obvious logarithmic recession because of these detention structures. For the purposes of predicting direct runoff volume, the detention structures are ignored because it is assumed that these structures primarily affect runoff timing and not total storm volume. The storage effects of these reservoirs are roughly accounted for in the modClark parameters that are used to transform rainfall excess to the watershed outlet.

In addition to these man-made detention structures, Allen and Naney (1991) report that 19.5 percent of the Little Washita watershed was controlled by farm ponds as of 1983. According to Allen and Naney, these farm ponds drain areas that do not contribute to runoff. In application, 19.5 percent of the direct runoff predicted by the model is assumed to flow to farm ponds where it is lost to evaporation. An option is available in the Visual Basic user interface to specify the fraction of contributing area. If this estimate of non-contributing areas is not accurate, then the calibrated model parameter values given in Chapter 5 would change slightly, but this is not likely to alter the conclusions reached in Chapter 5 because the same assumption is made for all modeling scenarios being compared.

3.4. Summary

A study of the available data and relevant literature has led to the development a soil-water balance and runoff model for which many of the required parameters can be estimated from available spatial databases. Before continuing on to a discussion of computer implementation (Chapter 4) and modeling results (Chapter 5), a summary of the key model features is provided here.

To implement the model, a watershed is divided into cells of uniform precipitation (NEXRAD rainfall cells in this case) and vertical flux calculations are made independently for each rainfall cell. Rainfall excess in each cell is

transformed to the watershed outlet using the modClark method developed at the Hydrologic Engineering Center.

Vertical flux calculations are dependent on soil hydraulic properties that vary in space. The model is designed so that different levels of spatial resampling in describing soil properties can be tested. Figure 3.4 shows that there are significant differences in the spatial detail provided by the 1:250,000 STATSGO soils data and the 1:24,000 30-m soils grid; however, the overall surface textural composition for the watershed predicted from the two data sets is similar (Figure 3.6b).

A straightforward method to estimate soil hydraulic properties (K_s , ϕ , θ_r , λ , h_b , θ_{fc} , and θ_{wp}) from soil texture is proposed. This method involves two lookup tables. The first table translates texture names in the STATSGO database into one of the 12 basic USDA texture classes or the "other" category, and the second table assigns mean hydraulic properties to each texture class. Two key papers by Rawls, Brakensiek, and Saxton (1982) and Carsel and Parrish (1988) tabulate mean values for hydraulic parameters in each texture class. The water retention parameter values (λ , h_b) reported in these two papers are considerably different. The reason(s) for these differences cannot be discerned from the literature but the Carsel and Parrish values have been selected for use here because they are more consistent with Figure 5.5.4 of Rawls *et al.* (1993). The sensitivity of model results to specifying a range of parameter values is discussed in Section 5.6.

Relatively simple infiltration, evaporation, and percolation models have been described. Simple infiltration (Green-Ampt) and percolation (kinematic) models described in the literature are easily amenable to a continuous soil-water balance scheme. Large uncertainties in parameter estimates and input data justify the use of simple flow models. Models available in the literature for predicting evaporation under soil moisture limited conditions are either theoretically weak or intractably complex. The possibility of developing a model of intermediate complexity was explored. An attempt was made to develop an empirical relationship between

evaporative surface resistance and soil suction using detailed meteorological data from DOE ARM CART measurement sites. Looking at this data, it is clear that this approach will not have general applicability because other factors besides soil moisture are strongly influencing surface resistance. This is a subject for further study. A conventional method for estimating evaporation discussed in Section 2.5 has been implemented in the proposed model.

It is a relatively simple task to partition the surface soils in a watershed into different texture classes, but considering increased vertical subdivision significantly complicates the problem. Based on the type of layer information available and the desire to keep the model as simple as possible, use of only a one-layer and a two-layer soil model are considered. The two-layer model uses more information provided in the soils databases. In the two-layer model, the top layer controls direct runoff while the bottom layer primarily serves as a storage reservoir for infiltrated water. Specific differences in model complexity, in terms of computer implementation, are described in Chapter 4.

CHAPTER 4. COMPUTER IMPLEMENTATION

To implement the model described in Chapter 3, there are three major steps: (1) collect spatial and time series data and convert these data into the required formats as necessary, (2) analyze spatial data to define modeling units and estimate model parameters, and (3) make hydrologic computations. Acquisition and formatting of input data is discussed briefly in Section 4.1.

Spatial analysis and parameter estimation are automated using the ArcView GIS and its Avenue script language. ArcView procedures are referred to as pre-processing steps. Hydrologic computations are done using Visual Basic. The Avenue scripting language is not used for the hydrologic calculations because the Avenue language is interpreted, and tends to be much slower than compiled languages like Visual Basic. Collectively, the programs developed in this research are given the name Soil Water Balance Modeling System (SWBMS). The ArcView pre-processor is referred to as AV-SWBMS and the Visual Basic programs are referred to as VB-SWBMS.

In addition to speed issues, an important reason for separating the spatial analysis computations from the hydrologic computations is to make it possible to pass parameter information derived in the GIS environment to existing hydrologic models developed elsewhere, like HEC-HMS. Working with researchers at HEC over the past several years, a simple strategy of passing parameter information from GIS to HEC-HMS through ASCII files has proven effective. The same scheme is used here, but hydrologic calculations are done using VB-SWBMS.

Sections 4.2 and 4.3 are devoted to a discussion of the two principal model components, AV-SWBMS and VB-SWBMS.

4.1. Collecting and reformatting input data

In this study, collecting and reformatting the spatial and time series data was the most tedious of the three major processing steps because it is the least

automated, but this step is typically only done once. The sources for acquiring spatial and time series data are given in Table 3.1. The preparation of time series data was more time consuming than the preparation of spatial data because the time series data that were obtained from different sources are distributed in different formats. Therefore, customized data reformatting programs are required for each time series data source so that the data can be read by the AV-SWBMS code. Since the programs for data conversion are not critical to the modeling concepts, a description of these programs is left to Appendix B.

The spatial data, including soils data, digital elevation models, and land use data are distributed in standard formats. Procedures for converting spatial data sources from their original formats to formats readable by the ArcView software are standard GIS operations. In addition to the information found in this chapter, information about converting these standard spatial data sources may be found at the web sites listed in Table 3.1, in the Arc/Info or ArcView software documentation, or in one of the references cited in Section 3.2. As discussed in Section 3.2, all spatial data must be converted to a common map projection.

4.2. The ArcView Pre-Processor (AV-SWBMS)

AV-SWBMS prepares parameter files for hydrologic calculations in VB-SWBMS. AV-SWBMS is packaged as an ArcView extension, which contains a set of scripts and associated menus that are added to the View GUI when the extension is loaded. The View GUI includes menus, buttons, tools that are seen when an ArcView user has a View window active. In ArcView, View windows are used to display and manipulate map layers called Themes. A Theme may contain vector or raster (gridded) data. A summary of the Themes and tabular data required to run the AV-SWBMS programs is provided in Table 4.1. All of the input Themes must provide complete coverage for the watershed of interest and be in the same map projection.

Table 4.1 Spatial data required to run AV-SWBMS

Theme	Suggested method of acquisition	Comments
A polygon Theme defining cells of uniform rainfall. (i.e. NEXRAD cells)	Programs for generating a polygon coverage of NEXRAD rainfall cells are described at www.ce.utexas.edu/prof/maidment/gis/hydro/seann/nexrad.htm and in Reed and Maidment (1995).	Although not needed for AV-SWBMS, a time series file containing a column for each rainfall cell must be related to cells in this Theme to run a hydrologic simulation. The rainfall cells do not have to be uniform in shape.
A watershed polygon	A watershed polygon can be derived from a digital elevation model using the Watershed Delineator, CRWR-Prepro, or the Hydrologic Modeling extension (Olivera, Reed, and Maidment, 1998). Information on obtaining digital elevation models through the Internet may be found at www.ce.utexas.edu/prof/maidment/gis/hyd97/library/websites/webtoc.htm .	At this time, the SWBMS system can only model single watersheds because there is no river routing component.
A grid Theme with values of flow length from each cell to the watershed outlet	The flow length grid can also be derived from a digital elevation model using either the Watershed Delineator, CRWR-Prepro, or the Hydrologic Modeling extension (Olivera, Reed, and Maidment, 1998).	
A STATSGO soil polygon Theme for the area of interest with the associated component (comp.dbf) and layer (layer.dbf) tables or a soil grid Theme and associated tables	www.ftw.nrcs.usda.gov/soils_data.html	The AV-SWBMS programs should also work with SSURGO vector data as is or with minor modifications. Use of SSURGO vector data has not been tested.
A land use polygon coverage for which the attribute table contains a field with Anderson Level II land use code.	www.ce.utexas.edu/prof/maidment/gis/hyd97/library/websites/webtoc.htm or www.epa.gov/ngispgm3/nsdi/projects/giras.htm	

The AV-SWBMS extension contains two menus, one called "SWBMS" and one called "SWBMS-Twolay," that become visible when a View is active. A screen capture of these two menus is shown in Figure 4.1.

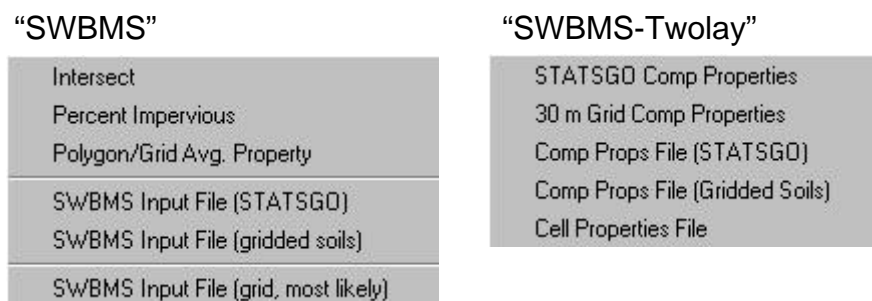


Figure 4.1 Screen capture of menus that are part of AV-SWBMS.

The "SWBMS" menu contains a sequence of programs that are run to create an input file for a one-layer model run, and the "SWBMS-Twolay" menu contains additional programs that are required to create input files for a two-layer model. A single ASCII file is created as input for a one-layer VB-SWBMS run, and two ASCII files are created for a two-layer VB-SWBMS run. Important differences in the data transfer between the one-layer and two-layer models are discussed in Sections 4.2.1 and 4.2.2.

For both the one-layer and two-layer models, separate algorithms are required to deal with the STATSGO soils data in vector format and the 30-m gridded soils. In addition, separate algorithms are required to prepare an input file for the different resampling levels.

4.2.1. Pre-processing for a one-layer model

ArcView pre-processing steps used to create a one-layer VB-SWBMS input file are summarized in Table 4.2. Table 4.2 lists each item under the menu "SWBMS" and explains its purpose. A more detailed description of each of these programs is provided in Appendix A.1. The first three menu items are generic tools that are

used both for the one-layer and the two-layer model while the last three menu items are specific tools that generate input files for VB-SWBMS.

The format of the VB-SWBMS input files is the same regardless of whether vector or gridded soils data are used as input. The transfer file format for NEXRAD cell level resampling is slightly different from that for no resampling as shown in Figure 4.2. Note that only one line of information is required for each NEXRAD cell in the sample input files shown in Figure 4.2. The actual input files are comma delimited but are presented here in columnar format to be more readable.

In the descriptions of the last three menu items in Table 4.2 there is no mention of creating an input file for watershed level resampling. To create input files for the watershed level resampling option in this study, it was easiest just to edit the input files for the no resampling option using Microsoft Excel. To do this, the percentages for the predominant watershed soil type (i.e. silt loam) were set to 100 for all cells, while the percentages for all other soil textures in all cells were set to 0.

Although all the pre-processing procedures described in Table 4.2 are automated, special situations may arise when it is necessary to manually edit an entry in one of the ASCII transfer files. A situation that requires manual editing occurs when only a tiny portion of the watershed being modeled intersects a NEXRAD cell. If this tiny intersected polygon is small enough so that it contains no underlying elevation grid cells, then the flow length from that tiny polygon to the watershed outlet is recorded as a Null Number. A problem will also occur if the program attempts to determine the soil type(s) within this polygon if gridded soils data are being used. This problem occurs where the Little Washita watershed intersects NEXRAD cell (553,306) forming a thin polygon with an area less than 0.01 km². Grid cell resolution is almost always an issue when dealing with both grid and vector data layers. In the author's experience, polygon/polygon operations are generally more robust than polygon/grid operations.

Table 4.2 Description ArcView pre-processing programs under the menu “SWBMS.”*

Step #	Must be preceded by steps	Menu item	Description
1		Intersect	Intersect watershed polygon with rainfall cells to define modeling units.
2	1	Percent Impervious	Compute percent imperviousness in each model polygon.
3	1	Polygon/Grid Avg. Property	Determine the average value of all grid cells in each model polygon or the most prevalent value of the grid cells in each model polygon. This program is used to compute the average flow length to the watershed outlet in each model polygon and is also used to compute the predominant soil type grid code in each cell when gridded soils data and NEXRAD cell level resampling are used.
4	1, 2, 3	SWBMS Input File (STATSGO)	Creates an input file for VB-SWBMS using STATSGO soils data. Tallies the percentage of each soil type that falls within that polygon. The user can choose between writing a file with NEXRAD cell level resampling or no resampling. Example input files for NEXRAD cell level resampling and no resampling are shown in Figure 4.1.
5	1, 2, 3	SWBMS Input File (gridded soils)	Creates an input file for VB-SWBMS using 30 m soils data. Tallies the percentage of each soil type that falls within each model polygon. Creates an input file with no resampling.
6	1, 2, 3	SWBMS Input File (grid, most likely value)	Creates an input file for VB-SWBMS using 30 m soils data and NEXRAD cell level resampling. Program assumes that predominant soil type in each model polygon has already been computed from the soils grid using the menu item Polygon/Grid Avg. Property.

* A more detailed description of each of these steps is provided in Appendix A.1.

Cell properties file for NEXRAD cell level resampling:

hrapx	hrapy	cellarea	flowlength	pct_imp	soiltype
560	311	1570369	7329	14	6
561	311	356931	5836	0	6
556	310	3402604	27999	0	3
557	310	10245727	25071	5	3
.
.

Notes:
 Units for cellarea are m².
 Units for flowlength are m.

Cell properties file for no resampling:

hrapx	hrapy	cellarea	flowlength	pct_imp	pct_S	pct_LS	pct_SL	pct_SCL	...
560	311	1570369	7329	14	0	0	6.364	0	...
561	311	356931	5836	0	0	0	0.557	0	...
556	310	3402604	27999	0	0	48.616	51.384	0	...
557	310	10245727	25071	5	0	10.409	89.591	0	...
.
.

No resampling file continued.

pct_L	pct_SIL	pct_CL	pct_SI	pct_C	pct_SC	pct_SICL	pct_SIC	pct_O
37.457	56.179	0	0	0	0	0	0	0
23.354	76.089	0	0	0	0	0	0	0
0	0	0	0	0	0	0	0	0
0	0	0	0	0	0	0	0	0
.
.

Figure 4.2 Example input files for the one-layer model.

4.2.2. Pre-processing for a two-layer model

Data processing for the two-layer model is much more complicated than that for the one-layer model. This is because more than one factor is used to distinguish mapped soil components in the two-layer model. In the one-layer model, surface texture is the only distinguishing factor while in the two-layer model there are three distinguishing factors for each soil component: top layer texture, bottom layer texture (which is the texture of the most restrictive layer in the layer table), and total soil zone depth. When the two-layer model is applied, only the no resampling option is used because it does not make sense to compute the predominant soil type in two different layers and the predominant soil zone depth independently of one another.

Another difference in the way the one-layer and two-layer models are implemented in this research is that hydraulic properties associated with each soil texture are assigned within AV-SWBMS for the two-layer model but within VB-SWBMS for the one-layer model. This difference reflects a change in philosophy that occurred during the course of this research. It now seems most logical keep the amount of information that is passed from AV-SWBMS to VB-SWBMS to a minimum. Passing only texture information rather than each parameter value associated with that texture is one way to reduce this amount of information. The one-layer model was developed more recently and therefore adheres to this newer philosophy.

The programs under the pull-down menu “SWBMS-Twolay” that are used to create input files for a two-layer SWBMS run are described in Table 4.3. Items 1, 2, and 3 from the “SWBMS” menu (Table 4.2) are prerequisites to run items 3, 4, and 5 in Table 4.3. Only a general description of the programs is provided in Table 4.3 with more details provided in Appendix A.1.

Two ASCII files get passed from AV-SWBMS to VB-SWBMS for the two-layer model, a cell properties file and a component properties file. The format for

both of these files is shown in Figure 4.3. Each line in the cell file contains a number indicating the number of components in that cell. The component file is ordered such that all of the components for the first cell are listed first, components for the second cell are listed second, and so forth. The actual input files are comma delimited but are presented here in columnar format to be more readable.

Table 4.3 Description of menu items used to create input files for a two-layer model.

#	Must be preceded by steps	Menu item	Description
1		STATSGO Comp Properties	This program processes the comp and layer soil attribute tables. The program loops through all components in the comp table and for each component loops through the associated layers. The program creates a new data table, which lists each component and the associated soil hydraulic properties for the top layer and the most restrictive layer in that component and the total depth for that component computed using the criteria described in Section 3.1.1.3.
2		30 m Grid Comp Properties	Performs exact same functions as above, but there are differences in the code to account for differences in the attribute tables.
3	1 from Table 4.1 and 1 from this table.	Comp Props File (STATSGO)	Creates one of two required input files for VB-SWBMS (the component properties file) using the STATSGO Theme as input. One line gets written to an ASCII file for each distinguishable component in each model cell. The format for this file is shown in Figure 4.3.
4	1 from Table 4.1 and 2 from this table	Comp Props File (Gridded soils)	Same as above except the 30-m soils grid is used as input. Algorithm is slightly different due to the use of gridded data but the result is identical.
5	1, 2, and 3 from Table 4.1 and either 3 or 4 from this table	Cell Properties File	Creates the second of two required input files for VB-SWBMS, the cell properties file. See Figure 4.3.

Cell properties file:

hrapx	hrapy	cellarea	numcomps	flowlength	pct_imp
560	311	2872067	12	7561.46	13
561	311	522941	4	6163.66	3
556	310	2678711	11	27812.3	0
.
.

The first 12 components listed in the component properties table are for cell (560,311).

Component properties file:

muid	gisclass	compct	totdepth	klu	porlu	theta_r	lambda	hb	fc	wp
51002	71	6.675	162.6	0.45	0.45	0.067	0.41	50	0.239	0.1037
51014	82	1.1595	116.8	0.45	0.45	0.067	0.41	50	0.239	0.1037
51015	83	0.6894	114.3	0.45	0.45	0.067	0.41	50	0.239	0.1037
51017	84	23.2216	182.9	0.45	0.45	0.067	0.41	50	0.239	0.1037
.
.
.

r_klu	r_porl	r_theta_r	r_lambda	r_hb	r_fc	r_wp
0.02	0.36	0.07	0.09	200	0.3367	0.2661
0	0.45	0.067	0.41	50	0.239	0.1037
0	0.45	0.067	0.41	50	0.239	0.1037
0	0.38	0.068	0.09	125	0.3466	0.2703
.
.
.

Figure 4.3 Example input files for the two-layer model.

4.3. The Visual Basic Hydrology Program (VB-SWBMS)

Several different versions of the VB-SWBMS program have been created to investigate the different modeling alternatives discussed in Chapter 3 and Chapter 5. All equations used to make calculations in VB-SWBMS are described in Chapter 3. The overall sequence of computations is the same for different program versions, although the details differ. The base time step for all model versions is one hour. The pseudo-code in Figure 4.4 summarizes the overall computational scheme for the main program. Several subprograms are called from the main program to perform tasks listed in Figure 4.4. A description of all the subprograms is provided in Appendix A.2.

-
- initialization and setup
 - open output files
 - initialize variables
 - read input files
 - cell properties file
 - component properties file (only for two-layer model)
 - texture to soil properties lookup table
 - precipitation file
 - climate data used to estimate potential evaporation
 - initial soil moisture levels (optional)
 - observed flow data (optional)
 - file specifying cells and components for which daily soil water content should be exported (optional)
 - loop through all computational cells
 - initialize precipitation and direct runoff arrays for the current cell
 - loop through soil components (or 12 possible soil types)
 - initialize soil hydraulic properties for current component
 - loop through simulation time steps
 - ❖ if rainstorm is reached
 - ✓ increment time steps and store storm precip array
 - ✓ compute direct runoff due to infiltration excess (GA algorithm - see Figure 3.25) and impervious cover and increment totals for the current cell for all storm time steps
 - ✓ make post-storm soil moisture adjustments (see Figures 3.36 and 3.37)
 - ✓ increment subsurface recharge for the current cell in all storm time steps
 - ❖ else if no rain
 - ✓ estimate evaporation and percolation based on initial water content in each layer

- ✓ compute mass balance on each soil layer
 - ✓ if change in effective saturation is greater than 0.1 then cut time step in half and repeat mass balance calculations
 - ✓ after mass balance, make sure physical limits on effective saturation are not violated -- adjust results if necessary
 - ✓ increment subsurface recharge for the current cell
 - ✓ increment time step
 - ❖ end if rain
 - end of loop through time periods
 - check mass balance on soil zone layers
 - end of loop through soil components
 - write final soil moisture values for each component to a file
 - convert units on direct runoff and subsurface recharge for each cell and for all times
 - compute modClark translated runoff array in each cell
- end of loop through cells
- route translated runoff array for each cell through modClark linear reservoir
- compute baseflow (optional)
- check mass balance on the entire watershed
- write output files
-

Figure 4.4 Pseudo-code describing the overall computational sequence for VB-SWBMS.

A number of checks were made during code development to eliminate errors. Two specific checks that are described here apply to two of the more complicated sections of code, infiltration calculations and soil layer mass balance calculations. The Green-Ampt infiltration code was checked against Example 5.4.1 in Chow, Maidment, and Mays (1988). There are two places in the VB-SWBMS where mass balance checks are written into the code. A mass balance check ensures that the inflow minus the outflow is equal to the change in storage within a specified tolerance. A mass balance check for the soil zone is included at the end of the loop through all time steps in each component. This check is applied both to the top layer and to the soil zone as a whole (in the two-layer model). A mass balance check for the watershed as a whole is also included at the end of the program. Error messages are given if tolerances get violated during these mass balance checks. The mass balance checks are not critical to the operation of the program, but are left in as a debugging tool to help with any future algorithm changes.

A list of input files required by VB-SWBMS is provided in Table 4.4 and a list of output files is provided in Table 4.5. The formats for the files that are used to

transfer spatial information from ArcView are described in Figures 4.1 and 4.2. The required formats for other input files and the formats for output files are described in Appendix A. A description of the VB-SWBMS user interface and brief operating instructions are also discussed in Appendix A.

Table 4.4 Input files for VB-SWBMS

File description	Notes
control file	Stores all input parameters and input filenames so that user does not have to redefine all this information each time the model is used
cell properties file	See Figure 4.2 or 4.3
component properties file	Only used in two-layer model versions (see Figure 4.3)
soil parameters lookup table	Only used in one-layer model versions; actual parameter values are passed in the two-layer model.
rainfall file	
potential evaporation file	This file may contain daily meteorological data in the format specified in Appendix A.2 or previously computed daily potential evaporation estimates using any method.
observed runoff data	optional
soil moisture initialization file	optional, If soil moisture is not initialized with a file then the user can specify a uniform initial effective saturation or a uniform suction head for the entire watershed being modeled.
list of components for which predicted soil water content data will be exported	optional

Table 4.5 Output files for VB-SWBMS

File description	Notes
flow file	Contains direct runoff, baseflow, total runoff, and observed flow (if available)
summary file	Summary of statistics and input parameters for simulation run
final storage values file	Could be used to initialize the soil moisture values in each layer and component and the subsurface storage level for a subsequent simulation
daily average soil moisture for selected components	optional, Used to compare predicted soil water contents with observed soil water contents in the Little Washita

4.4. Summary

The Soil Water Balance Modeling System code is divided into two parts, an ArcView pre-processor called AV-SWBMS and a Visual Basic component for hydrologic computations called VB-SWBMS.

A key aspect of this two part model is that spatial information is transferred from AV-SWBMS to VB-SWBMS using ASCII files. This information transfer becomes significantly more complicated for a two-layer model than for a one-layer model because there is more than one characteristic that differentiates soil components in the two-layer model. With no resampling and a one-layer model, the description of soil properties in each cell can always be accomplished with 13 values (percentage of soil in each texture class and the “other” class), no more and no less. With no resampling and the two-layer model, both the number of components in each cell and the properties associated with each component must be passed to the VB-SWBMS and the number of components will vary from cell to cell. At a minimum, the percent of the cell area covered, the total soil zone depth, the surface soil texture, and the percolation restricting texture must be passed for each component. In the current version, soil textures are converted to hydraulic parameters before this information is passed in the two-layer model (see Figure 4.3).

In addition to data transfer, the mass balance calculations for the two-layer model are significantly more complicated. Although code complexity does not preclude the use of a two-layer model, it is interesting to note that going from a one-layer to a two-layer model requires 3-4 times as many lines of code in AV-SWBMS and about 2 times as many lines of code in VB-SWBMS. These figures are estimated based only on code sections that significantly change between the two cases.

In previous research, Reed and Maidment (1995) developed programs to create a parameter file for the quasi-distributed modClark transform program that is now part of HEC-HMS. The modClark parameter file has a simple structure that is similar to the cell properties files shown in Figure 4.2. The modClark file includes HRAP cell coordinates, area, and average flow length for each rainfall cell. If it desired to implement a similar soil-water balance routine to that described here in HEC-HMS, it would be a straightforward task to add the additional columns shown in Figure 4.2 to the modClark parameter file. In a simple case, the one-layer model with NEXRAD cell level resampling, only the percent imperviousness and soil texture would need to be added to the modClark file. Other cases could be accommodated with the addition of more fields — 13 fields for the one-layer, no resampling case. Even the two-layer model could be accommodated by this data transfer structure (a two file data transfer scheme was used in this study), but the number of additional fields required would vary from cell to cell.

Different version of SWBMS are run in Chapter 5 to evaluate different modeling scenarios. The SWBMS programs are designed to answer specific research questions, not to provide a fool proof user interface (described in Appendix A.2). Based on the evaluation of different modeling scenarios in Chapter 5, future work can be geared towards cleaning up and integrating the most useful versions of SWBMS and making them more user friendly.

CHAPTER 5. ANALYSIS AND RESULTS

5.1. Overview

The purpose of this chapter is to examine the influence of the following factors on simulated direct runoff: (1) different levels of spatial detail in describing soil properties, (2) uncertainty in rainfall estimates, and (3) uncertainty in model parameter values associated with each of the basic USDA texture classes. This overview section lays out the strategy for making simulation runs, including a description of the alternatives being studied and the calibration and validation procedures.

As described in Section 3.2.4, three levels of resampling are considered for representing soil variability.

- No resampling: Estimate the percentage of each soil type or the percentage of all distinguishable soil components within each cell and make vertical flux calculations separately for each soil type.
- NEXRAD cell level resampling: Assign a representative soil type to each NEXRAD cell.
- Watershed level resampling: Assign a representative soil type to the entire watershed.

The rainfall excess in each cell is routed to the watershed outlet the same way in all three cases.

Several model variations in addition to spatial resampling are also of interest, including a study of the differences caused by the use of input data at two different map scales, the implications of choosing between a one-layer and a two-layer soil model, and the advantages and disadvantages of simulating baseflow versus using baseflow separation. Considering all of these factors, there are many combinations (3 resampling levels x 2 map scales x 2 layer options x 2 baseflow methods = 24 total

combinations) that may be of interest. A strategy is proposed here so that all of these combinations do not need to be analyzed. Insights about the one-layer versus two-layer approach and using baseflow simulation versus baseflow separation are derived for the most complex soil representation (no resampling and using the 30-m soils grid as input), and it is assumed that these insights hold for the simpler representations. The insights gained from these initial simulations lead the author to believe that using a one-layer soil model and baseflow separation is adequate to compare the remaining six scenarios which involve the three resampling levels and two map scales.

Another important issue to consider in these runoff modeling scenarios is the accuracy of the rainfall data. In examining the NEXRAD Stage III rainfall data and comparing it with data from the Little Washita Micronet, significant differences in rainfall magnitudes are noted for the brief period when Micronet data are available, although the spatial distributions of rainfall in the two data sets is similar. A data set in which the NEXRAD rainfall field has been adjusted to be more consistent with rainfall magnitudes reported by the Micronet is used for the majority of simulation runs. A comparison of NEXRAD and Micronet values and the preparation of this adjusted rainfall data set is described in Section 5.3.

The remainder of this chapter includes four sections.

- Section 5.2: A description of a general procedure for calibration and validation.
- Section 5.3: A comparison of NEXRAD rainfall estimates with Micronet rainfall estimates and creation of an adjusted NEXRAD rainfall field for subsequent simulation runs.
- Section 5.4: A comparison of the one-layer and two-layer simulation models and the implications for the use of a baseflow simulation or baseflow separation approach.
- Section 5.5: A study of simulations using the different horizontal soil representations (using three different resampling levels and using source data from two different map scales).

- Section 5.6: A sensitivity analysis aimed at understanding the impacts of model input uncertainties on runoff. Input uncertainties include rainfall error, soil moisture initialization, and the uncertainties inherent to specifying soil hydraulic properties based on USDA texture class.

5.2. Calibration and validation procedures

For each selected set of modeling options (i.e., a one-layer model with no resampling, 30-m soils data, and baseflow separation), both a calibration and a validation run are made. The calibration and validation runs are made for different time periods. In the calibration time period, model parameters are adjusted in an effort to provide the best match between simulated and observed flow data (and simulated and observed water content data in one case). For simulations during the validation time period, the optimal parameter values determined during the corresponding calibration time period are used. Performance during the validation phase is used to compare modeling scenarios.

5.2.1. Calibration

Calibration is done for a time period during the Southern Great Plains 1997 hydrology experiment so that both observed runoff data and observed soil moisture data can be used. The dates used for calibration are 6/18/97 – 7/22/97. Although a greater premium is placed on matching runoff data, it is interesting to see how well the variability of soil moisture is described by the model.

Runoff data recorded at 15 minute intervals were obtained from the Oklahoma U.S. Geological Survey and resampled to hourly average values for comparison with hourly modeled flows. As described in Section 3.2.6, gravimetric soil moisture samples were taken at 23 different sites in the Little Washita watershed from 6/18/97 – 7/16/97. The average of twice daily soil moisture measurements from selected sandy loam, loamy sand, loam, and silt loam sites are compared with simulated values in selected NEXRAD cells to assist with calibration.

A general calibration procedure is summarized here.

1. Initialize top layer soil moisture values using representative gravimetric soil moisture measurements from SGP97 for all sandy loams (SL), loamy sands (LS), loams (L), and silt loams (SIL) in the model. Other textures found in the watershed cover only a small fraction of the area but their water contents also must be initialized. To do this, the suction head of one of the texture values for which water content is known (SL, LS, L, or SIL) is used to estimate the initial water content in the other textures with the most similar properties. For example, the initial water content of sandy loam is known but the initial water content for sand is not known. The initial suction head for sandy loam is computed and then it is assumed that the initial suction head for sand is the same. Subsequently, the initial water content for sand is estimated using Equation 3.1. In the two-layer model runs, there are no data that can be used to assign initial water content for the bottom layer. Initial water content in the bottom layer may significantly influence baseflow. The top layer depth is set to 5 cm to compare results with observed soil moisture values that are from the top 5 cm of soil.
2. A user defined hydraulic conductivity calibration factor (k_f) is multiplied by the saturated hydraulic conductivity for each soil unit being modeled. This calibration factor is modified and calculations are repeated until either the total volume of simulated direct runoff matches the total observed direct runoff (baseflow separation case) or the total volume of modeled runoff and baseflow matches the total volume of observed streamflow (baseflow simulation case). Total observed direct runoff (ODR) and total simulated direct runoff (SDR) are computed using Equations 5.1 and 5.2.

$$\text{Equation 5.1} \quad \text{ODR} = \sum Q_o^d \Delta t$$

$$\text{Equation 5.2} \quad \text{SDR} = \sum Q_s^d \Delta t$$

In application, reasonable results are obtained through manual calibration and by carrying k_f to one decimal place for most cases. Calibrated k_f values range from 0.5 to 5.4 for different modeling options.

3. ModClark transform parameters (T_c , R) are modified to approximate the peak and spread in observed hydrographs. Changing these parameters will not influence the calibration of k_f unless a significant amount of surface water is still stored in the watershed at the end of the simulation time period. T_c and R parameters were adjusted manually in an attempt to minimize the HEC-1 objective function (HECOBJ) defined by Equations 5.3 and 5.4 (HEC, 1997). For all simulation results presented in this section, the values $R = 9$ hours and $T_c = 12$ hours are used. The HEC-1 objective function is designed to give greater weight to flow deviations associated with higher flows.

$$\text{Equation 5.3} \quad \text{HECOBJ} = \sqrt{\frac{\sum_{t=1}^n (Q_o(t) - Q_s(t))^2 \frac{(Q_o(t) + Q_A)}{2Q_A}}{n}}$$

$$\text{Equation 5.4} \quad Q_A = \frac{1}{n} \sum_{t=1}^n Q_o$$

4. The rooting depth parameter (d_r) is modified to get the closest fit to daily average soil moisture observations for the four available textures. The sum of absolute residuals (SAR) for 26 days and four different soil textures is used as a measure of the fit. The mathematical definition of SAR is given in Equation 5.5. Rooting depth values are calibrated manually to the nearest 5 cm. Calibration against soil moisture is only implemented in runs with no resampling because all of the correct textures do not exist in the correct rainfall cells with the other resampling levels. The rooting depth parameter values determined using the no resampling option are used for simulations with NEXRAD cell level and watershed level resampling.

$$\text{Equation 5.5} \quad \text{SAR} = \sum_{j=1,4} \sum_{k=1,2,6} |\bar{\theta}_o - \bar{\theta}_s|$$

5. After adjusting the rooting depth parameter (d_r), check to make sure that the optimal k_f value has not changed. If it has changed, repeat steps 2 and 4.

A summary of the model parameters that cannot be specified directly from the soils databases is provided in Table 5.1. In the third column of this table there is an explanation of how values for each of these parameters is determined.

Table 5.1 Model parameters not specified from soils databases.

Symbol	Description	Method of specification
k_f	hydraulic conductivity calibration factor	Determined through calibration against direct runoff. In this study, values of k_f range from 0.5 to 5.4, depending on the modeling options.
d_1	top layer depth	Taken as 5 cm for calibration and validation runs because observed soil moisture samples are from the top 5 cm of soil.
d_r	root zone depth	Determined through calibration against observed soil moisture. Values determined in different calibration runs were 35, 40, and 50 cm.
p_2	percolation out of layer 2 if it is underlain by a non-soil, low permeability layer	Used in two-layer model only. Varied in attempt to match observed baseflow (see Section 5.4). A value of $0.0015 \text{ cm hour}^{-1}$ seems reasonable.
χ	baseflow storage constant	Only required when baseflow is simulated. Estimated based on a visual comparison of simulated flow and the baseflow recession curve. A value of 240 hours seems reasonable.
n	baseflow separation parameter	Only required when baseflow separation is used. Taken as 60 hours.
T_c	modClark time of concentration	Initial estimates of T_c and R were determined by scaling estimates from a previous modClark study in another part of Oklahoma. Values of T_c and R were adjusted manually in an effort to minimize HECOBJ function during the calibration period. The resulting values used in all simulation runs were $R = 9$ hours and $T_c = 12$ hours.
R	modClark storage constant	see above

5.2.2. Validation

Validation runs are made during a time period preceding the calibration period, 6/01/97-6/18/97. A big storm occurs just prior to this validation period on 5/30/97 so the top layer soils are assumed to be initially saturated. The k_f and d_r values determined from the corresponding calibration run are used in validation runs. Modeled runoff from storms that occur on 6/10/97, 6/13/97, and 6/17/97 is compared with observed runoff.

For selected cases, validation runs are also made for the time period 5/7/97-5/24/97.

5.3. Comparison of NEXRAD and Micronet rainfall

Although the NEXRAD Stage III data are derived using both radar and rain gage information, the density of rain gage information used to develop the Stage III product is much less than that of the Micronet rain gage network. In this section it is assumed that when all Micronet stations are reporting, the Micronet data provide a better indicator of rainfall depths, and are used here to check the reliability of the NEXRAD data. Micronet data from the Agricultural Research Service are available for June, July, and August of 1997. As discussed in Section 3.2.6, there are 42 Micronet sites where rainfall measurements are taken; however, not all 42 stations reported valid data during a significant portion of June, 1997. Hourly rainfall totals have been computed from this data set by accumulating 5 minute data for each station. A summary of storm average rainfall totals computed based on Micronet data and NEXRAD data is provided in Table 5.2. The Micronet storm totals are computed by first determining the arithmetic average of the station values in a given hour and then summing the hourly averages for all hours in a storm. NEXRAD storm totals are computed similarly, first hourly arithmetic averages are computed from the values in all cells and then the hourly averages are summed over the storm duration. No area-weighting was used to determine the storm totals in Table 5.2.

The ratios of Micronet storm totals to NEXRAD storm totals (M/N) and the differences (M – N) between these quantities are tabulated in the last two columns of Table 5.2. For the ratios, there is no clear trend as to whether the NEXRAD totals tend to be greater than or less than the Micronet totals. The mean of the M/N ratio for all storms is 0.88 with a standard deviation of 0.31. The absolute differences between the two estimates are not exceptionally large in most cases except the storm of 7/10/97 where the NEXRAD data yield 2.72 cm more rain than the Micronet data. Since this is a critical storm within the selected calibration period, a further study of rainfall differences for this storm has been made.

Table 5.2 Comparison of storm rainfall totals between Micronet and NEXRAD data.

Storm begins	Storm duration (hrs)	Micronet Storm Totals, M (cm)	Nexrad Storm Totals, N (cm)	# of Micronet Stations Reporting	M/N	M - N
6/13/97 6:00	5	1.85	2.08	11	0.89	-0.24
6/15/97 4:00	3	0.10	0.17	16	0.57	-0.07
6/17/97 2:00	14	0.85	1.26	19	0.68	-0.40
6/22/97 22:00	22	1.24	0.83	23	1.50	0.41
6/26/97 12:00	12	0.19	0.17	32	1.10	0.02
6/27/97 18:00	28	0.42	0.91	36	0.46	-0.49
7/4/97 9:00	5	0.48	0.54	41	0.88	-0.06
7/9/97 19:00	6	0.17	0.16	41	1.09	0.01
7/10/97 19:00	16	4.78	7.51	42	0.64	-2.72
7/15/97 18:00	6	0.95	0.94	42	1.01	0.01

Maps in Figure 5.1 show the spatial distribution of rainfall estimated from the two data sources for 8 hours during the July 10, 1997 storm. The Micronet data are mapped using Thiessen polygons. There are actually fewer than 42 Thiessen polygons in these maps because some stations were missing data during part of the storm and no polygons were created for these stations. The fact that the number of rainfall stations reporting valid data changes with time is a clear drawback of using Thiessen polygons for spatially distributed modeling. Each time there is a missing station or an added station, the spatial network changes.

It is encouraging to see that the spatial distributions of rainfall from the two data sources are comparable. Differences in the areas covered by intense rainfall are evident at 7/11/97 00:00 GMT.

Micronet

7/10/97 20:00 GMT

NEXRAD



7/10/97 21:00 GMT



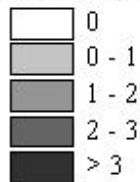
7/10/97 22:00 GMT



7/10/97 23:00 GMT



Rainfall (cm/hr)



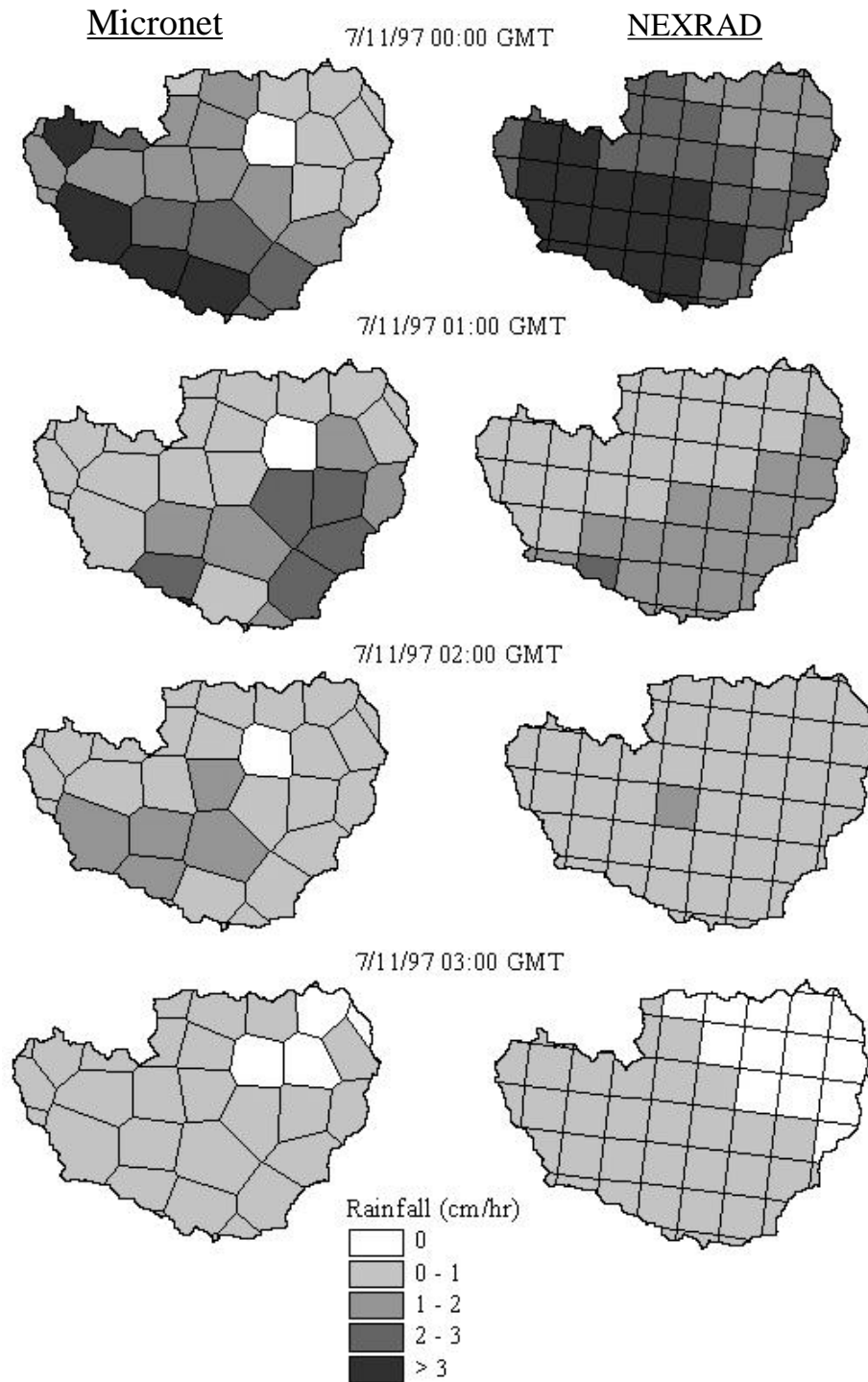


Figure 5.1 A comparison of Micronet and NEXRAD Stage III rainfall estimates for 8 hours of the 7/10/97 storm.

It is interesting to see how differences in rainfall magnitudes influence the values of parameters determined through calibration. A comparison is made here between a calibration run made using the NEXRAD rainfall field and a run using an adjusted NEXRAD rainfall field in which all rainfall values for the July 10, 1997 storm are multiplied by the M/N ratio for that storm (0.64). The one-layer model with 1:24,000 scale soils data, baseflow separation, and no resampling is used for this illustration. The calibrated parameter values (k_f and d_r) for the two cases are given in Table 5.3. Statistics for both the calibration and validation runs are given in Table 5.4.

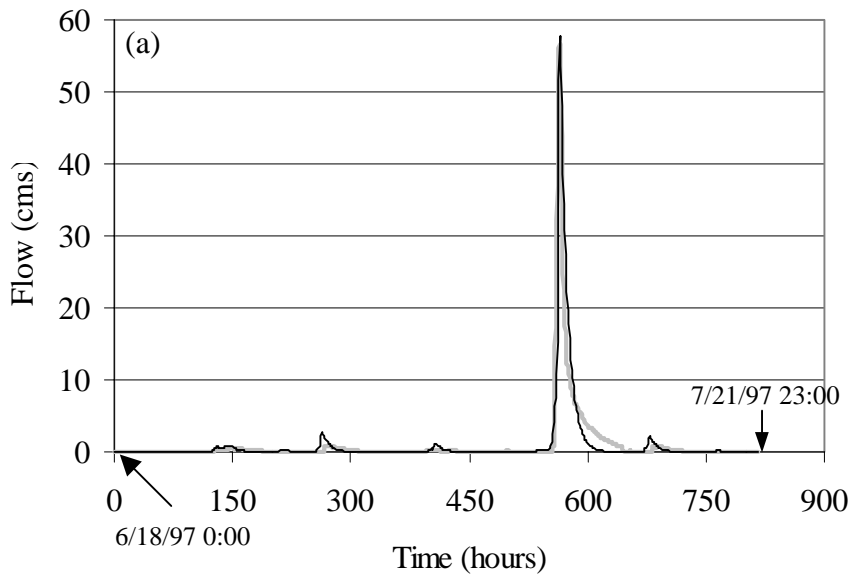
Figure 5.2 shows calibrated direct runoff (6/18/97-7/22/97) generated using the two rainfall input data sets and Figure 5.3 shows plots of direct runoff for the validation runs (6/1/97 – 6/18/97). As one might expect, there is little difference between the observed and predicted direct runoff during the calibration phase for both rainfall data sets because the value of k_f is modified to achieve the best fit in both cases. There is a big difference in the calibrated k_f values for the two cases, 5.4 for non-adjusted and 1.9 for adjusted rainfall. The validation results for the adjusted rainfall are significantly better than the validation results for non-adjusted rainfall as indicated by the SDR/ODR ratios in Table 5.4 and the direct runoff hydrographs shown in Figure 5.3.

Table 5.3 Calibrated parameter values for NEXRAD and adjusted NEXRAD simulations.

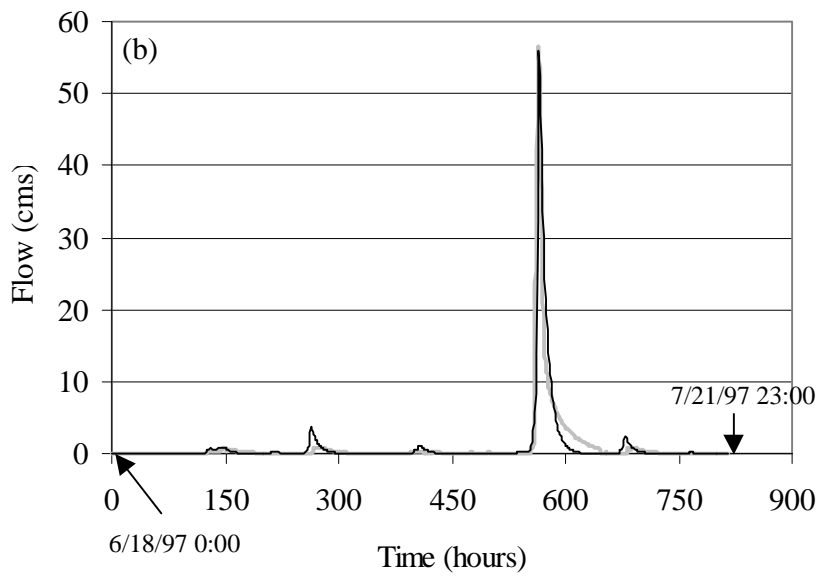
Parameter	NEXRAD	Adjusted NEXRAD
k_f	5.4	1.9
d_r	50 cm	40 cm

Table 5.4 Statistics describing NEXRAD and adjusted NEXRAD calibration and validation runs.

Statistic	NEXRAD	Adjusted NEXRAD
Calibration:		
ODR (m ³)	2,989,816	2,989,816
SDR (m ³)	2,965,103	2,935,168
SDR/ODR	0.99	0.98
HECOBJ (m ³ /s)	2.39	2.44
SAR for soil water content	4.91	4.45
Validation:		
ODR (m ³)	1,658,031	1,658,031
SDR (m ³)	741,265	1,225,445
SDR/ODR	0.45	0.74
HECOBJ (m ³ /s)	3.57	2.79

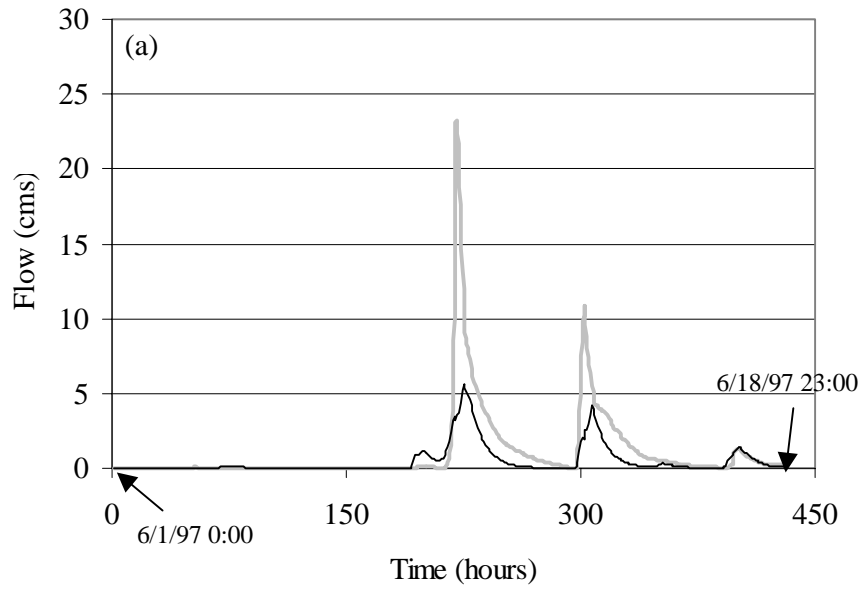


— Observed direct runoff (cms) — Simulated direct runoff (cms)

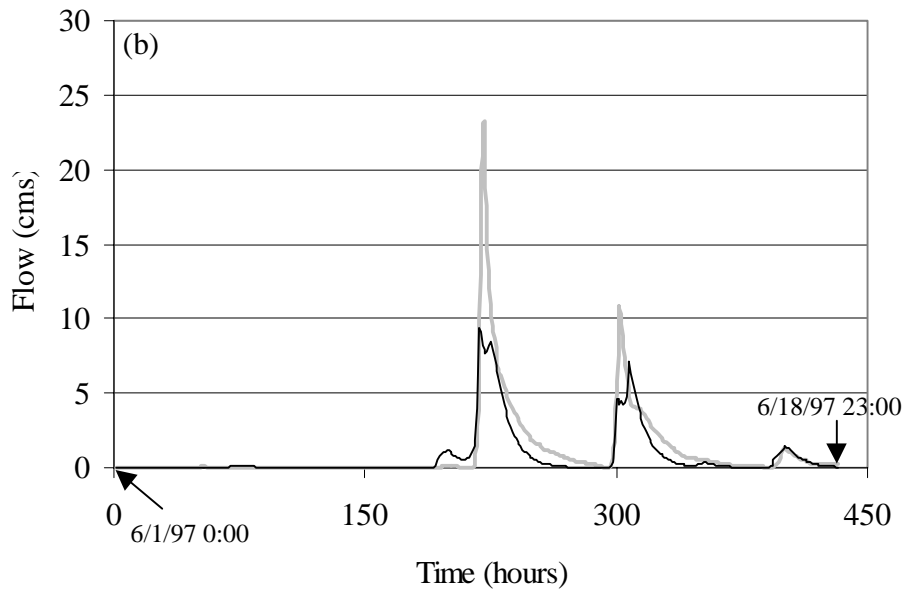


— Observed direct runoff (cms) — Simulated direct runoff (cms)

Figure 5.2 Calibrated flows using (a) NEXRAD and (b) adjusted NEXRAD rainfall.



— Observed direct runoff (cms) — Simulated direct runoff (cms)



— Observed direct runoff (cms) — Simulated direct runoff (cms)

Figure 5.3 Validation runs using parameters from Table 5.3. (a) NEXRAD and (b) adjusted NEXRAD rainfall.

As seen in Table 5.4, the SAR statistic between modeled and observed soil water content is lower for the case with adjusted rainfall, another indication that the model performs better using the adjusted rainfall. Figure 5.4 is included to give an idea of how well the model predicts average daily soil water content values when the adjusted rainfall is used. The graphs in Figure 5.4 represent the lowest overall SAR value that could be achieved by varying d_r by increments of 5 cm with k_f equal to 1.9. The best match for an individual soil type occurs with the loam soil ($SAR_1 = 0.72$). Although the trends make sense, there are considerable differences between observed and modeled soil water content values.

Given the comparisons between NEXRAD Stage III data and Micronet data and between simulations made using the original NEXRAD data and adjusted NEXRAD data, the adjusted NEXRAD data are used for simulations described in Sections 5.4, 5.5, and 5.6.

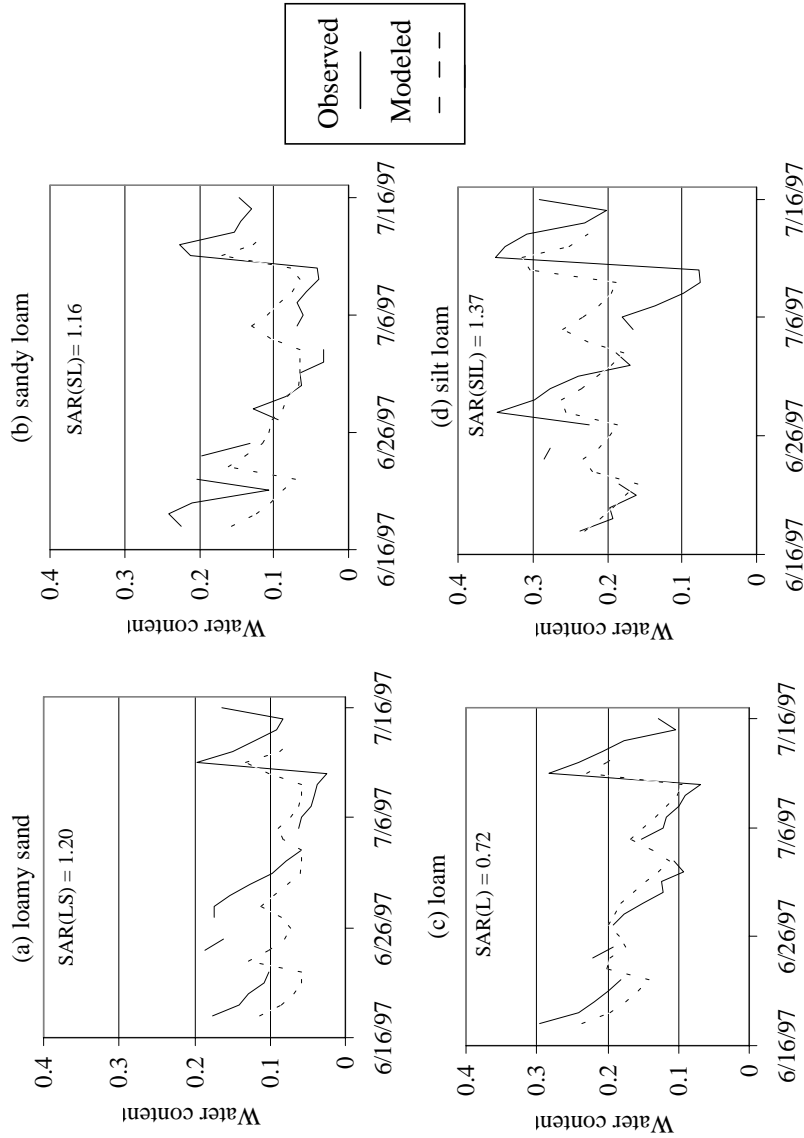


Figure 5.4 Comparison of modeled and observed average daily soil moisture for (a) a loamy sand in cell (557, 309) and observed data averaged from sites 3, 4, and 5; (b) a sandy loam in cell (559, 305) and observed data from site 17; (c) a loam in cell (560, 309) and observed data averaged from sites 11, 12, and 13; and (d) a silt loam in cell (555, 307) and observed data averaged from sites 8 and 9.

5.4. One-layer vs. two-layer model

In this section, the differences in predicted direct runoff from a one-layer and two-layer model are compared. In addition, simulations are presented showing the advantage of using a two-layer model when it is desired to simulate baseflow.

5.4.1. Direct runoff

To compare direct runoff, calibration and validation runs were made using the two-layer model and the one-layer model, each using the 1:24,000 scale spatial data and the baseflow separation option. Calibrated parameters for the one and two-layer models are given in Table 5.5 and statistics for these simulation runs are given in Table 5.6. Figure 5.5 shows the direct runoff generated by the one-layer and two-layer models during the validation period. Note that the one-layer results are identical to those from Section 5.3 (for the case of the adjusted rainfall field which is also used in this section).

Table 5.5 Calibrated parameter values for the one-layer and two-layer models.

Parameter	One-layer	Two-layer
k_f	1.9	1.8
d_r	40 cm	35 cm

Table 5.6 Statistics describing one-layer and two-layer calibration and validation runs.

Statistic	One-layer	Two-layer
Calibration:		
ODR (m ³)	2,989,816	2,989,816
SDR (m ³)	2,935,168	3,043,277
SDR/ODR	0.98	1.02
HECOBJ (m ³ /s)	2.44	2.52
SAR for soil water content	4.45	4.41
Validation:		
ODR (m ³)	1,658,031	1,658,031
SDR (m ³)	1,225,445	1,352,298
SDR/ODR	0.74	0.82
HECOBJ (m ³ /s)	2.79	2.65

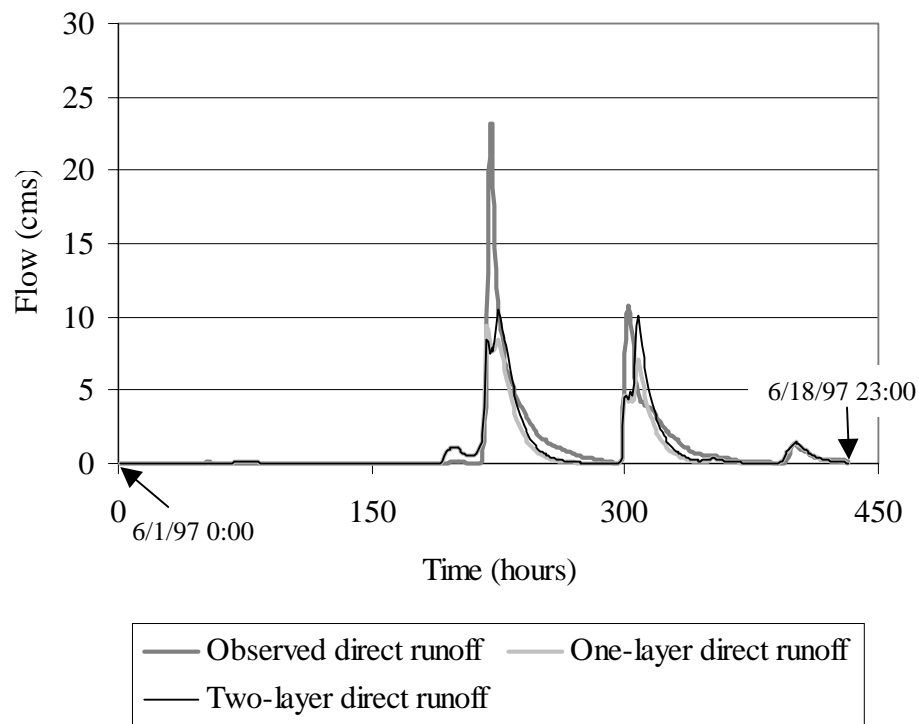


Figure 5.5 Flow during the validation period for the one-layer and two-layer models.

The calibrated parameter values for the one and two-layer models are very similar. The difference in the calibrated parameters is caused primarily by a difference in the assumption that is made to deal with non-soil cells in the 30-m soils grid (i.e. water, sewage lagoon, and limestone). Note that these non-soil cells are not assumed to be impermeable because this might be redundant with the land use data, which also identifies water bodies. The simplicity of data structure in the one-layer model made it easy to divide the percentage of each NEXRAD cell taken up by non-soil grid cells proportionally among the existing texture classes. Because of the greater complexity of the two-layer data structure, all non-soil cells are assigned the properties of a single soil type in this model. The differences that cause the calibrated k_f value to be 1.9 for the one-layer model and 1.8 for the two layer model are very subtle. The two-layer simulation with a k_f value of 1.8 is only slightly better than a two-layer simulation with a k_f value of 1.9. In fact, the best k_f value for both the one and two-layer models is close to 1.85. Thus, one reason why the validation run for the two-layer model is slightly superior to that for the one-layer model is due to rounding in the calibration phase.

For the two-layer model, a small amount of saturation excess runoff ($23,575 \text{ m}^3$) is generated during the validation phase when shallow soil components underlain by bedrock become saturated. This amount of saturation excess runoff constitutes only 1.7% of the simulated direct runoff during the validation phase. The amount of saturation excess that is generated is a function of the user specified percolation rate for non-soil, low permeability layers (p_2). The value assigned to p_2 for the simulations described in Table 5.6 and Figure 5.5 is 0.0015 cm/hour, which seems to be a reasonable value as discussed later in this section. The other major factor that influences the amount of saturation excess runoff is the depth of the soil zone. The small amount of saturation excess runoff in this example was generated from soils with less than 20 cm of total depth.

Based on the evidence in Tables 5.5 and 5.6, and Figure 5.5, the two-layer model is only slightly superior to the one-layer model in predicting direct runoff during the validation period; therefore, given the additional complications associated with using the two-layer model, the one-layer model is used for further analysis in Sections 5.5 and 5.6.

5.4.2. Baseflow

Although the simplicity of the one-layer model is preferred for simulating direct runoff, the second soil layer provides an advantage when simulating baseflow. Although the focus of this study is on direct runoff and not baseflow, a simple example is included here to illustrate this point.

If percolation out the bottom of a one-layer soil model is passed directly to a single linear reservoir for simulating baseflow, then this subsurface reservoir receives so much flow that it is not possible to match hydrograph recession. To show this, a calibration run is initialized with a recession constant of χ equal to 240 hours and a subsurface storage (S) of 2,510,000 m³ so that the initial streamflow is equal to the initial observed streamflow of 2.9 m³/s, (See Figure 5.6a). Provided there is not a large amount of initial percolation, a value of 240 hours for the recession constant is reasonable to approximate the recession rate for the first 120 hours in Figure 5.6a. However, when a storm occurs, the percolation influx to the subsurface creates unreasonably high subsurface storage and baseflow. This problem cannot be alleviated by simply increasing the subsurface storage constant. An extreme example of attempting to increase the subsurface storage constant is shown in Figure 5.6b. For Figure 5.6b, the subsurface storage constant is two years ($\chi = 17520$ hours) and the initial subsurface storage is set to 183,957,998 m³ in order to match the observed baseflow of 2.9 m³/s. With such a large storage constant, the ridiculously high baseflows of Figure 5.6a are eliminated but the baseflow curve becomes flat and cannot reflect the natural recession.

Using the two-layer soil model, the second soil layer provides a reservoir for infiltrated water which can subsequently evaporate or percolate to the subsurface reservoir. Simulation runs indicate that a more reasonable approximation for baseflow can be achieved using the two-layer model than using the one-layer model. Use of the two-layer model requires that the user specify a percolation rate (p_2) for soil components underlain by non-soil material such as weathered bedrock. As noted in Section 3.2.2.3, this percolation rate influences 47% of the Little Washita area being modeled. Using a recession constant of χ equal to 240 hours, an initial subsurface storage of 2,510,000 m³, and a non-soil percolation rate equal to 0.0015 cm/hour, a more reasonable baseflow hydrograph is simulated, as shown Figure 5.7. The simulation results shown in Figure 5.7 do not represent an optimal solution and are only presented with the intent to contrast the results of Figure 5.6.

The use of a two-layer model with baseflow simulation has not been fully explored in this research. Different combinations of p_2 , χ , initial subsurface storage, and initial water content in the second layer may provide equally valid or superior results to those shown in Figure 5.7. The second layer water content influences both the total amount of evaporation from the soil profile and the amount of percolation to the subsurface reservoir. Questions remain unanswered as to how the lower layer water content should be initialized and how realistic the final water content of the lower layer is relative to the initial water content. Perhaps, these are appropriate subjects for further research.

One important conclusion from the comparison of the one-layer and two-layer models is that for the validation period selected, the two-layer model does not significantly outperform the one-layer model in terms of predicting direct runoff. The one-layer model is much more practical to implement and is adequate to assess the effects of horizontal soil variability on direct runoff as described in the next section.

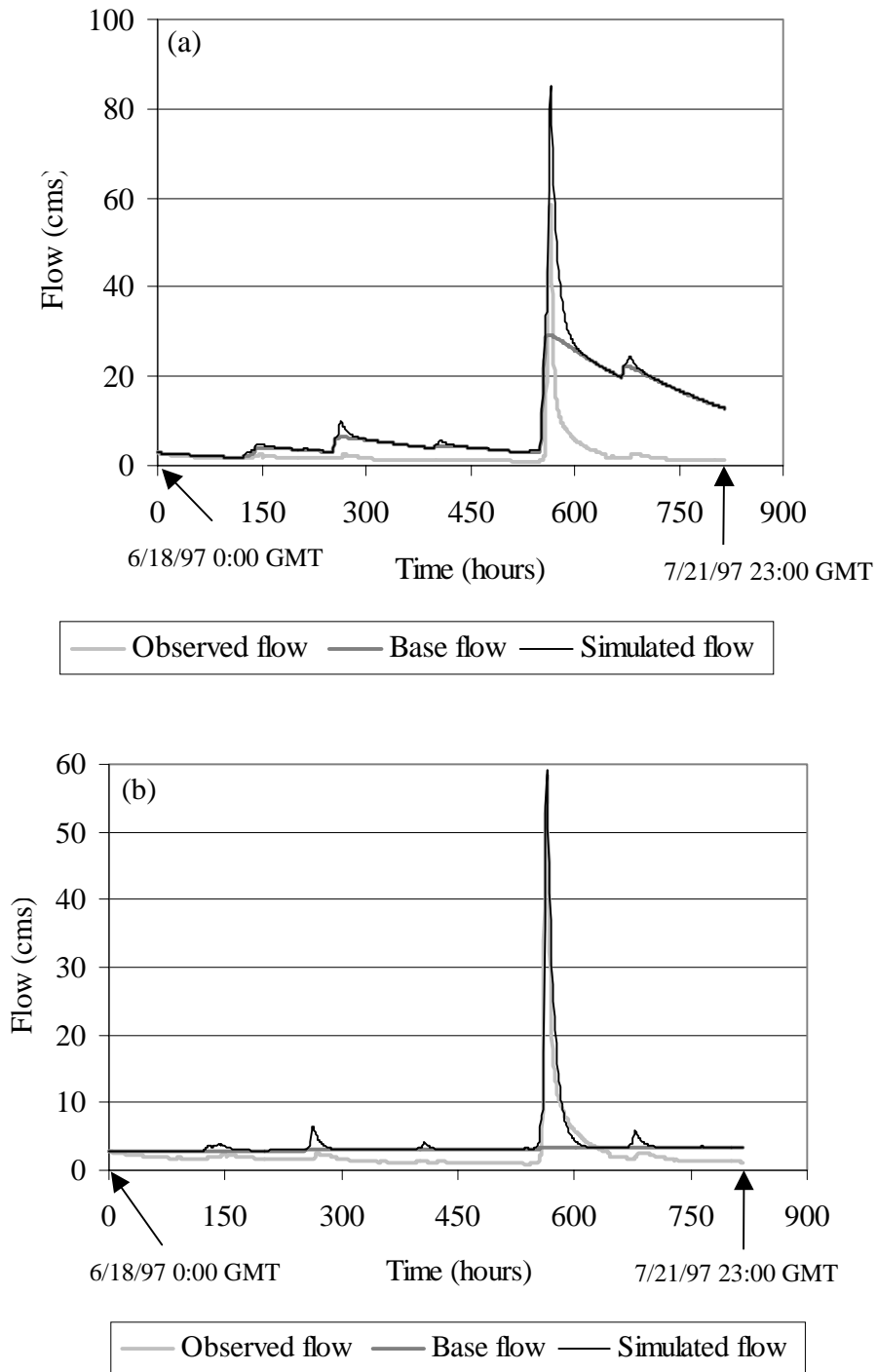


Figure 5.6 Attempts to simulate baseflow using the one-layer soil model. (a) recession constant $\chi = 240$ hours (b) recession constant $\chi = 17520$ hours.

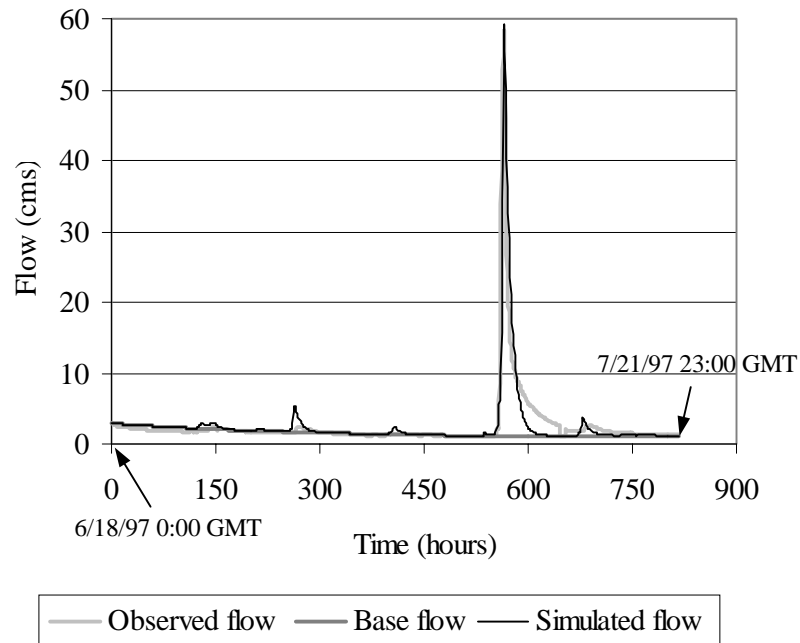


Figure 5.7 Hydrographs from two-layer simulation with $\chi = 240$ hours and $p_2 = 0.0015$ cm/hour.

5.5. Horizontal soil variations (spatial resampling and map scale issues)

An important objective of this research is to explore the implications of spatial resampling and map scale on runoff prediction. Six sets of calibration and validation runs using three resampling levels and two map scales are summarized in Table 5.7. Values of the ratio SDR/ODR closest to 1 are best while low values of HECOBJ are best. With one exception (watershed level resampling with STATSGO data), as spatial resampling decreases (meaning that spatial variability increases) the results improve. Looking at validation runs using the 30-m soils grid, the SDR/ODR ratio is the highest with no resampling (0.74) and decreases by 32% to 0.5 with NEXRAD cell level resampling and by another 8% to 0.46 with watershed level resampling. Still looking at validation runs using the 30-m soils grid, the HEC-1 objective function is the best (lowest) for no resampling and gets worse (increases) by 18% when NEXRAD cell level resampling is used. The HEC-1 Objective function

actually decreases slightly (3%) moving from NEXRAD cell level to watershed level resampling. Based on the numbers in Table 5.7, it appears that there is a significant drop-off in performance between no resampling and NEXRAD cell level resampling and a much smaller drop-off between NEXRAD cell level and watershed level resampling.

The differences between STATSGO and 30-m grid simulations are quite noticeable for watershed level resampling but not as marked for NEXRAD cell level resampling and no resampling. With NEXRAD cell level resampling, the ratio SDR/ODR indicates slightly better performance using STATSGO data, but the HECOBJ statistics indicate slightly better performance with the 30-m grid. With no resampling, the SDR/ODR ratio indicates slightly better performance using the 30-m grid data while the HECOBJ function values are identical. A graph of the validation flows for the no resampling, 30-m grid case was shown in Figure 5.3b.

Since the good performance of the watershed level resampling, STATSGO combination is inconsistent with the trend of improved performance with decreased model resampling, additional validation runs have been made to compare the watershed level resampling, STATSGO combination with the no resampling, 30-m grid combination. These validation runs were made for the time period 5/7/97 to 5/24/97 and the same parameter values determined from the original calibration runs (Table 5.7) were used. In theory, the same k_f should be applicable for this time period but perhaps not the same d_r value. Figure 5.8 shows graphical results from this second validation period and validation statistics are given in Table 5.8. Since no observed soil moisture data are available for this time period, all soils were initialized to the same effective saturation and this initial value was adjusted to get the best fit with observed data. Since the model overpredicts runoff for this period, a low effective saturation of 0.1 was used to initialize the model for the results shown here. The results in Figure 5.8 and Table 5.8 show that the no resampling, 30-m grid

combination significantly outperforms the watershed level resampling, STATSGO combination in this period.

Table 5.7 Calibrated parameter values and validation statistics for the one-layer model with different levels of model resampling and different soil map inputs.

Resampling	Soils Data Source	Calibrated parameter values		Statistics for validation runs	
		k_f	d_r^{***}	SDR/ODR	HECOBJ (m ³)
watershed	STATSGO**	0.49	40	0.66	2.5
watershed	30-m grid*	3.0	40	0.46	3.2
NEXRAD cell	STATSGO	2.2	40	0.55	3.4
NEXRAD cell	30-m grid	2.4	40	0.50	3.3
none	STATSGO	1.7	40	0.69	2.8
none	30-m grid	1.9	40	0.74	2.8

* Entire watershed assumed to be silt loam.

** Entire watershed assumed to be sandy loam.

*** d_r is only calibrated for the no resampling option.

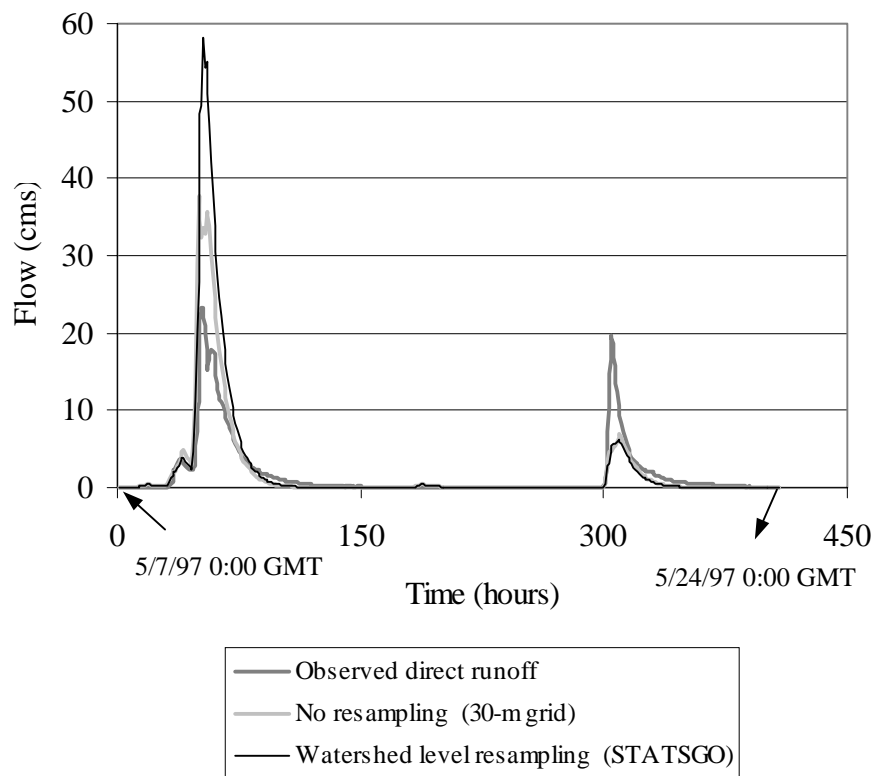


Figure 5.8 Comparison of direct runoff from watershed level resampling, STATSGO simulation with direct runoff from a no resampling, 30-m grid simulation for 5/7/97 - 5/24/97.

Table 5.8 Statistics for the watershed level resampling, STATSGO combination and the no resampling, 30-m grid combination for validation during 5/7/97 - 5/24/97.

Resampling	Soils Data Source	SDR/ODR	HECOBJ
watershed	STATSGO*	1.42	9.3
none	30 m grid	1.13	5.4

* Entire watershed assumed to be silt loam.

5.6. Sensitivity analysis

From the discussion in Section 3.2.2.2, it is clear that there is considerable uncertainty involved with specifying the soil parameter values (ϕ , θ_r , h_b , and λ) based on texture class. There is also considerable uncertainty in specifying K_s but this parameter is not considered here because the calibration factor k_f is used to adjust this parameter. To get a feel for how the uncertainty in input parameters influence model results, the nominal range method of sensitivity analysis is used. In this method, a model is run using high and low values for a given parameter while keeping the other parameters at their nominal values (Morgan and Henrion, 1990).

The mean soil parameter values reported by Carsel and Parrish (1988) are considered the nominal values. Low values and for each parameter are taken as the minimum of the Carsel and Parrish (1988) and Rawls, Brakensiek, and Saxton (1982) values corresponding to 1 standard deviation below the mean. High values are taken as the maximum of the Carsel and Parrish (1988) and Rawls, Brakensiek, and Saxton (1982) values for 1 standard deviation above the mean. This is equivalent to taking the minimum and maximum parameter values within each texture class from Figures 3.8 - 3.11. For some textures, the high values for θ_r exceeded the nominal wilting point values computed from the nominal h_b and λ values. In these cases, the high θ_r values were set equal to the wilting point to prevent an error in the model mass balance.

Sensitivity runs were made for the 6/18/97-7/22/97 using the model scenario that showed the best overall performance in Section 5.5, a one-layer model with no resampling that uses the 30-m soils grid. The results of the sensitivity analysis are presented in the form of a tornado diagram shown in Figure 5.9. The tornado diagram shows the deviations in the ratio SDR/ODR from the nominal case caused by using high and low parameter values. Parameters are ranked from top to bottom by the degree to which their uncertainty influences model results. In addition to uncertainty in soil parameter values, model sensitivity to uncertainty in rainfall and initial soil water content is also shown in Figure 5.9. The results of simulation runs with rainfall depths varied by +/-20% and +/-30% from the adjusted NEXRAD field are shown.

Model sensitivity to initial soil moisture is tested in two ways. In one set of sensitivity runs, the initial effective saturation (Θ_i) is set to high and low values of 1 and 0 for all soils on 6/18/97. In this case, the modeled direct runoff is insensitive to initial soil moisture because the major storm does not occur until 7/10/97. For the run with nominal values, soil moisture on 6/18/97 is initialized using observed data as described in Section 5.2.1. In a second set of runs, simulations are begun on 7/10/97, the morning of the big storm, and initial effective saturation values for all soils are set to high and low values of 1 and 0. In this case, the initial soil moisture does have a significant impact on the modeled runoff. The results for this case are denoted by the symbol Θ_i^* in Figure 5.9. Note that the nominal value of the ratio SDR/ODR changes for this case and this is reflected in the results shown.

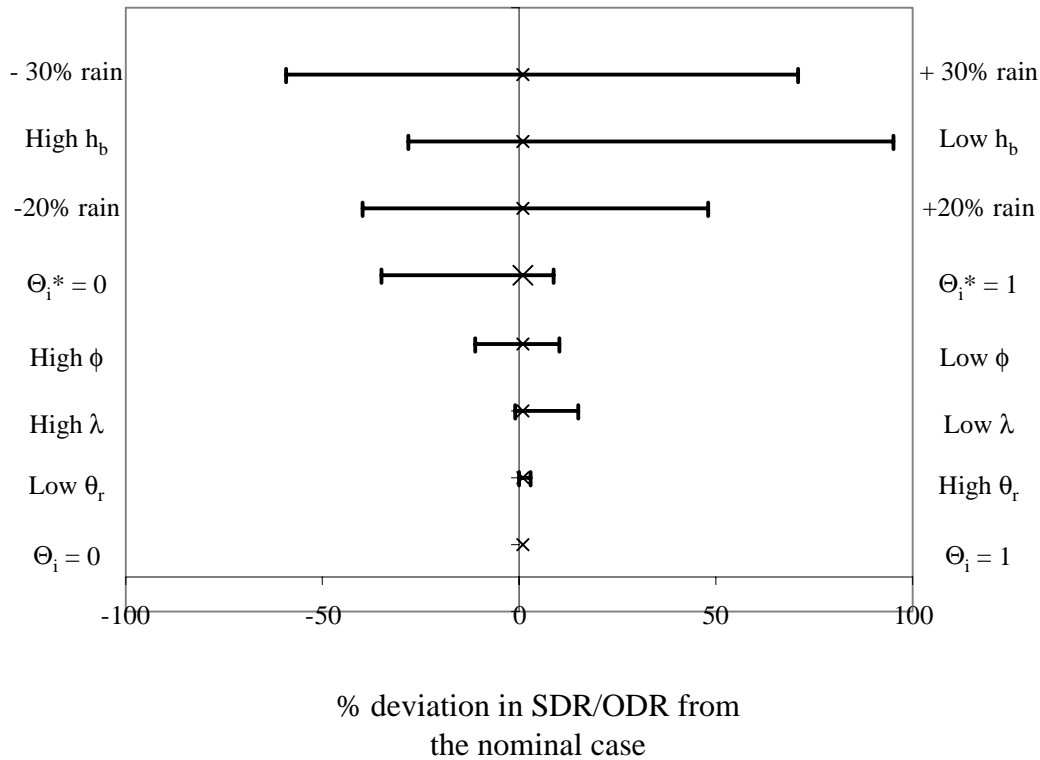


Figure 5.9 Tornado diagram showing deviations from the base case based on high and low parameter values.

The results shown in Figure 5.9 indicate that the uncertainty in specifying h_b causes more uncertainty in model output than the uncertainty in specifying ϕ , λ , or θ_r . Understanding the reasons for differences in the Carsel and Parrish and Rawls, Brakensiek, and Saxton parameter values would certainly reduce the uncertainty associated with specifying h_b because the ranges for h_b specified by these two studies are drastically different as indicated by Figures 3.9-3.12. Among the parameters ϕ , λ , θ_r , and h_b , part of the reason why the specification of h_b introduces the largest amount of uncertainty in the model output is because the coefficients of variation for this parameter tend to be higher (see Table 3.3). If averages of the coefficients of variation are computed for h_b and λ using the Rawls, Brakensiek, and Saxton data set (which exhibits a wider range of variability than the Carsel and Parrish data set), the

average coefficient of variation for h_b is 3.7 times higher than that for λ . Another indication of why the modeled direct runoff is less sensitive to λ than it is to h_b is that in Equation 3.27 for the Green-Ampt wetting front suction head, λ appears both in the numerator and the denominator.

CHAPTER 6. CONCLUSIONS AND RECOMMENDATIONS FOR FUTURE WORK

6.1. Conclusions

General objectives that have been met in this research include:

- A practical and automated method for using U.S. Department of Agriculture digital soil maps in a hydrology model has been developed and implemented.
- Model performance has been tested using different levels of spatial complexity to describe soil properties. This includes testing of a one and a two-layer conceptual soil model, three different levels of horizontally resampling soil properties, and the use of soils data from two different map scales (1:250,000 and 1:24,000).
- Uncertainties associated with soil parameter specification and rainfall inputs have been quantified.

The computer programs and the underlying conceptual model that have been developed for this dissertation are referred to collectively as the Soil Water Balance Modeling System (SWBMS). Summaries of important points and conclusions are grouped here according to specific modeling issues: spatial complexity, the use of NEXRAD Stage III rainfall data, parameterization, process representation, and computer implementation. It is important to point out that the conclusions below are based on a limited set of validation runs in a single watershed. Further work is suggested in Section 6.2 to verify these conclusions.

Spatial complexity

- Only minor differences were observed between the direct runoff volume predicted by a one-layer and a two-layer model conceptual model. Given the SWBMS conceptual model and the soil characteristics of the Little Washita watershed, only a small fraction of the direct runoff (1.7% of the total simulated

direct runoff) was generated due to the characteristics of the second layer in a validation run using the two-layer model.

- In SWBMS, a second soil layer serves as a storage reservoir from which water may evaporate or percolate to the groundwater reservoir. As discussed in Section 5.4, the combination of a single linear reservoir with a one-layer soil model is inadequate to simulate baseflow, but the inclusion of the second soil layer produces more reasonable baseflow results.
- Compared with a one-layer model, running a two-layer model requires significantly more complex pre-processing and simulation codes. In addition, the two-layer model requires the somewhat arbitrary specification of an additional parameter defining the non-soil (i.e. weathered bedrock) percolation rate and the specification of initial water content for the second layer.
- Resampling of soil properties is considered as an option to spatially simplify the water balance model. Three levels of resampling are considered: no resampling, resampling at the NEXRAD cell level, and resampling at the watershed level. When the spatial variability in surface soil texture is reduced through resampling, model performance decreases. In validation runs, when surface soil texture was resampled to the NEXRAD cell level and the 30-m soils grid was used, the ratio of total simulated to total observed direct runoff (SDR/ODR) decreased from 0.74 to 0.5 (a 32% decrease) and the HEC-1 objective function (lower is better) increased from 2.8 to 3.3 (18%). Based on these results, resampling is not recommended.
- When the no resampling or the NEXRAD cell resampling option is used, the differences in simulation results between using STATSGO soils data (1:250,000

map scale) and a 30-m soils grid (1:24,000 map scale) as input are relatively small when compared with the differences in simulation results among resampling levels. This result is consistent with the observation that the overall textural composition of the Little Washita watershed computed from the two data sources is similar (Figure 3.6b). It would be interesting to see if this result holds true in a watershed containing a broader range of soil textures.

NEXRAD data

- A comparison of Micronet gage rainfall estimates and NEXRAD StageIII rainfall estimates for a short period in June and July 1997 reveals substantial discrepancies in rainfall depth estimates; however, the spatial distribution of rainfall from these two data sources is similar for a storm on July 10, 1997. In a study of 10 storms, the mean ratio of average Micronet rainfall estimates to average NEXRAD StageIII estimates was 0.88 and these ratios ranged from 0.5 to 1.5.

Parameterization

- A practical scheme for estimating soil hydraulic properties from soils databases is proposed and implemented. The method involves the use of two lookup tables. The first table translates texture names in the STATSGO database into one of the 12 basic USDA texture classes or the "other" category, and the second table assigns mean hydraulic properties to each texture class.
- As discussed in Section 3.2.2.2.2, there are several reasons why the texture lookup table approach is used rather than trying to estimate individual parameter values from soil data table attributes other than texture. The Brooks and Corey parameters required to estimate the wetting front suction head and calculate

percolation cannot be estimated directly from the soil attribute tables and therefore must be estimated using either the regression equations of Rawls and Brakensiek (1985) or as a function of texture alone. In order to automatically apply the regression equations of Rawls and Brakensiek (1985), a complicated set of assumptions would be required to deal with layer table attributes that have missing values or internal inconsistencies. This level of complication does not seem justified when considering all the approximations in the modeling process. Therefore, the lookup table approach has been adopted.

- Several research papers have been published that deal with the specification of soil hydraulic properties as a function of texture class. Unfortunately, there are large discrepancies between some of the hydraulic parameter estimates reported in the two papers that have used the largest soils databases to develop parameter estimates — Rawls, Brakensiek, and Saxton (1982) and Carsel and Parrish (1988). The Carsel and Parrish values are used here, primarily because wetting front suction head values computed using Carsel and Parrish λ and h_b values are more consistent with Figure 5.5.4 in Rawls *et al.* (1993) than wetting front suction head values computed using Rawls, Brakensiek, and Saxton (1982) values.
- Among the parameters of interest in this study, saturated hydraulic conductivity (K_s) exhibits the most natural variability within a given texture class. For this reason, a hydraulic conductivity factor (k_f) is used for calibration. k_f is multiplied by the K_s value for all soil types at all points in space. In this study, values of k_f ranged from 0.5 to 5.4 depending on the modeling scenario being considered.

- Among the soil parameters not used for calibration (ϕ , h_b , λ , and θ_r), specification of the Brooks and Corey parameter (h_b) involves the most uncertainty and has the biggest impact on simulated runoff.
- Gravimetric estimates of soil-water content from the Little Washita watershed are used to calibrate a rooting depth parameter (d_r). Calibrated d_r values were 35 cm, 40 cm, and 50 cm for different modeling scenarios. Developing a physically based method to estimate the rooting depth (d_r) would require further research.

Process representation

- Simplified flow models for infiltration and percolation are used because the uncertainties in model inputs do not justify the use of more complex computational algorithms. The Green-Ampt model is used for infiltration and a simple kinematic model is used for percolation.
- Existing methods used to estimate evaporation from unsaturated soils range from simple empirical methods (bucket models) to complex soil-vapor-atmosphere transfer schemes (SVATS). The possibility of developing a model of intermediate complexity was explored using new data sets being generated at DOE ARM CART sites. Plots relating evaporative surface resistance to piezometric head were generated. Looking at this data, it is clear that this approach will not have general applicability because other factors besides soil-water potential are significantly influencing surface resistance.
- A conventional bucket model for estimating evaporation is used in this study. Initial results indicate that uncertainties in soil parameter specification and

rainfall have a greater impact on direct runoff than initial soil moisture. In light of this, perhaps no further complication in evaporation estimation is justified.

Computer implementation:

- Automated pre-processing routines are used to estimate hydrologic model parameters using ArcView GIS. The required spatial data describing soil, topography, and land use are readily available on the Internet for any location in the United States.
- Transfer of the required spatial information from the GIS (AV-SWBMS) to an external hydrologic model (VB-SWBMS) is easily achieved using an ASCII file. The proposed format of using a single line to describe the properties of each NEXRAD cell is compatible with the format of the modClark parameter file that is already used in HEC-HMS.
- The most tedious procedures in using the SWBMS model developed here are obtaining and reformatting the precipitation, climate, and runoff data. The GIS analysis of spatial data is more straightforward because the data formats for the original data sources are standardized.

6.2. Recommendations for future work

A key impetus for this research is the prospect of the eventual implementation of a GIS-based soil parameterization scheme within HEC-HMS. Based on limited trial simulations, use of the no resampling option showed better results than using either NEXRAD cell or watershed level resampling. Using a one-layer soil model, it would be a simple task to include a list of the percentages for 12 different soil textures (no resampling) on the line for each cell in an HEC-HMS parameter file (see Figure 4.2). Passing 12 values per cell versus passing one value per cell is not

overly cumbersome when procedures are computer automated. The number of vertical flux computations does increase when moving from NEXRAD level resampling to no resampling, although not necessarily by a factor of 12, if all 12 textures are not represented in each NEXRAD cell.

The observations in the preceding paragraph are immediately relevant to event simulation modeling in HEC-HMS. For continuous simulation, it would be interesting to try to combine the best features of the SWBMS model and the HEC Continuous Soil Moisture Accounting Model that is now under development. Baseflow simulation is an important component of continuous simulation. Issues involved with using the two-layer SWBMS to simulate baseflow have not been fully explored.

The SWBMS programs have only been applied in one watershed and for limited time periods. It would be prudent to apply SWBMS for different time periods and in different locations to verify the conclusions of this study. It would be interesting to test SWBMS in locations with a broader range of soil textures, particularly with regard to comparing the use of the STATSGO and SSURGO soil maps.

It would be interesting to explore the impacts of changing the top layer depth on model results. All simulations in this study were made with a top layer depth of 5 cm. A small top layer depth is more likely to be fully saturated after a storm but will also drain and return to mid-range saturation levels more quickly than a thicker top layer initialized at the same water content.

It is questionable whether the calibrated rooting depth values derived in this study would be appropriate to estimate evaporation during different seasons of the year. Use of remote sensing to estimate leaf area index values seems to be a promising avenue for improving the physical basis for evaporation estimates over large areas. This is a large research area that could be the subject of many future dissertations.

APPENDICES

The Appendices are divided into 5 parts.

- A. Description of the AV-SWBMS and VB-SWBMS programs.
- B. Time series data processing programs
- C. Description of files on the CD-ROM that was produced to archive the research presented in this dissertation.
- D. Table used to reclassify 719 STATSGO texture names into 12 basic USDA classes and the "other" category.

APPENDIX A: Description of the AV-SWBMS and VB-SWBMS programs.

A.1 AV-SWBMS

A general description of the subprograms in AV-SWBMS is provided in Chapter 4. A more detailed description of each of these programs and the actual filenames for these programs is provided here.

The only computer file required to access all of the capabilities of AV-SWBMS is called *swbms.avx*. The .avx filename extension indicates that this file is an ArcView “extension” file. To make this extension accessible to ArcView users, it should be placed in the directory ~/arcview/ext32 that gets created when ArcView is installed on PCs. When the AV-SWBMS extension is added to ArcView, two menus get added to the standard View GUI as shown in Figure A1.

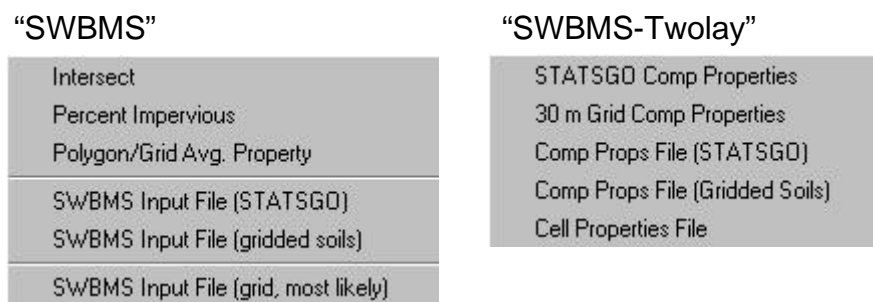


Figure A1. Menus for AV-SWBMS.

When each of the menu items is selected, an Avenue script gets executed. A list of menu items, script names, and a detailed description of the script functions is provided here. Inputs and outputs for each program are also described. The spatial data required to run AV-SWBMS are summarized in Table 4.1.

“SWBMS” Menu Items

Menu item: Intersect

Script name: swbp.intersect

Must be preceded by menu items: none

Description: Intersect watershed polygon with rainfall cells to define modeling units.

Input(s): watershed polygon, NEXRAD cell polygons

Output(s): intersected shapefile of model polygons (see Figure 3.17)

Menu item: Percent Impervious

Script name: swbp.percentimp

Must be preceded by menu items: Intersect

Description: Computes percent imperviousness in each model polygon. Adds a field called "pct_imp" to the model polygon attribute table. Impervious percent values associated with specific land use codes that are shown in Table 3.5 are hardwired into this program. The program loops through all model polygons and for each model polygon it loops through all intersecting land use polygons. For each land use polygon the percent imperviousness is determined based on the values in Table 3.5. An area-weighted average is used to determine the percent imperviousness for the entire model polygon.

Input(s): model polygons, land use polygons with a field containing the Anderson Level II classification code

Output(s): A new field called "pct_imp" is added to the model polygon attribute table (Figure 3.20 displays values for the pct_imp attribute.)

Menu item: Polygon/Grid Avg. Property

Script name: swbp.gridavg

Must be preceded by menu items: Intersect

Description: Given any grid and any polygon coverage, this program computes either the average value of all grid cells in each polygon or the most prevalent value of the grid cells in each polygon. The input polygon Theme must contain a field with a unique ID for each polygon. If the input polygon theme does not have a field with a unique ID for each polygon, then a field containing record numbers can easily be added to the polygon Theme using a script called View.AddrecnumfieldtoThemes that is freely available at www.esri.com. A copy of this script is saved in the scripts directory on the CD-ROM produced with this dissertation with the filename adrecno.ave. The attribute (either an average or a most prevalent value) computed by this program is written to a new field in the model polygon Theme. The user is prompted for the name of this new field. For the most prevalent value option, the input grid must be an integer grid. In AV-SWBMS, this program is used to compute the average flow length in each model polygon and is also used to compute the predominant soil type code in each cell when NEXRAD cell level resampling and gridded soils data are used.

IMPORTANT: In order for the subsequent scripts to work, the flow length field **MUST** be named "flength."

Input(s): flow length grid or integer soil texture classification grid (For the soil texture grid, the grid textural codes should be specified as follows: S = 1, LS = 2, SL = 3, SCL = 4, L = 5, SIL = 6, CL = 7, SI = 8, C = 9, SC = 10, SICL = 11, and SIC = 12), model polygons

Output(s): A field added to the model polygon Theme with a name specified by the user. The flow length field MUST be named "flength." (Average flow length values for each cell are shown in Figure 3.35.)

Menu item: SWBMS Input File (STATSGO)

Script name: swbp.writeinputfile

Must be preceded by menu items: Intersect, Percent Impervious, Polygon/Grid Avg. Property

Description: Creates an input file for VB-SWBMS using STATSGO soils data. Loops through each model polygon and tallies the percentage of each soil type that falls within that polygon. The user is given a choice as to whether a file is written with the predominant soil type only (NEXRAD cell level resampling) or with the percentage of each soil type (No resampling) in each model polygon.

Input(s): model polygons, soil comp table, STATSGO Theme, lookup table that translates STATSGO texture class into one of the 12 basic USDA classes or the "other" category (MUST be named statusda.txt)

Output(s): VB-SWBMS input file (see Figure 4.1)

Menu item: SWBMS Input File (gridded soils)

Script name: swbp.writeinputfilegrid

Must be preceded by menu items: Intersect, Percent Impervious, Polygon/Grid Avg. Property

Description: Creates an input file for VB-SWBMS using gridded soils data. Loops through each model polygon and tallies the percentage of each soil type that falls within that polygon. Writes a file with the percentage of each soil type in each model polygon (No resampling).

Input(s): model polygons, soil comp table, soil grid Theme, lookup table that translates STATSGO texture into one of the 12 basic USDA classes or the "other" category (MUST be named statusda.txt)

Output(s): VB-SWBMS input file (see Figure 4.1)

Menu item: SWBMS Input File (grid, most likely value)

Script name: swbp.writeinputfilegrid_b

Must be preceded by menu items: Intersect, Percent Impervious, Polygon/Grid Avg. Property

Description: Creates an input file for VB-SWBMS using NEXRAD cell level resampling and assuming that a predominant soil type for each model polygon has already been computed from a soils grid using Polygon/Grid Avg. Property. The

user is prompted for the name of the field in the model polygon Theme containing soil codes.

Input(s): model polygons — must contain field with predominant soil type computed with Polygon/Grid Avg. Property

Output(s): VB-SWBMS input file (see Figure 4.1)

“SWBMS-Twolay” Menu Items

Menu item: STATSGO Comp Properties

Script name: swbp.comp3

Must be preceded by menu items: none

Description: This program processes the comp and layer soil attribute tables and creates a new table which lists the key hydraulic properties for each component that are required for a two-layer VB-SWBMS model. The program loops through all components in the comp table and for each component loops through the associated layers to determine the required parameter values. This program uses both the "statusda.txt" lookup table to translate STATSGO texture names into the 12 basic USDA classes and the "usdapar.txt" lookup table to define hydraulic properties for each texture class. The lookup tables must have these names and be present in the project when the program is run. The program can process the comp and layer tables for the entire state of Oklahoma in less than 30 minutes on a PC with a 200 MHz processor.

Input(s): Lookup tables: statusda.txt, usdapar.txt (note that these two file names are hardwired into the codes), comp table, layer table; all of these tables must exist in the ArcView project.

Output(s): A table of component properties called compjoin.dbf (this filename is hardwired into the code) Attributes in this compjoin.dbf include the texture code, K_s , ϕ , θ_r , λ , h_b , θ_{fc} , and θ_{wp} for both the top layer and the soil layer with the lowest K_s value (most restrictive layer) and the total soil zone depth. Field names for the restrictive layer attributes start with "r_".

Menu item: 30 m Grid Comp Properties

Script name: swbp.compssurg2

Must be preceded by menu items: none

Description: Performs exacts same functions as the menu item STATSGO Comp Properties but there are differences in the code to account for differences in the table structures.

Input(s): Same as for menu item STATSGO Comp Properties

Output(s): Same as for menu item STATSGO Comp Properties except the filename for the table that gets created is not hardwired into the code.

Menu item: Comp Props File (STATSGO)

Script name: swbp.writecompprops

Must be preceded by menu items: Intersect, STATSGO Comp Properties

Description: Creates one of two files input files for a two-layer VB-SWBMS simulation — the component properties file — using the STATSGO soil map. One line gets written to an ASCII file for each distinct component in each model cell. Information on all components in the first cell is written, followed by all components for the second cell, etc. Each line contains information about the percent area taken by that component (compct), the total soil zone depth (totdepth) and K_s (k_lu), ϕ (por_lu), θ_r ($theta_r$), λ ($lambda$), h_b (hb), θ_{fc} (fc), θ_{wp} (wp) for both the top layer and the most restrictive layer (r_klu , r_porlu , r_theta , r_lambda , r_hb , r_fc , and r_wp). IMPORTANT: the compct here is not the same as the compct attribute in the STATSGO comp table. The compct here is weighted by the model cell fraction covered by the STATSGO component's mapunit. Adding all of the compct values for a given cell will yield 100%. Components with identical properties are eliminated from the lists written to the component properties file. The routine for eliminating redundant components is time consuming but saves time during the VB-SWBMS computations. It is expected that VB-SWBMS computations will be repeated many more times than the pre-processing routines.

Input(s): model polygons, compjoin.dbf table created using menu item STATSGO Comp Properties, STATSGO soils Theme

Output(s): Component properties file (see Figure 4.2 for an example). Adds an attribute to the model polygon Theme indicating the number of distinct soil components in each polygon. The field name for this attribute is “numcomps.”

Menu item: Comp Props File (Gridded soils)

Script name: swbp.writecomppropsgrid

Must be preceded by menu items: Intersect, 30 m Grid Comp Properties

Description: Creates the component properties file for VB-SWBMS using the 30 m soils grid. Procedures are identical to those above although the coding for spatial analysis differs because of the differences between grid and vector data.

Input(s): model polygons, component properties table created by menu item 30 m Grid Comp Properties, soil grid Theme

Output(s): Same as for menu item Comp Props File (STATSGO).

Menu item: Cell Properties File

Script name: swbp.writecellprops

Must be preceded by menu items: Intersect, Percent Impervious, Polygon/Grid Avg. Property

Description: Creates a cell properties file for VB-SWBMS. Reads attributes from the model polygon Theme that were created using menus Intersect, Percent Impervious, Polygon/Grid Avg. Property and either Comp Props File (STATSGO) or Comp Props File (Gridded soils). This program works independently of whether grid or vector soils data are being used.

Input(s): model polygons

Output(s): Cell properties file (see Figure 4.2).

Table A1 describes menu item sequences that were used to make input files for the modeling scenarios discussed in Chapter 5.

Table A1. Suggested AV-SWBMS menu sequences for different modeling options.

Model options	Menu sequence
One-layer, STATSGO, No resampling	Intersect, Percent Impervious, Polygon/Grid Avg. Property [create “flength” field], SWBMS Input File (STATSGO)
One-layer, STATSGO, NEXRAD cell level resampling	same as above
One-layer, gridded soils, No resampling	Intersect, Percent Impervious, Polygon/Grid Avg. Property [create “flength” field], SWBMS Input File (gridded soils)
One-layer, gridded soils, NEXRAD cell level resampling	Intersect, Percent Impervious, Polygon/Grid Avg. Property [create “flength” field], Polygon/Grid Avg. Property (create “soiltype” field), SWBMS Input File (grid, most likely)
Two-layer, STATSGO, No resampling	Intersect, Percent Impervious, Polygon/Grid Avg. Property [create “flength” field], STATSGO Comp Properties, Comp Props File (STATSGO), Cell Properties File
Two-layer, gridded soils, No resampling	Intersect, Percent Impervious, Polygon/Grid Avg. Property [create “flength” field], 30 m Grid Comp Properties, Comp Props File (Gridded Soils), Cell Properties File

A.2 VB-SWBMS

Several different versions of VB-SWBMS have been created. The source files for all program versions are stored on the project CD-ROM. Table A2 lists each model version and gives the source file names and directory locations. The two main model types are the one-layer and two-layer models for which there are significant differences in the code. The code differences among the one-layer versions and among the two-layer versions are not large. With more time for developing the user interface, it would be better to have a single interface to all modeling options of interest.

Table A2. VB-SWBMS File Names

Model version	Source file names	Directory location
one-layer, no baseflow simulation, no resampling	swbms1lay3.vpb, .vbw, .frm	single_layer
one-layer, baseflow simulation, no resampling	swbms1base.vbp, .vbw, .frm	single_layer_base
one-layer, no baseflow simulation, NEXRAD cell level resampling*	swbms1lay4.vbp,.vbw,.frm m	single_layer_pred
two-layer, baseflow simulation, no resampling	swbm2lay.vbp,.vbw,.frm, .frx	double_layer
two-layer, no baseflow simulation, no resampling	swbms2_24.vbp, .vbw, .frx, .frm	double_nobase

* Watershed level resampling can be achieved in any of the one-layer model versions by editing the cell parameter file.

A.2.1 Example user interface description

Since the user interface features are similar for all versions, only one example is given here. The user interface for a one-layer model without baseflow simulation is shown in Figure A2. In the upper left-hand corner of Figure A2, there is a File Listbox. Underneath this box is a Directory Listbox and a Drive Listbox. By clicking on these boxes with the mouse, a user can navigate the computer's directory structure and highlight a file of interest in the File Listbox. Rectangular shaped objects that appear raised and have writing on them are command buttons. A mouse click on one of these buttons executes a subprogram. The rectangular white boxes are text boxes. A user can add text to any of these boxes by inserting the cursor and typing. The small white squares are check boxes. A check placed in one of these boxes indicates that a given option is turned on. The small white circles are option

buttons. These buttons can be highlighted with a click of the mouse and are used to choose between different modeling options (i.e. between different options for specifying the initial soil-water content). Related buttons and text boxes have been grouped with the frames labeled “Identify Input Files,” “Simulation Times,” “Detention and Farm Ponds,” “Initial Conditions,” “PE Method,” “Reference Crop Parameters,” “User Defined and/or “Calibration” Factors,” and “Transform Parameters.”

The numbers that are seen labeling the command buttons serve only as a reference for this text description and do not appear on the actual program user interface. Buttons 1-4 and 6 are used to select the desired input files. For example, rather than typing the full path name of the input precipitation file, a user can simply navigate the directory structure, highlight the appropriate input file and click on command button 1, causing the full path name for the highlighted input file to be written in the text box next to button 1. Button 1 is used to specify the precipitation file. Button 2 is used to specify a file containing either the required data for estimating potential evaporation or pre-computed potential evaporation estimates depending on which option button is selected. Button 3 is used to specify the cell parameter file. Button 4 is used to specify the name of an observed runoff file. The check box next to this button should be checked if an observed runoff file is provided. If this box is not checked, then the user will not be able to write to the observed runoff text box. Button 5 is not used to specify an input file but is used to specify the name of an output file, the final soil moisture file. The full path name is not required for this file. All output files are written to the output directory written next to button 11. Button 6 is used to specify the filename for the soil parameter lookup table. In the two-layer user interface, there is an additional button to select the component properties file which is not shown in Figure A2.

The starting date and ending date for the simulation are specified by typing in the text boxes next to the words “Start Day” and “End Day.” Simulations always start and end at midnight and the time step is always one hour. The date format (mm/dd/yy) shown in Figure A2 should be used.

In the “Detention and Farm Ponds” frame, all items except the top text box can be ignored. The top text box is used to specify the percent contributing area or the “pond factor.” The other items were used to test detention storage models that are not used in this dissertation.

In the “Initial Conditions” frame, the user chooses from three different methods for specifying initial soil-water levels. In the example shown, the user has chosen to specify initial soil-water content from a file. The filename can be specified using button 7 in the same way that buttons 1-6 operate. Other options to specify the initial soil-water state are to specify initial suction head in cm or an initial effective saturation. These initial values can be typed in the appropriate text boxes and will apply to all soils in the watershed.

The “PE Method” frame is used to specify whether potential evaporation estimates will be made using raw meteorological measurements and the Penman/Monteith reference crop method or whether potential evaporation estimates are supplied in an input file.

If the “Penman/Monteith Reference Crop” option is selected, then “Reference Crop Parameters” need to be specified. “ra numerator” is the numerator for the aerodynamic resistance function like that of Equation 3.49. “rsmin” is the minimum stomatal resistance corresponding to conditions when soil moisture is not limiting evaporation.

The frame “User Defined and/or “Calibration” Factors” allows the user to type preferred values for model parameters.

The frame “Transform Parameters” is used to specify the modClark storage and time of concentration parameters.

Command button 13 is used to select a file that specifies soil components for which average daily soil moisture values are to be exported. Exporting these values only occurs if the box next to “Output WC for Selected Components” is checked.

Button 8 operates in the same way as buttons 1-6, but is used to select a model control file. The control file is just an ASCII file that contains a list of input files and model parameter values. If a control file is selected, clicking on button 9 will read all values from the control file into the user interface. Clicking on button 10 will write all current settings to a new control file. The file specified in the text box next to button 8 is the file which gets read from and written to. Clicking on button 10 will overwrite an existing control file or create a new file if the specified filename does not exist. Button 11 can be used to specify the model output directory. All output files are written to this directory. To set the output directory, highlight the desired directory in the Directory Listbox and then click on button 11. The selected directory name will get written to the text box next to button 11.

Once all input file names and parameter values have been set, button 14 is used to run a simulation. Optional text boxes include the observed runoff box and the output component list box. Only one of the text boxes in the “Initial Conditions” frame must contain a value. All other text boxes should contain text. The progress of a simulation will be indicated by a progress bar at the bottom of the form. Clicking on button 12 will exit the program.

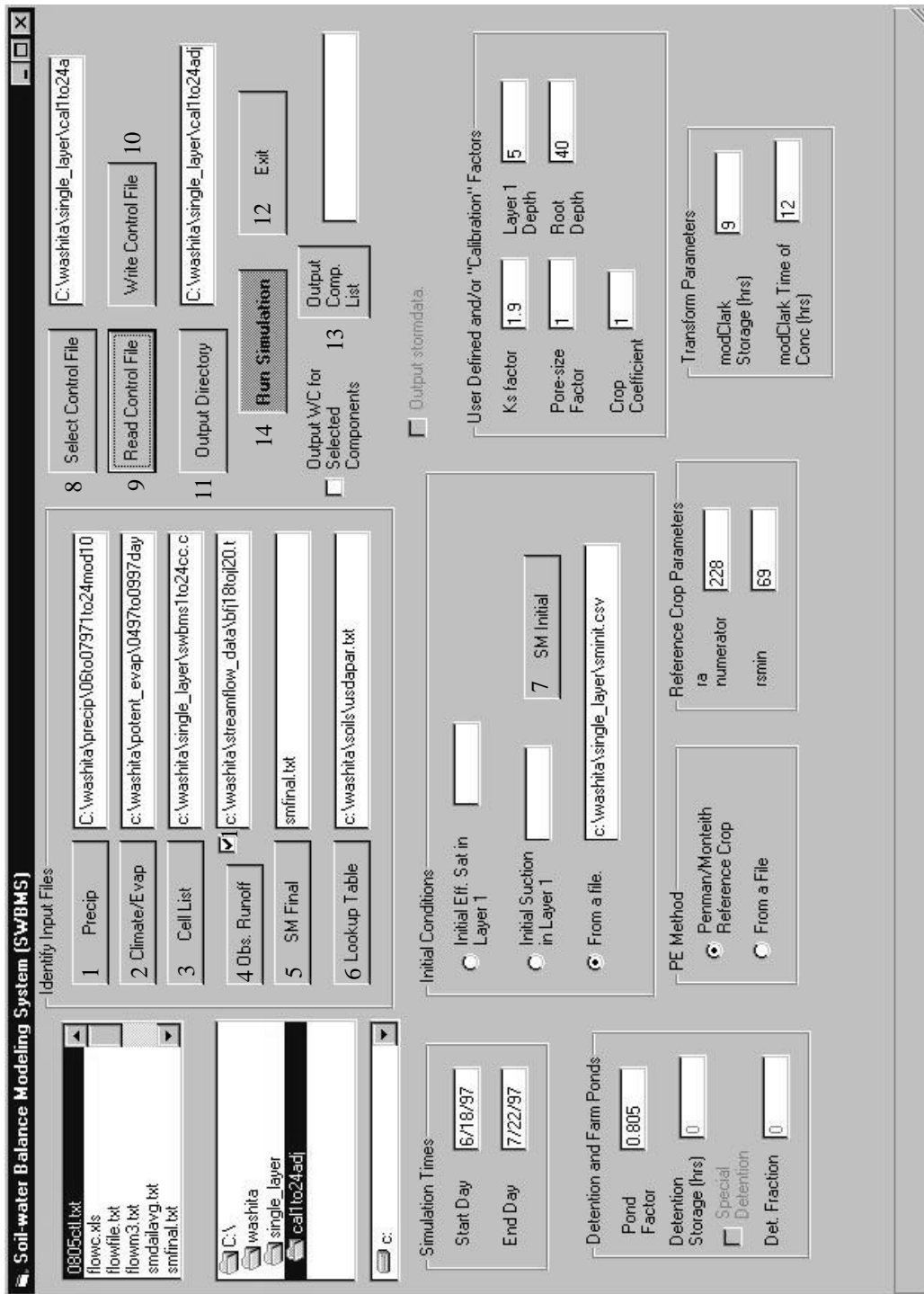


Figure A2. SWBMS user interface for a one-layer model with no baseflow simulation.

A.2.2 Formats for input and output files:

A list of input and output files is given in Tables 4.4 and 4.5. Input files include a control file, a soil parameter lookup table, a rainfall file, a potential evaporation file, an observed runoff file, a soil-water content initialization file, and a file listing components for which soil-water content will be exported. Examples that show the required formats for input files are given below. An example of a cell properties file and a component properties file (two-layer model only) are not given here because these files are illustrated in Figures 4.1 and 4.2. Procedures for creating a rainfall file, a potential evaporation file, and an observed runoff file are described in Appendix B. Output files include a flow file, a summary statistics file, a file with final storage values (soil-water content and subsurface reservoir storage), and daily average soil-water content for selected components (optional). For files that may be exceptionally long and/or wide (i.e. rainfall file), only a few lines and columns are shown to illustrate the format.

Example VB-SWBMS input files.

Example control file for a one-layer model with no baseflow simulation.

```
# Control file for Soil Water Balance Program
# full path names of input data files
C:\washita\precip\06to07971to24mod10.csv
c:\washita\potent_evap\0497to0997day1.txt
c:\washita\single_layer\swbms1to24cc.csv
c:\washita\streamflow_data\bfj18toj20.txt
c:\washita\soils\usdapar.txt
C:\washita\single_layer\cal1to24adj
c:\washita\single_layer\sminit.csv
smfinal.txt
# start time and end time for simulation
6/18/97
7/22/97
# soil moisture initialization method
fromfile
# initial effective saturation in layer 1

# initial soil suction in layer 1

# modClark storage (hours)
9
# modClark time of concentration (hours)
12
# Potential evaporation method: PMRC = Penman-Monteith Reference Crop, File = input values from a file
pmrc
# ks calibration factor
1.9
# layer 1 depth (cm)
5
# rooting depth (cm)
40
# Brooks and Corey pore-size index factor
1
# potential crop coefficient
1
# detention constant
0
# fraction of basin influence by detention
0
# farm pond factor
0.805
# numerator for aerodynamic resistance function
228
# minimum stomatal resistance
69
# use observed runoff
1
```

Example soil parameter lookup table.

class,abbrev,ks,poros,theta_r,fc,wp,lambda,hb
sand,S,29.7,0.43,0.045,0.0456,0.0450,1.68,6.90
loamy_sand,LS,14.59,0.41,0.057,0.0600,0.0570,1.28,8.06
sandy_loam,SL,4.42,0.41,0.065,0.0845,0.0657,0.89,13.33
sandy_clay_loam,SCL,1.31,0.39,0.1,0.1688,0.1111,0.48,16.95
loam,L,1.04,0.43,0.078,0.1645,0.0883,0.56,27.78
silt_loam,SIL,0.45,0.45,0.067,0.2390,0.1037,0.41,50.00
clay_loam,CL,0.26,0.41,0.095,0.2687,0.1493,0.31,52.63
silt,SI,0.25,0.46,0.034,0.2567,0.0897,0.37,62.50
clay,C,0.2,0.38,0.068,0.3466,0.2703,0.09,125.00
sandy_clay,SC,0.12,0.38,0.1,0.2666,0.1701,0.23,37.04
silty_clay_loam,SICL,0.07,0.43,0.089,0.3374,0.1962,0.23,100.00
silty_clay,SIC,0.02,0.36,0.07,0.3367,0.2661,0.09,200.00

Example of rainfall input file.

55 comma delimited columns (one for each cell)
 (54 for the 1:24,000 scale simulation runs) →

time (mmddyhh) ↓	time,p557_304,p558_304,p559_304,p554_305,p555_305,p556_305. .
	.
	5059702,0,0,0,0,0,0. . .
	5059703,0,0,0,0,0,0. . .
	5059704,0,0,0,0,0,0. . .
	5059705,0,0,0,0,0,0. . .
	5059706,48,0,0,0,0,0. . .
	5059707,204,227,295,0,0,0. . .
	5059708,0,0,0,0,0,0. . .
	. . .

Rainfall units are 1/100 mm. These are the units of the data distributed by ABRFC. SWBMS divides values from these files by 1000 and works with units of cm/hour.

Example input file for Penman-Monteith potential evaporation option.

```
"day,avail_heating,tempavg,tempmax,tempmin,presavg,rhavg,windavg,deficitavg"  
"04/01/97",38.13,14.31,18.96,9.7,96.9,.5926,5.1,.679  
"04/02/97",28.43,16.88,19.77,14.37,97.19,.7722,3.92,.449  
"04/03/97",40,16.4,20.89,13.25,96.74,.8038,3.74,.404  
"04/04/97",-59,16.11,17.6,15.46,95.69,.9894,3.96,.019  
"04/05/97",156.26,16.46,23.35,9.4,95.23,.5253,5.75,1.02  
"04/06/97",133.41,9.22,14.89,3.65,97.05,.4464,3.66,.689  
"04/07/97",138.71,12.54,20.32,4.24,97.3,.4649,3.35,.943  
"04/08/97",9.4,6.99,13.07,1.23,97.27,.8893,4.43,.149  
"04/09/97",62.67,6.16,11.24,1.49,97.47,.8622,3.34,.151  
"04/10/97",60.07,15.61,19.26,10.32,96.52,.7386,6.1,.487  
. . .  
. . .  
. . .
```

Units: avail_heating (W/m²), tempavg (C), tempmax (C), tempmin (C),
presavg (kPa), rhavg(none), windavg(m/s), deficitavg (kPa)

Example observed flow file.

```
date,observed_flow,base_flow  
#1997-06-18#,103,103  
#1997-06-18 01:00:00#,99.75,99.75  
#1997-06-18 02:00:00#,97,97  
#1997-06-18 03:00:00#,95.5,95.5  
#1997-06-18 04:00:00#,93.5,93.5  
#1997-06-18 05:00:00#,92.25,92.25  
#1997-06-18 06:00:00#,90.5,90.5  
#1997-06-18 07:00:00#,89.25,89.25  
#1997-06-18 08:00:00#,88.5,88.5  
#1997-06-18 09:00:00#,88,88  
#1997-06-18 10:00:00#,87,87  
. . .  
. . .  
. . .
```

Flow units: cfs.

Example soil-water content initialization file.

```
cell,S_wc,LS_wc,SL_wc,SCL_wc,L_wc,SIL_wc,CL_wc,SI_wc,C_wc,SC_wc,SICL_wc,SIC_wc
1,0.1,0.18,0.22,0,0.3,0.24,0.23,0,0.33,0,0.3,0
2,0.1,0.18,0.22,0,0.3,0.24,0.23,0,0.33,0,0.3,0
3,0.1,0.18,0.22,0,0.3,0.24,0.23,0,0.33,0,0.3,0
4,0.1,0.18,0.22,0,0.3,0.24,0.23,0,0.33,0,0.3,0
5,0.1,0.18,0.22,0,0.3,0.24,0.23,0,0.33,0,0.3,0
6,0.1,0.18,0.22,0,0.3,0.24,0.23,0,0.33,0,0.3,0
7,0.1,0.18,0.22,0,0.3,0.24,0.23,0,0.33,0,0.3,0
8,0.1,0.18,0.22,0,0.3,0.24,0.23,0,0.33,0,0.3,0
. . .
. . .
. . .
```

File listing soils for which soil-water content data will be exported. “Lwid” numbers correspond to the numbers in Figure 3.18.

```
lwid,hrapx,hrapy,soiltype
3_4_5,557,309,2
8_9,555,307,6
11_12_13,560,309,5
17,559,305,3
```

“Soiltype” codes.

S = 1, LS = 2, SL = 3, SCL = 4,
L = 5, SIL = 6, CL = 7, SI = 8,
C = 9, SC = 10, SICL = 11, SIC = 12

Example VB-SWBMS output files.

Example output flow file. This file is automatically named “flowfile.txt” and will overwrite any existing file with this name in the working directory.

```
date,direct_runoff,baseflow,total_runoff,observed_flow
#1997-06-18#,0,103,103,103
#1997-06-18 01:00:00#,0,99.75,99.75,99.75
#1997-06-18 02:00:00#,0,97,97,97
#1997-06-18 03:00:00#,0,95.5,95.5,95.5
#1997-06-18 04:00:00#,0,93.5,93.5,93.5
#1997-06-18 05:00:00#,0,92.25,92.25,92.25
#1997-06-18 06:00:00#,0,90.5,90.5,90.5
#1997-06-18 07:00:00#,0,89.25,89.25,89.25
#1997-06-18 08:00:00#,0,88.5,88.5,88.5
#1997-06-18 09:00:00#,0,88,88,88
#1997-06-18 10:00:00#,0,87,87,87
. . .
. . .
. . .
```

Units: cfs

Example output summary file. This file is automatically named "summary.txt" and will overwrite any existing file with this name in the working directory.

```
#1899-12-30 16:49:55#,#1899-12-30 16:56:10#
HEC Objective function: 146.740387455355
Total precipitation (m3): 51370941.7
Total evaporation (m3): 13723076.1
Total mod Clark runoff (m3): 2931621.6
Change in mod Clark storage (m3): 325.
Total modeled direct runoff (m3): 2931946.6
Total observed direct runoff (m3): 2989815.9
Modeled - observed direct runoff (m3): -57869.4
Total direct runoff due to impervious cover alone (m3): 903965.6
Total change in soil-water storage (m3): -3572678.4
Total volume diverted to ponds (m3): 710223.1
Total volume sent to subsurface (m3): 37578116.5
Net mass unaccounted for (m3): 257.9
Input precip file: C:\washita\precip\06to07971to24mod10.csv
Input climate file: c:\washita\potent_evap\0497to0997day1.txt
Input cell file: c:\washita\single_layer\swbms1to24cc.csv
Input observed runoff file: c:\washita\streamflow_data\bfj18toj120.txt
Soil moisture initialization file: c:\washita\single_layer\sminit.csv
Final soil moisture file: smfinal.txt
Simulation start time: 6/18/97
Simulation end time: 7/22/97
Initial effective saturation in layer 1:
modClark storage (hours): 9
modClark time of concentration (hours): 12
ks calibration factor: 1.9
Layer 1 depth (cm): 5
Rooting depth: 40
Brooks and Corey pore-size index factor: 1
Potential crop coefficient: 1
Farm pond factor: 0.805
Numerator for aerodynamic resistance function: 228
Minimum stomatal resistance 69
```

Final storage values example file. This example is for a one-layer model. The format is slightly different for a two-layer model. Reported values are water content.

```

cell,S_wc,LS_wc,SL_wc,SCL_wc,L_wc,SIL_wc,CL_wc,SI_wc,C_wc,SC_wc,SICL_wc,SIC_wc
1,0.,0.,0.,0.,0.1473,0.1894,0.,0.,0.,0.,0.
2,0.,0.,0.,0.,0.1392,0.1814,0.,0.,0.,0.,0.
3,0.07,0.0858,0.1206,0.,0.,0.23,0.,0.,0.,0.,0.
4,0.045,0.057,0.0747,0.,0.,0.,0.,0.,0.,0.,0.
5,0.,0.057,0.0657,0.,0.1141,0.1571,0.,0.,0.,0.,0.
6,0.,0.057,0.0651,0.,0.0975,0.1401,0.,0.,0.,0.,0.
.      .      .
.      .      .
.      .      .
The last line of this file will be the final subsurface reservoir storage (m3) if an SWBMS
version with baseflow simulation is being used.

```

Example of average daily soil-water content file.
The numbers in the header correspond to the numbers
in Figure 3.18.

```

3_4_5,8_9,11_12_13,17
0.113,0.229,0.236,0.156
8.46E-02,0.210,0.196,0.123
6.76E-02,0.192,0.175,0.105
5.72E-02,0.175,0.158,8.83E-02
5.70E-02,0.159,0.141,7.20E-02
0.126,0.214,0.197,0.156
.      .      .
.      .      .
.      .      .

```

A.2.3 Description of subprograms.

There are many subprograms within VB-SWBMS. The main program is called cmdrun_click and is initiated from button 14 (“Run Simulation”). This program calls several subprograms and functions to make the program more readable. A list of the most important subprograms and their description is provided here. Programs that perform tasks not essential to the hydrologic calculations (i.e. the programs that tell the File Listbox and the Directory Listbox how to communicate) are not included.

- `calcpevap`: Read average daily meteorological values from a climate file and compute potential evaporation using the Penman-Monteith method.
- `cmdctlread_click`: Read the selected control file and update text boxes, check boxes, and options in the user interface. Associated with the “Read Control File” button.
- `cmdctlwrite_click`: Write a control file based on the current entries and selections in the user interface. Associated with the “Write Control File” button.
- `cmdrun_click`: Main program. Initiated with a mouse click on the “Run Simulation” button. Tasks performed by this program are summarized in Figure 4.3. Calls many subprograms.
- `cuminffunct`: A function that calculates the left-hand-side of Equation 3.28 minus the right-hand-side of Equation 3.28 — used to solve for the root of this equation.
- `dcuminffunct`: A function that computes the derivative of the left-hand-side of Equation 3.28 minus the right-hand-side for use in the Newton-Raphson root finding subprogram.
- `green_ampt`: Computes cumulative infiltration for an event using the algorithm described in Section 3.3.1.
- `hecobject`: Compute the HEC Objective Function given input arrays of observed flow and simulated flow and an average observed flow value.
- `hffunct`: A function that computes the wetting front suction head as a function of the Brooks and Corey parameters and the initial effective saturation.
- `newt_raphs`: Solves for the cumulative infiltration at time step $t+\Delta t$ in Equation 3.28 using the Newton-Raphson root finding method.
- `outcompsub`: Assign values to the output array that stores average daily soil-water content values for selected components.
- `readprecip`: Read input precipitation file.
- `readpevap`: Read potential evaporation estimates from a file.

- readcell: Read cell parameter information contained in a file.
- readflowdata: Read observed streamflow data from a file.
- readoutcomps: Read the file containing a list of soil components for which average daily soil-water content will be written to a file.
- readsminit: Read soil-water content initialization file.
- readusdapar: Read soil parameter lookup table from a file.

APPENDIX B: Time series data processing programs

Many programs were written to process raw data files obtained from various sources and convert them into formats useful in this research. A summary of all data used in this research is provided in Table 3.1.

Many of the data processing programs are written in Visual Basic and run from the common GUI called "Data Processing Programs" shown in Figure B1. The Visual Basic files associated with the programs shown in Figure B1 are called readdata.vbp, readdata.vbw, and readdata.frm. Tasks performed by these programs include processing ARM data sets, processing 15 minute USGS streamflow data, baseflow separation, and processing Micronet rainfall data. An additional utility is provided to convert the flow units in the SWBMS output file (flowfile.txt) from cfs to cms. Processing programs not run from this interface include programs for processing NEXRAD data and a program for converting files in netCDF binary format into ASCII format. These programs are also described in this section.

As with any program, a user of these programs should always check input and output files to make sure the correct data transformations have been made.

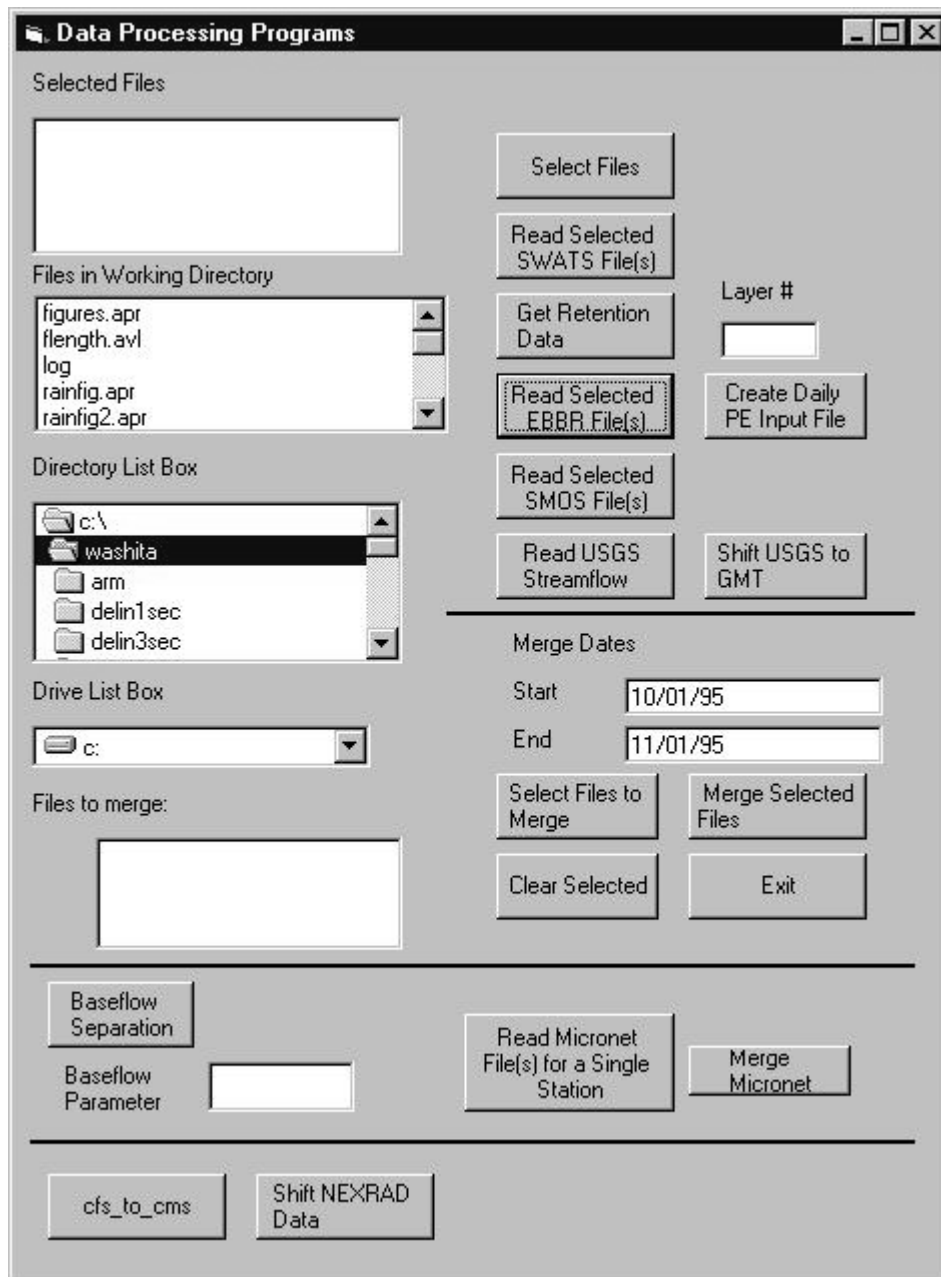


Figure B1 Graphical User Interface for several data processing programs.

B.1 Processing ARM data

Instructions for obtaining ARM data sets are available at www.archive.arm.gov/data/ordering.html. ARM data are distributed in netCDF (Network Common Data Format). Although there are FORTRAN and C utilities

distributed on the Internet for working directly with binary netCDF files, the approach taken in this research was to convert all netCDF files to ASCII files and then extract the desired data from these files using Visual Basic programs. A utility called ncdump was used to convert netCDF files from binary to ASCII format. The FORTRAN source code for this program was obtained through <http://unidata.ucar.edu>. Ncdump was compiled on a Sun UltraSparc1 workstation. Since the ncdump utility only operates on one file at a time, a semi-automated procedure using UNIX batch files was used to process many files at once. Here is an example of how this procedure works:

- 79 EBBR data files (one for each day from 5/01/97 to 8/22/97) are downloaded for site E4 to a single directory.
- A list of these files is written to an ASCII file called "files.txt" using the UNIX "ls" command.
- A C program called rdump.c is then run which creates a new file called "macro.txt" with a list of UNIX shell commands appropriate for running the ncdump program on each of EBBR files.
- In order to run the UNIX shell commands in "macro.txt," the chmod command must be used to make "macro.txt" an executable file. The program rdump.c is dependent on the file name length so it may need to be modified when applied to different data streams (for example, SWATS file names are 1 character longer than EBBR file names).

"Read Selected EBBR File(s)": Clicking on this button in Figure B1 executes a Visual Basic sub-program called "cmdebbr_click()." Two different tasks are performed by this sub-program — (1) EBBR data used for the analysis described in Section 3.3.2 are extracted from the ASCII versions of ARM data files and (2) EBBR data used by the SWBMS program to estimate potential evaporation are transformed to the correct format. In both cases, data from many files may be consolidated into a single file. The following steps are needed to execute this program:

- Using the Drive Listbox and the Directory Listbox shown in Figure B1, move to the directory where the raw ASCII files (that have been converted from netCDF format) are located.
- Highlight all files of interest in the "Files in Working Directory" box using the Windows standard combination of a mouse click and the shift key.
- Click the button "Select Files." All highlighted files should now be listed in the "Selected Files" list box. If a mistake is made in this selection, just click the "Select Files" button again and the previously selected file list will be overwritten.

- Click on "Read Selected EBBR File(s)."
- Enter an output file name including the desired file name extension. This file is written to the currently active directory in the Directory Listbox.
- As the program runs, the user has a choice of whether or not to create a file in simulation format. A file in simulation format is in a format that can be read by another data reformatting program, the result of which can be used as input to SWBMS if the Penman-Monteith option is selected for estimating potential evaporation. A file in simulation format is a comma delimited file with the following entries on each line for each 30 minute period: time (this time has been converted to Central Standard time from the Universal Standard Time reported in the ARM data files); net radiation [W m^{-2}]; ground heat flux [W m^{-2}]; temperature [$^{\circ}\text{C}$]; atmospheric pressure [kPa]; relative humidity; and wind speed [m s^{-1}]. If simulation format is selected then the user will get no further questions and a message saying when the computations are complete. A second program needs to be run to compute daily values for input to the SWBMS model from the file just created. To prepare a daily input file,
 - Locate the 30 minute file just created from the "Read Selected EBBR File(s)" button using the Directory Listbox. Highlight the file name with the mouse and click on "Select Files."
 - Type the start date and the end date for the time period of interest in the text boxes next to the words "Start" and "End." The start date must exist in the input file for the program to work. An acceptable format for the start and end dates is mm/dd/yy.
 - Click on the button "Create Daily PE Input File."
 - The user is prompted to name the output file. The file will be written to the active directory in the Directory Listbox. A message will appear when the program has completed. The file created is a comma delimited ASCII file with the following information: date, available heating ($R_n + G$) [W m^{-2}], average temperature [$^{\circ}\text{C}$], maximum temperature [$^{\circ}\text{C}$], minimum temperature [$^{\circ}\text{C}$], average pressure [kPa], average relative humidity, average wind speed [m s^{-1}], and average vapor pressure deficit [kPa].
- If the simulation format is not chosen, then a file in a different format is created. This file contains 30 minute values: time (CST), Bowen ratio, net radiation [W m^{-2}], latent heat flux [W m^{-2}], sensible heat flux [W m^{-2}], soil heat flux [W m^{-2}], and soil-water content. In order to come up with the estimate of soil-water content, the user must enter a porosity value. In some of the ARM data files, the surface soil texture at a given site is noted. This information may be used to estimate porosity. Suspect values for latent and sensible heat fluxes are flagged with -1.

“Read Selected SWATS File(s):” This button in Figure B1 runs a sub-program called “cmdswats_click().” This program does not prepare input data for the SWBMS program. The purpose of this subprogram is only to reformat SWAT ASCII files and put selected data in a format that is useful for making calculations and graphs described in Section 3.3.2. This program can be used to consolidate information from many files into one file. The following steps are required to run this program:

- Using the Drive Listbox and the Directory Listbox shown in Figure B1, move to the directory where the raw SWAT ASCII files (that have been converted from netCDF format) are located.
- Highlight all files of interest in the “Files in Working Directory” box using the Windows standard combination of a mouse click and the shift key.
- Click the button "Select Files." All highlighted files should now be listed in the "Selected Files" list box. If a mistake is made in this selection, just click the “Select Files” button again and the previously selected file list will be overwritten.
- Click on "Read Selected SWATS File(s)."
- The user is prompted to enter an output file name including the desired file name extension. This file is written to the currently active directory in the Directory Listbox.
- The program user is asked whether he/she wishes to use the “West Profile.” SWAT data files contain data for both an East profile and a West profile separated by 1 meter. Clicking yes will extract data for the West profile and clicking no will extract data for the East profile.
- The output from the program is an ASCII text file in which each line contains hourly observations of the following variables: time (CST), average water content from the top 3 measurement locations (wats_3), average suction head from the top 3 measurement locations [cm] (wats_3), water content from the top measurement location (wats_1), and piezometric head from all 8 measurement locations [cm] (watsp_1, watsp_2, watsp_3, watsp_4, watsp_5, watsp_6, watsp_7, watsp_8). Note that unit conversions have been made from the original SWAT files. The SWAT data files used in this study contain measurements from 8 depths: 5 cm, 15 cm, 25 cm, 35 cm, 60 cm, 85 cm, 125 cm, and 175 cm.

“Get Retention Data:” This button in Figure B1 runs a sub-program called “cmdretent_click().” This program extracts water content and water potential data for a selected layer so that a plot of the water retention curve for that layer can be made. The retention curves derived from the SWATS data files are not presented in this dissertation because calibrations used to convert matric potential to water

content are still being refined (as of June 1, 1998, www.arm.gov/docs/instruments/static/swats.html). This program can be used to consolidate information from many files into one file. The following steps are required to run this program:

- Using the Drive Listbox and the Directory Listbox shown in Figure B1, move to the directory where the raw SWAT ASCII files (that have been converted from netCDF format) are located.
- Highlight all files of interest in the “Files in Working Directory” box using the Windows standard combination of a mouse click and the shift key.
- Click the button "Select Files." All highlighted files should now be listed in the "Selected Files" list box. If a mistake is made in this selection, just click the “Select Files” button again and the previously selected file list will be overwritten.
- Type the layer number for which data will be extracted in the text box under the words “Layer #.”
- Click on "Get Retention Data."
- Enter an output file name including the desired file name extension. This file is written to the currently active directory in the Directory Listbox.
- The program automatically extracts data for the “West Profile” and creates an ASCII text file in which each line contains two values, water content (wat_cont) and matric potential [cm] (wat_pot), for the selected layer.

“Read Selected SMOS File(s)”: This button in Figure B1 runs a sub-program called “cmdsmos_click()”. This sub-program does not prepare input data for the SWBMS program. The purpose of this subprogram is only to reformat SMOS ASCII files and put selected data in a format that is useful for making calculations and graphs described in Section 3.3.2. This program can be used to consolidate information from many files into one file. The following steps are required to run this program:

- Using the Drive Listbox and the Directory Listbox shown in Figure B1, move to the directory where the raw ASCII files (that have been converted from netCDF format) are located.
- Highlight all files of interest in the “Files in Working Directory” box using the Windows standard combination of a mouse click and the shift key.
- Click the button "Select Files." All highlighted files should now be listed in the "Selected Files" list box. If a mistake is made in this selection, just click the “Select Files” button again and the previously selected file list will be overwritten.
- Click on "Read Selected SMOS File(s)."

- Enter an output file name including the desired file name extension. This file is written to the currently active directory in the Directory Listbox.
- The file created by this program contains 30 minute values for time (CST), precipitation [mm], snow depth [mm], wind [m s^{-1}], temp [$^{\circ}\text{C}$], relative humidity, and barometric pressure [kPa].

Select Files to Merge, Clear Selected, and Merge Selected Files: These buttons in Figure B1 are used to merge files containing EBBR, SWATS, and SMOS data. Merging the data from these files into one file made the analysis for Section 3.3.2 easier. The three input files containing EBBR, SWATS, and SMOS data must be in the format created by the “Read Selected EBBR File(s),” “Read Selected SWATS File(s),” and “Read Selected SMOS File(s)” buttons. These files must be named with the file extensions “.ebbr”, “.swat”, and “.smos”. To create a merged file,

- Using the Drive Listbox and the Directory Listbox shown in Figure B1, move to the directory where each input file is located and select each input file by clicking the “Select Files to Merge” button. Selected files get written to the “Files to merge” text box. Selected files can be cleared using the “Clear selected” button.
- Type the start date and end date for the data that you wish to merge in the text boxes next to the words “Start” and “End” (mm/dd/yy). The data for these dates must exist in the input files for the program to work.
- Click the “Merge Selected Files” button.
- The user is prompted to enter an output file name including the desired file name extension. The output file is written to the currently active directory in the Directory Listbox.

B.2 Processing Streamflow Data

“Read USGS Streamflow”: This button in Figure B1 runs a sub-program called “cmdusgs_click()”. This program was used to convert 15 minute flow data obtained from the Oklahoma office of the U.S. Geological Survey into a more useful format. The 15 minute data obtained from the USGS were in a complex, multi-column format with several lines of text separating the values for individual months. Cmdusgs_click() computes hourly average flows from the 15 minute data and creates a much simpler text file with only two columns, time and flow (cfs). No time conversions are made by this program. To convert the flow time series (which are reported in local time) to Greenwich Mean Time (GMT), the “Shift USGS to GMT” button is used. To run cmdusgs_click() ,

- Using the Drive Listbox and the Directory Listbox shown in Figure B1, move to the directory where the raw ASCII file is located.

- Highlight the file of interest in the “Files in Working Directory” box using the Windows standard combination of a mouse click and the shift key.
- Click the button "Select Files." The highlighted file should now be listed in the "Selected Files" list box. If a mistake is made in this selection, just click the “Select Files” button again and the previously selected file list will be overwritten.
- Click on "Read USGS Streamflow."
- Enter an output file name including the desired file name extension. The output file is written to the currently active directory in the Directory Listbox.

To shift the output flow file to GMT, repeat the above procedure for identifying the input file but select the output file that was just created as input. Click on the button “Shift USGS to GMT” (runs a subprogram called “cmdshift_click()”) to create a new ASCII file with hourly flow values in GMT.

“Baseflow Separation:” Clicking on this button in Figure B1 runs a sub-program called “cmdbflow_click()”. Cmdbflow_click() computes baseflow using the algorithm described in Section 3.3.6.2. The input file and output file format for this program are shown below. Flow can be in any units. A single line header must exist in the input file. An input file could be created using the “Read USGS Streamflow” button.

Input file format

```
Time,flow_cfs
#1997-06-18#,103
#1997-06-18 01:00:00#,99.75
#1997-06-18 02:00:00#,97
#1997-06-18 03:00:00#,95.5
#1997-06-18 04:00:00#,93.5
#1997-06-18 05:00:00#,92.25
. .
. .
. .
```

Output file format

```
date,observed_flow,base_flow
#1997-06-18#,103,103
#1997-06-18 01:00:00#,99.75,99.75
#1997-06-18 02:00:00#,97,97
#1997-06-18 03:00:00#,95.5,95.5
#1997-06-18 04:00:00#,93.5,93.5
#1997-06-18 05:00:00#,92.25,92.25
. .
. .
. .
```

- The baseflow parameter must be specified by typing a value into the text box next to the words “Baseflow Parameter” before clicking on the “Baseflow Separation” button. The baseflow parameter is in the same units as the time step for the input file (hours in the above example).
- The dates of interest must be specified in the “Start” and “End” text boxes. The program will not work if the start date does not exist in the input file.

- The input file is specified by using the Drive Listbox and the Directory Listbox shown in Figure B1, moving to the directory where the input file is located, highlighting the input file with the mouse, and clicking on the "Select Files" button so that the appropriate file is listed in the "Selected Files" box.

"Read Micronet File(s) for a Single Station" and "Merge Micronet:" These program buttons in Figure B1 are specifically designed to reformat the Little Washita Micronet 5 minute rainfall data. In the Micronet data downloaded from grl.ars.usda.gov/sgp97-1.html, there is a file for each day and each station. The format that was useful in this research was to have a single file that contains hourly rainfall values for all stations. Thus, the data processing procedure was divided into two steps. In the first step, data files for all days of interest from a single station are read, hourly values are computed and a single file with hourly values for that station is created. In the second step, data files from each station are merged into a single file.

- Clicking on the button "Read Micronet File(s) for a Single Station" (`cmdmicronet_click()`) will process all files listed in the "Selected Files" box. The only other input required by the user is an output file name.
- Clicking on the button "Merge Micronet" (`cmdmergemnet_click()`) will merge single station files listed in the "Selected Files" box into one file. Two output files are created by this program. One output file contains hourly data for all stations and the other file contains the hourly arithmetic average rainfall for all stations. NOTE: Even though this is a merge operation, the box labeled "Files to Merge" is not used. No dates need to be specified for this program to run.

cfs_to_cms: The button `cfs_to_cms` (`cmdcfsstocms_click()`) in Figure B1 was created to convert the units in the VB-SWBMS output flow file called `flowfile.txt` from cfs to cms. In future versions it will be more practical to just have VB-SWBMS write the output file in cms or give the user a choice of units. The `cfs_to_cms` button operates on a single file listed in the "Selected Files" box.

B.3 Processing NEXRAD StageIII Rainfall Data

Hourly NEXRAD StageIII data are archived by the Arkansas-Red Basin River Forecast Center (ABRFC — info.abrfc.noaa.gov) in network Common Data Format (netCDF — www.unidata.ucar.edu/packages/netcdf/). A semi-automated procedure was developed to facilitate the tedious task of downloading hourly netCDF files from ABRFC and extracting the data that covers the Little Washita watershed. This procedure could certainly be improved with more work.

As discussed in Section 3.2.4, the Hydrologic Rainfall Analysis Project (HRAP) grid is used to map radar rainfall estimates. The first step in the process of

using the StageIII data is to determine the HRAP grid cells which are completely or partially within the Little Washita watershed. Programs described at www.ce.utexas.edu/prof/maidment/gishydro/seann/nexrad.htm were used to create an HRAP grid coverage and a standard GIS intersection procedure was used to identify the cells of interest as shown in Figure 3.17. Based on the watershed delineation using the 3 arc-second digital elevation model, there are 55 HRAP cells that intersect the Little Washita watershed. These 55 cell HRAP ID's are:

```
hrapx, hrapy values
553, 306-309
554, 305-309
555, 305-309
556, 305-310
557, 304-310
558, 304-310
559, 304-310
560, 305-311
561, 306-311
562, 309
```

A subtle point that was not discovered by the author until all precipitation reformatting had been completed is that the watersheds delineated from the 3 arc-second digital elevation model and the 1 arc-second differ significantly enough so that tiny portions of the 1 arc-second watershed intersect HRAP cells that do not intersect with the 3 arc-second watershed. Tiny portions of HRAP cells (559, 311), (562, 308), and (562, 307) intersect with the 1 arc-second watershed but not with the 3 arc-second watershed. The total of the intersected areas for these cells amounts to only 0.1 km², so these cells were ignored in calculations made with the 1 arc-second data. Rainfall files used with the 1:24,000 data only contain data from 54 of the 55 cells because a tiny intersection with cell (553, 306) does not completely contain any 30-m grid cells.

The procedure used to extract the data for these cells was implemented on a Sun UltraSparc1 Workstation with the UNIX (cshell) operating system. To download StageIII files for June, 1997, the following sequence of commands was used.

```
ftp -i info.abrfc.noaa.gov
login: anonymous
password: your_email_address
cd archive/1997/jun/1hr_netcdf
bin
mget *
```


This procedure will take several minutes depending on the rate of data transfer. 720 zipped files, each with 53,265 data values get transferred.

A shell script containing the following commands is run to process the downloaded files for a month at a time and create a file in the correct format for input into VB-SWBMS. This procedure could certainly be streamlined with more work but serves its purpose.

Table B1: Procedure for processing NEXRAD StageIII data.

<code>gunzip -v *</code>	Unzip all files; unzipped files will have the .nc extension.
<code>\rm files.txt</code>	Delete any old versions of files.txt.
<code>ls .nc > files.txt</code>	Create a new file called files.txt which contains a list of files with the .nc ending.
<code>rdump</code>	Run rdump program. Rdump is a compiled version of a C program called rdump.c. Rdump creates a file called macro.txt which contains a list of commands necessary to convert all of the .nc files listed in files.txt into ASCII files with a .tx1 ending. The commands include a call to the utility ncdump described in the “Processing ARM Data” section of Appendix B. Note: As written, rdump.c requires a specific directory structure.
<code>macro.txt</code>	This command runs an executable text file called macro.txt (see above). This file can be made executable using the chmod command.
<code>\rm *.nc</code>	Remove all raw netCDF files to save space.
<code>\rm files1.txt</code>	Delete any old versions of files1.txt.
<code>ls *.tx1 > files1.txt</code>	List all *.tx1 files created by macro.txt to a file called files1.txt.
<code>replace2</code>	Run replace2 program. Replace2 is a compiled version of a C program called replace2.c. Replace2 eliminates all header information and delimiting commas from all of the *.tx1 files and creates a new set of files with the *.tx2 ending.
<code>\rm *.tx1</code>	Remove all *.tx1 files to save space.
<code>\rm files2.txt</code>	Delete any old versions of files2.txt.
<code>ls *.tx2 > files2.txt</code>	List all *.tx2 files in a file called files2.txt.
<code>readvals2</code>	Run readvals2 program. Readvals2 is a compiled version of a FORTRAN program

	called readvals2.f. Readvals2 reads through all the StageIII files (720 for a month) with the *.tx2 ending and extracts the data for the HRAP cells in the Little Washita listed above. This program must be changed to use it in any location other than the Little Washita. A comma delimited file called precip.txt with one line for each hour and one column for each rainfall cell is created.
mv precip.txt 0697prec.txt	Rename the precipitation file to so that it will not be overwritten during future processing. The text header with a list of cell IDs required by VB-SWBMS is not created by readvals2 and was created manually and copied to the top of each precipitation file. With the addition of this header, file 0697prec.txt would be in the input format required by VB-SWBMS.
\rm *.tx2	Remove all

The time stamp for each hourly NEXRAD StageIII data file represents the time at the end of the hour for which rainfall is recorded. Because the flow files used in this research have their time stamp at the beginning of the hour in which flow is recorded, the time stamps for the rainfall data are shifted to the beginning of the hour for consistency. Since this fact was not discovered until after the rainfall processing described above, a button was added to the Visual Basic “Data Processing Programs” shown in Figure B1 to shift the time stamp on the rainfall data.

Shift NEXRAD Data: The “Shift NEXRAD Data” button operates on a single file listed in the “Selected Files” box. The file format for the input and output files are the same as the rainfall input format for the VB-SWBMS program. The time stamp corresponding to each set of rainfall values is shifted back one hour.

Appendix C: Description of files on the CD-ROM that was produced to archive the research presented in this dissertation.

Type of File*	File Name	Description
* Filetypes: ascii (text), excel (Microsoft Excel), grid (Arc/Info Grid), shape (ArcView shapefile), cover (Arc/Info coverage), word (Microsoft Word), ppoint (Microsoft PowerPoint). Directories are denoted by Dir. Top level directories are printed in bold.		
Dir	avfiles	contains AV-SWBMS program files
ascii	swbms.apr	ArcView project file that contains scripts and menus for AV-SWBMS (also contains many scripts not used in AV-SWBMS)
ascii	swbms.avx	ArcView extension described in Appendix A.1
Dir	arm	contains EBBR, SMOS, and SWATS data files obtained from the DOE ARM data archive.
Dir	e4ebbr	contains data files with 30 minute energy budget bowen ratio (EBBR) measurements at site E4 in the Southern Great Plains Cloud and Radiation Testbed
ascii	sgp30ebbrE4.a1.970501.000000.txt	EBBR raw data file for 5/01/97. There are 79 data files with similar names for each day from 5/01/97 to 8/22/97.
ascii	0597.ebbr, 0697.ebbr, 0797.ebbr, 0897.ebbr	comma delimited text files containing selected 30 minute surface energy budget components for each month; these files were created using the "Read Selected EBBR File(s)" button in the "readdata" Visual Basic program.
Dir	e4merge	directory in which merged EBBR, SMOS, and SWATS data files for site E4 are analyzed
excel	e4julmerg_r.xls, e4junmerg_r.xls, e4maymerg_r.xls	spreadsheets used for analysis of data extracted from EBBR, SMOS, and SWATS data streams as described in Section 3.3.2.
Dir	e4smos	contains data files with 30 minute surface meteorological observation system (SMOS) measurements at site E4 in the Southern Great Plains Cloud and Radiation Testbed
ascii	sgp30smosE4.a1.970501.000000.txt	SMOS raw data file for 5/01/97. There are 80 data files with similar names for each day from 5/01/97 to 8/22/97.
ascii	0597.smos, 0697.smos, 0797.smos	comma delimited text files containing selected 30 minute SMOS data for each month; these files were created using the "Read Selected SMOS File(s)" button in the "readdata" Visual Basic program.
Dir	e4swats	contains data files with 30 minute soil water and temperature sensors (SWATS) measurements at site E4 in the Southern Great Plains Cloud and Radiation Testbed
ascii	DsgpswatsE4.a1.970521.000700.txt	SWATS raw data file for 5/21/97. There are 186 data files with similar names for each day from 5/21/97 to

		12/31/97. The upper case "D" at the beginning of the file name indicates that this data is from a developmental data stream.
ascii	0597.swats, 0697.swats, 0797.swats	comma delimited text files containing selected 30 minute SWATS data for the specified month; these files were created using the "Read Selected SWATS File(s)" button in the "readdata" Visual Basic program.
Dir	e7ebbr	contains data files with 30 minute energy budget bowen ratio (EBBR) measurements at site E7 in the Southern Great Plains Cloud and Radiation Testbed
ascii	sgp30ebbrE7.a1.970601.000000.txt	EBBR raw data file for 6/01/97. There are 110 data files with similar names for each day from 6/01/97 to 9/30/97.
ascii	0697.ebbr, 0797.ebbr, 0897.ebbr, 0997.ebbr	comma delimited text files containing selected 30 minute surface energy budget components for each month; these files were created using the "Read Selected EBBR File(s)" button in the "readdata" Visual Basic program.
Dir	e7merg	directory in which merged EBBR, SMOS, and SWATS data files for site E7 are analyzed
excel	e7augmerg_r.xls, e7julmerg_r.xls, e7junmerg_r.xls, e7sepmerg_r.xls	spreadsheets used for analysis of data extracted from EBBR, SMOS, and SWATS data streams as described in Section 3.3.2.
Dir	e7smos	contains data files with 30 minute surface meteorological observation system (SMOS) measurements at site E7 in the Southern Great Plains Cloud and Radiation Testbed
ascii	sgp30smosE7.a1.970609.000700.txt	SMOS raw data file for 6/09/97. There are 233 data files with similar names for each day from 6/09/97 to 3/07/98.
ascii	0697.smos, 0797.smos, 0897.smos, 0997.smos	comma delimited text files containing selected 30 minute SMOS data for each month; these files were created using the "Read Selected SMOS File(s)" button in the "readdata" Visual Basic program.
Dir	e7swats	contains data files with 30 minute soil water and temperature sensors (SWATS) measurements at site E7 in the Southern Great Plains Cloud and Radiation Testbed
ascii	DsgpswatsE7.a1.970609.000700.txt	SWATS raw data file for 6/09/97. There are 233 data files with similar names for each day from 6/09/97 to 03/07/98. The upper case "D" at the beginning of the file name indicates that this data is from a developmental data stream.
ascii	0697all.swat, 0797all.swat, 0897all.swat, 0997all.swat	comma delimited text files containing selected 30 minute SWATS data for the specified month; these files were created using the "Read Selected SWATS File(s)" button in the "readdata" Visual Basic program.

Dir	delin1sec	contains files related to watershed delineation and spatial analysis using the 1-second (30 m) DEM and the 30-m soils grid
grid	dem1alb	30-m DEM, vertical units are ft
grid	fdr_clip	flow direction grid derived from 30-m DEM, clipped to area draining to Ninnekah gage.
grid	filclip	filled DEM, vertical units are ft, clipped to area draining to Ninnekah gage
grid	filclip_m	filled DEM, vertical units are m, clipped to area draining to Ninnekah gage
grid	flen1clip	flow length grid derived from filclip_m
grid	shd1mask	mask of 30-m cells draining to Ninnekah gage, cells inside the watershed have the value 1, cells outside the watershed are assigned NODATA.
grid	soil30clip	30-m soils grid clipped to the area draining to the Ninnekah gage
grid	soil30m	30-m soils grid, unclipped
grid	soiltypes	30-m soils grid, values reclassified into basic USDA texture classes; 1 = S, 2 = LS, 3 = SL, 5 = L, 6 = SIL, 11 = SICL
	grayelev.avl	ArcView legend file for elevation grayshades
ascii	lwdemw.img	raw 30-m elevation data obtained from El Reno ARS
ascii	lwdemw.two	raw 30-m elevation data reformatted from a 1-dimensional to a 2-dimensional ASCII array.
ascii	onetotwo.f	FORTRAN program used to reformat lwdemw.img into lwdemw.two
shape	shd1secp.shp,.dbf,.shx	watershed polygon boundary delineated from 30-m DEM
shape	shdnex1.shp,.dbf,.shx	shd1secp.shp intersected with NEXRAD cells
shape	shdnex_clip.shp,.dbf,.shx	shdnex1.shp with 3 tiny polygons removed, these removed polygons correspond to HRAP cells (559, 311), (562, 308), and (562, 307); these tiny polygons do not appear in the equivalent coverage from the 3-arc second (100-m) delineation; contains flowlength and percent imperviousness attributes.
Dir	delin3sec	contains files related to watershed delineation and spatial analysis using the 3-second DEM, the 1:250k soils data, and land use data
grid	dem3al1	square portion of dem3alb clipped to the area of interest
grid	dem3alb	3-second DEM with data from USGS 1:250k quadrangles Clinton (East), Oklahoma City (West), Lawton (East), and Ardmore (West); grid has been merged and projected to a 90 m grid.
grid	demfclip	filled 3-second DEM clipped to the watershed boundary
grid	demfdr2	flow direction for demfill
grid	demfill1	filled dem3al1
grid	fdrclip	flow direction grid clipped to the watershed boundary
grid	flen1	flow length grid computed from demfill1

grid	flenclip	flow length grid clipped to the watershed boundary
grid	shdmask	mask of watershed boundary with 100-m cells
shape	cliptheme.shp,.dbf,.shx	rectangle used to clip other data sets
dBase	compjoin.dbf	dBase file containing computed component attributes (used for two-layer model only)
shape	landuse.shp,.dbf,.shx	1:250K GIRAS landuse polygons for Ardmore and Lawton quadrangles
shape	lwnexrad.shp,.dbf,.shx	NEXRAD cells in the vicinity of the Little Washita R.; a 12x9 mesh of HRAP cells; information about creating a mesh of HRAP cells may be found at www.ce.utexas.edu/prof/maidment/gishydro/seann/nexrad.htm
shape	modelp.shp,.dbf,.shx	intersection of NEXRAD cells and watershed boundary; KEY COVERAGE - contains cell attributes used for modeling
shape	nexlu.shp,.dbf,.shx	intersection of NEXRAD cells, land use, and watershed boundary
shape	nexshdsoil.shp,.dbf,.shx	intersection of NEXRAD cells, watershed boundary, and STATSGO soil polygons
shape	ninnekahshd.shp,.dbf,.shx	watershed boundary; area draining to the Ninnekah gage
shape	shdlu.shp,.dbf,.shx	watershed boundary intersected with land use polygons
shape	soillu2.shp,.dbf,.shx	STATSGO polygons intersected with land use polygons for the area of interest
shape	statnearlw.shp,.dbf,.shx	STATSGO polygons near the Little Washita R.
shape	statsclipfig.shp,.dbf,.shx	STATSGO polygons clipped for large area in central Oklahoma used to make Figure 3.5.
shape	statsshhd.shp,.dbf,.shx	STATSGO polygons intersected with the watershed boundary
Dir	double_layer	contains files used for simulations with two-layer model described in Section 5.4.
Dir	cal1to24adj	contains files for calibration runs (6/18/97-7/22/97) using 1:24K input data and adjusted rainfall
ascii	0807ctl.txt	control file for VB-SWBMS
excel	flow.xls	plot of simulated flows in Excel
ascii	flowfile.txt	VB-SWBMS flow output file (cfs)
ascii	flowm3.txt	VB-SWBMS flow output file converted to cms
ascii	smf.txt	output file from VB-SWBMS with final soil moisture values
ascii	summary.txt	summary output file created by VB-SWBMS
ascii	0810cellss.txt	cell parameter file for the two-layer model with 1:24K input data (“ss” stands for SSURGO)
ascii	0810compss.txt	component properties file for the two-layer model with 1:24K input data (“ss” stands for SSURGO)
ascii	cellsscompd24.txt	file which lists HRAP cell coordinates and the soil grid-code for locations at which modeled average daily soil water content values are to be compared with predicted values
ascii	sminit_d24.csv	file used to initialize soil moisture in the two-layer

ascii	sminit_d24_1.csv	model with 1:24K soils data (second layer is initialized to field capacity in this file)
	swbm2lay.frm, .vbp, .vbw	file used to initialize soil moisture in the two-layer model with 1:24K soils data (second layer is initialized to a water content of 0.1 in this file)
Dir	double_nobase	Visual Basic files for two-layer model with baseflow contains files used for simulations with two-layer model with no baseflow described in Section 5.4.
ascii	0810cellss.txt	cell parameter file for the two-layer model with 1:24K input data (“ss” stands for SSURGO)
ascii	0810compss.txt	component properties file for the two-layer model with 1:24K input data (“ss” stands for SSURGO)
ascii	cellscompd24.txt	file which lists HRAP cell coordinates and the soil grid-code for locations at which modeled average daily soil water content values are to be compared with predicted values
ascii	sminit_d24no.csv	soil-water content initialization file
	swbms2_24.frm, .frx, .vbp, .vbw	two-layer model modified to work specifically with the 1:24K input data and input data for the baseflow separation alternative
Dir	cal1to24adj	files associated with “double_nobase” calibration run using 1:24K input data
ascii	0807ctl.txt	VB-SWBMS control file
excel	flow.xls	spreadsheet used to plot flow results
ascii	flowfile.txt	VB-SWBMS output flow file
ascii	flowm3.txt	flowfile.txt converted from cfs to cms
ascii	smdailavg.txt	VB-SWBMS output file containing soil-water content values
ascii	smf.txt	VB-SWBMS output file of final soil-water content values
excel	soil_moist.xls	spreadsheet used to plot soil-water content results
ascii	summary.txt	VB-SWBMS output summary file
Dir	val1to24adj	files associated with “double_nobase” validation run using 1:24K input data
ascii	0807ctl.txt	VB-SWBMS control file
ascii	flowfile.txt	VB-SWBMS output flow file
ascii	flowm3.txt	flowfile.txt converted from cfs to cms
excel	flowv2.xls	spreadsheet used to plot flow results
ascii	smdailavg.txt	VB-SWBMS output file containing soil-water content values
ascii	smf.txt	VB-SWBMS output file of final soil-water content values
ascii	summary.txt	VB-SWBMS output summary file
Dir	micronet	contains unprocessed and processed Micronet rainfall data files
Dir	a110, a111, a121, etc. . . .	These 42 directories contain the raw data files for each of 42 Micronet stations for June, July, and August, 1997 (from grl.ars.usda.gov/sgp97-1.html). In each directory, there are raw 5 minute meteorological data files for each day in each month.

Each of these directories also contains two summary files for the months of June and July, 1997, containing hourly rainfall totals. These files are named after their respective directories concatenated with the endings “jul.txt” and “jun.txt.”

Dir	julsum	contains files summarizing rainfall values for July, 1997
ascii	jul10storm.txt	file used to help create Figure 5.1
excel	julyavg.xls	comparison of areal average hourly rainfall values from the Micronet and StageIII rainfall data sources
Dir	junsum	contains files summarizing rainfall values for June, 1997
excel	junavg.xls	comparison of areal average hourly rainfall values from the Micronet and StageIII rainfall data sources
shape	microdel.shp, .shx, .dbf	point shapefile of Micronet stations with reported data throughout the July 10 storm (36 points)
shape	microdth.shp, .shx, .dbf	thiessen polygons from microdel.shp
shape	micronet.shp, .shx, .dbf	point shapefile of all 42 Micronet stations
ascii	micronetloc.txt	latitude and longitude coordinates of Micronet stations
excel	micronetloc.xls	latitude and longitude coordinates of Micronet stations
shape	shdthiess.shp, .shx, .dbf	intersection of watershed boundary with microdth.shp (contains only 32 polygons)
Dir	office_docs	Microsoft Office documents
Dir	Excel	Microsoft Excel documents
excel	baseillust.xls	used to generate figures illustrating baseflow separation (Figures 3.39 and 3.40)
excel	radexample.xls	example DOE ARM EBBR data for July, 1997 – used to create Figures 3.27, 3.28, 3.29, 3.30, and 3.31
excel	soil_moist.xls	example comparison between predicted and observed soil-water content (see Figure 5.4)
excel	stypes.xls	used to create bar chart showing the distribution of surface soil textures in the Little Washita (Figure 3.6)
excel	tornado.xls	used to create Figure 5.9
excel	usdapar.xls	used to create Figures 3.9-3.12
Dir	Power Point	related Power Point Presentations
ppoint	defens_slides2.ppt	slides used at dissertation defense (Oct. 12, 1998)
ppoint	figures.ppt, figures0.ppt, figures2.ppt, figures3.ppt, figures4.ppt	figures used in dissertation
ppoint	hecoc98_c.ppt	slides for presentation at HEC (Oct. 9, 1998)
ppoint	rainfigs.ppt	used for Figure 5.1 of dissertation
ppoint	lecture_43098.ppt	GIS class lecture related to dissertation
Dir	Word	Microsoft Word Documents
word	anal_results.doc	Chapter 5: Analysis and results
word	appendices2.doc	Appendices
word	comp_imp.doc	Chapter 4: Computer implementation
word	conclusions.doc	Chapter 6: Conclusions
word	fpages.doc	Front Pages (copyright, title, etc.)

word	fpages2.doc	Fornt Pages (cont.—acknowledgements, TOC, etc.)
word	intro.doc	Chapter 1: Introductions
word	litreview.doc	Chapter 2: Literature Review
word	method.doc	Chapter 3: Methodology
word	references.doc	References
word	VITA.doc	Vita
Dir	potent_evap	contains data used to estimate potential evaporation
ascii	0497to0997day1.txt	daily average meteorological data from April to September, 1997 (used for Penman-Montieth calculations); this is an input file for VB-SWBMS model runs
Dir	precip	processed NEXRAD StageIII precipitation data and associated files
ascii	0197prec.csv, 0297prec.csv, 0397prec.csv, 0497prec.csv, 0597prec.csv, 0697prec.csv, 0797prec.csv, 0897prec.csv, 0997prec.csv, 1095prec.csv, 1196prec.csv, 1296prec.csv, 1to496prec.csv, 5to896prec.csv	StageIII hourly rainfall estimates in 55 cells for the month specified in the filename
ascii	06to07971to24.csv	StageIII hourly rainfall estimates in 54 cells for June and July, 1997; “1to24” indicates that this file was used in simulation runs using 1:24 k scale input data
ascii	06to07971to24mod10.csv	StageIII hourly rainfall estimates in 54 cells for June and July, 1997; “1to24” indicates that this file was used in simulation runs using 1:24 k scale input data; “mod10” indicates that the data for the July 10 th storm has been adjusted by a factor of 0.64 to reflect Micronet observations (see Section 5.3)
ascii	06to0797mod10.csv	StageIII hourly rainfall estimates in 55 cells for June and July, 1997; “mod10” indicates that the data for the July 10 th storm has been adjusted by a factor of 0.64 to reflect Micronet observations (see Section 5.3)
ascii	06to0797prec.csv	StageIII hourly rainfall estimates in 55 cells for June and July, 1997
ascii	exnexrad.bat	UNIX batch file used to process NEXRAD StageIII data described in Appendix B.3.
ascii	jul10storm.txt	hourly StageIII data for July 10, 1997 storm transposed so that rows are spatial units and columns are hours; used to create Figure 5.1
shape	lwxgeocprj.shp,.dbf,.shx	shapefile of NEXRAD cells before intersection with the Little Washita watershed (shown in Figure 3.18)
	ncdump	executable program compiled on a Sun Workstation used to convert netCDF files to ASCII files (see Section B.1 for further description)
ascii	rdump.c	C source code for program used to automate the conversion of hundreds of netCDF files to ASCII files (see Table B1)

ascii	readvals2.f	FORTRAN source code for program used to extract hourly StageIII estimates for only cells within the Little Washita watershed from larger files (see Table B1)
ascii	replace2.c	C source code for a program that reformats StageIII ASCII files created using ncdump (see Table B1)
Dir	prj	contains projection files
ascii	demtook.prj	projection file from decimal seconds to the projection defined in Table 3.2
ascii	geook.prj	projection file from decimal degrees to the projection defined in Table 3.2
ascii	utmttook.prj	projection file from UTM to the projection defined in Table 3.2
ascii	utmttook7.prj	projection file from UTM (NAD27) to the projection defined in Table 3.2
ascii	natok.prj	projection file from national Albers Equal-Area parameters to the projection defined in Table 3.2
Dir	readdata	contains source code for time series data processing programs
	readdata.frm, .vbp, .vbw	Visual Basic time series data processing programs described in Appendix B
Dir	referenc	data used for spatial reference
cover	hucsalb	USGS 8 digit HUCs for the Washita River
cover	okalb	state of Oklahoma boundary
cover	rf1	EPA River Reach File 1 for the Washita River
shape	arm7nd8.shp, .dbf, .shx	point shapefile of ARM stations EF7 and EF8
shape	kansok.shp, .dbf, .shx	shapefile of the Kansas and Oklahoma state boundaries
shape	lawhyd3p.shp, .dbf, .shx	1:100,000 scale hydrography DLG for the Lawton-3 quadrangle
shape	lawhyd4p.shp, .dbf, .shx	1:100,000 scale hydrography DLG for the Lawton-4 quadrangle
shape	lawt3.shp, .dbf, .shx	1:100,000 scale transportation DLG for the Lawton-3 quadrangle
shape	lawt4.shp, .dbf, .shx	1:100,000 scale transportation DLG for the Lawton-4 quadrangle
shape	okalb.shp, .dbf, .shx	shapefile of Oklahoma boundary
shape	okcitalb.shp, .dbf, .shx	shapefile of cities in Oklahoma
shape	okcntalb.shp, .dbf, .shx	shapefile of counties in Oklahoma
shape	paulval1.shp, .dbf, .shx	1:100,000 scale transportation DLG for the Paul Valley-1 quadrangle
shape	pvh1d1p.shp, .dbf, .shx	1:100,000 scale hydrography DLG for the Paul Valley-1 quadrangle
Dir	sgp97_grav_soil_data	contains observed gravimetric soil-water content data for the Little Washita from SGP97
ascii	bulkdens.txt	bulk density data for SGP sampling sites
	cellscompare.txt	SGP sites and cells where a comparison between modeled and observed soil-water content will be made
	figure11.gif	scanned map of Little Washita area
	figure11.tif	scanned map of Little Washita area

ascii	lwsweb.txt	gravimetric soil moisture data downloaded from the web (Little Washita data only) (daac.gsfc.nasa.gov/campaign_docs/sgp97/gravi_moist.html)
shape	smsites.shp, .dbf, .shx	approximate location of soil moisture measurement sites with points located visually
ascii	smweb.txt	gravimetric soil moisture data downloaded from the web (all sites) (daac.gsfc.nasa.gov/campaign_docs/sgp97/gravi_moist.html)
Dir	single_layer	contains program files and data files for single_layer simulation runs
ascii	cellscompare.txt	SGP sites and cells where a comparison between modeled and observed soil-water content will be made
ascii	senssminit.txt	soil-water content initialization file for soil moisture sensitivity runs
ascii	sminit.csv	soil-water content initialization file used with 1:250K runs
ascii	sminit1to24.csv	soil-water content initialization file used with 1:24K runs
	swbms1lay3.frm, .log, .vbp, .vbw	Visual Basic code for 1-layer model
ascii	swbms1to24cc.csv	cell parameter file used with 1:24K scale input data
ascii	swbms1to250.txt	cell parameter file used with 1:250K scale input data
ascii	swbmssil.txt	cell parameter file used when the watershed is assumed to be entirely silt loam (watershed level resampling with 1:24K soils data)
ascii	swbmssll.csv	cell parameter file used when the watershed is assumed to be entirely sandy loam (watershed level resampling with 1:250K soils data)
Dir	cal1to24	VB-SWBMS calibration files using 1:24K input data
ascii	0805ctl.txt	control file
ascii	flowfile.txt	VB-SWBMS output flow file (cfs)
ascii	flowm3.txt	flowfile.txt converted to cms
excel	flowoadj.xls	spreadsheet used to plot flow results
ascii	smdailavg.txt	VB-SWBMS daily average soil moisture output file
ascii	smfinal.txt	VB-SWBMS final soil moisture file
excel	soil_moist0.xls	spreadsheet used to compare observed and modeled soil moisture
ascii	summary.txt	VB-SWBMS output summary file
Dir	cal1to24adj	VB-SWBMS calibration files using 1:24K input data and adjusted rainfall for July 10 storm
ascii	0805ctl.txt	control file
ascii	flowfile.txt	VB-SWBMS output flow file (cfs)
ascii	flowm3.txt	flowfile.txt converted to cms
excel	flowc.xls	spreadsheet used to plot flow results
ascii	smdailavg.txt	VB-SWBMS daily average soil moisture output file
ascii	smfinal.txt	VB-SWBMS final soil moisture file
excel	soil_moist.xls	spreadsheet used to compare observed and modeled

ascii	summary.txt	soil moisture VB-SWBMS output summary file
Dir	cal1to250	VB-SWBMS calibration files using 1:250K input data
ascii	0805ctl.txt	control file
ascii	flowfile.txt	VB-SWBMS output flow file (cfs)
ascii	smdailavg.txt	VB-SWBMS daily average soil moisture output file
ascii	smfinal.txt	VB-SWBMS final soil moisture file
ascii	summary.txt	VB-SWBMS output summary file
Dir	cal1to250adj	VB-SWBMS calibration files using 1:250K input data and adjusted rainfall for July 10 storm
ascii	0805ctl.txt	control file
ascii	flowfile.txt	VB-SWBMS output flow file (cfs)
ascii	smdailavg.txt	VB-SWBMS daily average soil moisture output file
ascii	smfinal.txt	VB-SWBMS final soil moisture file
ascii	summary.txt	VB-SWBMS output summary file
Dir	calsiladj	VB-SWBMS calibration files using watershed level resampling, 1:24K input data, and adjusted rainfall for July 10 storm
ascii	0805ctl.txt	control file
excel	flow.xls	spreadsheet used to plot streamflows
ascii	flowfile.txt	VB-SWBMS output flow file (cfs)
ascii	flowm3.txt	flowfile.txt converted to cms
ascii	smdailavg.txt	VB-SWBMS daily average soil moisture output file
ascii	smfinal.txt	VB-SWBMS final soil moisture file
ascii	summary.txt	VB-SWBMS output summary file
Dir	calsladj	VB-SWBMS calibration files using watershed level resampling, 1:250K input data, and adjusted rainfall for July 10 storm
ascii	0805ctl.txt	control file
ascii	flowfile.txt	VB-SWBMS output flow file (cfs)
ascii	smdailavg.txt	VB-SWBMS daily average soil moisture output file
ascii	smfinal.txt	VB-SWBMS final soil moisture file
ascii	summary.txt	VB-SWBMS output summary file
Dir	senshb	VB-SWBMS files used for sensitivity analysis with h_b described in Section 5.6.
ascii	0805ctl.txt	control file
ascii	flowfile.txt	VB-SWBMS output flow file (cfs)
ascii	p_hbhigh.csv	parameter lookup table with high h_b values
ascii	p_hblow.csv	parameter lookup table with low h_b values
ascii	smdailavg.txt	VB-SWBMS daily average soil moisture output file
ascii	smfinal.txt	VB-SWBMS final soil moisture file
ascii	summary.txt	VB-SWBMS output summary file
Dir	senslam	VB-SWBMS files used for sensitivity analysis with λ described in Section 5.6.
ascii	0805ctl.txt	control file
ascii	flowfile.txt	VB-SWBMS output flow file (cfs)
ascii	p_lamhigh.csv	parameter lookup table with high λ values
ascii	p_lamlow.csv	parameter lookup table with low λ values
ascii	smdailavg.txt	VB-SWBMS daily average soil moisture output file

ascii	smfinal.txt	VB-SWBMS final soil moisture file
ascii	summary.txt	VB-SWBMS output summary file
Dir	senspor	VB-SWBMS files used for sensitivity analysis with porosity described in Section 5.6.
ascii	0805ctl.txt	control file
ascii	flowfile.txt	VB-SWBMS output flow file (cfs)
ascii	p_porhigh.csv	parameter lookup table with high porosity values
ascii	p_porlow.csv	parameter lookupt table with low porosity values
ascii	smdailavg.txt	VB-SWBMS daily average soil moisture output file
ascii	smfinal.txt	VB-SWBMS final soil moisture file
ascii	summary.txt	VB-SWBMS output summary file
Dir	sensrain	VB-SWBMS files used for sensitivity analysis with rain described in Section 5.6.
ascii	0805ctl.txt	control file
ascii	flowfile.txt	VB-SWBMS output flow file (cfs)
ascii	smdailavg.txt	VB-SWBMS daily average soil moisture output file
ascii	smfinal.txt	VB-SWBMS final soil moisture file
ascii	summary.txt	VB-SWBMS output summary file
Dir	senssm	VB-SWBMS files used for sensitivity analysis with soil moisture described in Section 5.6.
ascii	0805ctl.txt	control file
ascii	flowfile.txt	VB-SWBMS output flow file (cfs)
ascii	smdailavg.txt	VB-SWBMS daily average soil moisture output file
ascii	smfinal.txt	VB-SWBMS final soil moisture file
ascii	summary.txt	VB-SWBMS output summary file
Dir	sensthr	VB-SWBMS files used for sensitivity analysis with residual water content described in Section 5.6.
ascii	0805ctl.txt	control file
ascii	flowfile.txt	VB-SWBMS output flow file (cfs)
ascii	p_thrhigh.csv	parameter lookup table with high porosity values
ascii	p_thrflow.csv	parameter lookupt table with low porosity values
ascii	smdailavg.txt	VB-SWBMS daily average soil moisture output file
ascii	smfinal.txt	VB-SWBMS final soil moisture file
ascii	summary.txt	VB-SWBMS output summary file
Dir	val0507sl	VB-SWBMS files used for second validation run with watershed level resampling (assuming the entire watershed is sandy loam)
ascii	0805ctl.txt	control file
ascii	flowfile.txt	VB-SWBMS output flow file (cfs)
ascii	flowm3sl.txt	flowfile.txt converted to cms
excel	flowv1.xls	spreadsheet used to plot flows
ascii	smdailavg.txt	VB-SWBMS daily average soil moisture output file
ascii	smfinal.txt	VB-SWBMS final soil moisture file
ascii	summary.txt	VB-SWBMS output summary file
Dir	val1to250	VB-SWBMS validation files using 1:250K input data
ascii	0805ctl.txt	control file
excel	flowv1.xls	spreadsheet used to plot flows
ascii	flowfile.txt	VB-SWBMS output flow file (cfs)
ascii	smdailavg.txt	VB-SWBMS daily average soil moisture output file

ascii	smfinal.txt	VB-SWBMS final soil moisture file
ascii	summary.txt	VB-SWBMS output summary file
Dir	val1to250adj	VB-SWBMS validation files using 1:250K input data
ascii	0805ctl.txt	control file
ascii	flowfile.txt	VB-SWBMS output flow file (cfs)
ascii	smdailavg.txt	VB-SWBMS daily average soil moisture output file
ascii	smfinal.txt	VB-SWBMS final soil moisture file
ascii	summary.txt	VB-SWBMS output summary file
Dir	val1to24	VB-SWBMS validation files using 1:24K input data
ascii	0805ctl.txt	control file
excel	flow0.xls	spreadsheet used to plot flows
ascii	flowfile.txt	VB-SWBMS output flow file (cfs)
ascii	flowm3.txt	flowfile.txt converted to cms
ascii	smdailavg.txt	VB-SWBMS daily average soil moisture output file
ascii	smfinal.txt	VB-SWBMS final soil moisture file
ascii	summary.txt	VB-SWBMS output summary file
Dir	val1to240507	VB-SWBMS files for the second validation period using 1:24K input data
ascii	0805ctl.txt	control file
excel	flowv1.xls	spreadsheet used to plot flows
ascii	flowfile.txt	VB-SWBMS output flow file (cfs)
ascii	flowm3.txt	flowfile.txt converted to cms
ascii	smdailavg.txt	VB-SWBMS daily average soil moisture output file
ascii	smfinal.txt	VB-SWBMS final soil moisture file
ascii	summary.txt	VB-SWBMS output summary file
Dir	val1to24adj	VB-SWBMS validation files using 1:24K input data
ascii	0805ctl.txt	control file
excel	flowfig.xls	spreadsheet used to plot flows
ascii	flowfile.txt	VB-SWBMS output flow file (cfs)
ascii	flowm3.txt	flowfile.txt converted to cms
excel	flowv1.xls	spreadsheet used to plot flows
ascii	smdailavg.txt	VB-SWBMS daily average soil moisture output file
ascii	smfinal.txt	VB-SWBMS final soil moisture file
ascii	summary.txt	VB-SWBMS output summary file
Dir	valsiladj	VB-SWBMS validation files using watershed level resampling and 1:24K input data
ascii	0805ctl.txt	control file
ascii	flowfile.txt	VB-SWBMS output flow file (cfs)
ascii	flowm3.txt	flowfile.txt converted to cms
ascii	smdailavg.txt	VB-SWBMS daily average soil moisture output file
ascii	smfinal.txt	VB-SWBMS final soil moisture file
ascii	summary.txt	VB-SWBMS output summary file
Dir	valsldj	VB-SWBMS calibration files using watershed level resampling and 1:250K input data
ascii	0805ctl.txt	control file
ascii	flowfile.txt	VB-SWBMS output flow file (cfs)
ascii	smdailavg.txt	VB-SWBMS daily average soil moisture output file

ascii	smfinal.txt	VB-SWBMS final soil moisture file
ascii	summary.txt	VB-SWBMS output summary file
Dir	single_layer_base	VB-SWBMS files used for one-layer simulations with baseflow
	swbms1base.vbw, .vbp, .frm	Visual Basic code for 1-layer model which uses baseflow simulation
Dir	cal1to24adj	VB-SWBMS calibration files using 1:24K input data and adjusted rainfall for July 10 storm
ascii	0805ctl.txt	control file
excel	flowbig_cms.xls	spreadsheet plotting flows for example with a big baseflow storage constant (see discussion in Section 5.4)
ascii	flowfile.txt	VB-SWBMS output flow file (cfs)
ascii	flowm3_small.txt	VB-SWBMS output flow file converted to cms for the case of a small baseflow storage constant
ascii	flowm3big.txt	VB-SWBMS model flow output converted to cms for case with big baseflow storage constant
excel	flowsmall_cms.xls	spreadsheet plotting flows for example with a small baseflow storage constant (see discussion in Section 5.4)
ascii	smdailavg.txt	VB-SWBMS daily average soil moisture output file
ascii	smfinal.txt	VB-SWBMS final soil moisture file
ascii	summary.txt	VB-SWBMS output summary file
Dir	single_layer_pred	VB-SWBMS files used for one-layer simulations and the predominant soil type option (looping in the code is slightly different for this case)
	swbms1lay4, .frm, .frx, .vbp, .vbw	Visual Basic code for 1 layer model and the predominant soil type option
ascii	swbms1to24pred.csv	cell parameter file for VB-SWBMS for cases using 1:24K input data
ascii	swbms1to250pred.txt	cell parameter file for VB-SWBMS for cases using 1:250K input data
ascii	wcinit1to24pred.csv	soil-water content initialization file for the case of 1:24K input data and NEXRAD cell level resampling
ascii	wcinit1to250pred.csv	soil-water content initialization file for the case of 1:250K input data and NEXRAD cell level resampling
Dir	cal1to24adj	VB-SWBMS calibration files using 1:24K input data and adjusted rainfall for July 10 storm
ascii	0805ctl.txt	control file
ascii	flowfile.txt	VB-SWBMS output flow file (cfs)
ascii	smf.txt	VB-SWBMS final soil moisture file
ascii	summary.txt	VB-SWBMS output summary file
Dir	cal1to250adj	VB-SWBMS calibration files using 1:250K input data and adjusted rainfall for July 10 storm
ascii	0805ctl.txt	control file
ascii	flowfile.txt	VB-SWBMS output flow file (cfs)
ascii	smf.txt	VB-SWBMS final soil moisture file
ascii	summary.txt	VB-SWBMS output summary file
Dir	val1to24adj	VB-SWBMS validation files using 1:24K input

		data
ascii	0805ctl.txt	control file
ascii	flowfile.txt	VB-SWBMS output flow file (cfs)
ascii	smfinal.txt	VB-SWBMS final soil moisture file
ascii	summary.txt	VB-SWBMS output summary file
Dir	val1to250adj	VB-SWBMS validation files using 1:250K input data
ascii	0824ctl.txt	control file
ascii	flowfile.txt	VB-SWBMS output flow file (cfs)
ascii	smf.txt	VB-SWBMS final soil moisture file
ascii	summary.txt	VB-SWBMS output summary file
Dir	soils	contains soil maps and associated data tables
	30mcprop2.dbf	summary of component properties for 30-m soils grid created using AV-SWBMS
	compjoin.dbf	summary of component properties for Oklahoma STATSGO data created using AV-SWBMS
ascii	lookup.txt	lookup table to translate STATSGO texture names into the 12 basic USDA texture classes, created at Penn State and slightly modified here (see discussion in Section 3.2.2.2.2)
	lwcommod.dbf	modified version of lwcomp.dbf that contains only one entry for each "Gisclass" (a.k.a. grid-code)
	lwcomp.dbf	component attribute table associated with 30-m soils grid
	lwlayer.dbf	layer attribute table associated with 30-m soils grid
	lws30utm.bil, lws30utm.hdr	original spatial data for 30-m soils grid obtained from the ARS Grazinglands Research Laboratory in El Reno, OK (in the UTM coordinate system)
	lwsoils.wk4	original tabular data for 30-m soils grid obtained from the ARS Grazinglands Research Laboratory in El Reno, OK (in Lotus 1-2-3 format)
ascii	statusda.txt	lookup table (in ArcView readable, comma delimited, format) used to translate STATSGO texture names into USDA texture class names
ascii	usdapar.txt	parameter value lookup table based on Carsel and Parrish (1988) paper
ascii	usdapar_r.csv	parameter value lookup table based on Rawls, Brakensiek, and Saxton (1982) paper
Dir	info	contains Arc/Info "info" files (attribute tables)
grid	lws30alb	30-m soils grid in Arc/Info format and Albers projection (see Table 3.2)
Dir	statsgo	contains the STATSGO soil map and associated attribute files for the state of Oklahoma (organized into three directories that are created when the data is downloaded from the NRCS web site)
Dir	header	contains text files describing the mapextent and projection of the soils data
Dir	metadata	contains a text file with metadata (data about data)
Dir	spatial	contains 1:250K STATSGO soil maps and attribute

		tables
cover	Ok	STATSGO map in original national Albers Equal-area map projection
cover	oknat	STATSGO map in original national Albers Equal-Area projection with arc topology only
cover	okok	STATSGO map projected into an Albers Equal-Area projection with parameters used for making state-wide maps of Oklahoma
	comp.dbf	STATSGO component attribute table
	compyld.dbf	STATSGO table that stores crop yield information
	forest.dbf	STATSGO table that stores information for plant cover
	interp.dbf	STATSGO table
	layer.dbf	STATSGO layer table
	mapunit.dbf	STATSGO mapunit table
shape	oknat.shp, .dbf, .shx	shapefile with same data as the coverage "Ok"
	plantcom.dbf	STATSGO table that stores plant symbols and percent of plant composition
	plantnm	STATSGO table with the common and scientific names for plants
	rsprod.dbf	STATSGO table that stores range site productivity information for soils
	taxclass.dbf	STATSGO table that stores taxonomic classification for soil components
	windbrk.dbf	STATSGO table
	wlhabit.dbf	STATSGO table
	woodland.dbf	STATSGO table
	woodmgt.dbf	STATSGO table
	yldunits.dbf	STATSGO table
Dir	streamflow_data	contains hourly streamflow data for the gaging station (Ninnekah) shown in Figure 3.2
Dir	info	contains Arc/Info attribute tables
cover	usgsstel	point coverage of stations 07327447 and 07327550; attributes from the file usgsstel.txt can be joined to this coverage
ascii	0507to052497sf.txt	observed streamflow and separated baseflow for 5/7/97-5/24/97; units are cfs, baseflow separation parameter = 60 hours
ascii	0530to0731b.txt	observed streamflow and separated baseflow for 5/30/97-7/31/97; units are cfs, baseflow separation parameter = 60 hours
ascii	0601to0701.txt	observed streamflow and separated baseflow for 6/01/97-7/01/97; units are cfs, baseflow separation parameter = 60 hours
ascii	0601to0801.txt	observed streamflow and separated baseflow for 6/01/97-8/01/97; units are cfs, baseflow separation parameter = 60 hours
ascii	601to18base.txt	observed streamflow and separated baseflow for 6/01/97-6/18/97; units are cfs, baseflow separation parameter = 60 hours

ascii	709to718b15.txt	observed stramflow and separated baseflow for 7/09/97-7/18/97; units are cfs, baseflow separation parameter = 15 hours
ascii	709to718b30.txt	observed stramflow and separated baseflow for 7/09/97-7/18/97; units are cfs, baseflow separation parameter = 30 hours
ascii	709to718b60.txt	observed stramflow and separated baseflow for 7/09/97-7/18/97; units are cfs, baseflow separation parameter = 60 hours
ascii	bfj18tojl20.txt	observed stramflow and separated baseflow for 6/18/97-7/30/97; units are cfs, baseflow separation parameter = 60 hours
shape	chick_sf.shp, .dbf, .shx	locations of ARS streamflow stations in lat/lon
ascii	ninnekah	15 minute flows for the USGS gaging station East of Ninnekah (07327550) ; 10/1/95 – 10/29/97
excel	ninnflow2_s.xls	hourly flows for the USGS gaging station East of Ninnekah (07327550) ; 10/1/95 – 10/29/97 (cfs); computed from “ninnekah”; also includes separated baseflow with n = 60 hours
ascii	ninnflow2_s.txt	hourly flows for the USGS gaging station East of Ninnekah (07327550) ; 10/1/95 – 10/29/97 (cfs); computed from “ninnekah”
excel	ninnflowjj97.xls	hourly flows for the USGS gaging station East of Ninnekah (07327550) ; June and July 1997 (cfs)
shape	on1sec.shp, .dbf, .shx	USGS gaging station locations shifted onto streams defined by the 30 m DEM
shape	statalb.shp, .dbf, .shx	locations of ARS streamflow stations projected into an Albers Equal-area projection with parameters defined in Table 3.2
ascii	usgs.txt	attribute information for USGS gaging stations
ascii	usgssel.txt	attribute information that can be joined to the stations in the coverage usgssel
ascii	whatidid.txt	text file containing information about how the point coverage usgssel was created

Appendix D: Table used to reclassify 719 STATSGO texture names into 12 basic USDA classes and the "other" category.

STATSGO_name,USDA_t	BYX-CL, CL	CBA-FS, S
exture_class	BYX-COS, S	CBA-FSL, SL
BY-C, C	BYX-COSL, SL	CBA-L, L
BY-CL, CL	BYX-FS, S	CBA-LCOS, LS
BY-COS, S	BYX-FSL, SL	CBA-LS, LS
BY-COSL, SL	BYX-L, L	CBA-LVFS, LS
BY-FS, S	BYX-LCOS, LS	CBA-S, S
BY-FSL, SL	BYX-LFS, LS	CBA-SC, SC
BY-L, L	BYX-LS, LS	CBA-SCL, SCL
BY-LCOS, LS	BYX-LVFS, LS	CBA-SI, SI
BY-LS, LS	BYX-S, S	CBA-SIC, SIC
BY-LVFS, LS	BYX-SC, SC	CBA-SICL, SICL
BY-S, S	BYX-SCL, SCL	CBA-SIL, SIL
BY-SC, SC	BYX-SI, SI	CBA-SL, SL
BY-SCL, SCL	BYX-SIC, SIC	CBA-VFS, S
BY-SI, SI	BYX-SICL, SICL	CBA-VFSL, SL
BY-SIC, SIC	BYX-SIL, SIL	CBV-C, C
BY-SICL, SICL	BYX-SL, SL	CBV-CIND, O
BY-SIL, SIL	BYX-VFS, S	CBV-CL, CL
BY-SL, SL	BYX-VFSL, SL	CBV-COS, S
BY-VFS, S	C, C	CBV-COSL, SL
BY-VFSL, SL	CB-C, C	CBV-FS, S
BYV-C, C	CB-CL, CL	CBV-FSL, SL
BYV-CL, CL	CB-COS, S	CBV-L, L
BYV-COS, S	CB-COSL, SL	CBV-LCOS, S
BYV-COSL, SL	CB-FS, S	CBV-LFS, LS
BYV-FS, S	CB-FSL, SL	CBV-LS, LS
BYV-FSL, SL	CB-L, L	CBV-MUCK, OM
BYV-L, L	CB-LCOS, LS	CBV-S, S
BYV-LCOS, LS	CB-LFS, LS	CBV-SC, SC
BYV-LFS, LS	CB-LS, LS	CBV-SCL, SCL
BYV-LS, LS	CB-LVFS, LS	CBV-SIC, SIC
BYV-LVFS, LS	CB-S, S	CBV-SICL, SICL
BYV-S, S	CB-SC, SC	CBV-SIL, SIL
BYV-SC, SC	CB-SCL, SCL	CBV-SL, SL
BYV-SCL, SCL	CB-SI, SI	CBV-VFSL, SL
BYV-SI, SI	CB-SIC, SIC	CBX-C, C
BYV-SIC, SIC	CB-SICL, SICL	CBX-CL, CL
BYV-SICL, SICL	CB-SIL, SIL	CBX-COS, S
BYV-SIL, SIL	CB-SL, SL	CBX-COSL, SL
BYV-SL, SL	CB-VFS, S	CBX-FS, S
BYV-VFS, S	CB-VFSL, SL	CBX-FSL, SL
BYV-VFSL, SL	CBA-C, C	CBX-L, L
BYV-SL, SL	CBA-CL, CL	CBX-LCOS, LS
BYX-C, C	CBA-COS, S	CBX-LFS, LS
	CBA-COSL, SL	CBX-LS, LS

CBX-LVFS , LS	CNV-SIC , SIC	CRC-COSL , SL
CBX-S , S	CNV-SICL , SICL	CRC-FS , S
CBX-SC , SC	CNV-SIL , SIL	CRC-FSL , SL
CBX-SCL , SCL	CNV-SL , SL	CRC-L , L
CBX-SI , SI	CNV-VFS , S	CRC-LCOS , LS
CBX-SIC , SIC	CNV-VFSL , SL	CRC-LS , LS
CBX-SICL , SICL	CNX-C , C	CRC-LVFS , LS
CBX-SIL , SIL	CNX-CL , CL	CRC-S , S
CBX-SL , SL	CNX-COS , S	CRC-SC , SC
CBX-VFS , S	CNX-COSL , SL	CRC-SCL , SCL
CBX-VFSL , SL	CNX-FS , S	CRC-SI , SI
CE , O	CNX-FSL , SL	CRC-SIC , SIC
CEM , O	CNX-L , L	CRC-SICL , SICL
CIND , O	CNX-LCOS , LS	CRC-SIL , SIL
CL , CL	CNX-LS , LS	CRC-SL , SL
CN-C , C	CNX-LVFS , LS	CRC-VFS , S
CN-CL , CL	CNX-S , S	CRC-VFSL , SL
CN-COS , S	CNX-SC , SC	CRV-C , C
CN-COSL , SL	CNX-SCL , SCL	CRV-CL , CL
CN-FS , S	CNX-SI , SI	CRV-COS , S
CN-FSL , SL	CNX-SIC , SIC	CRV-COSL , SL
CN-L , L	CNX-SICL , SICL	CRV-FS , S
CN-LCOS , LS	CNX-SIL , SIL	CRV-FSL , SL
CN-LFS , LS	CNX-SL , SL	CRV-L , L
CN-LS , LS	CNX-VFS , S	CRV-LCOS , LS
CN-LVFS , LS	CNX-VFSL , SL	CRV-LS , LS
CN-S , S	COS , S	CRV-LVFS , LS
CN-SC , SC	COSL , SL	CRV-S , S
CN-SCL , SCL	CR-C , C	CRV-SC , SC
CN-SI , SI	CR-CL , CL	CRV-SCL , SCL
CN-SIC , SIC	CR-COS , S	CRV-SI , SI
CN-SICL , SICL	CR-COSL , SL	CRV-SIC , SIC
CN-SIL , SIL	CR-FS , S	CRV-SICL , SICL
CN-SL , SL	CR-FSL , SL	CRV-SIL , SIL
CN-VFS , S	CR-L , L	CRV-SL , SL
CN-VFSL , SL	CR-LCOS , LS	CRV-VFS , S
CNV-C , C	CR-LS , LS	CRV-VFSL , SL
CNV-CL , CL	CR-LVFS , LS	CRX-C , C
CNV-COS , S	CR-S , S	CRX-CL , CL
CNV-COSL , SL	CR-SC , SC	CRX-COS , S
CNV-FS , S	CR-SCL , SCL	CRX-COSL , SL
CNV-FSL , SL	CR-SI , SI	CRX-FS , S
CNV-L , L	CR-SIC , SIC	CRX-FSL , SL
CNV-LCOS , LS	CR-SICL , SICL	CRX-L , L
CNV-LFS , LS	CR-SIL , SIL	CRX-LCOS , LS
CNV-LS , LS	CR-SL , SL	CRX-LS , LS
CNV-LVFS , LS	CR-VFS , S	CRX-LVFS , LS
CNV-S , S	CR-VFSL , SL	CRX-S , S
CNV-SC , SC	CRC-C , C	CRX-SC , SC
CNV-SCL , SCL	CRC-CL , CL	CRX-SCL , SCL
CNV-SI , SI	CRC-COS , S	CRX-SI , SI

CRX-SIC ,SIC	FLX-COSL ,SL	GRC-L ,L
CRX-SICL ,SICL	FLX-FS ,S	GRC-LCOS ,LS
CRX-SIL ,SIL	FLX-FSL ,SL	GRC-LS ,LS
CRX-SL ,SL	FLX-L ,L	GRC-LVFS ,LS
CRX-VFS ,S	FLX-LCOS ,LS	GRC-S ,S
CRX-VFSL ,SL	FLX-LS ,LS	GRC-SC ,SC
DE ,O	FLX-LVFS ,LS	GRC-SCL ,SCL
FB ,OM	FLX-S ,S	GRC-SI ,SI
FL-C ,C	FLX-SC ,SC	GRC-SIC ,SIC
FL-CL ,CL	FLX-SCL ,SCL	GRC-SICL ,SICL
FL-COS ,S	FLX-SI ,SI	GRC-SIL ,SIL
FL-COSL ,SL	FLX-SIC ,SIC	GRC-SL ,SL
FL-FS ,S	FLX-SICL ,SICL	GRC-VFS ,S
FL-FSL ,SL	FLX-SIL ,SIL	GRC-VFSL ,SL
FL-L ,L	FLX-SL ,SL	GRF-C ,C
FL-LCOS ,LS	FLX-VFS ,S	GRF-CL ,CL
FL-LS ,LS	FLX-VFSL ,SL	GRF-COS ,S
FL-LVFS ,LS	FRAG ,O	GRF-COSL ,SL
FL-S ,S	FS ,S	GRF-FS ,S
FL-SC ,SC	FSL ,SL	GRF-FSL ,SL
FL-SCL ,SCL	G ,O	GRF-L ,L
FL-SI ,SI	GR ,O	GRF-LCOS ,LS
FL-SIC ,SIC	GR-C ,C	GRF-LS ,LS
FL-SICL ,SICL	GR-CL ,CL	GRF-LVFS ,LS
FL-SIL ,SIL	GR-COS ,S	GRF-S ,S
FL-SL ,SL	GR-COSL ,SL	GRF-SC ,SC
FL-VFS ,S	GR-FS ,S	GRF-SCL ,SCL
FL-VFSL ,SL	GR-FSL ,SL	GRF-SI ,SI
FLV-C ,C	GR-L ,L	GRF-SIC ,SIC
FLV-CL ,CL	GR-LCOS ,LS	GRF-SICL ,SICL
FLV-COS ,S	GR-LFS ,LS	GRF-SIL ,SIL
FLV-COSL ,SL	GR-LS ,LS	GRF-SL ,SL
FLV-FS ,S	GR-LVFS ,LS	GRF-VFS ,S
FLV-FSL ,SL	GR-MARL ,O	GRF-VFSL ,SL
FLV-L ,L	GR-MUCK ,OM	GRV-C ,C
FLV-LCOS ,LS	GR-S ,S	GRV-CL ,CL
FLV-LS ,LS	GR-SC ,SC	GRV-COS ,S
FLV-LVFS ,LS	GR-SCL ,SCL	GRV-COSL ,SL
FLV-S ,S	GR-SI ,SI	GRV-FS ,S
FLV-SC ,SC	GR-SIC ,SIC	GRV-FSL ,SL
FLV-SCL ,SCL	GR-SICL ,SICL	GRV-L ,L
FLV-SI ,SI	GR-SIL ,SIL	GRV-LCOS ,LS
FLV-SIC ,SIC	GR-SL ,SL	GRV-LFS ,LS
FLV-SICL ,SICL	GR-VAR ,O	GRV-LS ,LS
FLV-SIL ,SIL	GR-VFS ,S	GRV-LVFS ,LS
FLV-SL ,SL	GR-VFSL ,SL	GRV-S ,S
FLV-VFS ,S	GRC-C ,C	GRV-SC ,SC
FLV-VFSL ,SL	GRC-CL ,CL	GRV-SCL ,SCL
FLX-C ,C	GRC-COS ,S	GRV-SI ,SI
FLX-CL ,CL	GRC-COSL ,SL	GRV-SIC ,SIC
FLX-COS ,S	GRC-FS ,S	GRV-SICL ,SICL

GRV-SIL, SIL	MK-S, S	SH-SC, SC
GRV-SL, SL	MK-SC, SC	SH-SCL, SCL
GRV-VFS, S	MK-SCL, SCL	SH-SI, SI
GRV-VFSL, SL	MK-SI, SI	SH-SIC, SIC
GRX-C, C	MK-SIC, SIC	SH-SICL, SICL
GRX-CL, CL	MK-SICL, SICL	SH-SIL, SIL
GRX-COS, S	MK-SIL, SIL	SH-SL, SL
GRX-COSL, SL	MK-SL, SL	SH-VFS, S
GRX-FRAG, O	MK-VFS, S	SH-VFSL, SL
GRX-FS, S	MK-VFSL, SL	SHV-C, C
GRX-FSL, SL	MPT, OM	SHV-CL, CL
GRX-L, L	MUCK, OM	SHV-COS, S
GRX-LCOS, LS	NONE, O	SHV-COSL, SL
GRX-LFS, LS	PEAT, OM	SHV-FS, S
GRX-LS, LS	PT-SIC, SIC	SHV-FSL, SL
GRX-LVFS, LS	PT-SIL, SIL	SHV-L, L
GRX-S, S	RB-C, C	SHV-LCOS, LS
GRX-SC, SC	RB-CL, CL	SHV-LS, LS
GRX-SCL, SCL	RB-COS, S	SHV-LVFS, LS
GRX-SI, SI	RB-COSL, SL	SHV-S, S
GRX-SIC, SIC	RB-FS, S	SHV-SC, SC
GRX-SICL, SICL	RB-FSL, SL	SHV-SCL, SCL
GRX-SIL, SIL	RB-L, L	SHV-SI, SI
GRX-SL, SL	RB-LCOS, LS	SHV-SIC, SIC
GRX-VFS, S	RB-LS, LS	SHV-SICL, SICL
GRX-VFSL, SL	RB-LVFS, LS	SHV-SIL, SIL
GYP, O	RB-S, S	SHV-SL, SL
HM, OM	RB-SC, SC	SHV-VFS, S
ICE, O	RB-SCL, SCL	SHV-VFSL, SL
IND, O	RB-SI, SI	SHX-CL, CL
L, L	RB-SIC, SIC	SHX-L, L
LCOS, LS	RB-SICL, SICL	SI, SI
LCOS, LS	RB-SIL, SIL	SIC, SIC
LFS, LS	RB-SL, SL	SICL, SICL
LS, LS	RB-VFS, S	SIL, SIL
LVFS, LS	RB-VFSL, SL	SL, SL
MARL, O	S, S	SP, OM
MI-SIL, SIL	SC, SC	SR, O
MK-C, C	SCL, SCL	SR-, O
MK-CL, CL	SG, O	SR-SIL, SIL
MK-COS, S	SH-C, C	ST-SIL, SIL
MK-COSL, SL	SH-CL, CL	ST-C, C
MK-FS, S	SH-COS, S	ST-CL, CL
MK-FSL, SL	SH-COSL, SL	ST-COS, S
MK-L, L	SH-FS, S	ST-COSL, SL
MK-LCOS, LS	SH-FSL, SL	ST-FS, S
MK-LFS, LS	SH-L, L	ST-FSL, SL
MK-LS, LS	SH-LCOS, LS	ST-L, L
MK-LVFS, LS	SH-LS, LS	ST-LCOS, LS
MK-MARL, O	SH-LVFS, LS	ST-LFS, LS
MK-PEAT, OM	SH-S, S	ST-LS, LS

ST-LVFS,LS	STX-SCL,SCL	SYX-COSL,SL
ST-MUCK,OM	STX-SI,SI	SYX-FS,S
ST-S,S	STX-SIC,SIC	SYX-FSL,SL
ST-SC,SC	STX-SICL,SICL	SYX-L,L
ST-SCL,SCL	STX-SIL,SIL	SYX-LCOS,LS
ST-SI,SI	STX-SL,SL	SYX-LS,LS
ST-SIC,SIC	STX-VFS,S	SYX-LVFS,LS
ST-SICL,SICL	STX-VFSL,SL	SYX-S,S
ST-SIL,SIL	SY-C,C	SYX-SC,SC
ST-SIL-,SIL	SY-CL,CL	SYX-SCL,SCL
ST-SL,SL	SY-COS,S	SYX-SI,SI
ST-VFS,S	SY-COSL,SL	SYX-SIC,SIC
ST-VFSL,SL	SY-FS,S	SYX-SICL,SICL
STV-C,C	SY-FSL,SL	SYX-SIL,SIL
STV-CL,CL	SY-L,L	SYX-SL,SL
STV-COS,S	SY-LCOS,LS	SYX-VFS,S
STV-COSL,SL	SY-LS,LS	SYX-VFSL,SL
STV-FS,S	SY-LVFS,LS	UWB,O
STV-FSL,SL	SY-S,S	VAR,O
STV-L,L	SY-SC,SC	VFS,S
STV-LCOS,LS	SY-SCL,SCL	VFSL,SL
STV-LFS,LS	SY-SI,SI	WB,O
STV-LS,LS	SY-SIC,SIC	-
STV-LVFS,LS	SY-SICL,SICL	
STV-MPT,OM	SY-SIL,SIL	
STV-MUCK,OM	SY-SL,SL	
STV-S,S	SY-VFS,S	
STV-SC,SC	SY-VFSL,SL	
STV-SCL,SCL	SYV-C,C	
STV-SI,SI	SYV-CL,CL	
STV-SIC,SIC	SYV-COS,S	
STV-SICL,SICL	SYV-COSL,SL	
STV-SIL,SIL	SYV-FS,S	
STV-SL,SL	SYV-FSL,SL	
STV-VFS,S	SYV-L,L	
STV-VFSL,SL	SYV-LCOS,LS	
STX-C,C	SYV-LS,LS	
STX-CL,CL	SYV-LVFS,LS	
STX-COS,S	SYV-S,S	
STX-COSL,SL	SYV-SC,SC	
STX-FS,S	SYV-SCL,SCL	
STX-FSL,SL	SYV-SI,SI	
STX-L,L	SYV-SIC,SIC	
STX-LCOS,LS	SYV-SICL,SICL	
STX-LFS,LS	SYV-SIL,SIL	
STX-LS,LS	SYV-SL,SL	
STX-LVFS,LS	SYV-VFS,S	
STX-MUCK,OM	SYV-VFSL,SL	
STX-PEAT,OM	SYX-C,C	
STX-S,S	SYX-CL,CL	
STX-SC,SC	SYX-COS,S	

REFERENCES

- Allen, P.B., and J.W. Naney, "Hydrology of the Little Washita River Watershed, Oklahoma: Data and Analyses," U.S. Department of Agriculture, Agricultural Research Service, ARS-90, 74 pp., 1991.
- ASCE, *Evapotranspiration and Irrigation Water Requirements*, ASCE Manuals and Reports on Engineering Practice No. 70, Jensen, M.E., R.D. Burman, and R.G. Allen, eds., ASCE, 1990.
- Anderson, M.G., and T.P. Burt, "Automatic Monitoring of Soil Moisture Conditions in a Hillslope Spur and Hollow," *Journal of Hydrology*, 33, 27-36, 1977.
- Anderson, J.R., E.E. Hardy, J.T. Roach, and R.E. Witmer, 1976, "A Land Use and Land Cover Classification System for Use with Remote Sensor Data," U.S. Geological Survey, Professional Paper 964, Reston, VA.
- Atmospheric Radiation Measurement Program (ARM), www.arm.gov, 1998.
- Bennett, T., "Development of the Continuous Soil Moisture Accounting Model for HEC-HMS — DRAFT," unpublished material obtained through personal communication, January, 1998.
- Betson, R.P., "What is watershed runoff?," *Journal of Geophysical Research*, 69, 8, 1541-1552, 1964.
- Beven, K.J., and Kirkby, M.J., "A Physically-based Variable Contributing Area Model of Basin Hydrology," *Hydrol. Sci. Bull.*, 24, 1, pp. 43-69, 1979.
- Beven, K.J., "Runoff Production and Flood Frequency in Catchments of Order n: An Alternative Approach," *Scale Problems in Hydrology*, Gupta, V.K., I. Rodriquez-Iturbe, and E.F. Wood, eds., D. Reidel Publishing, Dordrecht, Holland, 1986.
- Bouwer, H., "Rapid Field Measurement of Air Entry Value and Hydraulic Conductivity of Soil as Significant Parameters in Flow System Analysis," *Water Resources Research*, 2, 4, pp. 729-738, 1966.
- Bouwer, H., "Infiltration of Water into a Non-uniform Soil," *Journal of the Irrigation and Drainage Division, ASCE*, 451-462, December, 1969.

Brutsaert, W., *Evaporation into the Atmosphere: Theory, History, and Applications*, D. Reidel Publishing Company, Dordrecht, Holland, 1982.

Burnash, R.J., R.L. Ferral, and R.A., McGuire, "A Generalized Streamflow Simulation System Conceptual Modeling for Digital Computers," U.S. National Weather Service and State of California Department of Water Resources, March, 1973.

Burt, T.P., and D.P. Butcher, "Topographic Controls of Soil Moisture Distributions," *Journal of Soil Science*, 36, pp. 469-486, 1985.

Canadell, J., R.B. Jackson, J. Ehleringer, H.A. Mooney, O.E. Sala, and E.D. Schulze, "Maximum rooting depth of vegetation types at the global scale," *Oecologia*, 108, 583-595, 1996.

Carsel, R.F., and R.S. Parrish, "Developing Joint Probability Distributions of Soil Water Retention Characteristics," *Water Resources Research*, 24, 5, 755-769, 1988.

CRWR-ESRI, GISHydro98 CD-ROM,
www.crwr.utexas.edu/gis/gishyd98/GisHyd98.htm, 1998.

Charbeneau, R.J., "Liquid Moisture Redistribution: Hydrologic Simulation and Spatial Variability," *Unsaturated Flow in Hydrologic Modeling Theory and Practice*, H.J. Morel-Seytoux (ed.), Kluwer Academic Publishers, 127-160, 1989.

Chow, V.T., D.R. Maidment, and L.W. Mays, *Applied Hydrology*, McGraw-Hill, Inc., New York, 1988.

Clapp, R.B., and G.M. Hornberger, "Empirical Equations for Some Soil Hydraulic Properties," *Water Resources Research*, v. 14, no. 4, August, 1978.

Coles, N.A., M. Sivapalan, J.E. Larsen, P.E. Linnet, and C.K. Fahrner, "Modeling Runoff Generation on Small Agricultural Catchments: Can Real World Runoff Responses be Captured?" *Hydrologic Processes*, 11, 111-136, 1997.

Dawdy, D.R., R.W. Lichty, and J.M. Bergmann, "A Rainfall-Runoff Simulation Model for Estimation of Flood Peaks for Small Drainage Basins," Professional Paper 506B, U.S. Geological Survey, pp. B1-B28, 1972.

DeVries, J.J., and T.V. Hromadka, "Computer Models for Surface Water," *Handbook of Hydrology*, Ch. 21, ed. D.R. Maidment, McGraw-Hill, Inc., 1993.

Dickinson, R.E., "Modeling Evapotranspiration for Three-dimensional Global Climate Models," *Climate Processes and Climate Sensitivity, Geophys. Monogr. Ser.*, J.E. Hansen and T. Takahashi, eds., 29, 58-72, AGU, Washington, D.C., 1984.

Dingman, S.L., *Physical Hydrology*, Prentice Hall, Englewood Cliffs, NJ, 1994.

Doorenbos and Pruitt, "Guidelines for Predicting Crop Water Requirements," Food and Agriculture Organization of the United Nations Irrigation and Drainage Paper 24, Rome, 1977.

Dunne, T., "Field studies of hillslope flow processes," *Hillslope Hydrology*, Chapter 7, M.J. Kirkby (ed.), 1978.

Dunne, T., T.R. Moore, and C.H. Taylor, "Recognition and Prediction of Runoff-Producing Zones in Humid Regions," *Hydrological Sciences Bulletin*, 20, 305-327, 1975.

Dyck, S., "Overview on the Present Status of the Concepts of Water Balance Models," IAHS Publ. 148, Wallingford, pp. 3-19, 1983.

Entekhabi, D., and P.S. Eagleson, "Land Surface Hydrology Parameterization for Atmospheric General Circulation Models Including Subgrid Scale Spatial Variability," *Journal of Climate*, 2, 816-831, 1989.

Famiglietti, J.S., and E.F. Wood, "Multiscale Modeling of Spatially Variable Water and Energy Balance Processes," *Water Resources Research*, 30, 11, 3061-3078, November 1994.

Finnerty, B., and D. Johnson, "Comparison of National Weather Service Operational Mean Areal Precipitation Estimates Derived from NEXRAD Radar vs. Rain Gage Networks," presented at International Association for Hydraulic Research (IAHR), XXVII Congress, San Francisco, CA, August 10-15, 1997.

Franchini, M., and M. Pacciani, "Comparative Analysis of Several Conceptual Rainfall-Runoff Models," *Journal of Hydrology*, v. 122, 161-219, 1991.

Fukami, K., E.T. Engman, P. Kumar, A. Terakawa, "A Study on Basin-wide Soil-layer Modeling in the Little Washita Basin in Oklahoma, USA," Proceedings of the Consultative Meeting on Soil Moisture and Ocean Salinity Measurement Requirements and Radiometer Techniques, ESA WPP-87, ESTEC, Noordwijk, The Netherlands, 35-40, April 20-21, 1995.

Goldman, D.M., "Loss Rate Representation in the HEC-1 Watershed Model," *Unsaturated Flow in Hydrologic Modeling Theory and Practice*, H.J. Morel-Seytoux (ed.), Kluwer Academic Publishers, 1989.

Govindaraju, R.S., D. Or, M.L. Kavvas, D.E. Rolston, and J. Biggar, "Error Analyses of Simplified Unsaturated Flow Models Under Large Uncertainty in Hydraulic Properties," *Water Resources Research*, v. 28, no.11, 2913-2924, November 1992.

Greene, D.R., and M.D. Hudlow, "Hydrometeorologic Grid Mapping Procedures," AWRA International Symposium on Hydrometeorology, Denver, CO, June 13-17, 1982 (DRAFT).

HEC, "GridParm: Procedures for Deriving Grid Cell Parameters for the ModClark Rainfall-Runoff Model, User's Manual," U.S. Army Corps of Engineers Hydrologic Engineering Center, Davis, CA, CPR-71, November 1996.

HEC, "HEC-HMS Hydrologic Modeling System User's Manual," U.S. Army Corps of Engineers Hydrologic Engineering Center, Davis, CA, 1997.

HEC, "modClark User's Manual," U.S. Army Corps of Engineers Hydrologic Engineering Center, Davis, CA, 1995.

Hellweger, Ferdinand, *HEC-Prepro: A GIS Pre-processor for HMS*, Master's Thesis, University of Texas at Austin, May, 1997.

Hewlett, J.D., and A.R. Hibbert, "Factors Affecting the Response of Small Watersheds to Precipitation in Humid Areas," International Symposium on Forest Hydrology, W.E. Supper and H.W. Lull, eds., Pergamon Press, Oxford, 275-290, 1967.

Hydrocomp Simulation Programming Operations Manual, Hydrocomp International, Inc., Palo Alto, CA, 1970.

Jackson, T.J., J. Schmutge, and E.T. Engman, "Remote Sensing Applications to Hydrology: soil moisture," *Hydrological Sciences*, 41, 4, 1996.

Jenson, S.K., Domingue, J.O. : Extracting topographic structure from digital elevation data for geographic information system analysis. *Photogrammetric Engineering and Remote Sensing* 54, 1593-1600, 1988.

Jury, W.A., Gardner, W.R., and Gardner, W.H., "Soil Physics : Fifth Edition," John Wiley and Sons, Inc., New York, 1991.

Kanemasu, E.T., S.B. Verma, E.A. Smith, L.J. Fritschen, M. Wesely, R.T. Field, W.P. Kustas, H. Weaver, J.B. Stewart, R. Gurney, G. Panin, and J.B. Moncrieff, "Surface Flux Measurements in FIFE: An Overview," *Journal of Geophysical Research*, v. 97, No. D17, 18547-18555, November 30, 1992.

Leavesley, G.H., R.W. Lichty, B.M. Troutman, and L.G. Saindon, "Precipitation-runoff Modeling System: User's Manual," *Water-Resources Investigations Report 83-4238*, USGS, 1983.

Maidment, D.R., and Mizgalewicz, P. : Digital delineation of watersheds and stream networks in the Allegheny basin. Report prepared for the Hydrologic Engineering Center, U.S. Army Corps of Engineers, Davis, CA, 1993.

McFadden, D.E., "Soil Moisture Accounting in Continuous Simulation Watershed Models," Master's Project Report, University of California at Davis, 1994.

McCuen, R.H., W.J. Rawls, and D.L. Brakensiek, "Statistical Analysis of the Brooks-Corey and the Green-Ampt Parameters Across Soil Textures," *Water Resources Research*, 17, 4, 1005-1013, 1981.

Mein, R.G., and C.L. Larson, "Modeling Infiltration During a Steady Rain," *Water Resources Research*, 9, 2, 384-394, 1973.

Miller, D.A. and R.A. White, "A Conterminous United States Multi-Layer Soil Characteristics Data Set for Regional Climate and Hydrology Modeling," *Earth Interactions*, 2, 1998. (More information at: www.essc.psu.edu/soil_info/index.cgi?soil_data&index.html).

Monteith, J.L., "The Development and Extension of Penman's Evaporation Formula," *Applications of Soil Physics*, Chapter 10, D. Hillel (ed.), Academic Press, 247-253, 1980.

Monteith, J.L., Szeicz, G., and Waggoner, P.E., "The Measurement and Control of Stomatal Resistance in the Field," *J. Appl. Ecol.*, 2, 345-355, 1965.

Moore, I.D., Grayson, R.B., Ladson, A.R.: Digital terrain modelling : a review of hydrological, geomorphological, and biological applications. *Hydrological Processes* 5, 3-30, 1991.

Moore, I.D., E.M. O'Loughlin, and G.J. Burch, "A Contour-based Topographic Model for Hydrologic and Ecological Applications," *Earth Surface Process Landforms*, 13, pp. 305-320, 1988.

Moore, I.D., S.M. Mackay, P.J. Wallbrink, G.J. Burch, and E.M. O'Loughlin, "Hydrologic Characteristics and Modelling of a Small Forested Catchment in Southeastern New South Wales. Pre-logging Condition," *Journal of Hydrology*, 83, 307-335, 1986.

Morgan, M.G., and M. Henrion, *Uncertainty, A Guide to Dealing with Uncertainty in Quantitative Risk and Policy Analysis*, Cambridge University Press, 1990, p. 178.

Neuman, S.P., "Wetting Front Pressure Head in the Infiltration Model of Green and Ampt," *Water Resources Research*, 12, 3, 564-566, 1976.

Noilhan, J., and S. Planton, "A Simple Parameterization of Land Surface Processes for Meteorological Models," *Monthly Weather Review*, 117, 536-549, 1989.

O'Callaghan, J.F., Mark, D.M. : The extraction of drainage networks from digital elevation data. *Computer Vision, Graphics and Image Processing* 28, 323-344 (1984).

Olivera, F., D.R. Maidment, and R.J. Charbeneau, *Spatially Distributed Modeling of Storm Runoff and Non-Point Source Pollution using Geographic Information Systems*, CRWR Online Report 96-4, December 1996.

Olivera, F., S. Reed, and D. Maidment, "HEC-PrePro v. 2.0: An ArcView Pre-Processor for HEC's Hydrologic Modeling System," paper presentation at the 1998 ESRI User's Conference, San Diego, CA, July 25-31, 1998 (www.ce.utexas.edu/prof/olivera/esri98/p400.htm).

O'Loughlin, E.M., "Saturation Regions in Catchments and their Relations to Soil and Topographic Properties," *Journal of Hydrology*, 53, 229-246, 1981.

O'Loughlin, E.M., "Prediction of Surface Saturation Zones in Natural Catchments by Topographic Analysis," *Water Resources Research*, 22, 5, pp. 794-804, May 1986.

Peters, J., personal communication, 1998.

Peters, J., and D. Easton, "Runoff Simulation Using Radar Rainfall Data," *Water Resources Bulletin*, 32, 4, 753-760, 1996.

Peppler, R.A., Sisterson, D.L., and Lamb, P.J., "Site Scientific Mission Plan for the Southern Great Plains CART Site: July-December 1997," ARM-97-002, prepared for the U.S. Department of Energy under Contract W-31-109-Eng-38.

Peppler, R.A., Sisterson, D.L., and Lamb, P.J., "Site Scientific Mission Plan for the Southern Great Plains CART Site: January-June 1998," ARM-98-002, prepared for the U.S. Department of Energy under Contract W-31-109-Eng-38.

Pilgrim, D.H., and I. Cordery, "Flood Runoff," *Handbook of Hydrology*, Chapter 9, D.R. Maidment (ed.), McGraw-Hill, Inc., 1993.

Rawls, W.J., Ahuja, L.R., Brakensiek, D.L., and A. Shirmohammadi, "Infiltration and Soil Water Movement," *Handbook of Hydrology*, ed. D. Maidment, Chapter 5, McGraw-Hill, Inc., 1993.

Rawls, W.J., D.L. Brakensiek, and N. Miller, "Green-Ampt Infiltration Parameters from Soils Data," *J. Hydraul. Div. Am. Soc. Civ. Eng.*, 109, No. 1, pp. 62 - 70, 1983.

Rawls, W.J., D.L. Brakensiek, K.E. Saxton, "Estimation of Soil Water Properties," *Transactions of the ASAE*, ASAE Paper No. 81-2510, pp. 1316-1320, 1982.

Rawls, W.J., and D.L. Brakensiek, "Prediction of Soil Water Properties for Hydrologic Modeling," *Watershed Management in the Eighties*, ASCE, pp. 293-299, 1985.

Reece, C.F., "Evaluation of a Line Heat Dissipation Sensor for Measuring Soil Matric Potential," *Soil Sci. Soc. Am. J.*, 60, 1022-1028, 1996.

Reed, S.M., and D.R. Maidment, *A GIS Procedure for Merging NEXRAD Precipitation Data and Digital Elevation Models to Determine Rainfall-Runoff Modeling Parameters*, CRWR Online Report 95-3, September 1995.

Reed, S.M., and D.R. Maidment, "Coordinate Transformations for Using Nexrad Data in GIS-based Hydrologic Modeling," accepted for publication in the *Journal of Hydrologic Engineering*, April 21, 1998.

Sellers, P.J., "Biophysical Models of Land Surface Processes," *Climate System Modeling*, Chapter 14, K.E. Trenberth (ed.), Cambridge University Press, 1992.

Sellers, P.J., Y. Mintz, Y.C. Sud, and A. Dalcher, "A Simple Biosphere Model (SiB) for Use with General Circulation Models," *Journal of the Atmospheric Sciences*, 43, 6, 1986.

Schneider, J.M., and D.K. Fisher, "Meeting GEWEX/GCIP Measurement Needs by Adding Automated Measurement of Soil Water and Temperature Profiles to the DOE ARM/CART Southern Great Plains Site," AMS 13th Conference on Hydrology, 265-268, 1997.

Shedd, R.C., and Fulton, R.A., "WSR-88D Precipitation Processing and its Use in National Weather Service Hydrologic Forecasting," *Engineering Hydrology: Proceedings of the Symposium Sponsored by the Hydraulics Division of the American Society of Civil Engineers*, San Francisco, CA, July 25-30, 1993.

Shuttleworth, J.W., "Evaporation," *Handbook of Hydrology*, D.R. Maidment Editor, McGraw-Hill, Inc., 1993.

Sivapalan, M., K. Beven, and E.F. Wood, "On Hydrologic Similarity. 2. A Scaled Model of Storm Runoff Production, *Water Resources Research*, 23, 12, pp. 2266-2278, 1987.

Sivapalan, M., and E.F. Wood, "Spatial Heterogeneity and Scale in the Infiltration Response of Catchments," *Scale Problems in Hydrology*, V.K. Gupta et al. (eds.), D. Reidel Publishing Company, 81-106, 1986.

Smith, J.A., D.J. Seo, M.L. Baeck, and M.D. Hudlow, "An Intercomparison Study of NEXRAD Precipitation Estimates," *Water Resources Research*, v. 32, no. 7, 2035-2045, July, 1996a.

Smith, M.B., D.J. Seo, B.D. Finnerty, V. Koren, "Distributed Parameter Hydrologic Modeling and NEXRAD for River Forecasting: Scale Issues Facing the National Weather Service," presented at the North American Water and Environment Congress '96, ASCE, Anaheim, California, June 24-28, 1996b.

Soil Conservation Service, National Engineering Handbook, Section 4, Hydrology, U.S. Department of Agriculture, U.S. Government Printing Office, Washington, D.C., 1972.

Southern Great Plains Hydrology Experiment (SGP 97),
daac.gsfc.nasa.gov/CAMPAIGN_DOCS/SGP97/sgp97.html, 1997.

United States Army Corps of Engineers (USACE), *Flood-runoff Analysis - Engineer Manual*, Manual No. 1110-2-1417, Washington, D.C., August 31, 1994.

United States Department of Agriculture, *Soil Survey Manual*, Handbook No. 18, U.S. Government Printing Office, August, 1951.

United States Department of Agriculture, *Soil Survey Manual*, Handbook No. 18, U.S. Government Printing Office, October, 1993.

United States Department of Agriculture Natural Resources Conservation Service, "State Soil Geographic (STATSGO) Data Base Data Use and Information," Misc. Publication No. 1492, December, 1994.

United States Department of Agriculture Natural Resources Conservation Service, "Soil Survey Geographic Data Base Data Use and Information," Misc. Publication No. 1527, January, 1995.

U.S. Geological Survey Open-File Report 95-727 (CD-ROM), "Watershed Boundaries and Digital Elevation Model of Oklahoma Derived from 1:100,000-scale Digital Topographic Maps," 1995.

Watershed Modeling System, www.ecgl.byu.edu/software/wms/, 1998.

Wood, E.F., M. Sivapalan, K. Beven, and L. Band, "Effects of Spatial Variability and Scale with Implications to Hydrologic Modeling," *Journal of Hydrology*, v. 102, 29-47, 1988.

Zahner, R., "Refinements in Empirical Functions for Realistic Soil-moisture Regimes Under Forest Cover," International Symposium of Forest Hydrology, W.E. Sopper and H.W. Lull, eds., Pergamon Press, New York, 261-274, 1967.

Zaslavsky, D., Sinai, G., "Surface hydrology : 1 – explanation of phenomena," *Journal of the Hydraulics Division. Proceedings of the American Society of Civil Engineers*, 107, 1-16, 1981.

VITA

Seann Mischa Reed was born in Ithaca, New York on August 17, 1971, the son of John and Kathleen Reed. Seann graduated from Oak Ridge High School, Oak Ridge, Tennessee, in 1989. In the fall of 1989 he enrolled at Cornell University in Ithaca, New York where he received a Bachelor of Science Degree in Civil Engineering in May 1993. From the fall of 1993 to the present, Seann has been a graduate student at The University of Texas at Austin. For his five-plus years at The University of Texas at Austin, Seann has been a research assistant at the Center for Research in Water Resources and has been a teacher and teaching assistant for several short courses dealing with GIS, hydrology, and hydraulics. Seann received a Master of Science degree in Civil Engineering from The University of Texas at Austin in May 1995.

Permanent Address: 2952 Cyrandall Valley Rd., Oakton, VA 22124

This dissertation was typed by the author.